INFORMATION TO USERS

This manuscript has been reproduced from the microfilm master. UMI films the text directly from the original or copy submitted. Thus, some thesis and dissertation copies are in typewriter face, while others may be from any type of computer printer.

The quality of this reproduction is dependent upon the quality of the copy submitted. Broken or indistinct print, colored or poor quality illustrations and photographs, print bleedthrough, substandard margins, and improper alignment can adversely affect reproduction.

In the unlikely event that the author did not send UMI a complete manuscript and there are missing pages, these will be noted. Also, if unauthorized copyright material had to be removed, a note will indicate the deletion.

Oversize materials (e.g., maps, drawings, charts) are reproduced by sectioning the original, beginning at the upper left-hand corner and continuing from left to right in equal sections with small overlaps. Each original is also photographed in one exposure and is included in reduced form at the back of the book.

Photographs included in the original manuscript have been reproduced xerographically in this copy. Higher quality 6" x 9" black and white photographic prints are available for any photographs or illustrations appearing in this copy for an additional charge. Contact UMI directly to order.

UMI

A Bell & Howell Information Company
300 North Zeeb Road, Ann Arbor MI 48106-1346 USA
313/761-4700 800/521-0600

ASYMMETRIC DIGITAL SUBSCRIBER LINE (ADSL) LOOP ENVIRONMENT

by

Ajit Reddy

A dissertation submitted to the Graduate Faculty in Computer Science in partial fulfillment of the requirements for the degree of Doctor of Philosophy, The City University of New York.

1997

The City University of New York

This Manuscript has been read and accepted for the Graduate Faculty in Computer Science in satisfaction of the dissertation requirement for the Doctor of Philosophy.

Jan 29, 1997
Date

Professor Syed V. Ahamed
Chair of Examining Committee

January 28, 1997
Date

Professor Stanley Habib
Executive Officer

Professor Syed V. Ahamed
Professor Stanley Habib
Professor Michael Anshel
The City University of New York

Dr. Jean Jacques Werner
Lucent Technologies

Supervisory Committee

THE CITY UNIVERSITY OF NEW YORK

Abstract

Asymmetric Digital Subscriber Line (ADSL) Loop Environment

by

Ajit Reddy

Advisor: Professor Syed V. Ahamed

Simulation study of the matching circuits and functions for the transhybrid loss in the ADSL subscriber loop environment. The sixteen loops in the Digital Subscriber Loop Environment called as the Bellcore /ANSI Standard Loops have been considered for the study of the feasibility of increasing the transhybrid loss in the active hybrid circuits using optimization methods. This optimization attempts to reduce the near-end reflection which occurs as a result of the overlap of the forward and the reverse channel in the digital subscriber lines (ANSI) for the ADSL environment for DS2, DSC1 and DS1 rates in the forward channel and fractional DS1 or T1 rates (384 kb/s) in the reverse channel using Coefficient Relaxation and Component Relaxation techniques. The performance of these matching functions obtained by the two methods are compared and evaluated in terms of the maximum transhybrid loss obtained in either case. Time Domain Hybrid Attenuation using digital adaptation and analog cancellation has been discussed and their performance for fixed and adaptive models are also evaluated and implementation using Analog and Digital techniques are presented.

The City University of New York

Acknowledgments

I wish to express my deep appreciation and gratitude to Professor Syed V. Ahamed for being my Advisor and for his continuous supervision, guidance, encouragement and help during the course of this research. I also thank Professor Stanley Habib and Professor Michael Anshel for serving as members of my doctoral thesis committee and who have also guided me and encouraged me throughout my doctoral studies.

My appreciation is also expressed to Dr. Jean Jacques Werner of Lucent Technologies for serving on my thesis committee and also for his guidance. My thanks to Dr. Victor Lawrence (Director) and Mr. Krishna Murti (Head) of Advanced Communications Technologies (ACTS) at Lucent Technologies for providing support and facilities for my research. I would like to thank Dr. Nickolas Zervos for his encouragement, guidance, cooperation and for sharing some of his views and thoughts with me.

Finally I would like to thank Professor Stephen Lucci (Chairman) of City College of New York and Professor Michael Kress (Chairman) of College of Staten Island for their continuous help and support during the course of my studies.

CONTENTS

List of Tables

List of Figures

Chapter 7

Chapter 1

Introduction

1.0 Digital Transmission Systems

In the early days of communication copper wire was used to carry information on a single channel. In order to make the effective use of the physical link ways were developed in which multiple channels could be transmitted on the same physical link which came to be called as the carrier. The digital signals are now transmitted from one point to another using different media such as twisted wire pair, coaxial cable, radio, optical fibers and satellite. A typical T-carrier system consists of channel service units, channel banks, multiplexers, transcoders and digital cross connects.

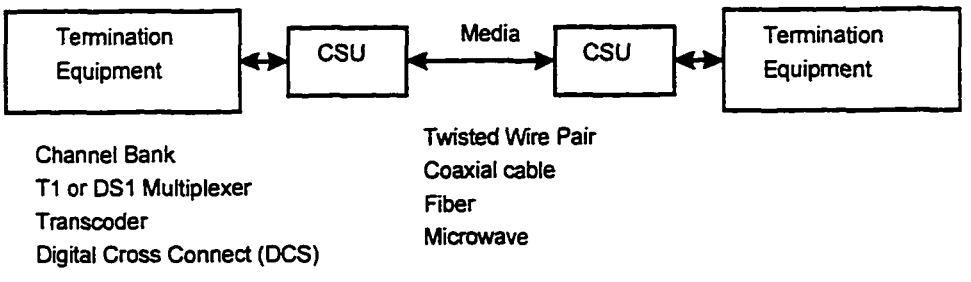

Figure 1.1: Digital Transmission System

1.1.1 Channel Service Unit

The channel service unit (CSU) is the bridge between the channel and the termination equipment. It is a protective interface which connects the premises distributed equipment (PDE) to the digital transmission line. The basic function of a CSU is to ensure that a good quality digital signal is maintained in the network. It also has feature for testing and monitoring the access of the signals transmitted and received to and from the data termination equipment (DTE) in order to isolate the fault if any that arises in the network. The CSU has a transmit side which regenerates the digital signal received from the subscriber by doing error correction and then retransmitting the signal on the DS1 transmission facility. The receive side of the CSU regenerates the DS1 signal received from the network and checks for the remote loop back codes and sends it to the customer.

1.1.2 Multiplexer

These are devices which convert the digital information from different channels into a single stream of digital data. However the data rate of the output channel of the multiplexer would be higher than the data of the incoming channels. Approximately the data rate of the outgoing channel could be considered to be the data rate of the incoming channels times the number of incoming channels. Various *time division multiplexing (TDM)* techniques are used like synchronous time division multiplexing

and statistical time division multiplexing. In synchronous TDM number of input signals are multiplexed onto the same channel. The incoming signals which carry digital data are first buffered which are then scanned sequentially to form a composite data stream whose data rate is equal to the total sum of the data rates of all the input channel. Synchronous TDM is so called not because of synchronous transmission is used but because time slots are pre-assigned to sources and fixed. The time slots for each source are transmitted irrespective of whether the source has data to send or not.

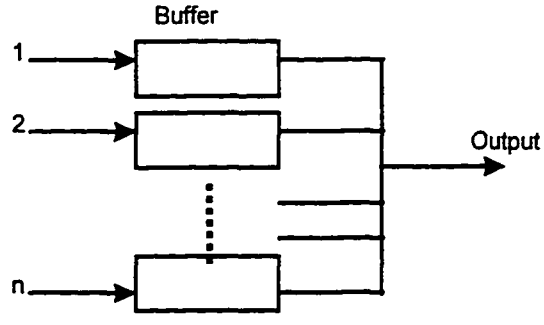

Figure 1.2: Synchronous Time Division Multiplexing

In statistical time division multiplexing also known as asynchronous TDM and intelligent TDM the statistical multiplexer exploits the common property of data transmission by dynamically allocating time slots on demand. Statistical TDM takes advantage of the fact that the attached device are not all transmitting all of the time. In statistical TDM it is not known ahead of time which source's data will be in any

particular slot. Since data arrive from and are distributed to I/O lines unpredictably, address information is required to assure proper delivery, which means there is more overhead per slot for statistical TDM since each slot carries an address as well as data.

1.1.3 Channel Bank

A channel bank performs the first step of call handling. It multiplexes a group of channels into a higher frequency band and conversely, demultiplexes the higher frequency band into the respective individual channels. The digital channel banks convert the analog voice to digital data using pulse code modulation (PCM) and vice versa and they also multiplex several of these streams into a single stream using time division multiplexing (TDM).

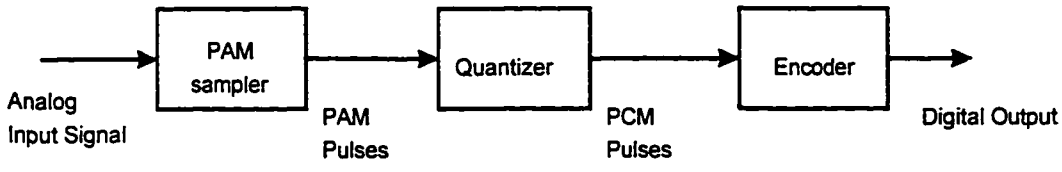

Figure 1.3: Pulse Code Modulation

Pulse code modulation is based on the sampling theorem which states that "If a signal f(t) is sampled at regular intervals of time and at a rate higher than twice the

highest significant signal frequency, then the samples contain all the information of the original signal. The function f(t) may be reconstructed from these samples by the use of a low pass filter." In PCM the signal is sampled and the samples obtained are represented as narrow pulses whose amplitude is proportional to the value of the original signal. This process is known as *pulse amplitude modulation (PAM).* The PAM samples are now quantized by which the original are now approximated to give the PCM pulses. The PCM pulses are then encoded whose output is a digital output . Thus the channel banks act as an interface from the analog world to the digital world and each channel provides the interface between the *central office (CO)* and the terminal at the subscriber end.

1.1.4 Transcoder

The transcoders accept two DS1 rate (1.544Mbps) PCM channels and code translate the two streams using adaptive differential pulse coded modulation (ADPCM) techniques onto a single DS1 channel retaining the framing format of the DS1 standard. In ADPCM the signal is encoded and then decoded and therefore requires an encoder and a decoder. The ADPCM encoder accepts the PCM compressed signal samples and by means of adaptive prediction and adaptive quantization reduces the output to half of its input.

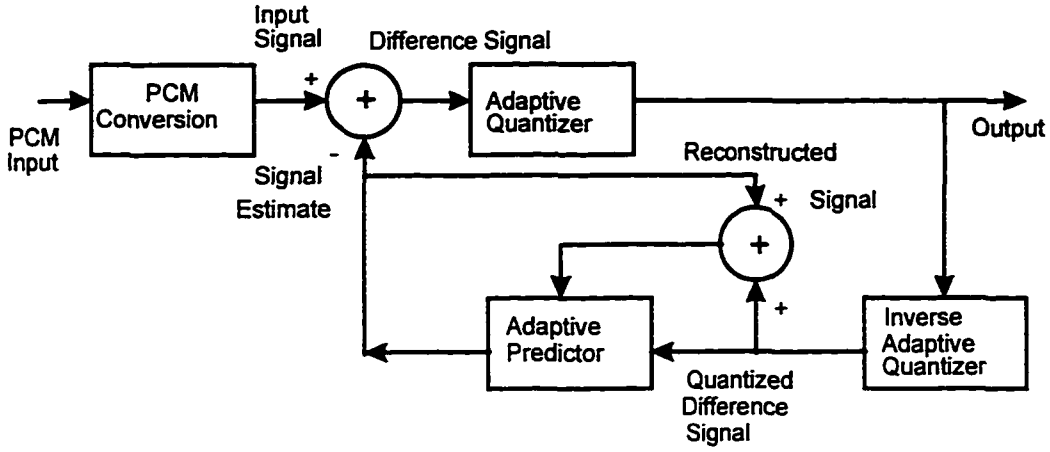

Figure 1.4: ADPCM Encoder

The ADPCM decoder accepts the input which has been reduced by the encoder and reconstructs the signal in the form of the PCM compressed signal which was fed to the input of the ADPCM encoder.

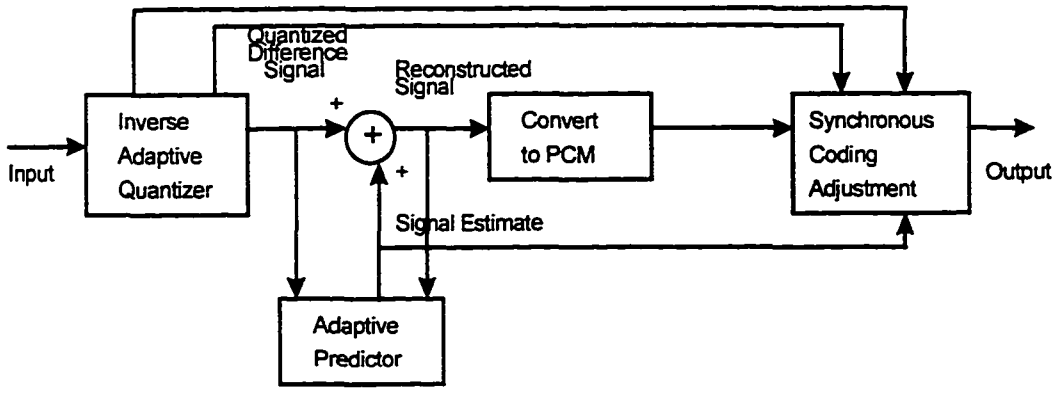

Figure 1.5: ADPCM Decoder

1.1.5 Digital Cross Connect

Digital cross connects are the interconnection points for terminals, multiplexers and transmission systems. It is a computerized facility that allows DS1 lines to be remapped electronically at the DS0 level. It allows the assignment and redistribution of 64Kbps channels among various DS1/T1 systems connected to the digital cross connect system (DCS) at the digital level and can therefore be considered as the DS1 switch at the first level in the PCM hierarchy.

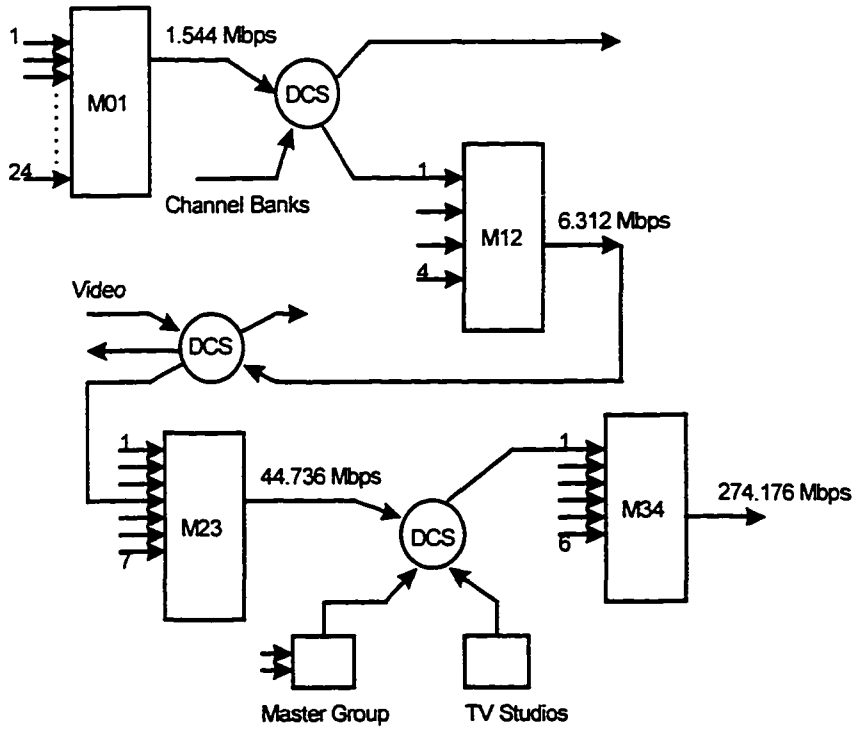

Figure 1.6: Digital Cross Connect

1.2 The TDM Hierarchy (North America)

The traditional PCM hierarchy consists of levels DS0 to DS4. These digital streams produced by channel banks and other multiplexing equipment are by design independent of the target transmission media. The voice band channels which are between 0 to 4KHz are first pulse code modulated and then multiplexed using multiplexers onto higher bit rates. The voice band channel is 0 to 4KHz and so the sampling frequency is twice that of the signal frequency or 8KHz which means the voice signal has to sampled at twice the rate of the signal frequency which amounts to 8000 samples per second. Each of the samples obtained are of 8 bits and therefore for 8000 samples it is 64,000 bits and hence the channel capacity of the DS0 is fixed at 64Kbps. Twenty four of the DS0 channels are multiplexed to form the DS1 channel which is 1.544 Mbps channel. Two of the DS1 channels are multiplexed to form the DS1C channel which has a channel capacity of 3.152 Mbps, also four of the DS1 channels are multiplexed to form the DS2 channel which can handle data rates of 6.312 Mbps. Seven of the DS2 channels are multiplexed to form the DS3 channel which can handle a data rate of 44.736 Mbps and finally six of the DS3 channels are multiplexed to form the DS4 channel which can handle data rates of 274.176 Mbps.

These are also called as the T1, T2, T3 and T4 channels which are the same as the DS1, DS2, DS3 and DS4 channels only in terms of channel capacities. However if the frame format of DS1 and T1 is considered then there is some difference since the T1

is formed by multiplexing 24 of the 64 Kbps channels and the frame for the T1 channel consists of 193 bits with 192 bits being the data (8 bits per input) of the 24 inputs to multiplexer and one frame bit is used for synchronization which is bit 193. In the case of the DS1 format 23 channels are data and the twenty fourth channel position is reserved for special sync byte which allows faster and more reliable reframing following a framing error. Within each DS0 channel seven bits per frame are used for data with the eighth bit used to indicate if the channel contains user data or system control data. With seven bits per channel and each of the DS0 frame being repeated 8000 times a data rate of 56 Kbps is provided by the DS0.

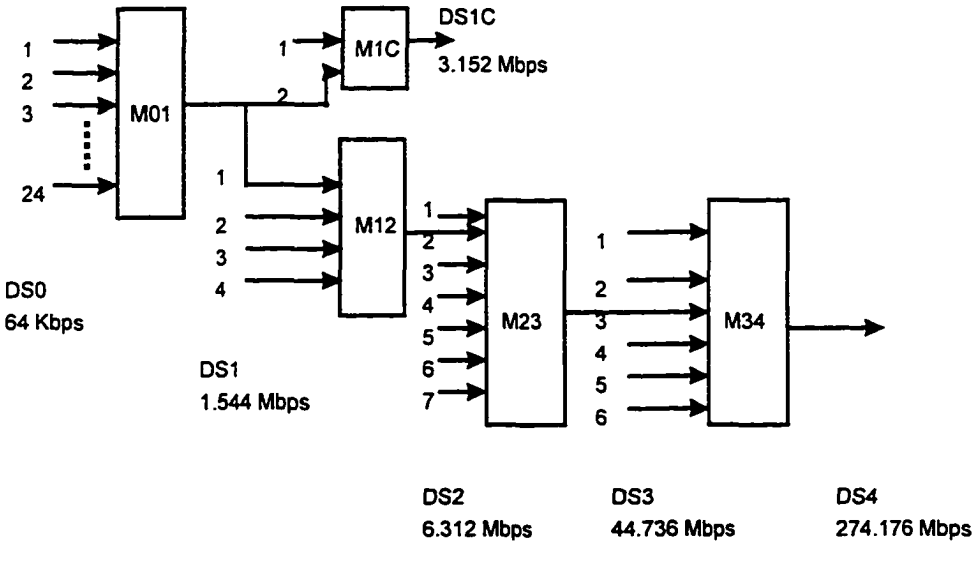

Figure 1.7: North American Hierarchy

1.3 Residential Video Services

The local exchange companies have not taken an active part in the distribution of video services to the subscriber even though television is an integral part of the customer in the United States. The main reason for this being the regulation which had kept the telephone companies out the business of engaging themselves in the transmission of video information to the residents. The technology now being used in the local exchanges have the capability to transmit video information to the customers. The advances in digital video technologies have made the local exchange companies to conduct research in these areas and also to equip themselves with the growing needs of the customers. The fact that the customers are not quite satisfied with the broadcast media and the cable television companies has called for the regulatory bodies to re-examine the local exchange companies delivering video information on a large scale. One of the forerunners in this area is the Bell Atlantic company which has been conducting experiments in the residential video services and delivery. The need for viewing selected video information from the cable televisions and the broadcast media by the customers at their own leisure is fast emerging and also a desire for face to face communication (video conferencing) among various family members when one or more are homebound.

1.3.1 Restrictions

The major problem is that if the local exchange companies were to transmit video information on the existing twisted wire pairs to the customers than the video quality has to be good. This means better video coding and compression algorithms with high bit rates on the digital subscriber loops. The customer has to get accustomed to the voice response units (VRU) which employ voice prompts and respond with the dual tone multifrequency (DTMF) signals. The VRU's could be combined with a series of dynamic on line menus providing the users with the necessary control options. The delivery device ultimately should respond to the control units.

1.3.2 Video On Demand (VOD)

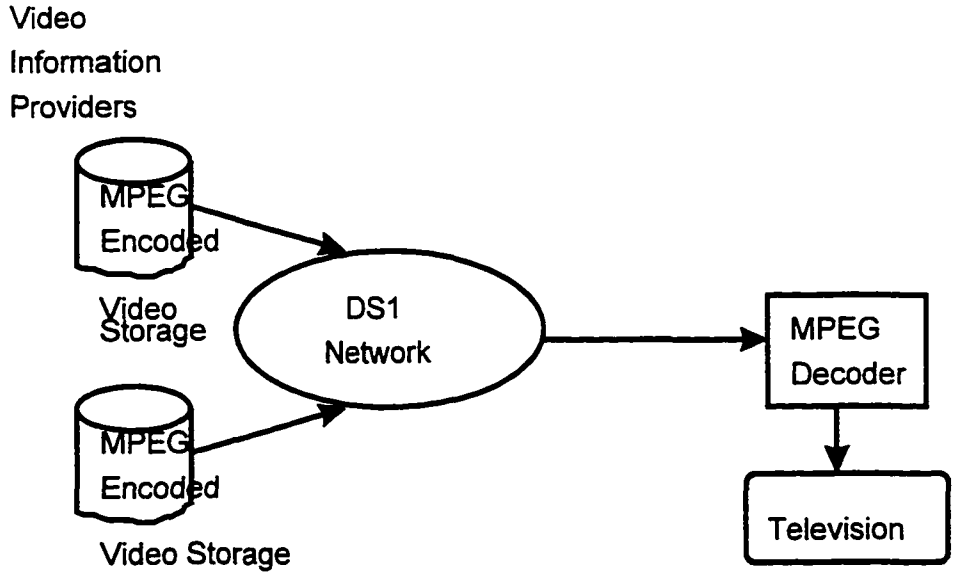

Figure 1.8: Basic Video On Demand Architecture

It is an electronic device which the customer who wants this service has to rent . Customers seeking certain video information at their schedule can access the video information such as entertainment video services (News, movies, etc.) and education video services (classroom lectures) for the students. The VOD implementation uses DS1 line (1.544Mbps) and motion pictures experts group (MPEG) coding and compression techniques.

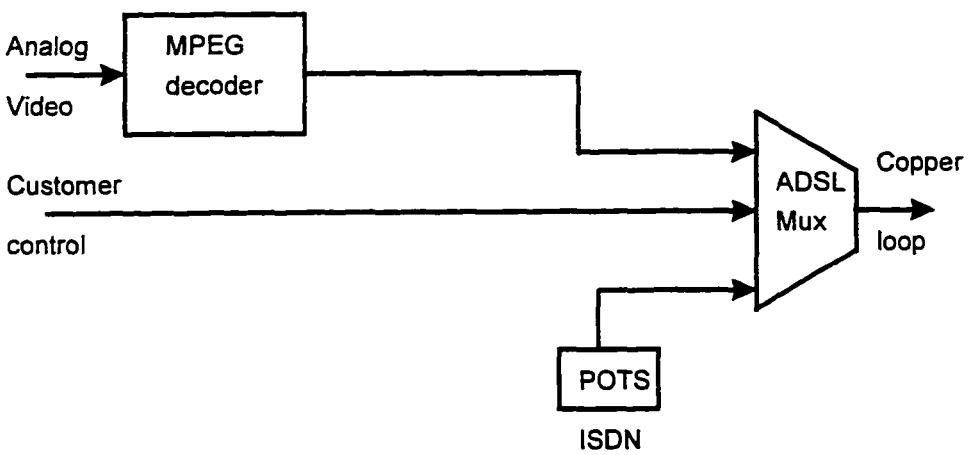

Figure 1.9: Video On Demand Equipment

The encoding and compression using MPEG takes a long time and hence the video information is encoded compressed and stored on the large disk drives.

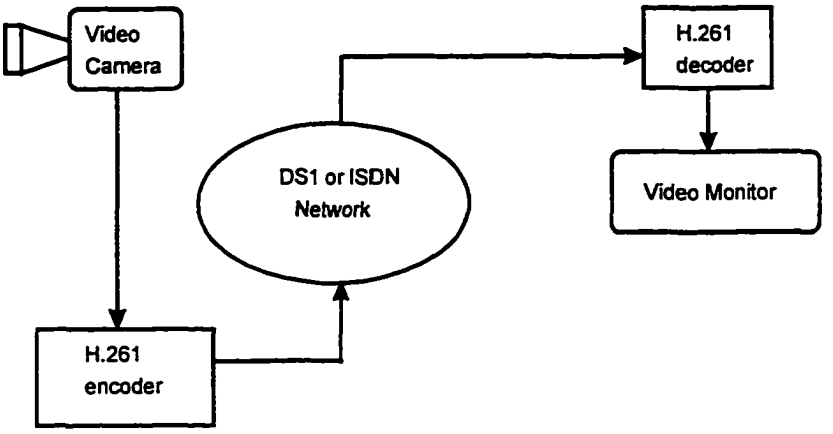

Figure 1.10: Distance Learning Service

1.3.3 Telecommuting and Learning

In this case the customer does not require the two way conference, but would require remote video monitoring functionality. These services rely on ISDN or DS1 line and H.261 video compression technology. The H.261 which is CCITT standard is a video transmission protocol specified for its use in real time video information delivery at bandwidth the increments of 64Kbps ((1 to 30) x 64Kbps). The image quality increases with bandwidth but at present its quality is less than the existing VCR quality at 1.544 Mbps.

1.3.4 Multimedia

Services such as a combination of text still images, audio and motion video are considered multimedia services. Entertainment and education generally involve a greater amount of interactivity source. The architecture for such a service employs the same setup as that required for VOD services, utilizing ISDN or DS1 line to allow users to access the remote multimedia databases. The multimedia technology primarily employs ISO's joint photographic experts group (JPEG) standard for still image delivery and MPEG for the delivery of motion video. Another ISO standard which is considered is multimedia hypermedia experts group (MHEG) which will provide a combined standard for still image, motion video and audio.

1.3.5 Cable Television

The use of optical fiber by the local exchange companies provides some potential for the delivery of cable television company program to its subscribers. At present only analog video technology is considered. The use of digital video technology needs more advances in digital video technology and deploying of fiber by the local exchange companies between the subscriber and the central office or the use of fibers in digital subscriber loops.

1.4 Local Loop Environment

The copper loop between the Central Office (CO) and the customer is usually made up of pairs from the sections of several cables. A loop can include several gauge changes and bridge taps. Bridged taps are open circuit pairs, either intentionally placed along a main cable route in anticipation of possible service demand at another location or resulting from past service disconnection's and rearrangements. The segment of the network between the local office and the customer is copper based. About 25% of the subscriber loops have load coil which flatten the frequency at the upper edge of the voice band (3500Hz). Load coils are mostly used for long loops in excess of 18 Kft.

In an effort to improve the line characteristics and bandwidth Carrier Serving Area administration guidelines were introduced which were aimed at shortening the distribution of loop lengths, eliminating longer loops, and eliminating the use of load coils in order to position the loop plant to provide new digital services at speeds in the region of 64 Kbps. The CSA guidelines specifies the following loop lengths 9 Kft of 26 gauge, 12Kft of mixed 26 and 24 gauge. The guidelines also restrict the working length of the loops with bridged taps and limit bridged tap length and excessive mixing of gauges.

1.4.1 Loop Impairments

Since the frequency responses of the subscriber loops drop off rapidly at higher frequencies, it calls for the use of equalizers for the voice service to flatten the channel at higher frequencies. The phase response is not strictly linear in the case of the copper loop since it provides a dispersive communications channel. If a pulse is transmitted down the loop, the phase non linearity will cause the pulse to spread out in time. In a pulse train, the smeared out pulses will overlap with each other causing *inter symbol interference (ISI).* ISI usually comprises most of the energy in the received pulse samples. It is anticipated that the post-cursor ISI will be cancelled out by the Decision Feedback Equalizer (DFE). The complexity of the filters used in the Feedback Equalizers depend on the line codes used. The pre-cursor ISI can be reduced by the use of Feed-Forward Filters, which also reduces the crosstalk noise. The length of the filters used to reduce all types of ISI depends not only on the line codes used but also on the subscriber loops.

The pulses also undergo considerable attenuation which are compensated by the equalizer and the timing recovery circuits. For economic reasons two-wire transmission has been chosen for the voice service where transmission takes place in both the directions. This is achieved by the use of a hybrid balance network which separates the two directions of transmission by using a four port balanced bridge. The same principle is also followed for the transmission of data in both the directions over

the same twisted wire pair in full duplex manner. One of the impairments arising from this type of technique is that the residual echo which occurs due to the imbalance between the hybrid and the line impedance and also due to the bridge taps in the subscriber loops causes some of the transmit energy to leak into the receive path and thereby causing an *echo* at the receiving end. Echoes can be cancelled by the use of transversal filters. The length of the transversal filters used depends on line codes used. Some line codes cause bigger echoes than the others which leads to different levels of echo cancellation which can cause non-linearities in performance of the canceler that can be rectified by additional canceler complexity. High levels of echo cancellation means that the sensitivity of the echo canceler is an important issue with respect to the timing jitter. When the echo cancellation is done after the A/D the received signal also contains echoes which are quantized and this results in residual echo which arises from the quantization errors. The residual echoes could be held to an acceptably low levels by going in for echo cancellation in the analog domain.

Several active wire pairs are grouped together to form the binder group of the cable. Since these wire pairs carry signals and are in close proximity for long distances coupling takes place and these wire pairs *crosstalk* into each other. A major impairment in any two-wire transmission system is the near end crosstalk (NEXT).

Electromechanical switches, dial pulses and voltage surges due to the heavy inductive circuits close to the transmission cables induce noises into these wire pairs in the cables termed as *impulse noise*. Studies conducted have shown that the impulse noise varies substantially in the frequency of occurrence, intensity, and characteristics from location to location, and from time to time at the same location. Because of the variability of the characteristics of impulse noise, it is essentially the mean-square loss inherent in a line code that affects its impulse noise performance, and not explicitly its transmission bandwidth or its baud. the line code spectrum affects its loss, with those codes concentrated at lower frequencies having lower loss. However in analysis of performance of line codes for high speed data transmission systems are considered impulse is not a major impairment, the two major impairments being ISI and NEXT.

The other types of noise that are prevalent in transmission systems are the *thermal noise* which is the result of Brownian motion and is inherent in all the amplifiers. For practical reasons this noise is assumed to be Gaussian having a flat spectral density over the entire band of interest. *Quantizing noise* is also another impairment caused by the different types of converters used specially the Analog to Digital converters (A/D).

The early telephone systems used hybrid transformers and fixed passive analog equalizers. The requirements for higher data rates required higher bandwidth services and therefore more complex equalizers and hybrids balance circuits were required. Advancements in technology led to adaptive equalization and echo cancellation techniques to be used to two wire transmission systems.

References

[1] J.G. Proakis, Digital Communications, MacGraw Hill, New York.

[2] B.E.Keiser, Broadband Coding, Modulation and Transmission Engineering", Prentice Hall, New York.

[3] W.Y.Chen, J.L.Dixon and J.L.Waring, "High-Bit Rate Digital Subscriber Line Echo Cancellation", IEEE JSAC, Vol. 9, No. 6, August 1991, pp. 848-860.

[4] S.V.Ahamed, P.P.Bohn and N.L.Gottfried, "A Tutorial on Two Wire Digital Transmission in the Loop Plant", IEEE Transactions on Communications, Vol. COM 11, Nov. 1981, pp. 1554-1564.

[5] J.J.Werner, "The HDSL Environment", IEEE JSAC, Vol. 9, No. 6, August 1991.

[6] W.Stallings, "Data and Computer Communications Systems", MacMillan, New York.

[7] J.Sutherland and L.Litteral, "Residential Video Services", IEEE Comm. Mag. July 1992.

Chapter 2

Transmission Technologies

About twenty years ago the maximum achievable speed on the copper wires were considered to be about 1.2 kbps. With the bandwidth of the voice grade telephone line at 3.3 kbps today voice grade modems are able to achieve faster speeds of about 28.8 kbps with advances in algorithms, digital signal processing and VLSI. Even higher speeds can be attained in the future over the voice grade telephone line with the voice grade modems with improvement in the algorithms, line codes and digital signal processors.

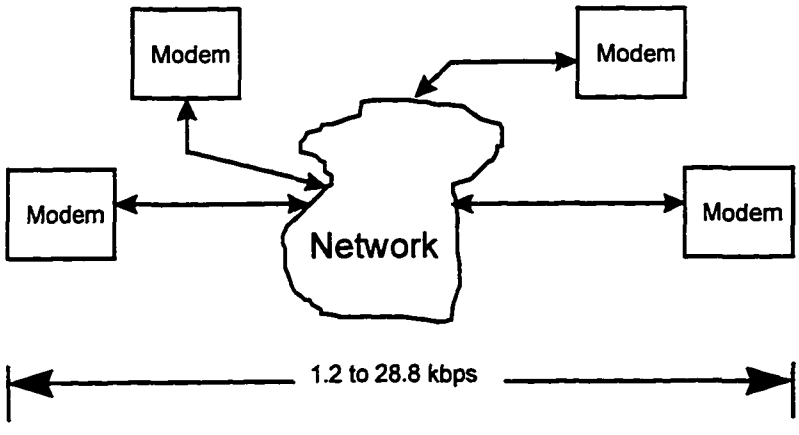

Figure 2.1: Voice Grade Modem Connection Over Existing Copper Lines

The voice grade modems operate at the subscriber end of voice grade lines and transmit signals through the core switching network without alteration and the network which connects the two ends or points of communication treating them exactly like voice signals.

Attenuation of the signal increases with the increase in the line length and therefore there is a limitation on the line lengths used which also plays a major role in the data rate over the twisted wire pair. The use of filters also limits the voice grade bandwidth to about 3.3 kbps without which higher speeds can be attained. The practical limits on the data rate in one direction for the given line length for the 24 gauge twisted wire pair are as follows:

Carrier	*Data Rate*	*Length*
DS1 (T1)	1.544 Mbps	18,000 feet
E1	2.048 Mbps	16,000 feet
DS2	6.312 Mbps	12,000 feet
E2	8.448 Mbps	9,000 feet
STS-1 (1/4)	12.960 Mbps	4,500 feet
STS-1 (1/2)	25.920 Mbps	3,000 feet
STS-1	51.840 Mbps	1,000 feet

Table 2.1: Data Rate Limits for 24 Gauge Wire Pair

These rates vary from country to country and in some countries 18,000 feet would cover almost every subscriber, whereas in certain places in North America especially

United States 18,000 feet would barely cover 80% or even less number of subscribers. For applications such as Video on demand and internet accesses 1.544 Mbps would be enough in the forward channel serving subscribers within distances of 18,000 feet. Data rates of 6 Mbps for distances of 4500 feet would be required for digital television, but for HDTV data rates of 20 Mbps would be required but this would be carried only for short distances on the twisted wire pair as indicated in the table.

2.1 T1 (DS0) and E1 Line

T1 a concept which evolved from Bell Labs in the sixties assumes the voice bandwidth to be about 4000 Hz and sampling this voice signal at Nyquist frequency which is twice the highest frequency component in the voice signal and at 8 bits per sample would need 64 Kbps of data stream to transmit the digitized voice signal. Twenty four channels were grouped together to form the T1 frame in which 8 bit of each channel was organized in the 24 slots of the frame with an additional framing bit used for synchronization thus resulting in DS1 frame of 193 bits long, and created an equivalent data rate of 1.544 Mbps for the structured DS1 signal and T1 being the raw data rate. E1 also uses the same number of bits to transmit voice (64 Kbps), but it multiplexes 30 voice channels each of 64 Kbps and two additional channels of 64 Kbps for synchronization purposes thus forming an equivalent data rate of 2.048 Mbps. T1 and E1 both use Alternate Mark Inversion (AMI) as the line code with a

repeater first placed after 3000 feet from the Central Office (CO) and 6000 feet thereafter.

2.2 Digital Subscriber Loop

The digital subscriber line was developed in the 1980's for ISDN basic rate access (2B + D) using different adaptive techniques available then for equalization and echo cancellation. Adaptive filtering techniques have been extremely of great use in loop application because of the different channel characteristics due to the different cable loops, loops which contain cables which are of different length, gauge and often containing bridge taps.

2.3 Digital Subscriber Loop Components

The fundamental components of a DSL are scrambler, encoders, filters, 2 to 4 wire line hybrid, adaptive digital echo canceler, A/D converter, adaptive digital equalizer, decoder, descrambler and timing recovery circuit.

2.3.1 Scrambler / Descrambler

The input serial bit stream when fed into the scrambler randomizes the data thus producing a pseudorandom sequence. The main purpose of the scrambler is to whiten the spectrum of the transmitted data which utilizes the bandwidth of the channel more

efficiently making carrier recovery and timing synchronization easy and also makes the adaptive equalization and echo cancellation possible.

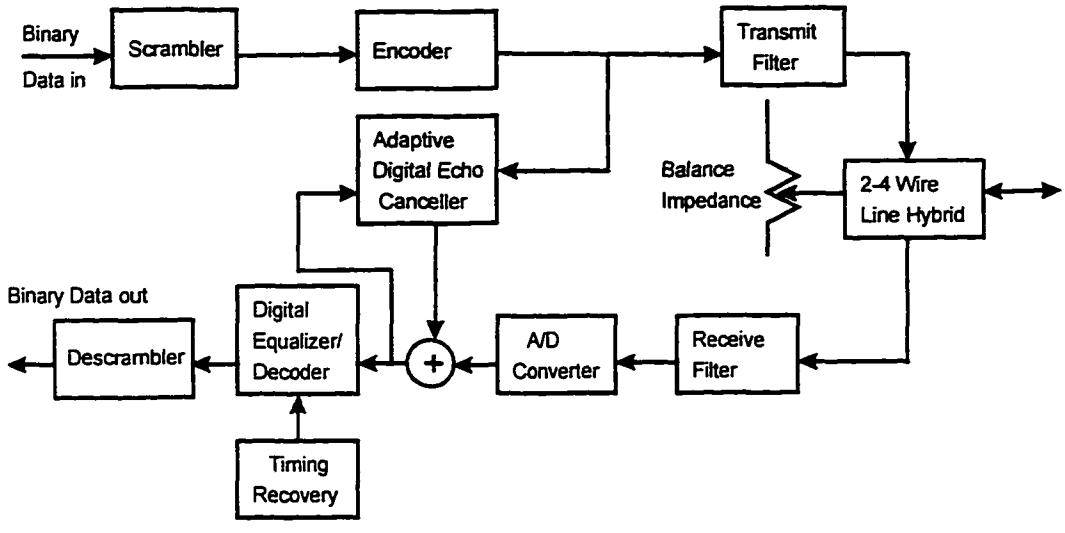

Figure 2.2: DSL Components

The pseudorandom sequence s(t) which is transmitted is produced by the modulo 2 addition of the data sequence d(t) and the feedback sequence g(t) produced by using the linear shift register.

$$s(t) = d(t) \oplus g(t)$$

Assuming that no transmission errors have occurred the data recovered at the receiving side is as follows.

$$d'(t) = s(t) \oplus g(t) = d(t) \oplus g(t) \oplus g(t) = d(t)$$

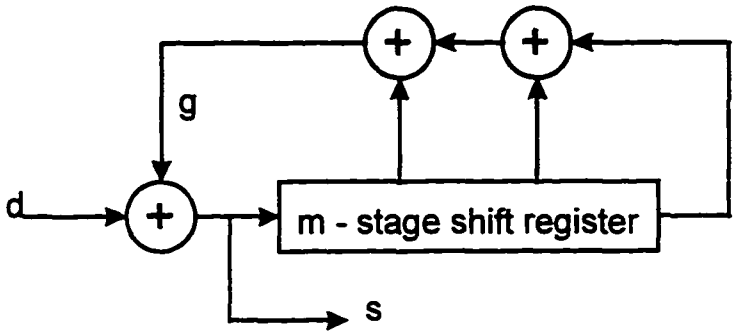

Figure 2.3: Scrambler

Thus the original data is recovered without any errors and the randomizing sequence is self synchronizing. If the channel is noisy it introduces errors and the received sequence is

$$r(t) = s(t) \oplus e(t)$$

The output of the descrambler is then

$$d'(t) = d(t) \oplus e(t) \oplus g(t)$$

The purpose of the scrambler is to insure transitions in the input bit stream. The shift register taps are chosen by a primitive polynomial over the algebraic field, GF(2), the data output of the scrambler will respond to the periodic input with an output whose period is the either the period of the input or the least common multiple of the input and $2^m - 1$.

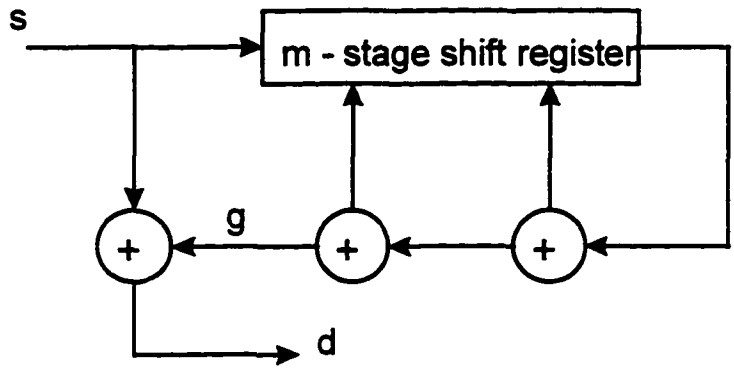

Figure 2.4: Descrambler

The transition density of the output stream satisfies the following bounds

$$1/2 * (2^m - 2) / (2^m - 1) \leq \delta \leq 2^{m-1} / (2^m - 1)$$

Thus the scrambler produces an output data stream with an average transition density of 0.5. At the receiving the descrambler needs time to synchronize with the transmitter. When there are no channel errors then the synchronization time is equal to the length of the shift register. When there are channel errors then the length of the shift register should be made short so that the re-synchronization time could be minimized.

2.3.2 Line Encoders

These are devices which map the output of the scrambler obtained to the line code that is being used in the transmission system. The selection of the line code for any Digital Communication System is critical to its performance which determines the

transmission characteristics of the signals, the line impairments, the complexity of the loop plant and the complexity of the system components used. The line codes could be broadly classified based on the number of levels and the number of dimensions the line codes use for the transmission of data. Some of the line codes used in the Digital Transmission Systems are as follows:

One Dimension Line Codes

In the case of the 1-D code each of the symbol is mapped to one of the 2^m different levels.

- *2B1Q (2 binary 1 quartenary)* In this code the binary digital data, two consecutive bits (binary bits) are taken which is grouped into a single four-level pulse (quartenary level) for transmission, due to which the baud rate is half its information rate. This is a saturated code.
- *3B2T (3 binary 2 ternary)* This code converts three binary bits (eight possible combination) to two three-level (ternary) signals (nine possible combinations). This code needs lower baud to transmit the same information using 2B1Q. In this code there is some redundancy thereby making the code an unsaturated code.
- *4B3T (4 binary 3 ternary)* This code uses three, three level signals (ternary) (27 possible combinations) to transmit 4 binary bits of information (16 possible combinations). This code has a greater redundancy than the 3B2Q code and also

needs lower baud to transmit the same number of information bits as compared to the 3B2Q code.

- *AMI (Alternate Mark Inversion)* It is a three-level (ternary) code which reverses the polarity of one, or mark, from that of the previous mark. In this case the line encoder is called as bit-to-bit encoder as compared to the block encoder in the above cases. Since this code uses a bit-by-bit encoding the baud rate is the same as the information rate.
- *MDB (Modified Duobinary)* It is a partial response code in which each information bit leads to a transmitted pulse in a time slot followed by an identical pulse of opposite polarity in a time slot one time interval removed. Use of this code leads to the overlapping of the transmitted symbols. In this case the line coder is a bit-by-bit encoder using a three-level signal (ternary) which results in the overlap of the transmitted symbols. It is a redundant code with no baud rate reduction.
- *Bi-phase* This code has a positive and a negative excursion within the same time interval offering no baud rate reduction. It is a binary code which is saturated code.

In addition to the above line codes there are many other one dimensional codes like NRZ, NRZI, Manchester codes etc., which are used in data communication systems for transmission of information.

Two Dimension Codes

In the case of two dimensional coders successive blocks of m bits are mapped into two separate symbol streams. Assuming that the payload is evenly distributed between the different symbols then each symbol represents m / 2 bits and has to take $2^{m/2}$ levels. This theory can be extended to multidimensional code as well, in which the number of symbol streams would be equal to the number of dimensions. If there are n dimensions then each symbol represents m / n bits and has to take $2^{m/n}$ different levels. Among the many multidimensional codes that have been proposed the most commonly used ones are the *Quadrature Amplitude Modulation (QAM)* in which the two sets of symbols a_n and b_n are mapped to a constellation point $a_n + jb_n$ in which a_n is the inphase component of the signal and b_n is the quadrature component of the signal. The complex point is then spectrally shifted, at the receiving end the signal has to be demodulated before the symbols are recovered. *Carrierless Amplitude Modulation (AM) / Phase Modulation (PM) (CAP)* on the other hand is a bandwidth efficient passband line code which is exactly the same as the QAM in terms of performance except that it does not require any modulation or demodulation at transmitter and receiver respectively, which makes CAP encoded systems easy to implement.

Error correction due to various channel impairments is incorporated in the encoder which resides between the scrambler and the line encoders. In all coding of error

correction such as block codes and the convolution codes for combating errors consist of a subset of valid codewords of all the possible combination of the n-bit code. Good codes are those codes whose subset of valid codewords is large enough which also means that the distances between the allowed members is large enough such that the channel impairments will not cause the message that was transmitted to be confused with another valid codeword. For the binary error-correcting codes the distances used are the *Hamming distances* whereas for the modulating type of error-correcting codes the distances used are called as the *Euclidean distances.* The Hamming distance between two valid codewords can be defined as the number of places (bits) the two codewords differ, whereas the Euclidean distance is the difference in energy between the two constellation points. Whenever error-correction is introduced in the transmission systems there is an addition (additional binary bits to be appended to the actual data) overhead which thereby reduces the actual number of information bits that are transmitted across the channel.

2.3.3 Filters

Two distinct approaches to filtering exist one for the baseband systems and one for the frequency translated systems. The transmit filter is used to limit out-of-band signal energy. This type of filtering is required where the out-of-band energy would interfere with other services sharing the same loop-plant cable bundle. The cutoff frequency of such a filter is chosen to be equal to or greater than the sampling

frequency, it thus causes little impairment to the data signal. The receive filters are used to limit the thermal and impulse noise input and out-of-band crosstalk from other systems. Again the cutoff frequency is placed to insure little degradation of the desired data signal. These two filters are of low orders and therefore are simply realized. For higher transmission rates the orders of the filter have to increased. If the cutoff frequency of either of these two filters is chosen to be below the sampling frequency then major degradation of the data signal results.

In the case of the modulated systems the baseband frequency is frequency translated both before and after transmission. These systems permit the transmission of signal over the existing or planned facilities with poor low frequency characteristics. They also allow for the packing, over one facility, of several independent signals using frequency division multiplexing (FDM). However in both these cases the translated signals are bandwidth limited. The multiplexed systems needs extra hardware for its implementation which thus makes it complex and expensive as compared to the baseband systems.

Three parameters that ultimately determine the bit rate are: sampling rate (baud rate) number of quantization levels (bits / baud) and modulation scheme. Increase in the b / s per Hz can be obtained by using special bandlimiting filters. Among these class of

filters are the *raised cosine filters* which enables efficient spectral shaping. The design of the impulse response of such a filter is based on two main observations.

- The discrete levels representing the bits need not be defined for the entire pulse duration, which means that these levels need be defined only at the center of the pulse.
- Defining the discrete levels at a specified time instant, the duration of the pulse need not be restricted to one symbol period.

Pulses conforming to the above design rules are termed as the Nyquist pulses. The Fourier transform of the Nyquist pulse shows that it does not have any side lobes at higher frequencies and has a bandwidth much less than the other pulses such as the NRZ pulse. The analytical expression for the *Nyquist pulse* is given by

$$g(t) = \frac{\sin(\pi\ t/T)}{\pi\ t/T}.$$

In the transition region from $(1-\alpha)f_N$ to $(1+\alpha)f_N$ the curve is half a cosine cycle offset or it is raised by 0.5, f_N is the Nyquist frequency, f_S is the sampling frequency and α is the excess bandwidth or the roll-off factor. The roll-off can range from 0 (Nyquist cutoff frequency f_S) to 1. One important characteristic of this class of filters is that its impulse response produces zero ISI, which is obvious from the second rule of the Nyquist pulse, that is ISI can be avoided between the neighboring pulses by having the pulse's amplitude go zero at regular spaced time instants. This can be generalized by saying that smaller the excess bandwidth longer the impulse response of the shaping filter. Another filter which belongs to this class is *square-root raised cosine*

filter. Expressions for the pulses generated by the above two filters belonging to this class of filters are as follows:

Raised-Cosine Nyquist pulse

$$g(t) = \frac{\sin(\pi t / T)}{\pi t / T} \frac{\cos(\alpha \pi t / T)}{1 - (2\alpha \pi t / T)^2}$$

$$G(f) = \begin{cases} T & 0 \le | f | \le \frac{1}{2T}(1 - \alpha) \\ \frac{T}{2} - \frac{T}{2} \sin \frac{\pi T}{\alpha} (f - \frac{1}{2T}) & \frac{1}{2T}(1 - \alpha) \le | f | \le \frac{1}{2T}(1 + \alpha) \end{cases}$$

Square-Root Raised-Cosine Pulse

$$g(t) = \frac{\sin [\pi (1 - \alpha) t'] + 4\alpha t' \cos [\pi (1 + \alpha) t']}{\pi t' [1 - (4\alpha t')^2]} \qquad t' = t / T$$

$$G(f) = \begin{cases} T & 0 \le | f | \le \frac{1}{2T}(1 - \alpha) \\ \frac{T}{\sqrt{2}} \sqrt{1 - \sin \frac{\pi T}{\alpha} (f - \frac{1}{2T})} & \frac{1}{2T}(1 - \alpha) \le | f | \le \frac{1}{2T}(1 + \alpha) \end{cases}$$

For 1 - D line code expression for the bandwidth can be derived

$$W - 1/(2T) = \alpha * 1 / (2T)$$

$$\alpha = \frac{W - 1/(2T)}{1/(2T)}$$

Solving for W we get

$$W = (1 + \alpha) * 1/(2T)$$

For 2-D code we arrive at slight different results

$$W - 1/T = \alpha * 1 / T$$

$$\alpha = \frac{W - 1/T}{1/T}$$

Solving for W we get

$$W = (1 + \alpha) * 1/T$$

In a Double Sideband Amplitude Modulated Suppressed Carrier (DSBAM-SC) the transmit low-pass filter used is a band-limiting Nyquist filter. The bandpass filter at the transmitter is required to reject the sideband. At the receiver also a bandpass filter is used for noise rejection and which acts as a matched filter which selects the signal. When an ideal channel is assumed then the matched filter for the transmitted signal is a complex conjugate of the Nyquist filter. Most low-pass filters (LPF) have a non-overlapping passband and stop band. In the Nyquist filters the transition region is always specified. In addition, the group delay characteristic for Nyquist filters must be constant up to their cutoff frequency $(1 + \alpha)f_N$. The receive Nyquist filter must be designed to have flat delay and its squared amplitude impulse response must provide low ISI. The transmit Nyquist filter must also provide a function to convert the coders square pulse outputs into impulses for driving the Nyquist filters. Depending upon the system application, the transmit Nyquist filter will likely have additional stringent

conditions in order to reduce the interchannel interference. Passband realization of Nyquist filters are even more difficult since they have the additional requirement of conjugate symmetry about the carrier frequency. This can be avoided by the use of Nyquist filters at the baseband and then spectrally shifting the filtered signal. Nyquist filters can be realized with digital or analog circuitry. In an all digital realization, the receive filter is more complex due a needed analog band-limiting filter, a higher than baud-rate sampling frequency to mitigate aliasing and a high resolution A/D to reduce the quantization noise. The transmit filter is less complex as compared to the receive filter since the filter input is PAM signal easily generated from an n-bit conversion of the digital data stream.

2.3.4 Line Hybrids

In a two wire transmission the communication is carried out in both directions. The center of this connection is a four wire separation of the transmission at either end. There is a potential feedback of the transmitted signal at the receiver leading to the impairment in the received signal due to the imperfect matching of the loop components, in the worst case leading to oscillations called as singing. The hybrid is a device which provides a high loss, thus reducing this impairment. In order that this path not have an appreciable attenuation, it is necessary for the hybrid not to have appreciable attenuation in its two wire or four wire port. There are two distinct echoes which the hybrid has to handle one is the talker echo in which case the talker hears a

delayed version of his own speech and the other is the listener echo whereby the listener hears a delayed version of the talker's speech. A reasonable attenuation for short delays is 6 dB and for large delays the signal has to be highly attenuated.

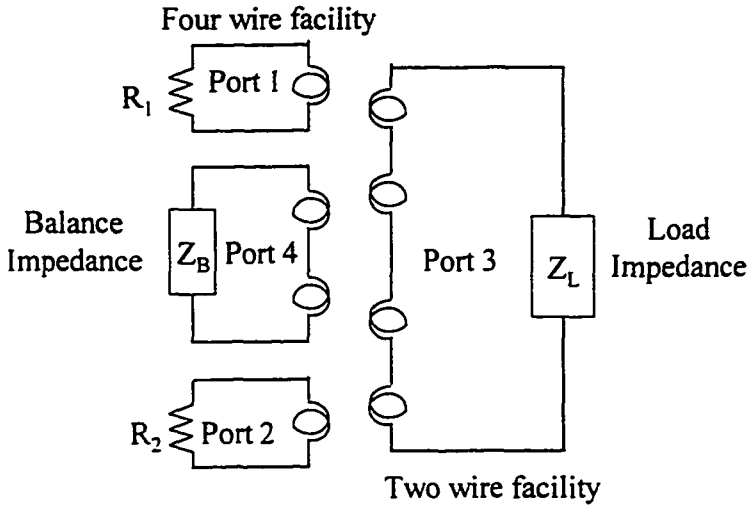

Figure 2.5: Two Transformer Hybrid

Two different implementations of the hybrid is the transformer method as shown in the figure 2.5 and this is the older method, and the new electronic hybrid method is as shown in the figure 2.6 . Consider the figure 2.5 in which let the balance impedance Z_B be equal to the load impedance Z_L, and that the four wire resistor's R_1 and R_2 are also equal. In such the turns ratio of the transformer of port 1 and port 2 would be a conjugate of each other and similarly the turns ratio of the transformer of port 3 and port 4 are conjugate of each other, this means that if the source is

delivering power to port 1 and hence port 3 a very small amount of power will flow into the port 3 and hence port 4.

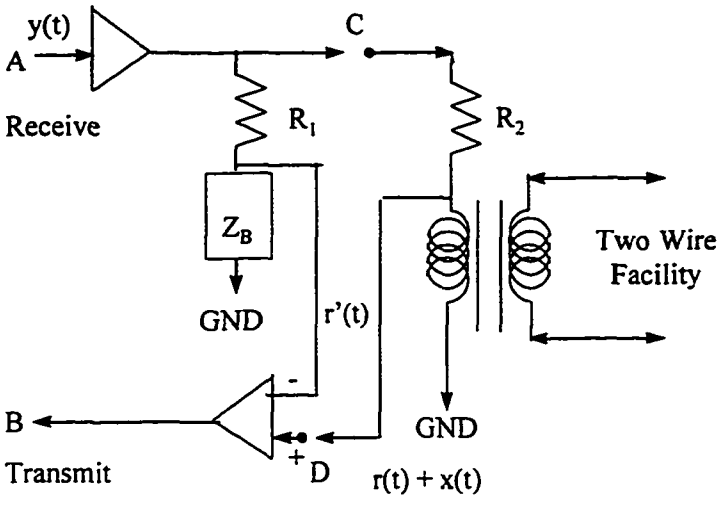

Figure 2.6: Electronic Hybrid

The hybrid provides an infinite loss between the receive four wire port which is port 1 and the transmit four wire port 2. The two talker speech paths are from port 1 to port 3 and from port 3 to port 2. The so called load impedance Z_L in this case also contains the image impedance of the loop, and hence Z_L varies from one loop to another. The balancing impedance Z_B is so chosen that it matches perfectly the impedance Z_L for any given loop. In the electronic hybrid shown in the figure 2.6 , the transformer does not serve as an integral part of the hybrid but is used as isolation transformer to isolate the balanced and the unbalanced side. The four wire receive port uses an amplifier in order to make up for the loss which the hybrid and transformer would

introduce. Here the operational amplifier on the transmit side as shown in the figure is operated in differential mode, wherein the positive terminal of the op-amp is connected to the voltage divider circuit formed by the resistor R_2 and the combined impedance formed by the load impedance and the loop image impedance Z_L. The negative terminal of the op-amp is connected to another voltage divider circuit formed of the resistor R_1 and the balancing impedance Z_B. The signal to the positive terminal of the op-amp is the combined signal which consists of the near-end talker x(t) and the feedthrough r(t) in the voltage divider. The undesired effect of the feedthrough is canceled by the voltage divider circuit consisting of the resistor R_1 and the balancing impedance network Z_B (fixed or variable) connected to the negative terminal of the op-amp which generates the replica r'(t) and the difference amplifier subtracts the replica across the signal from the transformer. The main purpose of this electronic hybrid is to cancel the feedthrough in the voltage divider by choosing a suitable value of Z_B such that the transfer functions of the two voltage dividers are matched. The transfer function of the voltage divider is $H_{bal}(j\omega) = \frac{R_1}{R_1 + Z_B}$ and the transfer function of the voltage divider with the loop impedance is given by $H_{loop}(j\omega) = \frac{R_2}{R_2 + Z_L}$. For a perfect match to occur $H_{bal}(j\omega) = H_{loop}(j\omega)$. When $R_1 = R_2$ then a perfect match could be achieved when Z_B is made equal to Z_L.

2.3.5 Echo Cancelers

A basic block diagram for the echo canceler is as shown in the figure 2.7 for full duplex digital transmission on two wire lines. An identical unit is used at the opposite end of the line. The reflections along the transmission line and the analog hybrid circuit which causes imperfect impedance matching will leak through to the receiver. This leakage which is caused is denoted as the echo path. The typical attenuation of the echo path is 10-20 dB for conventional analog hybrids. Thus an extra compensation circuit is required in order to reduce the echoes to an acceptable level for the attenuation to a reasonable level which is required in a practical system application.

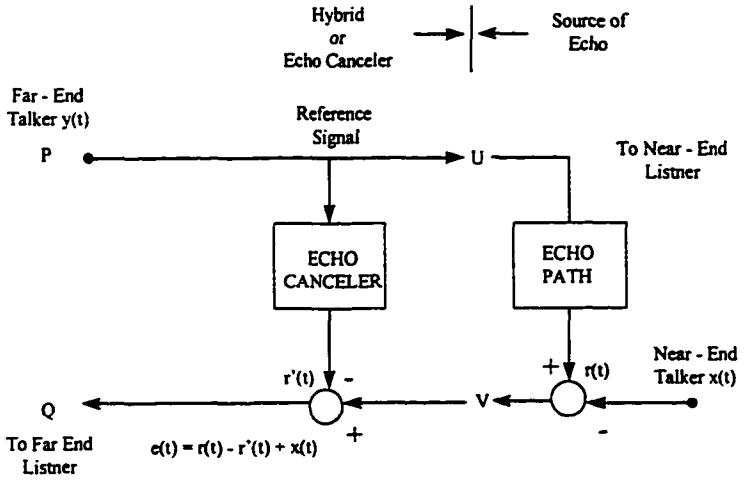

Figure 2.7: Principle of Echo Cancellation

Echo cancellation is done by the use of analog circuitry and digital circuitry in which case the transversal filters are used. With increasing round trip delay the subjective effect of echo becomes more annoying. Echo canceler controls the echo effectively eliminating the echo which acts as an impairment even on long delay channels. The portion of the four-wire connection near the two wire interface is as shown in the figure 2.7, with one direction of transmission between the ports P and Q and the other direction between the ports U and V. The far end talker is shown by y(t) and the near-end talker is represented by x(t), the undesired effect on the signal which is echo is represented by r(t). At the port V the near-end talker is superimposed by the undesired echo. The far-end talker y(t) at the port P also called as the reference signal is used by the canceler to generate the replica of the echo alone r'(t). This replica is then subtracted from the echo pulse near end talker to get e(t) which should ideally contain the near end talker but this would happen only when the replica generated is identical to the echo in the received signal.

2.3.6 Equalizers

In considerably long transmission lines the transmitted ideal square digital pulse will be distorted, attenuated and dispersed over several neighboring signaling intervals which is called as the Inter-symbol Interference (ISI). In baseband systems the signal dispersion is entirely caused by the channel amplitude distortion and group delay distortion and the derivative with respect to frequency of the channel phase

characteristics has little effect.The equalizer used in the baseband systems is designed in such a way that its transfer function is set approximately to the inverse channel characteristics 1/C(ω). The equalizer as such is designed as a simple fixed gain circuit with gain G to correct for the low frequency loss of the channel (flat loss). and a fixed zero network with zero z to correct for high frequency shape of the channel that is $E(\omega) = (1 + j\omega z)$. Digital or analog circuitry can be used to realize the desired equalizer function. A digital realization would require an anti-aliasing filter and an analog-to-digital (A/D) converter as the front end of the equalizer. In the case when the channel is time varying an adaptive equalizer is necessary to adapt to the channel variations. The adaptive equalizer must be able to detect the changing characteristics of the channel and the distorted signals it receives based on which it estimates computes and performs the necessary corrections required to reduce the channel impairments at a rate equal to the variations of the channel.

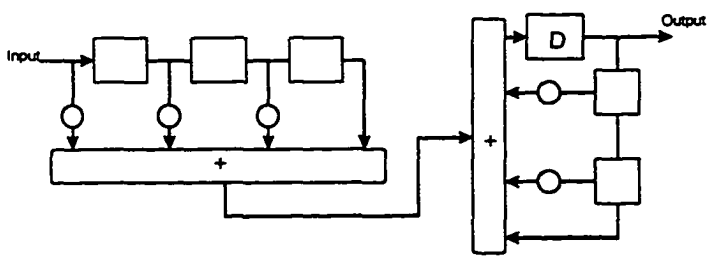

Figure 2.8: Decision Feedback Equalizer

Conventional approaches to the channel equalization exploit the fact that the channel though it is time varying it is linear so that its effect on the transmitted signal can be

modeled as a convolution operator. The equalizer is at least approximately the inverse deconvolution operator. It is considered enough to equalize the channel impulse response in view of the linearity of the distortion mechanism. Equalizers used in the high speed transmission networks are adaptive equalizers base on the two-stage equalizer architecture in which precursors, signal samples preceding the main pulse are dealt with by means of feed-forward transversal processor (tapped delay line) while precursor are removed by means of a feedback processor as shown in the figure 2.8. based on the Least MeanSquared (LMS) or the Stochastic Gradient Algorithm. The presence of a decision feedback shown as D in the figure regenerates the multi-level digital signal and feeds back.

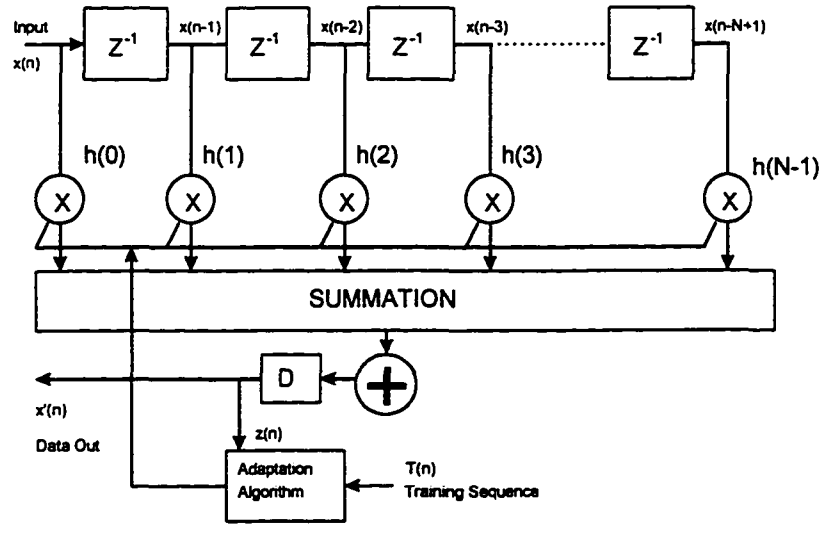

Figure 2.9: Tapped Delay-Line Adaptive Equalizer

This renders a non-linear operation which can be shown that this is beneficial in removing some of the unwanted noise accompanying the wanted signal and ensuring the stability of the feedback loop. The Feed-forward and the Feedback filters used in the decision feedback equalization are adaptive filters The unequalized baseband signal is applied on the left, propagates through the delay line towards the right and symbol-delayed which are held in the taps are multiplied by the tap coefficients h_0, h_1, .. h_{N-1} which are updated at regular intervals due to the varying characteristics of the transmission lines. The products are summed up before being sent to the decision device D which is a slicer and finally sent out as the equalized data. During the training period the training sequence is sent and the adaptive filter computes the tap coefficients by using the LMS algorithm and continues to do until a equalized response is obtained during which time the tap coefficients can be said to have converged to the desired value.

$$h_n(k+1) = h_n(k) - s(e_k * x(n-pn+kn))$$

where e_k is the error at time kT between the partially equalized output z(n) and either the training sequence T(kT), or the output data x(n); i:e., e_k = z(kn) - T(kT) during training or e_k = z(n) - x'(kT) during tracking. In the above equations during training the resulting error is multiplied by the delayed received signal r(n-pn+kn) to determine the magnitude and polarity of the adjustment to the corresponding tap, s is a fixed constant which scales the step size of each adjustment in order to ensure

smooth convergence. Once the training mode is over the equalizer switches over to the tracking mode and derives its reference from the reconstructed data x'(n), by making decisions on the equalized signal z(n).

2.3.7 Analog to Digital (A/D) Converters

Analog to Digital (A/D) converters are used to convert the analog signal to digital data. The A/D converters are integrated along with the sample and hold component thus forming the sampling converter. This integration of the two devices thus simplifies some of the timing issues and also amounts for some of the optimization for the best performance.

Some of the architectures used for the implementation of A/D's are as follows:

Successive Approximation Converter In this architecture which is the most accepted architecture by the industry today has the combination of very high resolution along with the speed which can be obtained in a VLSI implementation at a low cost. The building blocks of the A/D converter consists of a comparator, Digital to Analog (D/A) converter and control logic which uses a Successive Approximation Register (SAR) are a shown in the figure 2.10. The analog input drives one of the input of the comparator while the other input is driven by the output of the Digital to Analog (DAC) converter. The conversion technique consists of comparing the unknown input against a precise voltage or current generated by the DAC. Once the SAR and the

converter is initialized, the conversion command is applied when the DAC along with the SAR and control logic tries to produce an output using the Successive Algorithm and the resolution of the A/D depends on the output of the DAC. Once the conversion is complete, that is when held analog input is equal to the set digital output of the DAC the conversion complete bit is set.

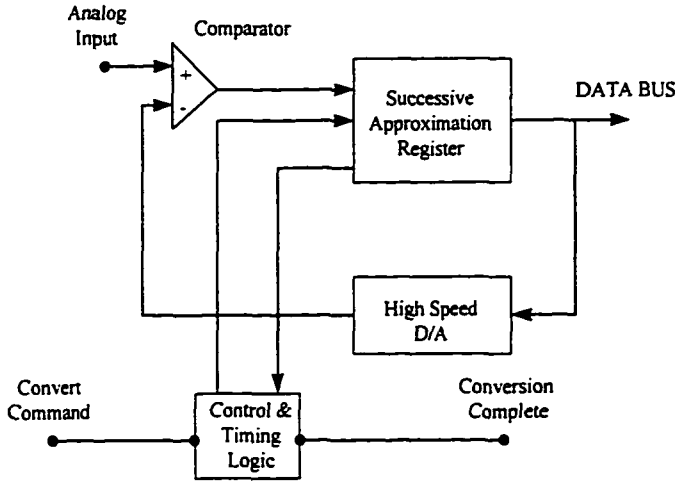

Figure 2.10: Successive Approximation Converter (SAC)

Flash A/D Converter High speed comparators called as flash converters are often used as building blocks as shown in the figure 2.11. The analog input signal to be digitized is applied simultaneously to 2^N - 1 latched comparators, where N is the number of bits. The reference input voltage is derived for each comparator from the resistive voltage divider. The reference voltage for each comparator is one LSB

higher than the comparator immediately below it. When an analog voltage is applied to the input of the comparator bank, all comparators which have a reference voltage below the input voltage will assume an output of '1' and those of the comparators which have a reference voltage above the input voltage will assume an output voltage of '0'.

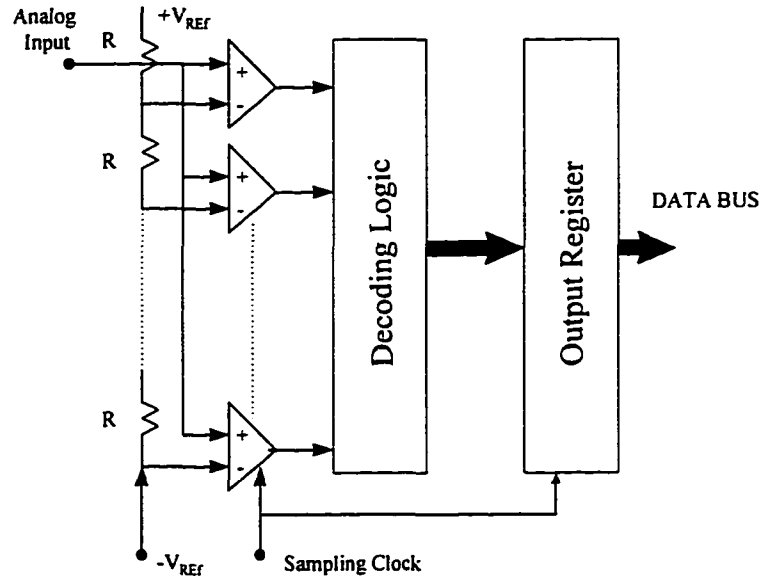

Figure 2.11: Flash Converter

The outputs of these comparators is then fed to the decoding logic circuitry which decodes into a digital output word which is latched using the output register block as shown in the figure 2.11.

2.3.8 Decoders

These are devices which does the reverse of the line encoders, that is it maps the received symbols after the error correction is performed to the binary bit stream depending upon the type of line codes used, that is one, two or *n* dimensional line codes. If error correction codes were used at the transmitting side then decoding has to done by the respective decoder based on the error correcting codes such as the block codes (Hamming code, Reed-Solomon code) or the convolution codes in which case the Viterbi decoder could be used for decoding. The error correction decoders as mentioned above should be placed before the line decoders.

2.3.9 Timing Recovery Circuit

The receiver extracts its clock from the signal it receives. In timing recovery the functioning of the other devices such as the equalizers and echo cancellers are very important in addition to the other peripheral chips of the associated digital subscriber loop components. The equalizer precedes the timing recovery circuit and it takes of the signal amplitude and the distortion that the signal undergoes during the transmission of the signal over the channel. The echo canceler also which precedes the timing recovery circuit cancels out a large amount of the echo that the signal contains. Thus the signal when it reaches the timing recovery circuit is relatively clean with well defined transitions. In practice the timing recovery circuits, equalizers, echo cancellers and the phase locked loops all work in co-ordination. The

proper working of the equalizers and echo cancelers are important in the timing recovery and the timing recovery is important also in the accurate functioning of the equalizers and echo cancelers. In order to understand the extraction of the timing signal it is necessary to know the type of the signal, that is the type of encoding that is used to encode the signal at the transmitter side. Assuming the signal to be a PCM signal to be a randomly encoded NRZ signal it can be mathematically represented as

$$z(t) = \sum_{n=-\infty}^{\infty} a_n \, g(t - nT) + n(t)$$

where a_n is the two level data with equal probability, n(t) is the additive white gaussian noise, g(t) is the individual pulse waveform and T the symbol period. In the case of NRZ line code g(t) is a rectangular pulse with duration equal to the symbol period. In general the symbol can be considered to be pulse amplitude modulated (PAM). In the case of the line codes such as the NRZ or the AMI code the power spectrum seems to contain no energy at the frequency corresponding to the symbol rate. If Fourier series analysis was to be done for the NRZ code assuming that the data was alternating ones and zeros then the spectrum would contain frequency components at 1/2 the symbol period and odd harmonics at one and half times the symbol period. For purely random data the probability of a very long data sequence approaches zero which means that the designer cannot rely upon the period components for timing in the PCM signal. One of the primary design ideas in the designing of a timing recovery circuit is to create a signal component at the symbol period

During the time when DSL was proposed it was understood that it would support higher data rates over short ranges 56 kbps and later to 160 kbps. Different line codes were studied and multilevel line codes such as 2B1Q , AMI and 4B3T were used. A multilevel line code maps the inputs into one of M different pulse amplitudes that are transmitted over the loop.

2.4 High Speed Digital Subscriber Line (HDSL)

Recent advancements in adaptive filtering techniques using VLSI led to intense research in high bit rate digital subscriber lines (HDSL) which is capable of delivering 1.544Mbps over the CSA loops. HDSL is a simply a better way of transmitting T1 or E1 over the twisted wire pair and thus acts as not only an alternate means for T1 or E1 but it also is an improved method which not only uses less bandwith but also requires no repeaters unlike the T1. HDSL uses advanced modulation techniques and transmits data at the rate of 1.544 Mbps or 2.048 Mbps in bandwidths ranging from 80 kHz to 240 kHz. HDSL operates in the dual duplex mode in the Carrier Serving Area (CSA) over distances of 12,000 feet using 24 gauge wire. With the advent of high speed digital subscriber lines (HDSL) in recent years a number of new high speed transport concepts have been proposed in the communications industry. Among these newly proposed transport concepts are asymmetrical digital subscriber lines (ADSL) .

2.5 Single Line Digital Subscriber Line (SDSL)

Single Line Digital Subscriber Line (SDSL) and Very High-speed Digital Subscriber Line (VHDSL). The need for these high bit rate services is due to the increasing demand by the subscriber for residential video services.

SDSL is simply a single line version of HDSL, transmitting T1 or E1 signals over a single twisted wire pair operating over POTS so that it can support both POTS and T1/E1 over the same line. SDSL will service the needs of the customers who are in need of symmetric access (such as servers and power remote LAN users). It also complements ADSL, however it has a limitatation of only about 10,000 feet over which ADSL operates with data rates of about 6 Mbps in the forward channel.

2.6 Asymmetric Digital Subscriber Line (ADSL)

The ADSL is designed to operate on the last leg of the customer premises outside the CSA where the HDSL and the SDSL fails to carry data at higher rates. The ADSL as the name indicates carries high speed data in the forward channel and very low speed data in the reverse channel. The twisted wire pairs are grouped in a cable. The reason for twisting the wires was to reduce the interference of signals from one cable to another. When many symmetric signals are sent within the same binder group of the cable there is a limitation on the length of the cable and on the data rate. Services such as Video on Demand, Home Shopping, Internet Access, remote LAN access,

Multimedia Access and specialized PC services all feature high data rate demands on the forward channel and relatively low data rates on the reverse channel which will be mainly used for control purposes. For the above mentioned services 1.5 Mbps to 9.0 Mbps would be enough in the forward channel and 16 Kbps to 640 Kbps in the reverse channel. The forward channel speeds for the ADSL depends on the distances and is as shown in the table below.

Distance in feet	*Data rate in Mbps*
18,000	1.544
16,000	2.048
12,000	6.312
9,000	8.448

Table 2.2: Distance Versus Data Rates

ADSL transmits digitally compressed video signals which includes error correction using block and convolution error correcting codes which is intended to reduce the effect of impulse noise on video signals. The use of error correcting codes introduces an overhead in terms of delay of about 20 ms which is a bit too much for certain type of applications. ADSL will be used in circuit switched, packet switched networks and eventually with ATM based networks.

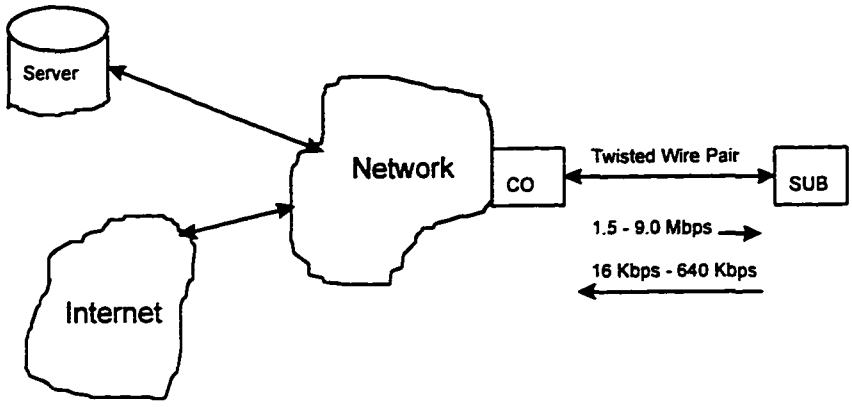

Figure 2.12: ADSL Network

2.7 Very High-speed Digital Subscriber Line (VHDSL)

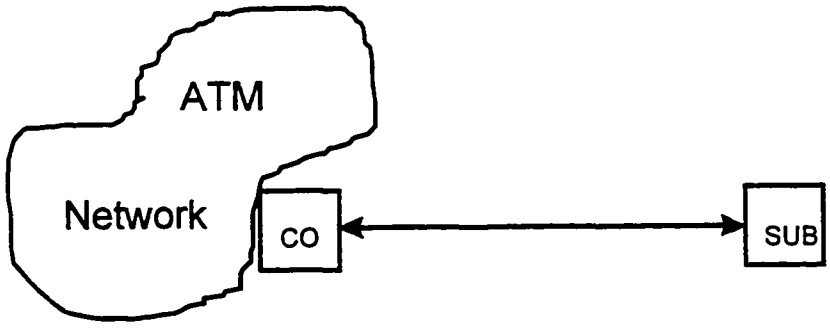

Figure 2.13: VHDSL Network

For higher data rates VHDSL or VDSL would be used. The VDSL would also use copper wire pair to carry high quality video signals for shorter lengths. It would be connected to the ATM network either directly or through a multiplexor.

The data rates supported along with the distances are as shown below

Data Rate in Mbps	*Length in feet*
12.96	4,500
25.82	3,000
51.84	1,000

Table 2.3: Distance Versus Higher Data Rates

In many ways VHDSL is easier to implement than the ADSL since it imposes far fewer transmission constraints so the basic transceiver technology is much less complex even though it operates at much higher speeds as compared to the ADSL.

References

[1] K.W. Cattermole, "Principals of Digital Line Coding," Int. J. Electron., Vol. 55, no. 1, pp.3-33, 1983.

[2] S.V. Ahamed , P.P. Bohn, and N.L. Gottfried, "A Tutorial on Two Wire Data Transmission in the Loop Plant," IEEE Trans. on Commun., Vol. COM-29, no. 11, pp. 1,554-1,564, Nov. 1981.

[3] J.W. Lechleider, "DSLs for use with Correlated Line Codes," IEEE Trans. on Commun., Vol. COM-35, no. 10, pp. 1,029-1,036, Oct. 1987.

[4] British Telecommunications Research Laboratories, "Further Comparisons of Line Codes for the Network Side of NT1, "ECSA contribution T1D1.3

Chapter 3

New Transport Technologies

Advancement in VLSI technology and demand for increase information rate on the digital subscriber lines up to DS1 rates have given rise to two such digital transport systems both of which use the copper wires as the physical media.

1. High-Bit-Rate Digital Subscriber line (HDSL)
2. Asymmetrical Digital Subscriber Line (ADSL)

3.1 High-Bit-Rate Digital Subscriber Line

The HDSL is considered to be alternative to the existing T1 lines to support repeaterless DS1 rate over the copper loops that conform to the CSA design rules within the CSA environment. The HDSL architecture consists of dual full duplex two-wired metallic cable pairs which are non-loaded each of the wire pairs capable of transmitting 784 kb/s in either direction thereby making HDSL provide a full duplex transmission rate of T1 which is 1.544 Mb/s. Each of the wire pairs are treated as a separate identity which means that each of them have a separate monitoring, framing and timing overhead functions. The main advantages of HDSL over the T1 lines are

a. The HDSL lines need not be conditioned.

b. Repeaters are not used within the CSA environment.

c. Single bridged taps are allowed.

d. The binder group separation is not required.

3.1.1 Access Configurations at the Customer Side

At the Customer or the Subscriber Side the entire bandwidth of DS1 is available to the customer. Some of the possible subscriber access circuit configurations are as follows:

- ***Repeaterless DS1 Access***

In this case the entire bandwidth of DS1 rate is dedicated and delivered to the subscriber.

- ***Repeaterless DS1, ISDN Primary Rate Access***

The HDSL has the capability to transport the Primary Rate ISDN service which provides digital access at DS1 rates. The Primary Rate Access uses up to the 1.539 Mb/s net payload capacity of the 1.544 Mb/s DS1 bandwidth. PR-ISDN consists of 23 B channels of 64 kb/s each and a D channel of 64 kb/s. The other variations of this could be that it contains certain channels of H0 of 384 kb/s or a H1 line of 1536 kb/s with a D channel being in the companion line.

- ***Switched-DS1/Switched Fractional DS1 (SWF-DS1):***

HDSL can also provide SWF-DS1 service which is a dialable, public, circuit switched service which provides digital service from 128 kb/s to 1536 kb/s in steps of 64 kb/s.

For the SWF-DS1 clear channel capability is required and all the digital trunks having the capability of supporting the SWF-DS1 feature should be B8ZS line code compatible.

- ***Switched Multi-megabit Data Service (SMDS):***

HDSL should provide DS1 based access lines to support SMDS. SMDS is a connectionless, public, packet switched data transport service that extends Local Area Network (LAN) like performance and features beyond the subscriber's premises across a metropolitan area thereby making HDSL as an alternative which provides a Subscriber Network Interface (SNI) to a Metropolitan Area Network (MAN) or Metropolitan Switching System (MSS).

- ***Repeaterless DS1, Extension Access:***

HDSL can provide DS1 rate access between the fiber based remote electronics and the customer premises

3.1.2 HDSL Loop Plant Environment

When it comes to the successful deployment of the HDSL technology in the metallic loop plant, the transceivers must satisfy performance objectives for all the Carrier Serving Area (CSA) loops without binder separation, bridged-tap removal or other pair conditioning and achieve spectrum compatibility with the transmission

equipment. Loops that conform to the CSA guidelines are characterized in detail to which the HDSL technology will be applied.

HDSL equipment is expected to operate over loops that conform to CSA design guidelines. Some of the loop criteria for the operation of the HDSL are

1. All loops are non-loaded.
2. Maximum allowable length for the 26 gauge cable is 9000 ft. including bridged taps
3. The maximum allowable length for cables that are coarser than the 26 gauge cable is 12000 ft. including bridged taps.
4. The maximum allowable of a single bridged tap is 2000 ft. and the total length of all the brigded taps in the loop should not be greater than 2500 ft.
5. The total length of the heterogeneous cable makeup with the 26 gauge cable should not be greater than 12-[(3*L26)/(9-LBTAP)] kft where L26 = total length of the 26 gauge cable without bridged tap and LBTAP = total length of the all bridged tap.

Generally it is suggested not to use cables of heterogeneous nature consisting of cables of not more than two wire gauges. In addition to the loop wiring Central Office consists of wiring typically of 26 gauge or 26 gauge and may be up to 1 kft. The customer premises wiring consists of typically 26 gauge with some 24 wire gauge and may up to 1 kft. long. The HDSL must be capable of operating with all this wiring.

3.1.3 HDSL Spectrum Characteristics

HDSL systems will be installed along with the existing transmission systems in the exchange plant. The HDSL signal should not interfere with the other HDSL signals or other services such as POTS, ISDN and T1 lines which exist within the same binder group.

3.1.3.1 Crosstalk

Among the many impairments that exist crosstalk such as the Near-end crosstalk (NEXT) between pairs in the same cable is the main source of degradation of other HDSL signals in the cable. The NEXT coupling is directly proportional to the frequency which increases at a rate of 15 dB/decade for frequencies above 20 kHz within the band of the HDSL. The NEXT is also dependent on the loop length, cable makeup, waveform of the transmitted signals, spectral characteristics of the systems involved as well as the receiver characteristics. Since the loop length and the cable makeup cannot be changed for the given loop that already exists, the only way of controlling crosstalk is by the design of effective filters at the receiver side, transmitted signal waveforms and the spectrum of the transmitted line code. Self-NEXT, NEXT that is caused by the same cable transmitting the same line code, has been found to be the worst case form of NEXT. There are two main attributes that affect NEXT performance, the insertion loss of the loop and the frequency spectrum of the self-NEXT.

3.1.3.2 Conditions for the NEXT Model

1. The disturbing transmitters use the same binder group of the cable as the disturbed system.

2. The disturbing transmitters are co-located with the disturbed receiver.

3. The termination impedance's are matched to the characteristic impedance of the cable pairs at each frequency.

4. The loop configurations contain no bridged taps or gauge changes.

5. The loops are long enough that they effectively appear as infinite length from a crosstalk point of view.

3.1.4 The HDSL Architecture

In figure 3.1 a block diagram of the HDSL architecture is shown. The units shown at the Central Office side and the Subscriber side each contain two transceivers capable of sending and receiving information at the rate of 784 Kbps and a DS1 interface circuit which enables the units at either side to be connected to a DS1 line. The units receive the DS1 signal introduce the necessary overhead required and split the signal into 784 Kbps and transmit it. At the receiving side the split signals are combined and the overhead bits removed to get back the DS1 signal. The transceiver units at either side consist of impedance matching circuits for the hybrid and echo cancelers to remove the echoes caused due to the reflections of the transmitted signal from

discontinuities such as bridged taps, non-uniform wire gauges, and mismatch of the impedance of the hybrids used and equalizers to remove the inter symbol interference.

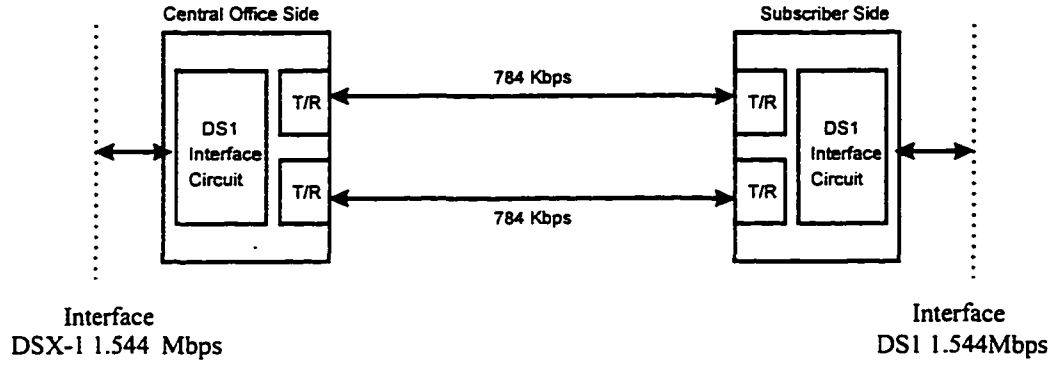

Figure 3.1: HDSL Architecture

3.1.4.1 HDSL Transmission

Two CSA loops which are uniform would be used to provide transmission at a data rate of 1.544 Mb/s. Each of the loops would consist of an echo canceler and a matching hybrid for the transhybrid attenuation to provide full duplex operation. The system design is based on the fact that it would operate on the non-loaded subscriber loops meeting the CSA design criteria.

3.1.4.2 Line Code

The line code that would be used for the HDSL transmission system will be 2B1Q (2 binary, 1 quaternary) a multilevel pulse amplitude modulated code (PAM) without redundancy. The 2B1Q mapping for the 4 level code is as follows.

First bit (sign)	Second bit (magnitude)	Quartenary Symbol (Quat)
1	0	+3
1	1	+1
0	1	-1
0	0	-3

Table 3.1: 2B1Q Bit to Voltage Mapping

3.2 Asymmetric Digital Subscriber Line (ADSL)

The overall network of the ADSL is as shown in the figure 3.2 below gives the technical guidelines for architectures, protocols and interfaces for telecommunications networks incorporating ADSL transceivers. The figure 3.2 below describes the overall network elements incorporated in multimedia communications suggesting the group

of transport configurations ADSL will encounter as network migrate from Synchronous Transport Mode (STM) to Asynchronous Transport Mode (ATM).

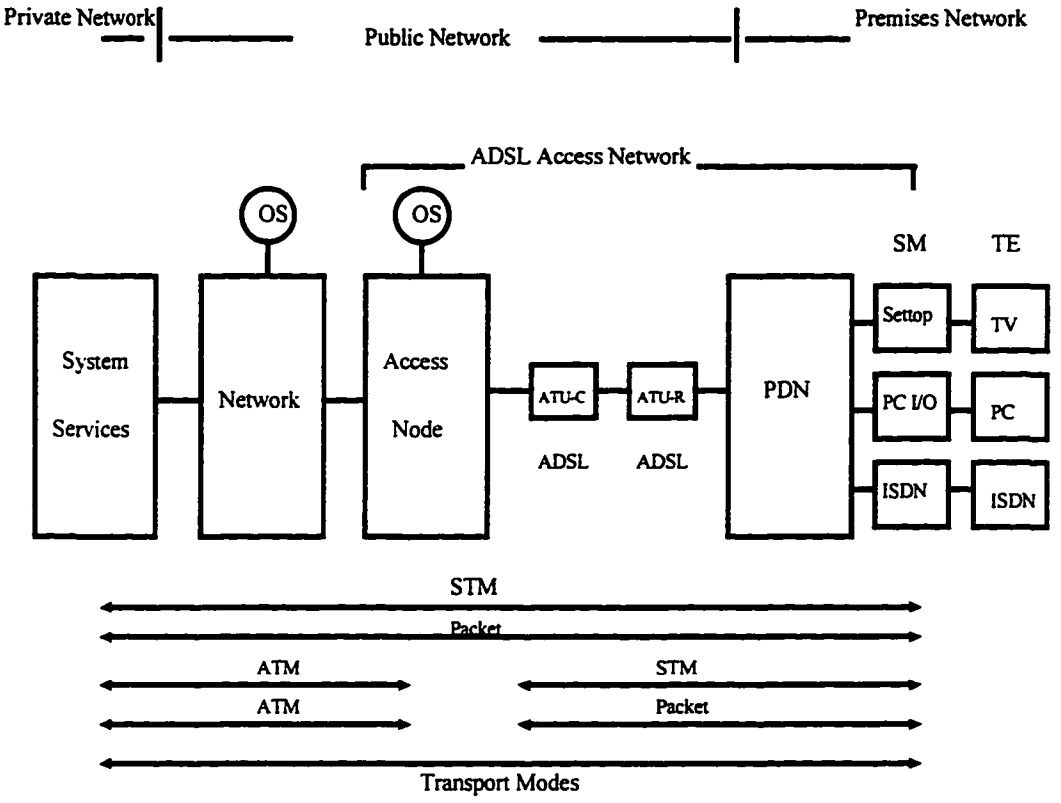

Figure 3.2: ADSL Network Architecture

In the figure 3.2 the system services are the on-line services, Internet access, local area network access, interactive video and video conferencing. The network consists of broadband network (data rates above 1.5/2.0 Mbps), narrowband network (data rates at or below 1.5/2.0 Mbps) and packet switched network. The network and the

access node have operations system (OS). The connecting link between the access node and the premises distribution network (PDN) is the asymmetric digital subscriber line (ADSL) which consists of the ATU-C the ADSL Transmission Unit at the Central Office side or at the network end and the ATU-R the ADSL Transmission Unit at the subscriber's side or at the customer premises end. The PDN connects the ATU-R to the service modules (SM) in point-to-point manner or in the multipoint manner. The connection maybe passive wiring or an active network. In the multipoint connection it could be a bus or a star. The various modules are settop, PC I/O and ISDN. The terminal equipment (TE) (TV, PC and ISDN terminal) is connected to the service modules (SM) .

3.2.1 ADSL Transceivers

The two different techniques that have been proposed for the implementation of the ADSL transceivers are as follows.

1. Discrete Multitone (DMT).
2. Carrierless Amplitude Modulation/ Phase Modulation (CAP)

3.2.1.1 Discrete Multitone (DMT) System

Multitone has been considered for ADSL since it has the following interesting properties, it uses many narrow bandwidth tones instead of a single tone, could be

used over channel with null in the transfer function, its main property is that it approximates Shannon's "water filling" solution., it is used with QAM over twisted wire pair channel.

In the case of the DMT systems the basic principle involved is to use frequency division multiplexing (FDM) techniques to divide the channel of the main transmission system into subchannels which are modulated and demodulated independently. A diagram involving the principle of transmission of data using DMT is as shown in figure 3.3.

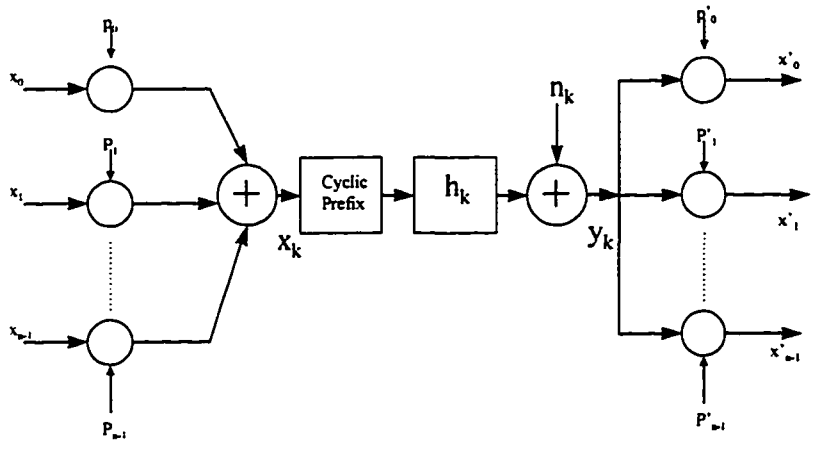

Figure 3.3: Discrete Multitone (DMT) Principle

A block of input bits is divided into N sub-symbols x_n, $0 \leq n \leq N-1$, such that N is a power of two. Each of the sub-symbols x_n are independently modulated by the N

dimensional sampled sinusoid modulating vectors P_n, and then summed to form an N-dimensional block of modulated transmit signal samples x_k, k=0, .. N-1. The nth modulating vector is given by

$$\mathbf{P}_n = [\, P_{n,0}\, P_{n,1} \ldots P_{n,N-1}]$$

where

$$P_{n,k} = \frac{1}{\sqrt{N}} e^{+j(2\pi/N)kn} \quad k,n = 0, \ldots, N-1$$

the inverse discrete Fourier Transform (IDFT) vector. DMT can be considered to consist of N/2, QAM channels. The modulation is carried out digitally without the explicit use of any carrier modulation frequencies or modulators. Assume an impulse response h_k to be of finite length and also n_k to be AWGN introduced by the channel, the symbol y_k received at the receiving end is $y_k = x_k + h_k + n_k$ where x_k is the transmitted symbol. At the receiving end when the symbol is received, the signal undergoes demodulation which is done by the inner product of the corresponding N channel outputs $y_0, \ldots, y_{N-1}$ with P_n^*. In practice however the modulation and demodulation is implemented by the use of FFT algorithms which perform FFT computation in an efficient manner.

3.2.1.1.1 DMT ADSL transmitter

The DMT ADSL transmitter is as shown in the figure 3.4 In this implementation where the transmission rate in the forward channel is T1 rates with very low speeds

in the reverse channel. The implementation discussed is only for the forward channel transmitter with data rates of 1.6 Mbps. For this the sampling rate is fixed at 640 kHz, v to be a maximum of 8 and N=512. For the single twisted wire pair to carry a data stream at rates R equal to 1.6 Mbps the input data is divided into M-bit blocks, where M=(N+v)R/S=1300. These bits are then transformed into (a maximum of) N/2 = 256 QAM subsymbols that are then applied to a trellis encoder. The trellis encoder sequentially processes the frequency-indexed symbols to avoid the large latency and memory requirement that would occur with multiple trellis encoders. This process requires that the subchannel indexes be shuffled to avoid any minor correlation between the noise on adjacent frequency subchannels. The input of the trellis encoder is then modulated, as described earlier, through the use of an N = 512 inverse FFT. An eight-sample cyclic prefix is placed at the beginning of the corresponding block of modulated transmit samples, and extended block of N+v samples is then applied to the channel through the digital-to-analog converter (DAC) and the line -interface unit. The sampling rate is 640 kHz, which leaves the 256 subchannels effectively separated by 1.25 kHz. This corresponds to a block symbol period of 512 + 8 = 520 samples or 812.5 μs. A simple equalizer is used to contain the inter-symbol interference.

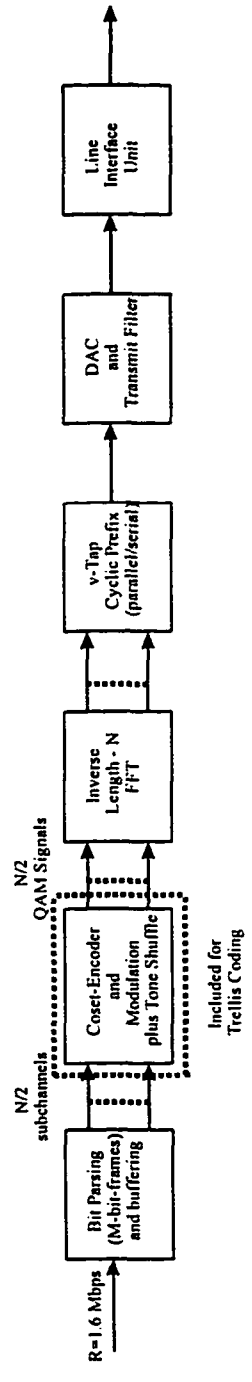

Figure 3.4: Discrete Multitone (DMT) Transmitter

3.2.1.1.2 DMT ADSL Receiver

A general block diagram of the DMT ADSL receiver is as shown in the figure 3.5. A simple equalizer is used at the input of the receiver which does not completely remove the inter-symbol interference (ISI), but rather confines the impulse response h(D) = a(D) / p(D) so that its length is approximately v +1 sample periods or less. By setting the equalizer to p(D), we will have a minimum mean square error approximation of an additive white noise channel with impulse response characterized by a(D), which has a response length of v+1 sample periods or less. The last N samples of the N + v samples that correspond to the transmit block are extracted from the equalizer output. An N-point FFT is performed on the equalizer output. The FFT outputs, Z_n, (n = 0,1, ... , N-1), are multiplied by N complex, 1-tap adaptive filters, W_n, (n = 0,1, ... , N-1) so that a common decision device can be used to estimate the sub-symbols on each of the sub-channels. The initial tap setting for W_n is:

$$W_n = A_n^{-1}, n = 0,1, \ldots, N\text{-}1$$

where

$$A_n = \sum_{k=0}^{N-1} a_k \, e^{-j(2\pi/N)kn}, n = 0,1, \ldots, N\text{-}1$$

the FFT of a(D). The resulting output data $v_n = w_n z_n$, n = 0,1, ... , N-1 can then be decoded, which in the case of an applied trellis code requires a Viterbi decoder as shown. The symbol decisions are used (in the coded case) only to derive an error signal, so that the adaptive updating mechanism can be used to allow for slight

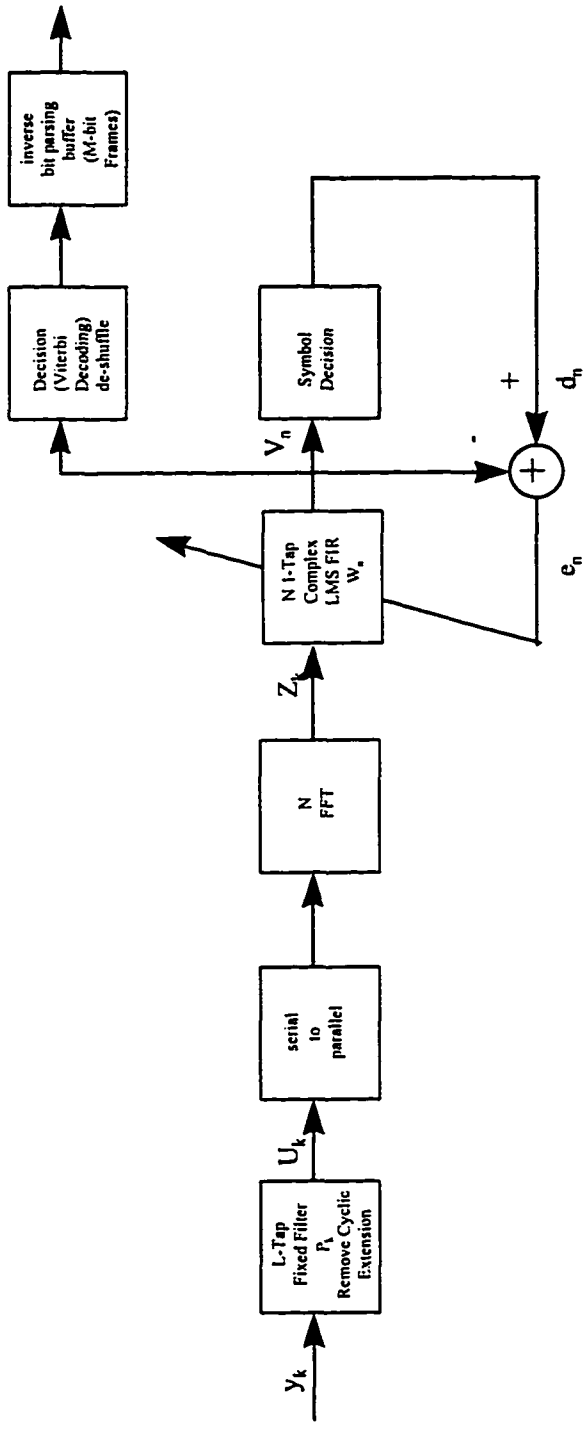

Figure 3.5: Discrete Multitone (DMT) Receiver

channel variation. The corresponding error is $e_n = d_n - v_n$, n = 0,1, ... , N-1. Standard LMS algorithm is used for the updating of $w_n = w_n + 2\mu_n e_n z_n^*$, n = 0,1, ... , N-1 where μ_n is the step size for each sub-channel, and can be adjusted independently to optimize the rate of convergence.

3.2.1.2 Carrierless Amplitude Modulation / Phase Modulation (CAP)

The Carrierless AM/PM (CAP) is a bandwidth-efficient two dimensional passband line code that was originally derived from the closely related quadrature amplitude modulation (QAM) line code [3] and has the following properties.

1) It does not need explicit modulation and demodulation functions.

2) There is no special relationship between carrier and bit rate.

3)The spectral characteristics of CAP is the same as QAM but less complicated to be implemented digitally.

4) From the performance point of view CAP is the same as QAM.

3.2.1.2.1 Derivation of CAP from QAM

In the case of a QAM communication system the QAM transmitter is as shown in the figure 3.6.

In figure 3.6, $\omega=2\pi f_0$ and $a_n, b_n = \pm 1, \pm 3 \ldots \pm (m-1)$.

$s(t) = \Sigma\, a_n\, g(t-nT) \cos 2\pi f_0 t - \Sigma\, b_n\, g(t-nT) \sin 2\pi f_0 t.$

The above equation can be rewritten as

$s(t) = \mathrm{Re}\ \{ \Sigma\ a_n\, g(t-nT)\, e^{j2\pi f_0 t} \}$

where $a_n = a_n + j\, b_n$.

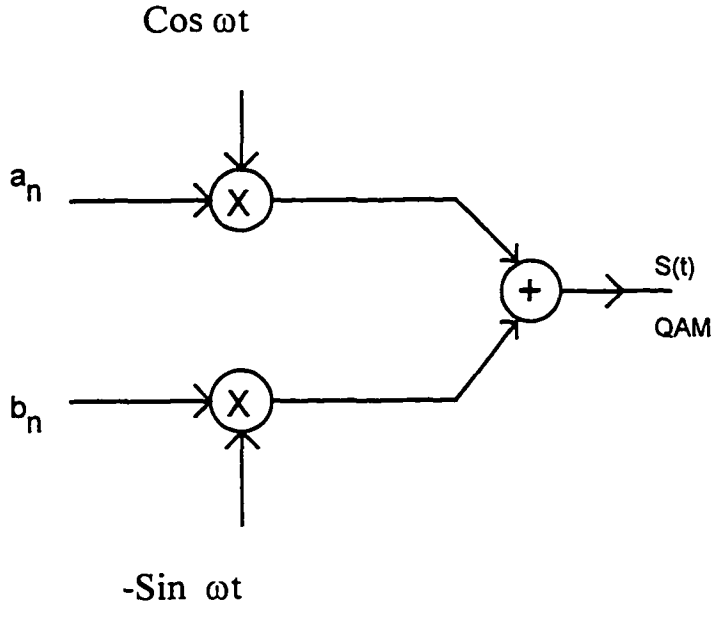

Figure 3.6: QAM Transmitter

The QAM receiver is as shown in figure 3.7.

$y_1(t) = r(t) \cos 2\pi f_0 t * h(t)$

$y_2(t) = - r(t) \sin 2\pi f_0 t * h(t)$

$$y_1(t) = \int_{-\infty}^{\infty} r(t-\tau)\,\mathrm{Cos}\,\omega(t-\tau) * h(\tau)\,d\tau$$

$$y_2(t) = -\int_{-\infty}^{\infty} r(t-\tau)\,\mathrm{Sin}\,\omega(t-\tau) * h(\tau)\,d\tau$$

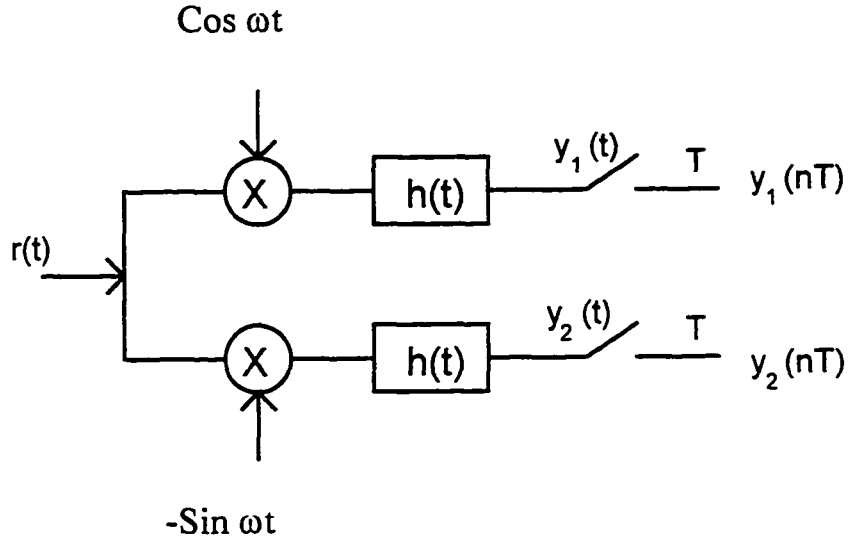

Figure 3.7: QAM Receiver

When the signal is sampled

$$y_1(nT) = \int_{-\infty}^{\infty} r(nT-\tau)\,Cos\,\omega(nT-\tau) * h(\tau)\,d\tau$$

$$y_2(nT) = -\int_{-\infty}^{\infty} r(nT-\tau)\,\mathrm{Sin}\,\omega(nT-\tau) * h(\tau)\,d\tau$$

The above two equations can be rewritten as

$$\tilde{Y}(nT) = \{ \int_{-\infty}^{\infty} r(nT-\tau)^* h(\tau)\, e^{-j\omega(nT-\tau)} d\tau \}$$

where $\tilde{Y}(nT) = y_1(nT) + jy_2(nT)$.

$$s(t) = Re \{ \Sigma a_n\, e^{j\omega nT} g(t-nT)\, e^{j\omega(t-nT)} \}$$

$$= Re \{ \Sigma \tilde{A}_n \tilde{P}(t-nT) \}$$

where $\tilde{A}_n = a_n\, e^{j\omega nT}$ and $\tilde{P}(t) = g(t)\, e^{j\omega t}$

The spectrum of $\tilde{P}(t)$ is one sided and $\tilde{A}_n$ represents a_n rotated by $e^{j\omega nT}$ radians.

$$\tilde{P}(t) = g(t)\, e^{j\omega t} = g(t)\,[\cos \omega t + j \sin \omega t]$$

$$= p_1(t) + j\, p_1^-(t)$$

where $p_1(t) = g(t) \cos \omega t$ and $p_1^-(t) = g(t) \sin \omega t$.

s(t) can now be rewritten as

$$s(t) = Re \{ \Sigma \tilde{A}_n\, (p_1(t-nT) + j\, p_1^-(t-nT)) \}$$

Now at the receiver side

$$Y(nT) = \{ e^{-j\omega nT} \int_{-\infty}^{\infty} r(nT-\tau)^* h(\tau)\, e^{j\omega\tau} d\tau \}$$

$$= \{ e^{-j\omega nT} \int_{-\infty}^{\infty} r(nT-\tau)^* \tilde{Q}(\tau) d\tau \}$$

where $\tilde{Q}(\tau) = h(\tau) e^{j\omega\tau}$ which is one sided spectrum.

Rewriting as

$$\tilde{Q}(\tau) = h(\tau)\,[\,\mathrm{Cos}\,\omega\tau + j\,\mathrm{Sin}\,\omega\tau\,]$$

$$\tilde{Q}(\tau) = q_1(t) + j\,q_1^{-}(t)$$

where

$$q_1(t) = h(t)\,\mathrm{Cos}\,\omega t$$

$$q_1^{-}(t) = h(t)\,\mathrm{Sin}\,\omega t$$

At the transmitter side $\tilde{A}_n = a_n\, e^{j\omega nT}$ where the symbol a_n is rotated by $e^{j\omega nT}$ at the receiving side the received symbol is rotated by $e^{-j\omega nT}$. So the rotation operations can be completely ignored.

Now s(t) takes the form

$$s(t) = \mathrm{Re}\,\{\,\Sigma\, a_n\,(p_1(t-nT) + j\,p_1^{-}(t-nT))\,\}$$

$$= \Sigma\, a_n\, p_1(t-nT) - \Sigma\, b_n\, p_1^{-}(t-nT))$$

This clearly indicates that in the CAP transmitter no modulation is required.

At the receiving side

$$\tilde{Y}(nT) = \{\int_{-\infty}^{\infty} r(nT-\tau)[q_1(t) + j\,q_1^{-}(t)]\,d\tau\,\}$$

$$y_1(nT) = \{\int_{-\infty}^{\infty} r(nT-\tau)\,q_1(t)\,d\tau\,\}$$

$$y_2(nT) = \{ \int_{-\infty}^{\infty} r(nT-\tau) q_2(t)\, d\tau \}$$

Hence the receiver uses no demodulation. However the transmitter requires pulse shaping filters and the receiver needs matching filters.

3.2.1.2.2 Digital CAP Transmitter

The structure of an uncoded digital CAP transmitter is as shown in the figure 3.8. With multilevel encoding the signal mapper maps blocks of bits into multilevel symbols. If m is the number of bits in the block and R is the bit rate, the symbol rate is then 1/T=R/m.

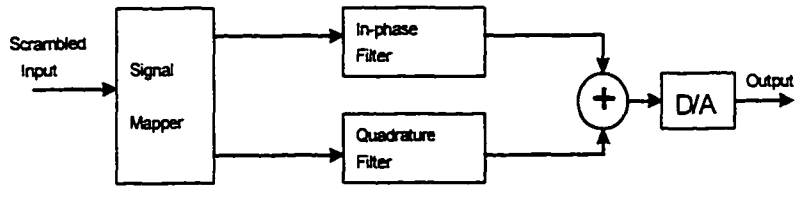

Figure 3.8: CAP Transmitter Structure

The multilevel encoding improves the bandwidth efficiency and decreases the rate at which the square pulses are sent through the channel. The signal mapper as shown in the above figure 3.8, is a 2-D encoder which maps the blocks of bits into two symbol

streams a_n and b_n. The two stream of symbols obtained from the output of the signal mapper is now fed to the inputs of the two parallel in-phase and quadrature digital shaping filters. The outputs are then subtracted (or added) and the result is fed to a digital to analog converter (D/A) as shown in figure 3.8.

3.2.1.2.3 CAP Encoding and Symbol Rate

In the case of 16 CAP blocks of 4 bits are mapped into one of the 16 possible 2-D symbols in each symbol period. The points in the 16 CAP signal constellation are Gray Coded and the symbols in the constellation represent a 4 bit block obtained from the scrambler. The symbol rate depends on the input data rate and the signal constellation chosen.

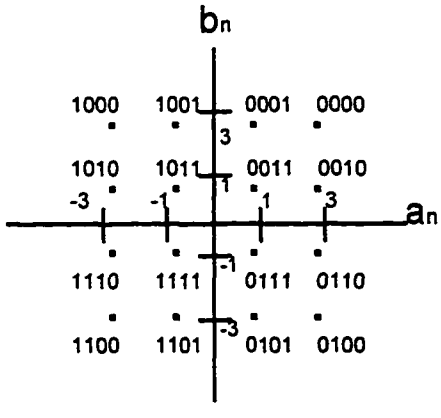

Figure 3.9: 16 Cap Signal Constellation

For T2 rates the symbol rate, if a 16 CAP signal constellation was used would be 6.312/4 = 1.544 Mbauds. Using a 15% excess bandwidth for the 16 CAP transmitter the theoretical utilization of the line code is then obtained which is w = 1.544(1 + 0.15) = 1.8147 MHz. The signal constellation for the 16 CAP line code is as shown in figure 3.9. Table 3.2, provides the corresponding values for 32 CAP and 64 CAP line codes.

Symbol Rate and Theoretical Bandwidth for k-CAP Systems Bit Rate R = 6.312 Mbps Excess Bandwidth alpha=15%			
Line Code	Bits/Symbol	Symbol Rate	Bandwidth
16 CAP	4	1.578 Mbauds	1.8147 MHz
32 CAP	5	1.262 Mbauds	1.4517 MHz
64 CAP	6	1.052 Mbauds	1.2098 MHz

Table 3.2: Excess Bandwidth at DS2 Rates

The bandwidth is then taken and the sampling rate (1/T ') is determined for the FIR digital shaping filters [3]. The input to these filters are digital data which is fed after the 4 bits blocks are mapped to the symbols in the 16 CAP signal constellation. The output from the digital filters are binary numbers which are then subtracted or (added) and fed as input to the D/A converter followed by an interpolating low pass filter (LPF).

3.2.1.2.4 Digital CAP Receiver

The CAP receiver has a structure as shown in the figure 3.10, where the input signal to the Analog to Digital Converter (A/D) is sampled at a rate 1/T' which is 3/T or 4/T depending on the excess bandwidth.

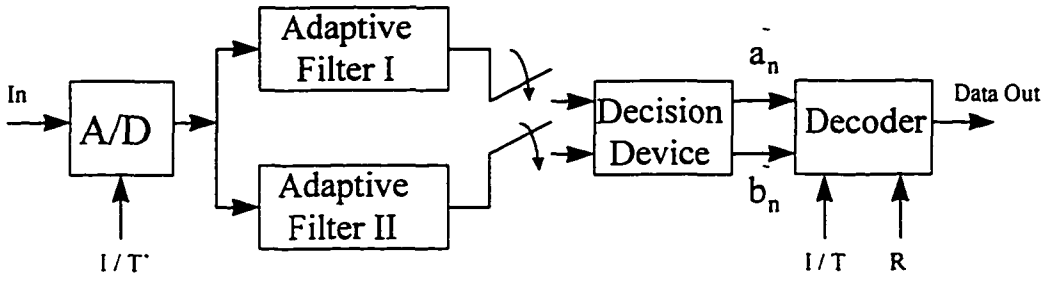

Figure 3.10: CAP Receiver Structure

The digital output of the A/D is now fed to the two adaptive FIR filters, filter I which is the in-phase filter and the filter II is the quadrature filter. These filters are called as the fractionally spaced linear equalizers (FSLE). When the symbol rate is 1/T the sampling is given by 1/T' = j/T where j=3 or 4 and the linear equalizer used is called as the T/j equalizer. The FSLE minimizes the combined power of the noise and the ISI. The taps of the FIR filter are updated using the Least Mean Squared (LMS) algorithm. The output from these filters $y_i(n)$ and $y_q(n)$ are then fed to the decision with a rate change that from 1/T' to 1/T. The in-phase and the quadrature component

now fed to the input of the decision device has channel noise combined with the symbol data, that is

$$y_i(n) = a_n + e_i(n)$$

and

$$y_q(n) = b_n + e_q(n)$$

the decision device then computes the error from the received signal and the previous history, the error in this case is due to sampled noise, in which case

$$e_i(n) = y_i(n) - \tilde{a}_n$$

and

$$e_q(n) = y_q(n) - \tilde{b}_n .$$

In most cases the decision device will correct the received symbol $\tilde{a}_n = a_n$ and $\tilde{b}_n = b_n$, but when error due to the noise sample is too large then it may not be able to correct in which case the decision taken by the device could be wrong. The outputs from the decision device is now taken to the input of the decoder which based on the decided values of a_n and b_n decodes it to the binary bit blocks based on the n-CAP line code used. The output of the data is the actual data that was transmitted which is in the form of the binary data stream. The decoder could also consists of the Viterbi

decoder part built into it if trellis encoding was done at the transmitter side or even Reed-Solomon decoder if block encoding was done at the encoder of the transmitter.

3.2.2 Design Rules for ADSL

1. All loops are non-loaded.

2. All loops are to consist of 26 gauge wires or coarser cables. The cable makeup can be homogenous or heterogeneous.

3. Maximum allowable loop length including bridged taps is 18 kft.

4. Reverse channel to be operated at lower rates which is to be used for control purposes.

5. The ASDL is to be super-imposed on the same line that delivers BR-ISDN and POTS.

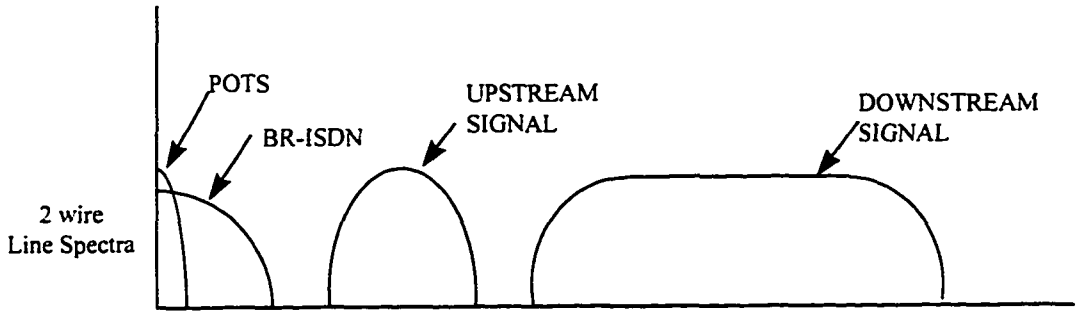

Figure 3.11: ADSL Spectrum Architecture using CAP

3.2.3 Impairments in ASDL

The main impairments in ADSL are

1. Inter-symbol Interference (ISI).

2. Far End Crosstalk (FEXT) from the other ADSL services within the same wire pair.

3. Near End Crosstalk from the other baseband services.

4. Reflections which could impair the received signal when there is an overlap of the upstream and the downstream signal.

References

[1] Bellcore, "Generic Requirements for High-Bit-Rate Digital Subscriber Lines", Technical Advisory TA-NWT-001210, issue 1, Oct. 1991.

[2] A.Reddy & S.V.Ahamed, "Parallel Digital Cap Transmitter", ISCA, Vol.3, No. 2, Aug. 1996, pp. 86-91.

[3] W.Y.Chen, G.H.Im & J.J.Werner, "Design of Digital Carrierless AM/PM Transceivers", T1E1.4/92-149.

[4] I.Kalet, "The Multitone Channel", IEEE Trans. Commun., Vol. 37, no. 2, pp. 119-124, Feb. 1989.

[5] J.S.Chow, J.C.Tu & J.M.Cioffi, " A Computationally Efficient Adaptive Transceiver for High-Speed Digital Subscriber Lines", ICC '90, Vol. 4, pp. 1750-1753.

[6] T.Russel Hsing & J.W.Lechleider, "Digital Signal Processing for High-Speed Digital Transport Technology in the Copper Loop Plant", Globecom '91, pp. 1987-1991.

[7] R.D.Gitlin & S.B.Weinstein, "Fractionally-Spaced Equalization: An improved Digital Tranversal Equalizer ", Bell System Technical Journal, Vol. 60. 1981, pp. 275-296.

Chapter 4

Transmission Line Characteristics

4.1 Types of Transmission Lines

Transmission lines can be generally classified as *balanced* or *unbalanced* types. In the case of the balanced lines both the conductors carry current in each line with a phase offset of 180°. In the case of the unbalanced lines one of the lines is at the ground potential while the other carries all the current. The advantage of using the balanced line is that it provides very high immunity to the noise interference. The balanced lines can be connected to the unbalanced lines by the use of special transformers called as *baluns* (balanced to unbalanced) thereby allowing the co-existence of both the types of lines in any communication network. The transmission lines can be *open-wire transmission line*, *twin lead, twisted-pair cable, shielded cable pair* or *coaxial transmission lines.*

The open-wire transmission line is a two-wire parallel conductor consisting of simply two parallel wires closely spaced but separated by air, while the twisted-lead is also a two-wire parallel conductor with spacers in between. The twisted-pair cable is formed by twisting together two insulated conductors. These pairs are then combined together into units and then cabled together to form cores. The cores are covered with various

types of sheaths depending on its intended type of use. The adjacent pairs are twisted with a different pitch so as to reduce the interference between the two pairs due to mutual induction. The primary constants of the twisted wire pair are its electrical parameters such as resistance, inductance, conductance and capacitance. In order to provide better protection to signals from the radiation losses and interference, parallel two wire transmission lines are often enclosed in a conductive metal braid. The braid used acts as a shield and is connected to the ground. This braid also protects the signal from radiating beyond its boundaries and keeps the electromagnetic interference (EMI) from reaching the other conductors. For high frequency applications coaxial transmission lines are extensively used since they offer better immunity to radiation and dielectric losses and other external interference. The coaxial cable consist of a conductor in the center and surrounded by an outer conductor which is at a uniform distance from the center. The outer conductor used in the coaxial cable provides excellent shielding at higher frequencies but at lower frequencies the shielding is ineffective.

4.2 Line Characteristics

The characteristics of a transmission line are determined by its electrical properties such as wire conductivity and insulator dielectric constant and its physical properties such as the wire diameter and conductor spacing. These properties in turn determine series dc resistance R, series inductance L, shunt capacitance C and shunt

conductance G. Resistance and inductance occur along the line whereas the conductance and the capacitance occur between the two conductors. The primary constants are distributed throughout the length of the line and are therefore called as the distributed parameters. The transmission characteristics of a transmission line are called secondary constants and are determined from the four primary constants. The secondary constants are characteristic impedance and the propagation constant. For maximum transfer of the source energy to the load, that is there no reflected energy, the transmission line must be terminated in a purely resistive load equal to the characteristic impedance of the line. The characteristic impedance of a transmission line is a complex ac quantity which is expressed in ohms. The derivation for the characteristic impedance is as shown in the appendix A. Using the primary constants the characteristic impedance can be computed by the following equation.

$$Z_0 = \sqrt{\frac{R + j\omega L}{G + j\omega C}}$$

From the equation it is clear that the characteristic impedance varies according to the length of the loop and also the frequency. For extremely low frequencies the resistance's dominate in which case the characteristic equation is similar to $Z_0 = \sqrt{\frac{R}{G}}$ whereas for very high frequencies it is seen that the inductance and capacitance begin to dominate and therefore the characteristic impedance now gets modified to $Z_0 = \sqrt{\frac{j\omega L}{j\omega C}} = \sqrt{\frac{L}{C}}$. The characteristic impedance for a transmission

line can also be determined in addition to the methods explained in the appendix A by the use of Ohms's law by the ratio of the source voltage V_s to the source current I_s.

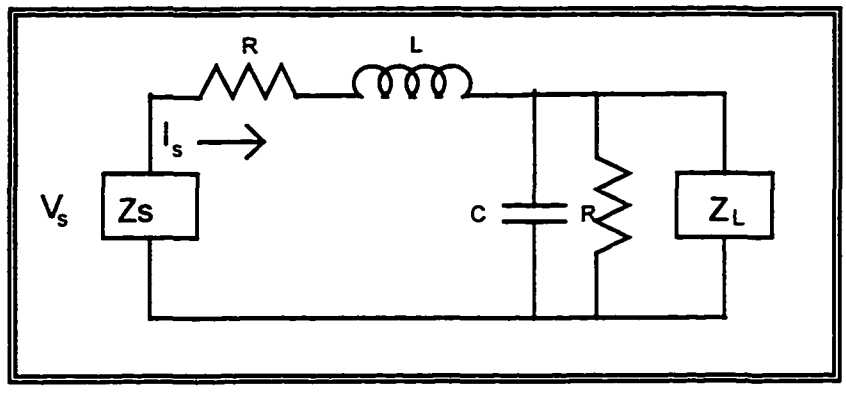

Figure 4.1: Equivalent Circuit for Transmission Line

The transmission lines can be designed and analyzed by the following rules.

1. The input impedance of an infinitely long line at radio frequencies is resistive and equal to Z_0.

2. When the electromagnetic waves travel down the line without reflections such a line is called as the nonresonant line.

3. The ratio of the voltage to current along any part in the line should be equal to the characteristic impedance.

4. The incident voltage and the current along the line should be in phase.

5. Line losses on the nonresonant line are minimum per unit length.

6. Any transmission line that is terminated with a purely resistive load equal to the characteristic impedance acts like an infinite line which means that $Z_0 = Z_L$, there are no reflected waves, the voltage and the current are in phase and there is a maximum transfer of power from the source to the load.

Propagation constant sometimes also called as the propagation coefficient γ is used to express the signal loss and the phase shift in the line. As the wave moves along the line from the transmitted side to the receiver side the amplitude of the wave decreases with the distance. The propagation constant is used to determine the reduction in the voltage and the current as the signal travels down the transmission line. When the line is terminated with a matched load $Z_0 = Z_L$, no energy is returned or reflected back towards the source. Mathematically it can be that the propagation constant $\gamma = \alpha + j\beta$, where α is the attenuation constant (nepers per unit length) and β is the phase constant (radians per unit length). The propagation constant is computed from the primary constants where

$$\gamma = \sqrt{(R + j\omega L)(G + j\omega C)}$$

The phase shift of 2π radians occurs over a distance of one wavelength, then $\beta = 2\pi/\lambda$. The phase constant is generally computed from the primary constants for a given section of length l in which case the phase constant is

$$\beta = \sqrt{\left[1/2\left\{\sqrt{((R^2 + \omega^2 L^2)(G^2 + \omega^2 C^2))} - (RG - \omega^2 LC)\right\}\right]}$$

and the attenuation is given by the equation

$$\alpha = \sqrt{\left[1/2\left\{\sqrt{((R^2 + \omega^2 L^2)(G^2 + \omega^2 C^2))} + (RG - \omega^2 LC)\right\}\right]}$$

From the appendix A we have

$$\alpha^2 - \beta^2 = RG - \omega^2 LC$$

$$2\alpha\beta = \omega(LG + RC)$$

At higher frequencies the inductance and the capacitance begins to dominate where ωL is greater than the resistance R and ωC is greater than the conductance G. At higher frequencies the attenuation constant α is small and therefore RG and α^2 can be neglected so that $\beta = \omega\sqrt{LC}$. The attenuation constant α is then $\alpha = 1/2(R / Z_0 + G Z_0)$ where $Z_0 = \sqrt{\frac{L}{C}}$. The current and voltage distribution along the transmission line that is terminated in a load equal to its characteristic impedance is now shown as follows:

$$I = I_s e^{-l\gamma}$$

$$V = V_s e^{-l\gamma}$$

where

I_s = current at the source end of the line

V_s = voltage at the source end of the line

γ = propagation constant

l = length of the line at which the current or voltage is determined

For a matched load $Z_L = Z_0$ the loss in signal voltage or current and phase shift for a given length of cable is equal to γl.

An ordinary transmission line is bi-directional and the power can propagate equally well in both directions. The signal that originates from the transmitter side and travels towards the load side is called as the *incidence signal* or *wave* and the part of the signal which gets bounced back due the mismatch in the impedance at the receiving or anywhere along the line is called as the *reflected signal* or *wave*. When we talk about the incidence and the reflected waves of the signals we talk about the voltages and the currents corresponding to the signals. The incident voltage and the current of a particular signal emitted from the transmitter are always in phase. When the line is considered to be infinitely long the incident power is absorbed by the line and there is no reflected power, also when the line is perfectly terminated by a purely resistive load equal to the characteristic impedance of the line the load is said to absorb all the incident power, which means that the line is lossless. Reflected power of the signal is that part of the signal that is not completely absorbed by the load and therefore the reflected signal is always much lower in power then that of the incident signal.

When the line is infinitely a long line or is perfectly terminated with a load impedance then the line is said to be *flat* or *nonresonant* since it has no reflected component present in it. Reflections are caused when the load side is either open or short-circuited. When a lossless line is assumed then the voltage and the current remain constant throughout the length of the line. When the source is assumed to be open or short-circuited and assuming the line to be lossless then the energy present in the

transmission line would continue to oscillate back and forth thus creating a line called as the *resonant line* where the energy is alternately transferred between the magnetic and electric fields of the distributed inductance and capacitance.

The reflection coefficient

$$\rho(x) = (V_r / V_i) e^{2\gamma x}$$

$$V_r / V_i = [(V_r - I_r Z_0) / 2] / [(V_r + I_r / Z_0) / 2] = (Z_r - Z_0) / (Z_r + Z_0)$$

$$\rho(x) = [(Z_r - Z_0) / (Z_r + Z_0)] e^{2\gamma x}$$

At $x = 0$

$$\rho(x) = [(Z_r - Z_0) / (Z_r + Z_0)]$$

From the above equations it is clear that the reflection coefficient takes a maximum value when the reflection voltage becomes equal to the incident voltage and a minimum value when the reflected voltage is zero which means the reflection coefficient also becomes zero which is an ideal case. When all the incident power is absorbed by the load impedance then the line is called as a matched line when $Z_0 = Z_L$ as has been discussed before. When $Z_0 \neq Z_L$ then the line is said to be an unmatched or mismatched line. When a line is mismatched there are two waves traveling in the line but in opposite directions very often the amplitude of the two waves are not the same. When the incident and the reflected waves pass each other they appear to stationary and these stationary waves are called as standing waves. The standing wave ratio (SWR) is defined as the ratio of the maximum voltage or the maximum current to the minimum voltage or current of a standing wave of a transmission line. SWR is

the mismatch between the load impedance and the characteristic impedance of the line.

$$SWR = V_{max} / V_{min}$$

The voltage maximum occurs when the both the incident and the reflected waves are in phase, that is when the maximum peaks of both the waves pass the same point at the same time, and the voltage minimum occurs when both the waves are out of phase by 180°.

$$V_{max} = V_i e^{-\gamma l} + V_r e^{-\gamma l}$$

$$V_{min} = V_i e^{-\gamma l} - V_r e^{-\gamma l}$$

$$SWR = V_i e^{-\gamma l} (1 + \rho) / V_i e^{-\gamma l} (1 - \rho) = (1 + \rho) / (1 - \rho)$$

$$\rho = SWR - 1 \ / SWR + 1$$

When there is a mismatch that is the transmission line is not flat then maximum transfer of power from the source to the load does not occur, the reflections that occur in the line cause more and more power loss and also these reflections cause ghost images. Mismatches also cause noise interference. The standing waves so produced due to the mismatch has some of the following characteristics when the load end is open, it has a maximum voltage when at the open end and a minimum at one quarter of the wavelength whereas the current is a minimum at the open end and reaches a maximum value at one quarter of a wavelength, the voltage of the standing wave is reflected without any phase reversal, the current is reflected back as if it were to continue with a phase reversal of 180°, the sum of the incident and the reflected

currents is a minimum at the open but the sum of the incident voltage and reflected voltage is a maximum at the open. When the standing wave encounters a shorted line then the voltage which is incident at the shorted end gets reflected back with a phase reversal of 180° and the current is reflected back in the same manner. It can be concluded that for the transmission line with a shorted end has a minimum voltage at that end whereas the current is maximum at that end with current and voltage repeating every quarter wavelength, that there is an inversion of the impedance at every quarter wavelength. The characteristics of a standing wave on a line having a shorted end has the incident voltage reflected back by a phase of 180° whereas the current is reflected back with the same phase, the sum of the incident and the reflected voltage is a minimum (zero) at the shorted end whereas the incident and the reflected currents are a maximum at the shorted end.

4.3 Digital Subscriber Test Loops

The Bellcore/ANSI have specified certain standard test loops which is supposedly said to cover certain types of loops that exits in the North American Subscriber Loop Environment called as the Bellcore/ANSI Standard Test Loops. There are sixteen such standard test loops which have been defined for HDSL and ADSL which are as follows.

Loop #1

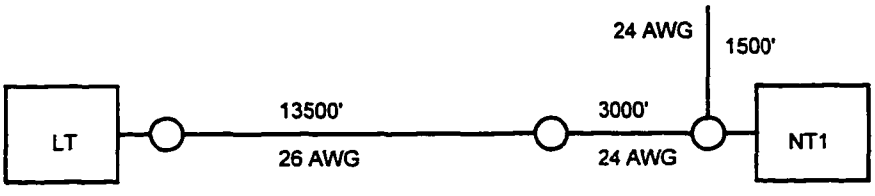

Loop #2

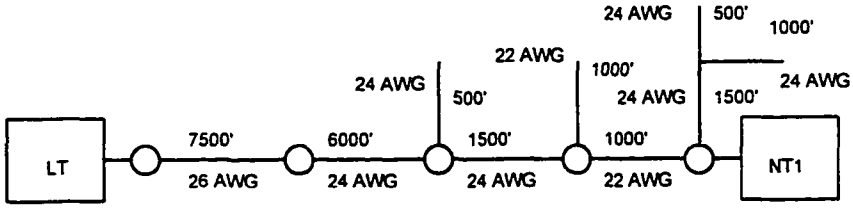

Loop #3

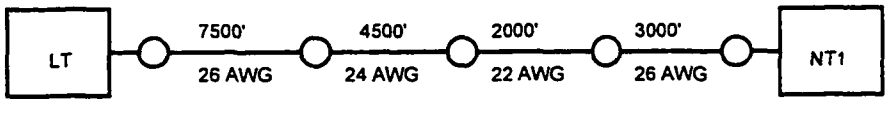

Loop #4

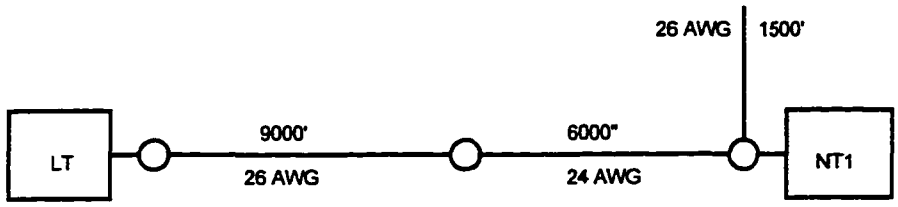

Loop #5

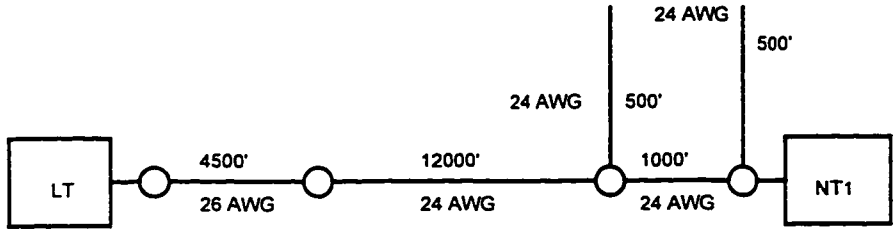

Loop #6

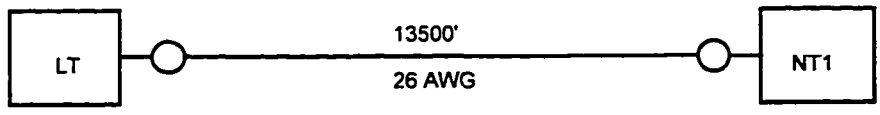

Loop #7

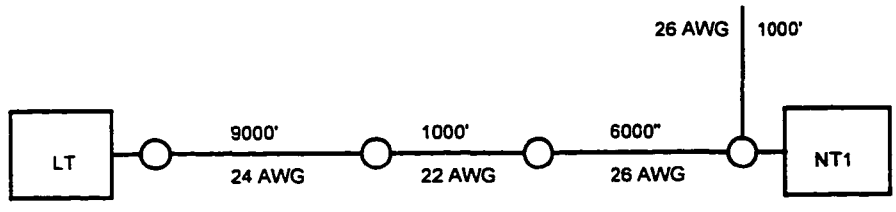

Loop #8

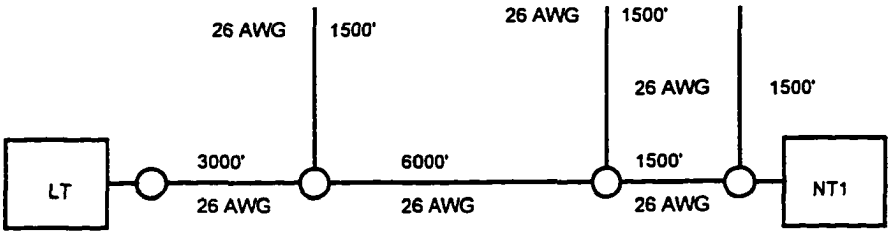

Loop #9

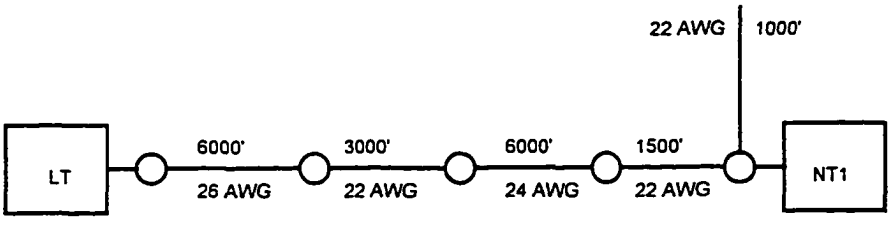

Loop #10

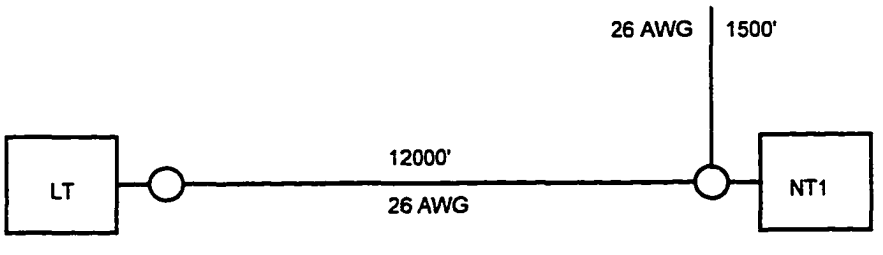

Loop #11

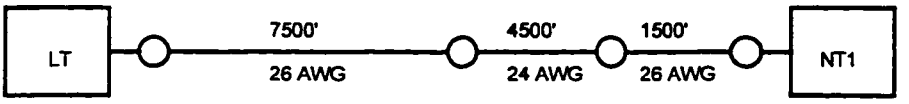

Loop #12

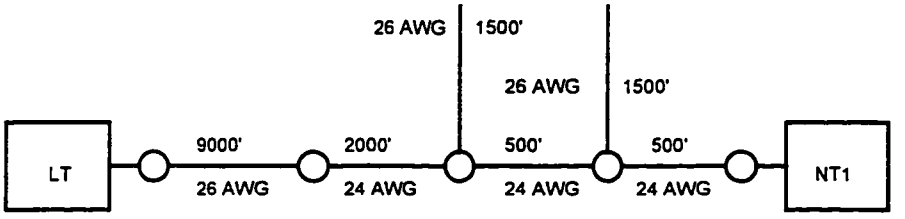

Loop #13

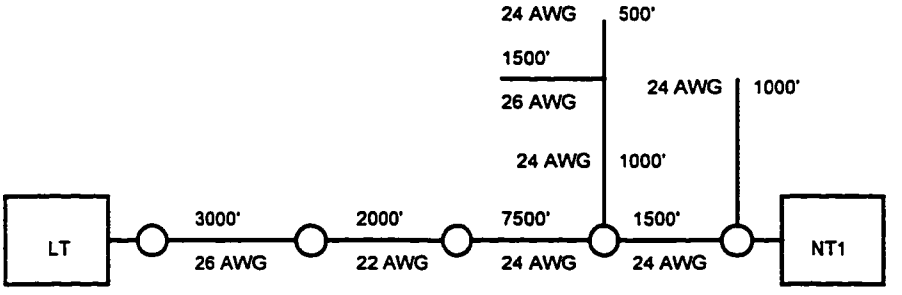

Loop #14

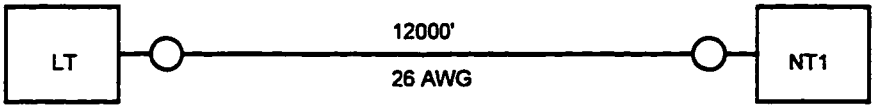

Loop #15

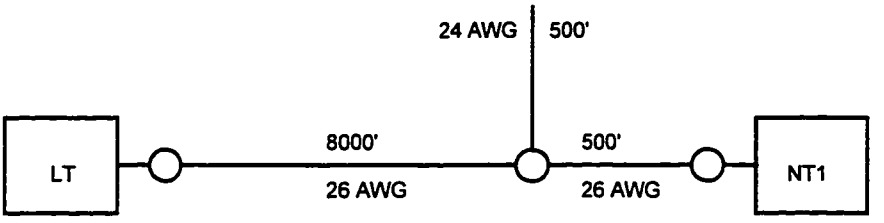

Loop #16

Figure 4.2: Bellcore/ ANSI Standard Test Loops

4.4 Computation of Input Impedance

Accordingly the line input or the line impedance Z_1 from the central office (CO) to the subscriber (SUBS) may be written as

$$Z_1 = (Z_L A + B) / (Z_L C + D)$$

and Z_2 the line in put impedance from the subscriber to the CO as

$$Z_2 = (Z_L D + B) / (Z_L C + A)$$

where A, B, C and D represent the four complex elements of the composite ABCD loop matrix. From transmission line theory [Appendix A] one can derive the elements A, B, C and D for a single gauge homogenous line with no discontinuity as

$$[ABCD] = \begin{bmatrix} \cosh \gamma\, l & Z_0 \sinh \gamma\, l \\ 1/Z_0 \sinh \gamma\, l & \cosh \gamma\, l \end{bmatrix}$$

where γ and Z_0 are the propagation constant and characteristic impedance respectively derived from the primary constants R, L, G and C of the homogenous line of length l units. The presence of gauge discontinuities in the loop requires the cascading of individual ABCD matrices for each loop section that is itself homogenous. When only gauge discontinuities exist, the composite matrix for the loop is the product of each individual ABCD matrix for the corresponding uniform gauge section. Cascading then implies generating the overall ABCD matrix as a product matrix from the central office side to the subscriber side in the order in which the cable sections are encountered. When bridged taps are encountered it is necessary to compute the ABCD parameters for each bridge tap and then the composite $A_{eq}B_{eq}C_{eq}D_{eq}$ matrix is computed A'B'C'D'. The input impedance Z_{in} is computed from the load impedance Z_L and the composite matrix $A_{eq}B_{eq}C_{eq}D_{eq}$ thereby obtaining

$$Z_{in} = \left(\frac{A_{eq} Z_L + B_{eq}}{C_{eq} Z_L + D_{eq}} \right)$$

The bridged taps are generally left opened instead of being terminated and thus the ABCD matrix of the bridged tap represented by its input impedance Z_{BT} across the loop has the form

$$[ABCD]_{BT} = \begin{bmatrix} 1 & 0 \\ 1/Z_{BT} & 1 \end{bmatrix}$$

where $1/Z_{BT} = Y_0' \tanh \gamma l$ and $Y_0' = (1.0 + j\ 0.0) / Z_0' = \sqrt{(C'D')/(A'B')}$

propagation constant $\gamma'(\omega) = \alpha'(\omega) + j\beta'(\omega) = \sqrt{(R' + j\omega L')(G' + j\omega C')}$

image impedance $Z_0' = \sqrt{\frac{(R' + j\omega L')}{(G' + j\omega C')}}\Omega = \sqrt{\frac{A'B'}{C'D'}}\Omega$

R′ is resistance for the bridged tap in Ω / unit length, L′ is the inductance for the bridged tap in henries / unit length, G′ is the conduction for the bridged tap in mhos /unit length and C′ is the capacitance for the bridged tap in farads / unit length. $\omega = 2\pi f$ radians /second or frequency hertz.

The real part $\alpha'(\omega)$ of $\gamma'(\omega)$ gives the attenuation coefficient in nepers / unit length and imaginary part $\beta'(\omega)$ of $\gamma'(\omega)$ yields the phase angle in radians / unit length.

$$\gamma' l = \Gamma = \text{complex } [\log (0.5 * (A' + D' + B'/Z_0' + C'Z_0'))]$$

Z_0' is the characteristic impedance and Γ the propagation constant of the entire bridged tap. When the impedance for the entire bridged tap is computed, then by taking into account all the characteristic impedance's of the various normal sections of the transmission line which is heterogeneous in its makeup (consisting of more than one section made up of different wire gauges) the image impedance is computed. Similarly the values of A′, B′, C′ and D′ are the values of the entire bridged tap. In this way the matrix reduction continues in the presence of loop multiple discontinuities. The composite ABCD matrix is obtained by normal multiplication techniques for the entire subscriber loop with one or more bridged taps where bridged taps upon bridged taps are encountered as shown in the figure 4.5, then the matrix reduction is done in a similar way.

4.5 Matrix Representation and Reduction of the Subscriber Loop

There are various types of subscriber loops. There are metallic loops with gauge discontinuities as shown in figure 4.3(a)

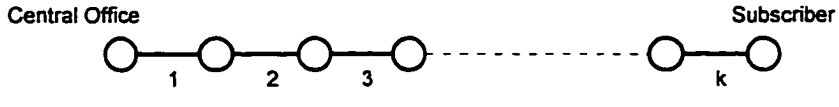

Figure 4.3(a): Loop with Gauge Discontinuity

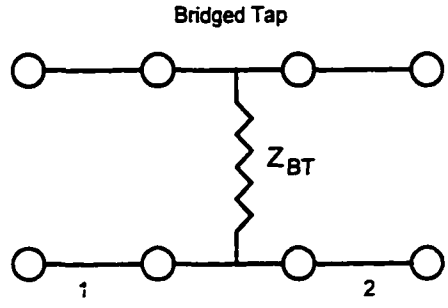

Figure 4.3(b): Cascaded Bridged Tap Loop

The loop shown in figure 4.3(b) is a cascaded loop with equivalent bridged tap 2 ports. There are also metallic loops with gauge discontinuities and bridged taps.

The equivalent ABCD matrix for the figure 4.3 is

$$\begin{bmatrix} A_1 & B_1 \\ C_1 & D_1 \end{bmatrix} \begin{bmatrix} 1 & 0 \\ 1/Z_{BT} & 1 \end{bmatrix} \begin{bmatrix} A_2 & B_2 \\ C_2 & D_2 \end{bmatrix}$$

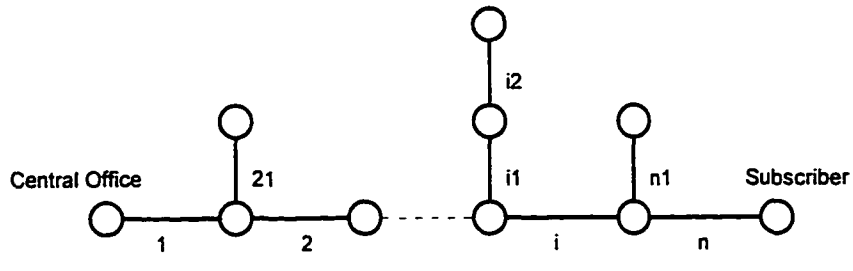

Figure 4.4: Multisection Bridged Tap Loop

The loop is sometimes much more complicated than a simple loop having one or two sections with a single bridged tap. A generalized loop is as shown in figure 4.4. It could consist of any number of normal sections of different wire gauges such as 19, 22, 24 and 26 AWG, with multiple bridged taps and bridged taps over bridged taps.

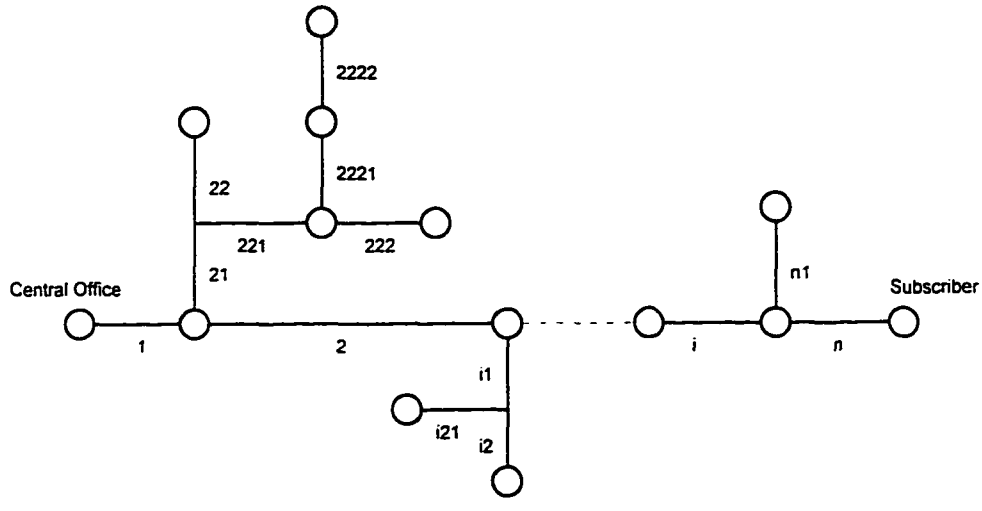

Figure 4.5: Bridged Tap Over Bridged Tap Loop

The computation of the equivalent A'B'C'D' matrix for the loop such as the one shown in figure 4.5 increases the computational complexity, matrices for each of the sections in the loop for the figure 4.5 is computed as shown below

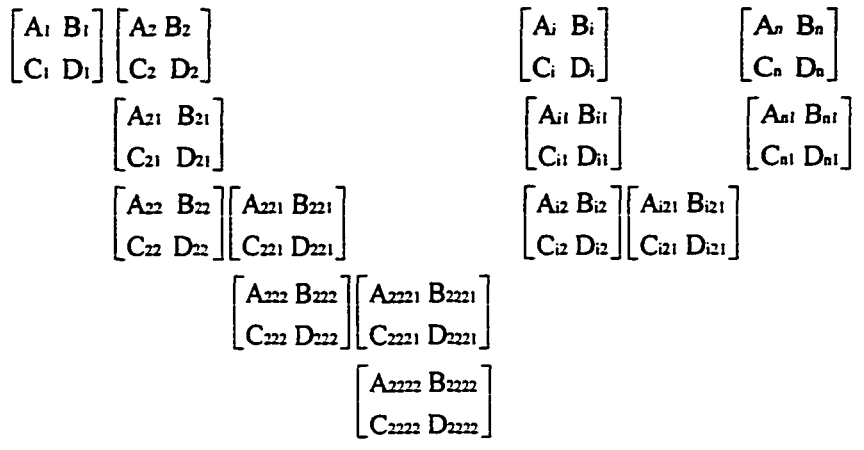

Figure 4.6: Computational Complexity of ABCD Matrix

Matrix representation of a metallic loop with gauge discontinuities and bridged taps upon bridged taps is as shown in figure 4.6.

In principle ABCD matrix of the parallel impedance of the outermost bridged tap is derived from its individual ABCD matrix. This in turn is cascaded with the inner bridged tap matrix. Next the new matrix of the bridged tap upon bridged tap structure is generated and cascaded with the rest of the loop. This process is repeated throughout the entire loop configuration. An algorithm for generating the general ABCD matrix for any loop whose topology can be represented as a tree structure has been derived from these basic principles. In order to provide new services such as

video on demand, tele-commuting, distance learning , interactive multimedia, high speed data transmission etc., it is necessary to study high frequency transmission characteristics of the subscriber loop environment considered for these services to be provided. Characteristics of the transmission line such as the image impedance, return loss, insertion loss for the frequency band under which these loops are suppose to operate needs to be determined. The loops such as the ANSI standard loops considered for these studies are a mixture of homogenous (cable consisting of the same gauge) and heterogeneous (cable consisting of different wire gauges) with or without bridged taps for the asymmetric mode of data transmission on these lines.

4.6 Voltage Transfer Function

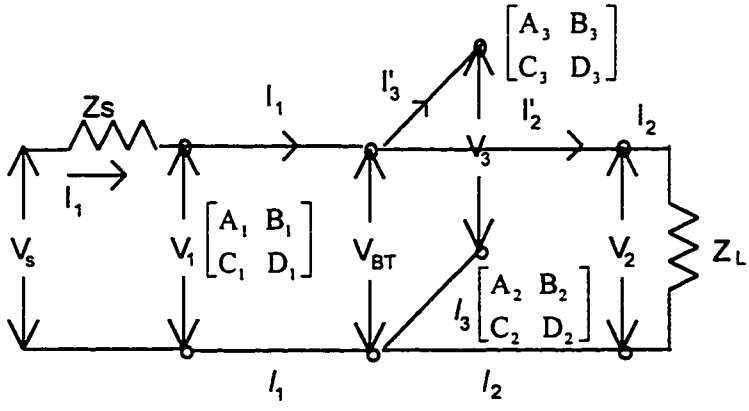

Figure 4.7: Transmission Line with Bridged Tap

Consider the following line shown in figure 4.7 consisting of different lengths and made up of different wire gauges including a bridged tap. Let Z_S be the source impedance Z_L the load impedance. Let Z_1 and Z_2 be the characteristic impedance's of the two normal sections of length l_1 and l_2 respectively. We know that from the derivations in Appendix A that $A = D = \text{Cosh}\gamma l$, $B = Z_0 \text{ Sinh}\gamma l$ and $C = 1/ Z_0 \text{ Sinh}\gamma l$. Here Z_0 is the characteristic impedance and γ is the propagation constant. From the properties of symmetry of the transmission line A = D and from the properties of reciprocity AD - BC =1. In this case when we consider the properties of symmetry and reciprocity then it is assumed that the transmission line is homogenous with bridged taps if any is only at the center of the line. From the two port network theory it is clear that

$$\begin{bmatrix} V_1 \\ I_1 \end{bmatrix} = \begin{bmatrix} A & B \\ C & D \end{bmatrix} \begin{bmatrix} V_2 \\ I_2 \end{bmatrix}$$

Applying this to the figure 4.7 above we get

$$V_1 = A_1V_{BT} + B_1I_1', \; I_1 = C_1V_{BT} + D_1I_1', V_{BT} = A_2V_2 + B_2I_2, \; I_2'$$

$$= C_2V_2 + D_2I_2$$

$$I_1' = I_3' + I_2', \; V_{BT} = A_3V_3 \text{ and } I_3' = C_3V_3.$$

Now

$$\begin{bmatrix} V_1 \\ I_1 \end{bmatrix} = \begin{bmatrix} A_{eq} & B_{eq} \\ C_{eq} & D_{eq} \end{bmatrix} \begin{bmatrix} V_2 \\ I_2 \end{bmatrix}$$

Substituting for I_1', I_2', I_3' and V_{BT} we get

$$V_1 = A_1 V_{BT} + B_1 (C_2 V_2 + D_2 I_2) + \frac{B_1 C_3}{A_3} V_{BT}$$

$$= V_{BT} (A_1 + \frac{B_1 C_3}{A_3}) + B_1 (C_2 V_2 + D_2 I_2)$$

$$= A_1 (A_2 V_2 + B_2 I_2) + \frac{B_1 C_3}{A_3} A_2 V_2 + \frac{B_1 C_3}{A_3} B_2 I_2 + B_1 C_2 V_2 + B_1 D_2 I_2$$

$$= (A_1 A_2 + B_1 C_2 + \frac{B_1 C_3}{A_3} A_2) V_2 + (A_1 B_2 + B_1 D_2 + \frac{B_1 C_3}{A_3} B_2) I_2 \quad - (1)$$

$$I_1 = C_1 V_{BT} + D_1 I_1'$$

$$I_1' = I_2' + I_3' = (C_2 V_2 + D_2 I_2) + \frac{C_3}{A_3} V_{BT}$$

$$= [C_1 + \frac{D_1 C_3}{A_3}] V_{BT} + D_1 C_2 V_2 + D_1 D_2 I_2$$

$$= C_1 A_2 V_2 + C_1 B_2 I_2 + A_2 V_2 \frac{D_1 C_3}{A_3} + B_2 I_2 \frac{D_1 C_3}{A_3} + D_1 C_2 V_2 + D_1 D_2 I_2$$

$$= [C_1 A_2 + D_1 C_2 + A_2 \frac{D_1 C_3}{A_3}] V_2 + [C_1 B_2 + D_1 D_2 + B_2 \frac{D_1 C_3}{A_3}] I_2 \quad - (2)$$

$$A_{eq} = A_1 A_2 + B_1 C_2 + B_1 \frac{A_2 C_3}{A_3}$$

$$= \text{Cosh}\gamma l_1 \text{Cosh}\gamma l_2 + Z_0 \text{Sinh}\gamma l_1 \; 1/Z_0 \; \text{Sinh}\gamma l_2 + Z_0 \text{Sinh}\gamma l_1 \frac{\text{Cosh}\gamma l_2 \; \text{Sinh}\gamma l_3}{Z_0 \; \text{Cosh}\gamma l_3}$$

$$= \text{Cosh}\gamma (l_1 + l_2) + \text{Sinh}\gamma l_1 \, \text{Cosh}\gamma l_2 \, \text{Tanh}\gamma l_3 \quad - (3)$$

$$B_{eq} = A_1 B_2 + B_1 D_2 + B_1 B_2 C_3 / A_3$$

$$B_{eq} = \text{Cosh}\gamma l_1 \; Z_0 \text{Sinh}\gamma l_2 + Z_0 \text{Sinh}\gamma l_1 \; \text{Cosh}\gamma l_2 +$$

$$Z_0 \text{Sinh}\gamma l_1 \; Z_0 \text{Sinh}\gamma l_2 \; 1/Z_0 \; \frac{\text{Sinh}\gamma \, l_3}{\text{Co s h}\gamma \, l_3}$$

$$= Z_0\{ \text{Sinh}\gamma(l_1+l_2) + \text{Sinh}\gamma l_1 \, \text{Sinh}\gamma l_2 \, \text{Tanh}\gamma l_3 \} \qquad \text{- (4)}$$

$$C_{eq} = C_1A_2 + D_1C_2 + D_1A_2C_3 / A_3$$

$$\text{Cosh}\gamma l_2 \; 1/Z_0 \text{Sinh}\gamma l_1 + 1/Z_0 \text{Sinh}\gamma l_2 \; \text{Cosh}\gamma l_1 +$$

$$1/Z_0 \text{Cosh}\gamma l_1 \; \text{Cosh}\gamma l_2 \; \frac{\text{Sinh}\gamma \, l_3}{\text{Co s h}\gamma \, l_3}$$

$$= 1/Z_0\{ \text{Sinh}\gamma(l_1+ l_2) + \text{Cosh}\gamma l_1 \, \text{Cosh}\gamma l_2 \, \text{Tanh}\gamma l_3 \} \qquad \text{- (5)}$$

$$D_{eq} = C_1B_2 + D_1D_2 + D_1B_2C_3 / A_3$$

$$= 1/Z_0 \text{Sinh}\gamma l_1 \; Z_0 \text{Sinh}\gamma l_2 + \text{Coh}\gamma l_1 \; \text{Cosh}\gamma l_2 +$$

$$Z_0 \text{Cosh}\gamma l_1 \; \text{Sinh}\gamma l_2 \; 1/Z_0 \; \frac{\text{Sinh}\gamma \, l_3}{\text{Co s h}\gamma \, l_3}$$

$$= \text{Cosh}\gamma(l_1+ l_2) + \text{Cosh}\gamma l_1 \, \text{Sinh}\gamma l_2 \text{Tanh}\gamma l_3 \qquad \text{- (6)}$$

From the above equations it is clear that when $l_1 = l_2$ even with a bridged tap at the center, the network is symmetrical and reciprocal and the network is only reciprocal when $l_1 \neq l_2$ for transmission line with a bridged tap. When the line has no bridged taps $l_3 = 0$ and $\text{Tanh}\gamma l_3 = 0$ resulting in a total chain matrix for the transmission line which is the product of two or more sub matrices for the heterogeneous line.

$$V_2 = Z_L \, I_2, \; V_s = I_1Z_L + V_1 = I_1Z_s + V_1$$

$$V_1 = A_{eq}V_2 + B_{eq}I_2 = A_{eq}Z_LI_2 + B_{eq}I_2$$

$$I_1 = C_{eq}V_2 + D_{eq}I_2 = C_{eq}Z_1I_2 + D_{eq}I_2$$

$$H(j\omega) = \frac{V_2}{V_s} = \frac{Z_L}{A_{eq} Z_L + B_{eq} + Z_s(C_{eq} Z_L + D_{eq})}$$

When $Z_L = Z_S = Z$ then

$$\frac{V_2}{V_s} = \frac{1}{A_{eq} + B_{eq} / Z + (C_{eq} Z + D_{eq})} = 1/S_r$$

$S_r = \{ Z_L / Z_0(\text{Sinh}\gamma(l_1 + l_2) + \text{Cosh}\gamma l_1 \text{Cosh}\gamma l_2 \text{Tanh}\gamma l_3) +$

$(\text{Cosh}\gamma(l_1 + l_2) + \text{Cosh}\gamma l_1 \text{Sinh}\gamma l_2 \text{Tanh}\gamma l_3) +$

$(\text{Cosh}\gamma (l_1 + l_2) + \text{Sinh}\gamma l_1 \text{Cosh}\gamma l_2 \text{Tanh}\gamma l_3) +$

$(Z_0 / Z_L (\text{Sinh}\gamma(l_1 + l_2) + Z_0 \text{Sinh}\gamma l_1 + \text{Sinh}\gamma l_1 \text{Sinh}\gamma l_2 \text{Tanh}\gamma l_3)\}$

$= \text{Sinh}\gamma(l_1 + l_2) (Z_L / Z_0 + Z_0 / Z_L) + \text{Tanh}\gamma l_3 (Z_L / Z_0 \text{Cosh}\gamma l_1 \text{Cosh}\gamma l_2 +$

$Z_0 / Z_L \text{Sinh}\gamma l_1 \text{Sinh}\gamma l_2) + 2 \text{Coh}\gamma(l_1 + l_2) + \text{Tanh}\gamma l_3 \text{Sinh}\gamma(l_1 + l_2)$

When $Z_0 = Z_L$ we get

$$S_r = \text{Sinh}\gamma(l_1 + l_2) (2 + \text{Tanh}\gamma l_3) + \text{Coh}\gamma(l_1 + l_2) (2 + \text{Tanh}\gamma l_3)$$

$$= (\text{Sinh}\gamma(l_1 + l_2) + \text{Coh}\gamma(l_1 + l_2)) (2 + \text{Tanh}\gamma l_3)$$

$$V_2 / V_S = \frac{e^{-\gamma(l_1 + l_2)}}{2 + \tanh\gamma l_3}$$

This is the formula which gives a picture about the reflections that occur due to the bridge tap. When no bridge tap is used $l_3 = 0$ and

$$V_2 / V_S = \frac{e^{-\gamma(l_1 + l_2)}}{2}$$

which means that maximum voltage is transferred in the absence of the bridged tap. When a bridged tap is present then minimum voltage gets transferred when $\tanh\gamma l_3 = 1$, that when $\gamma l_3 = \pi / 4$, then

$$V_2 / V_S = \frac{e^{-\gamma(l_1 + l_2)}}{3}$$

The figure 4.8 and figure 4.9 shows the image impedance computed for all the ANSI standard loops. These are the test loops used by the HDSL and the ADSL environment. The image impedance shown in the figure 4.8 are for the ADSL with operating frequency range being 100 kHz - 1350 kHz in the forward channel or downstream that is from the central office side to the subscriber side. and in figure 4.9 the image impedance is shown at an operating frequency range of 10 kHz - 90 kHz in the reverse channel or upstream from the subscriber side to the central office. The above frequency ranges would be able to support data rates of 6.312 Mbps with an excess bandwidth of 15% for the forward channel using bandwidth efficient line codes such as the CAP 64 and in the reverse channel data rates of 384 Kbps would be supported with an excess bandwidth of 15% with the use CAP 64 line code. The image impedance is computed for the loop by first computing the $A_{eq}B_{eq}C_{eq}D_{eq}$ parameters for each of these loops and then from these parameters the image impedance is computed as discussed above. For computing the image impedance of the reverse channel the same $A_{eq}B_{eq}C_{eq}D_{eq}$ parameters are taken and then the A_{eq} and

D_{eq} parameters are swapped and the image impedance is once again computed as before using the same equation for the image impedance $Z_o' = \sqrt{\frac{A_{eq} B_{eq}}{C_{eq} D_{eq}}} \Omega$.

4.7 Classification of Loops

Loops could be classified broadly as

1. Homogenous Loops

When homogenous loops are considered, they could be sub-classified as

a. loops without any bridged taps

b. loops with single bridged taps

c. loops with multiple single bridged taps

d. loops with a combination of single and bridged tap over bridged tap.

In the case of homogenous loops all the sections including the bridged taps are of uniform wire gauge, that is the wire gauges used in the loops are the same.

2. Heterogeneous Loops

In the heterogeneous loops it has the same classification as that of the homogenous loops except that the different sections of the loop need

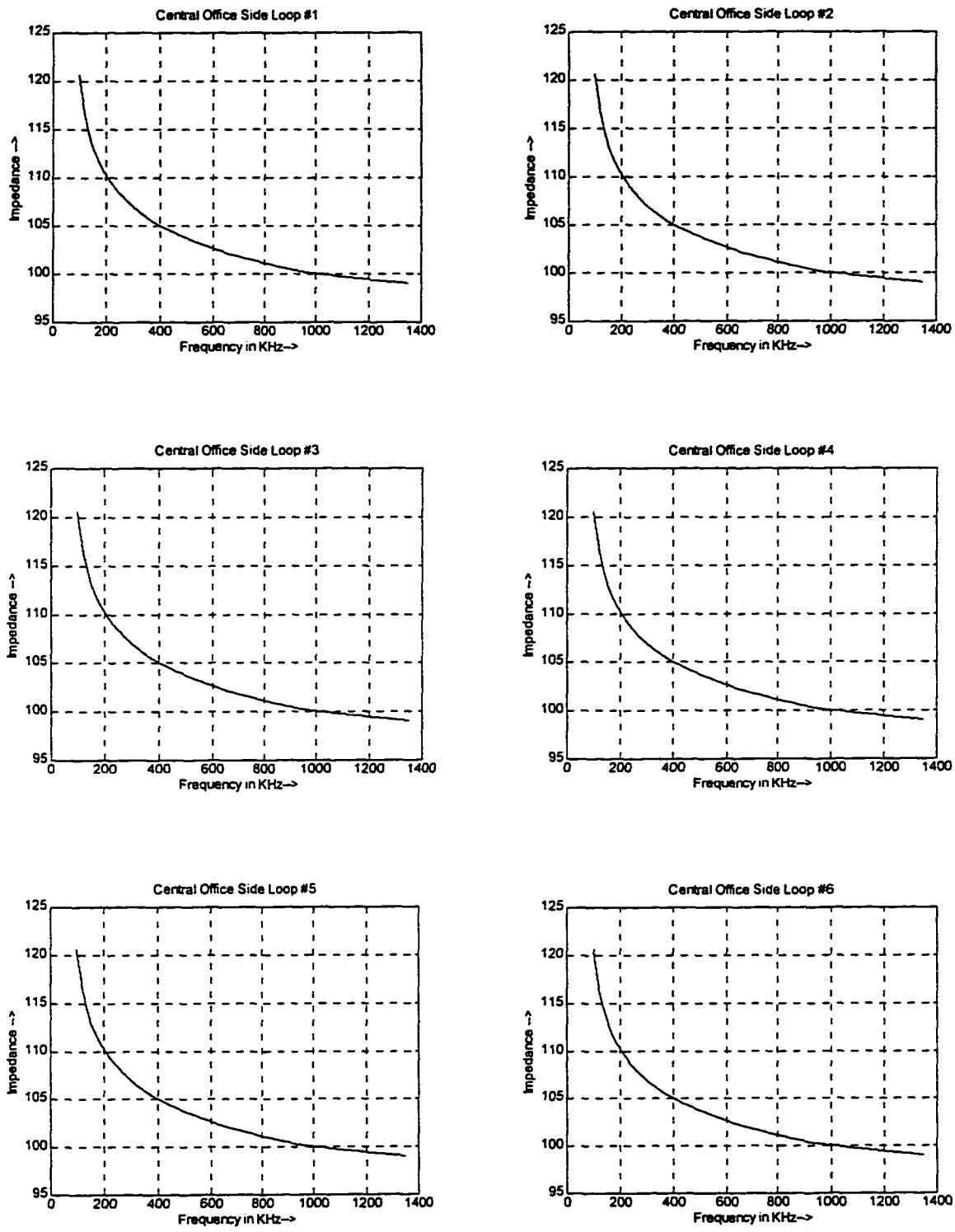

Figure 4.8: Central Office Side Image Impedance

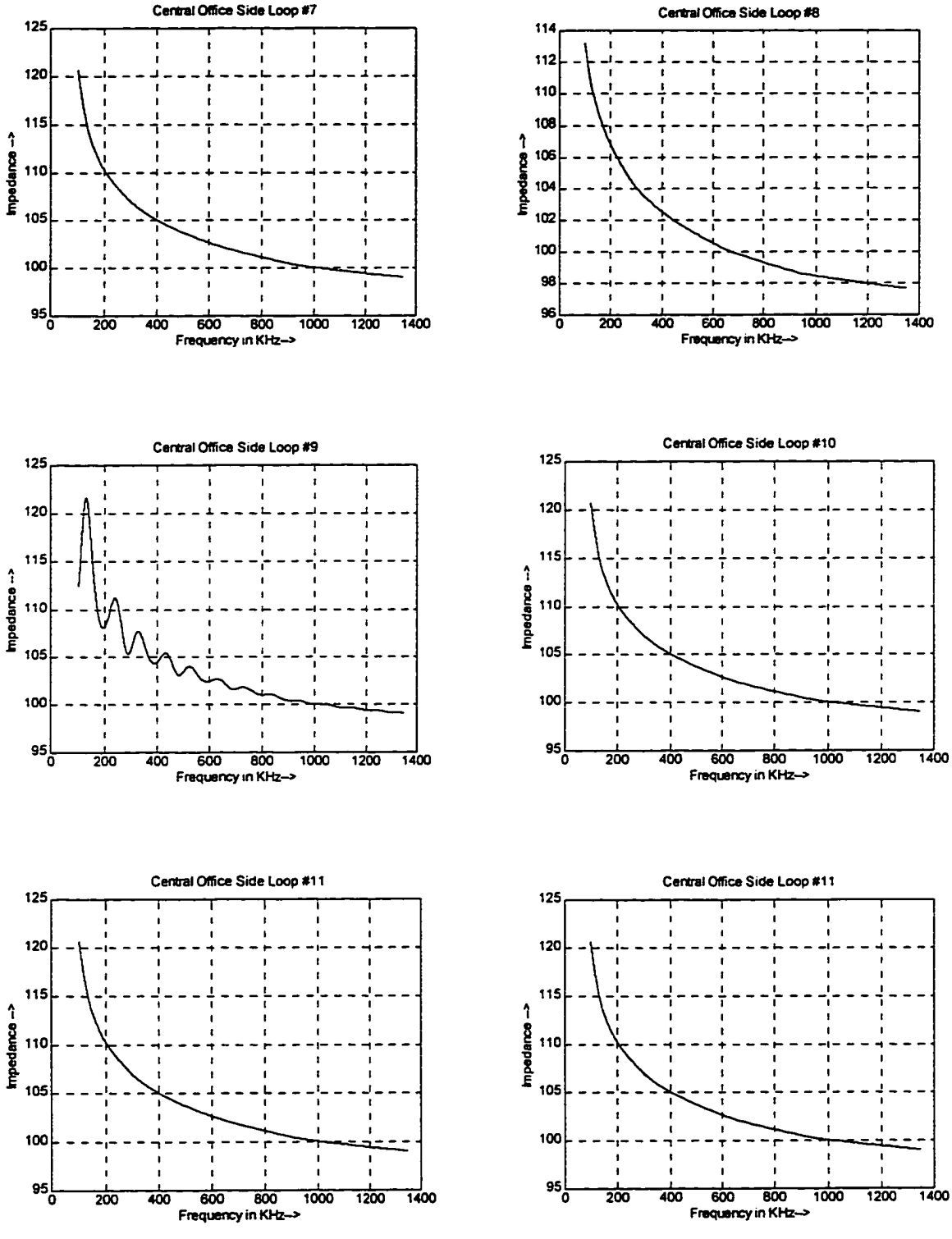

Figure 4.8: Central Office Side Image Impedance

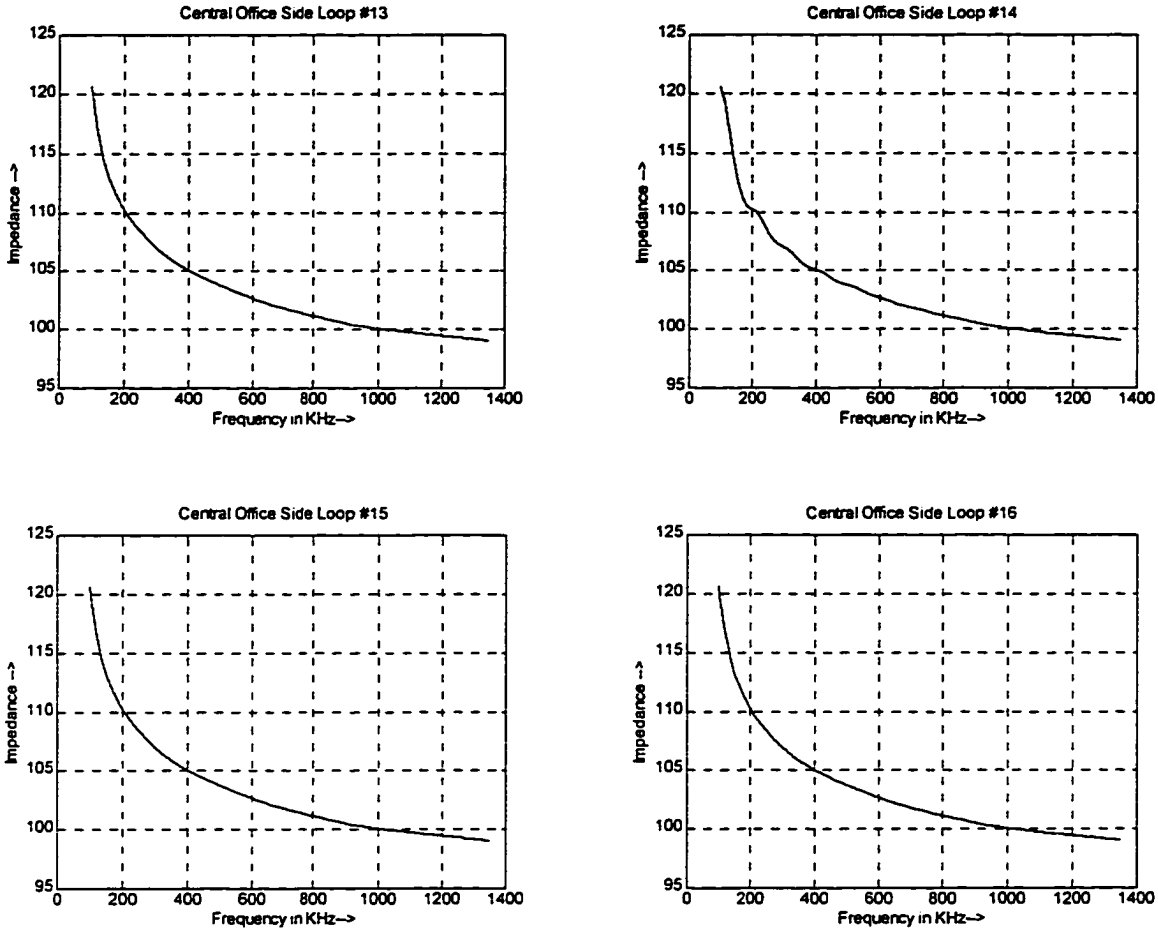

Figure 4.8: Central Office Side Image Impedance

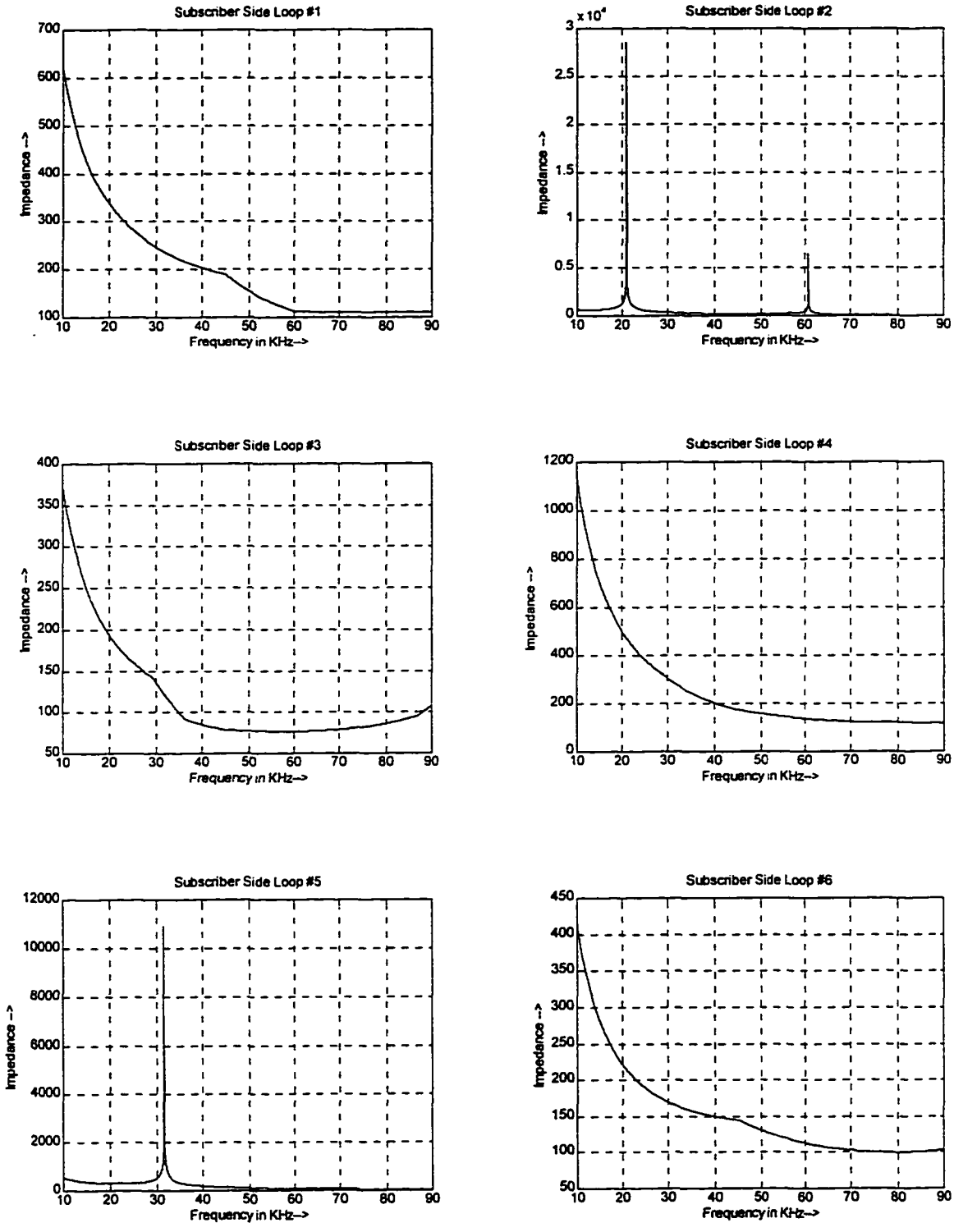

Figure 4.9: Subscriber Side Image Impedance

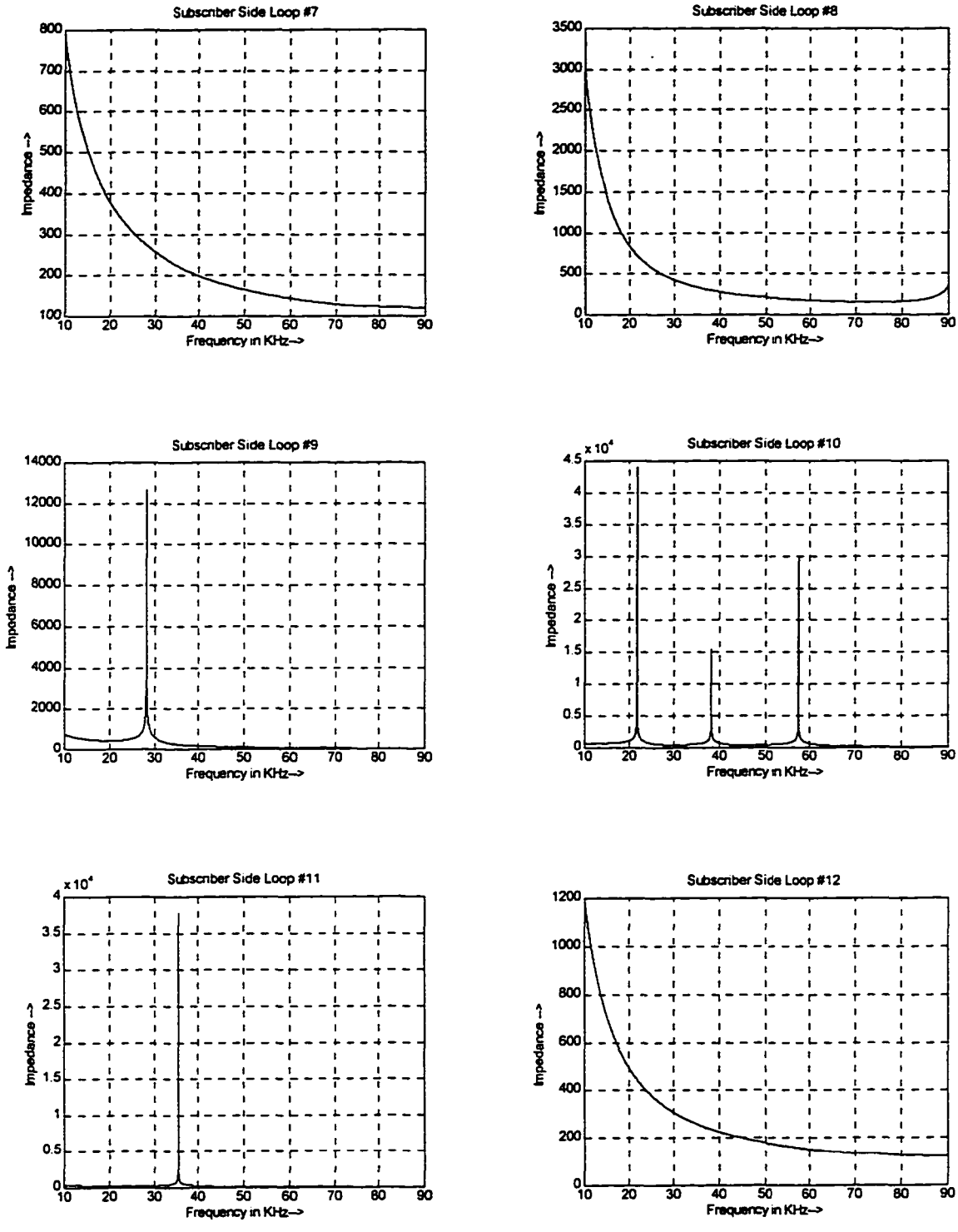

Figure 4.9: Subscriber Side Image Impedance

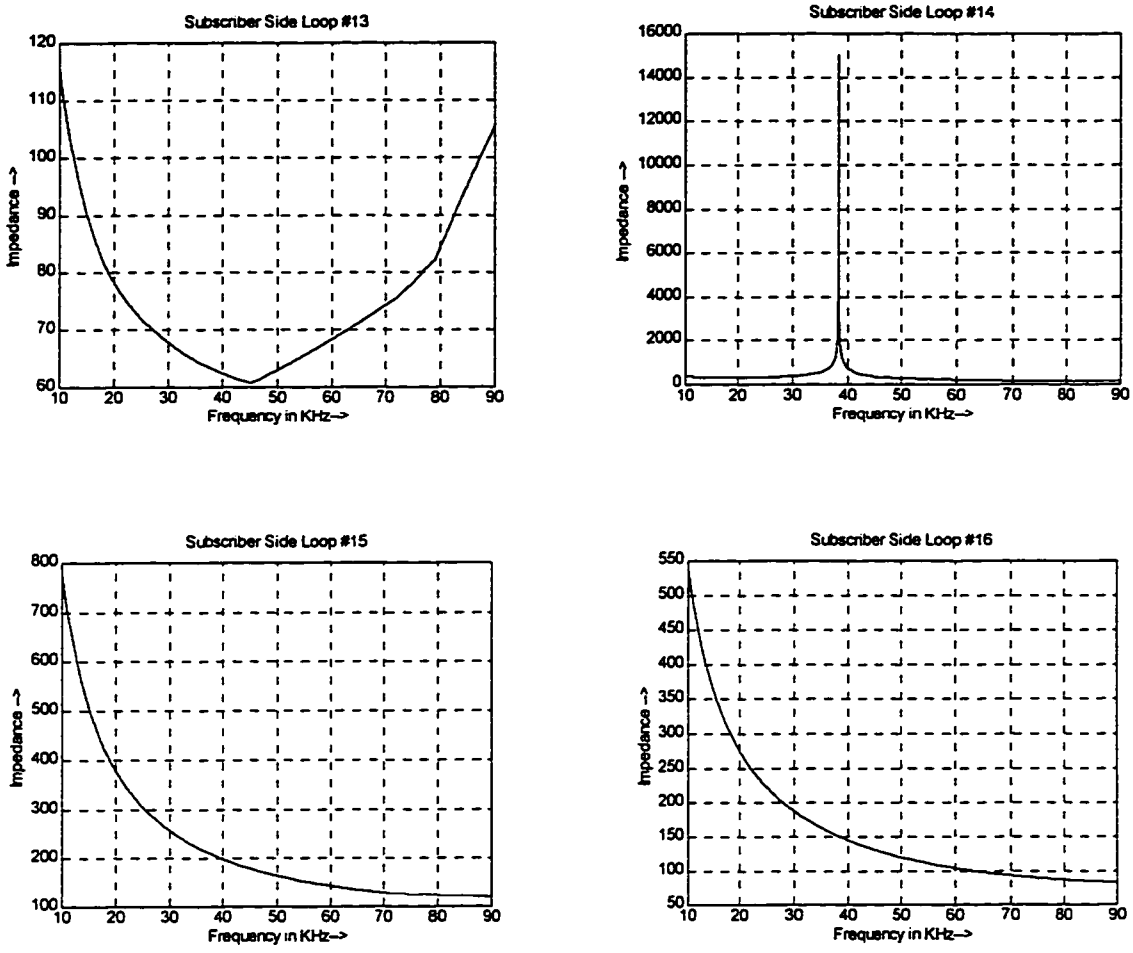

Figure 4.9: Subscriber Side Image Impedance

Loop #	Central Office Side (Ohms)	Subscriber Side (Ohms)
1	103.99	200.05
2	103.94	336.86
3	103.89	117.45
4	103.95	259.63
5	103.91	202.25
6	103.87	151.93
7	104.01	222.38
8	101.68	433.28
9	103.91	253.19
10	103.88	582.74
11	103.95	187.33
12	103.96	270.29
13	103.88	75.17
14	103.88	320.04
15	104.01	222.38
16	103.98	160.40

Table 4.1: Mean Values of Image Impedance for CO and SUB Side for the ANSI Loops

not necessarily be of the same wire gauge, that is some of the sections could be made of different wire gauges. The wire gauges used both in the case of the homogenous and the heterogeneous loops are 19 to 26 AWG. The mean values of the image impedance for both the Subscriber (SUB) side and the Central Office (CO) side are as shown in the table 4.1.

4.8 Results of the Loop Impedance

The ANSI standard loops as shown in the figure 4.2 consists of loops with various types of cable make-up which fall into one of the classifications as discussed above. Considering the loops with uniform wire gauge, loops 7, 15 and 11 are such loops except that loop 11 has a single bridged tap. All the other ANSI standard loops shown in the figure 4.2 fall into the category of heterogeneous loops. Among the so called heterogeneous loops, loops 1,4 and 12 are loops without bridged taps, loops 2,5,6,8,9,10,13 and 16 are loops with single bridged taps and loops 3 and 14 are those loops with a combination of single bridged taps and bridged tap over bridged tap.

The image impedance's for all the loops at the Central Office is as shown in the figure 4.8. Since the frequency range for the forward channel is 100 kHz to 1350 kHz for most of the loops the image impedance starts from 120 ohms at 100 kHz and falls down to about 98 ohms at about 1350 kHz, and the drop is relatively very smooth by

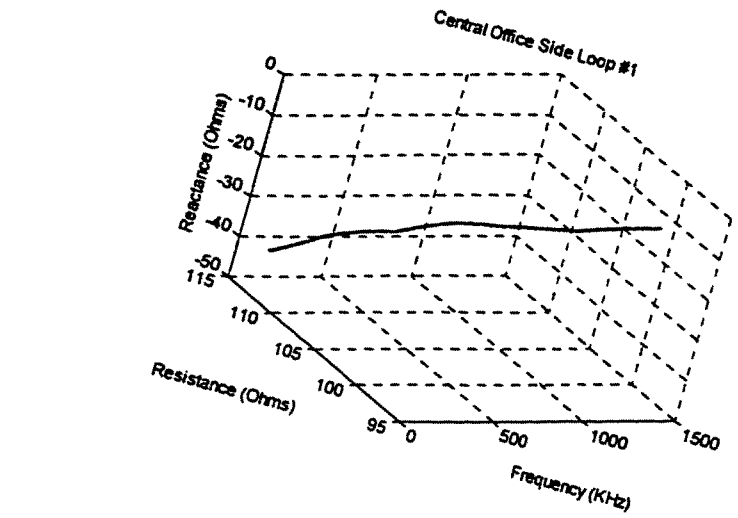

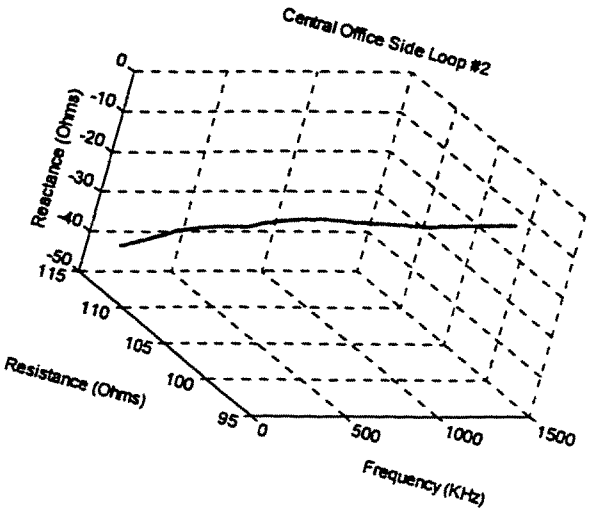

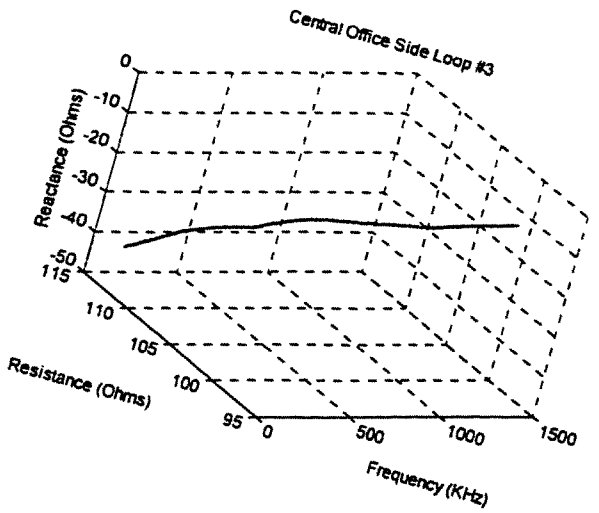

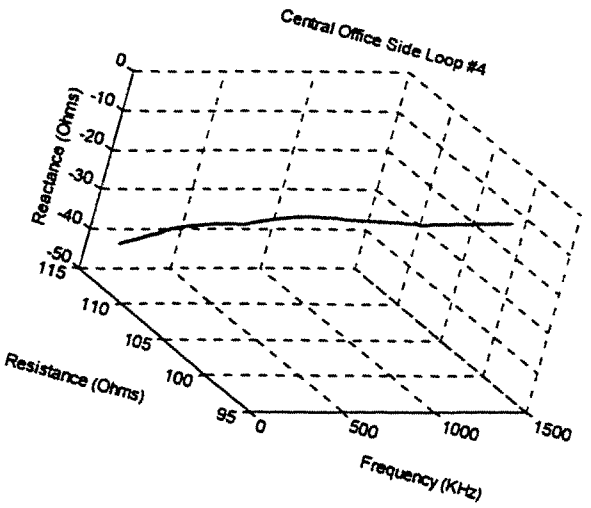

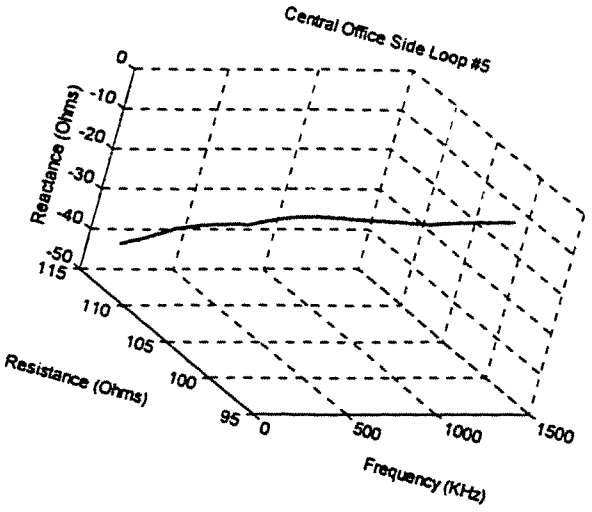

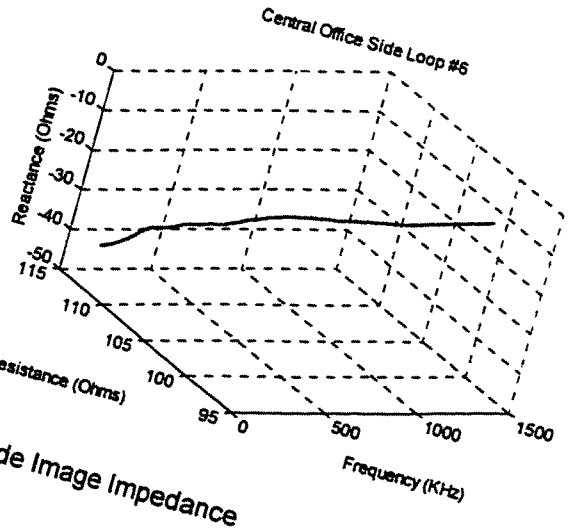

Figure 4.10: Central Office Side Image Impedance

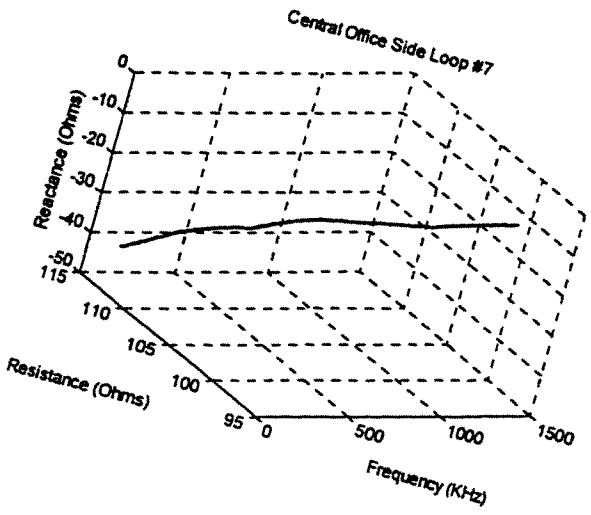

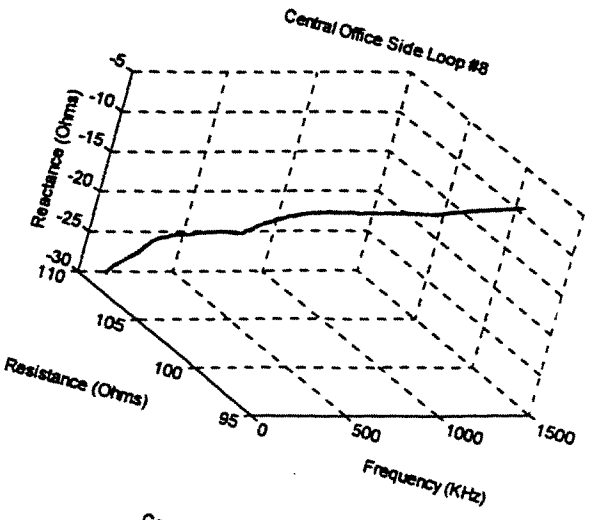

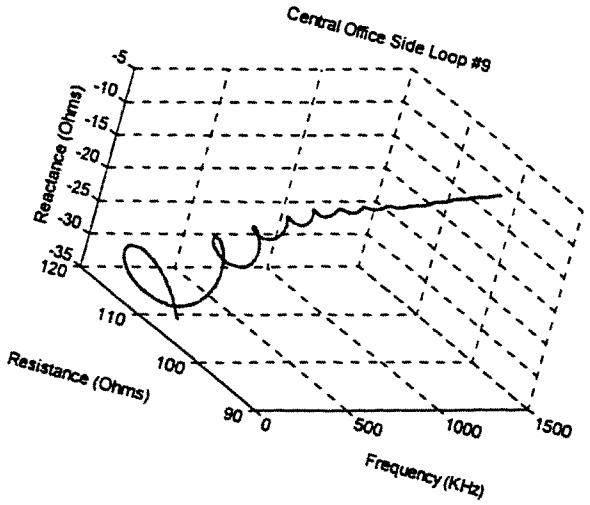

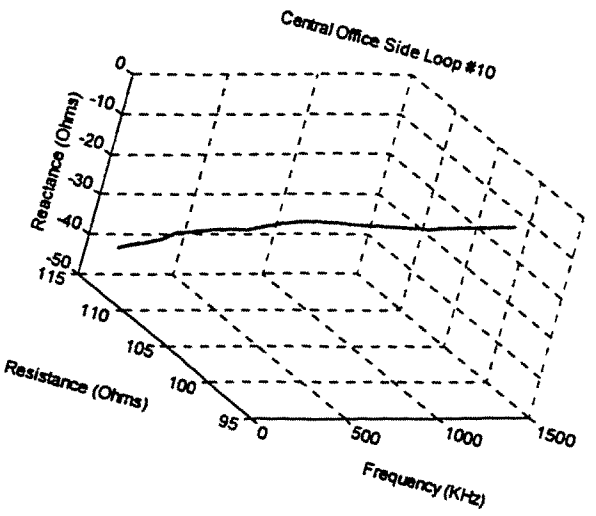

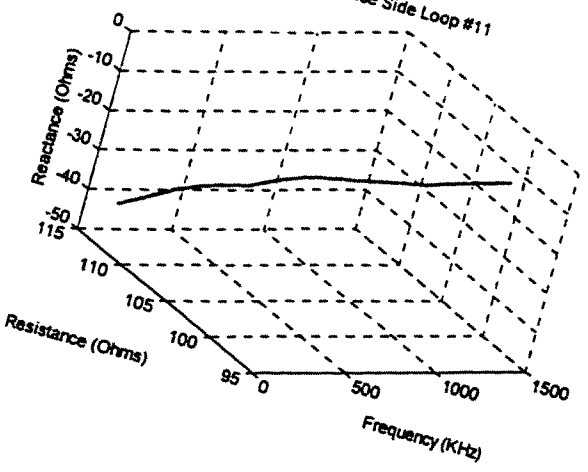

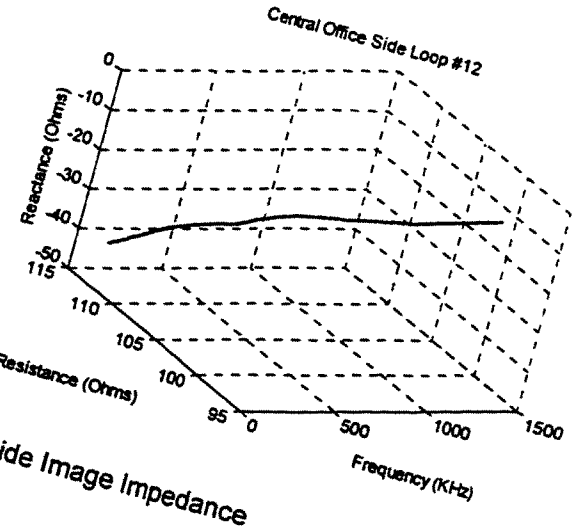

Figure 4.10: Central Office Side Image Impedance

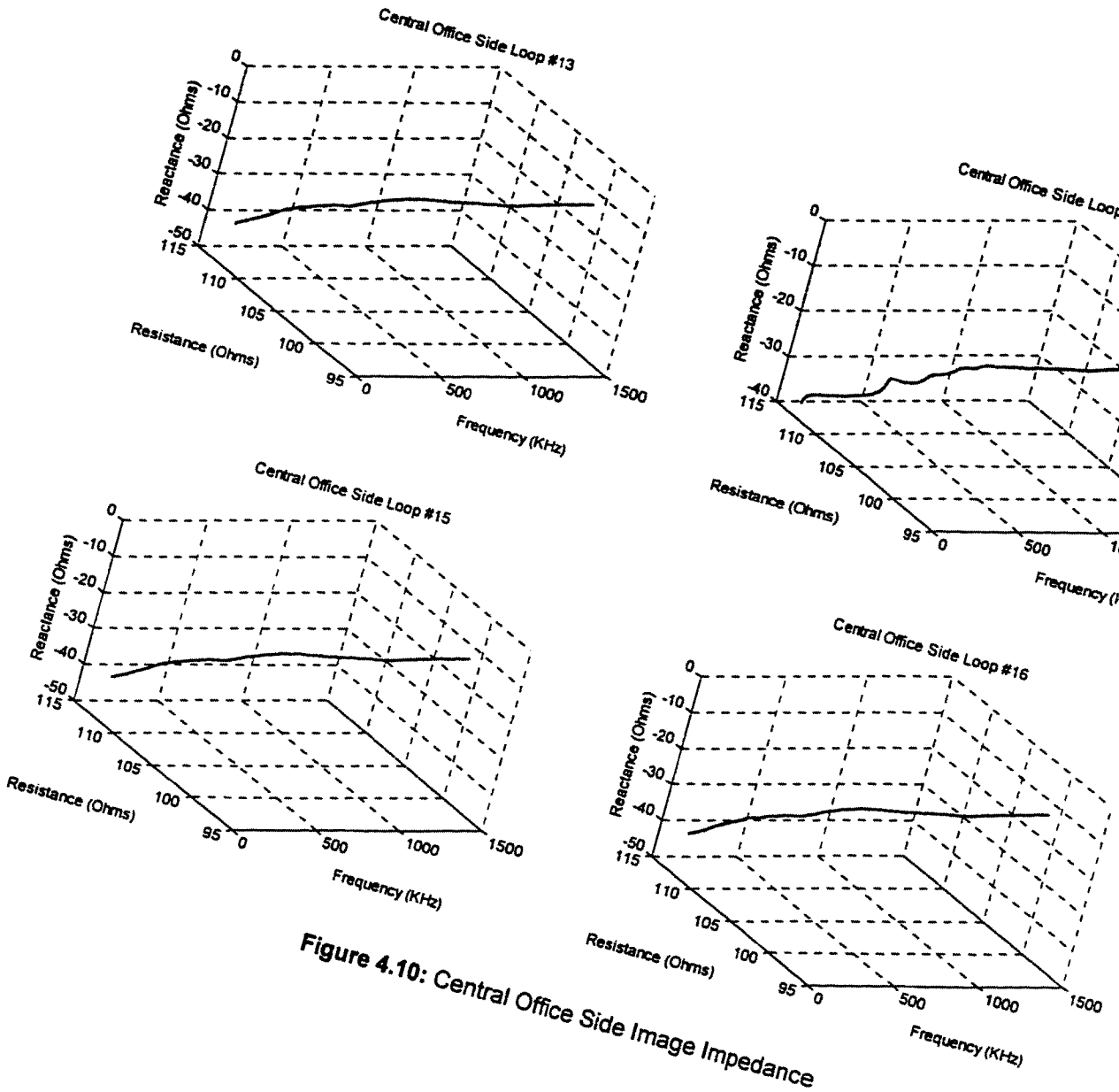

Figure 4.10: Central Office Side Image Impedance

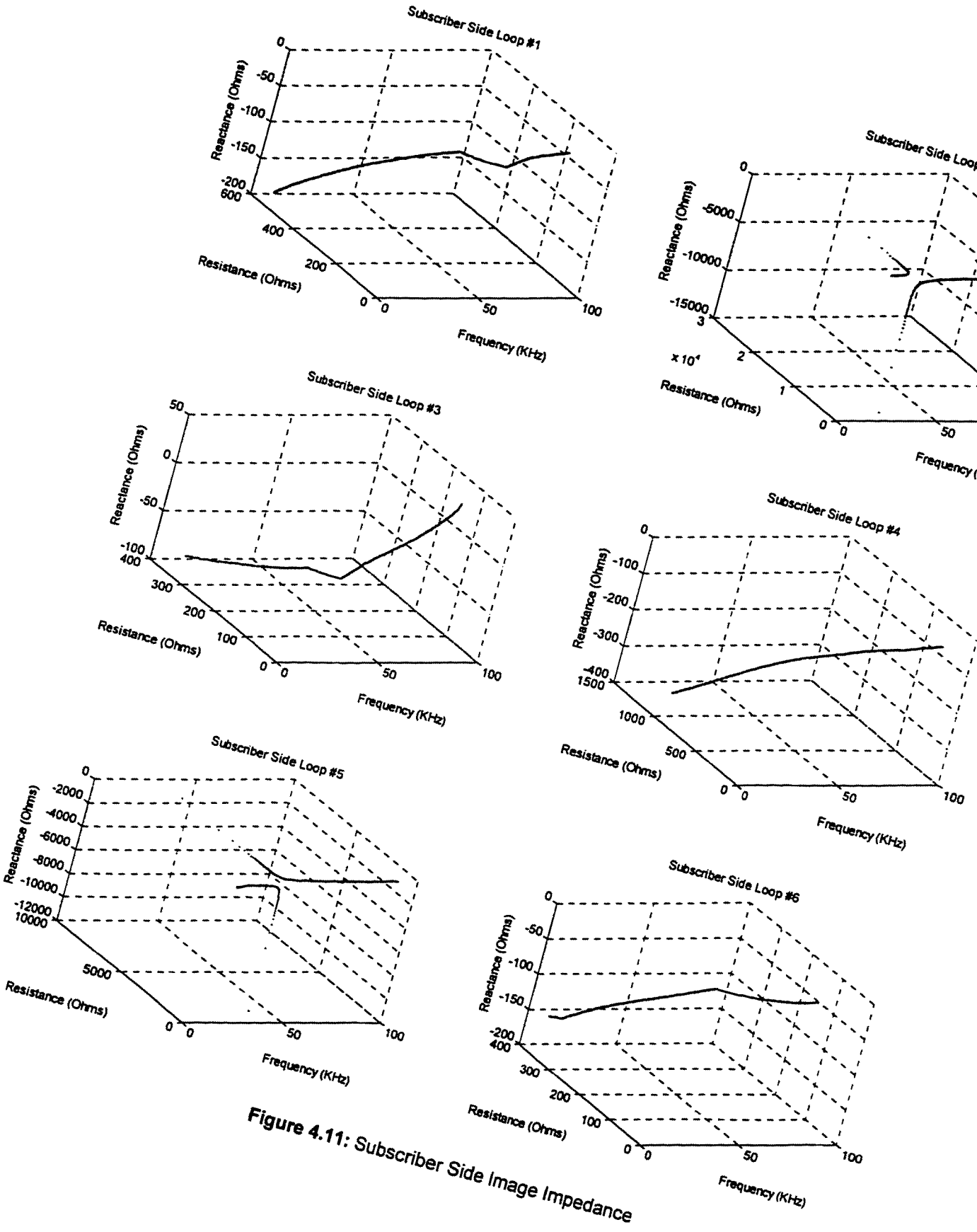

Figure 4.11: Subscriber Side Image Impedance

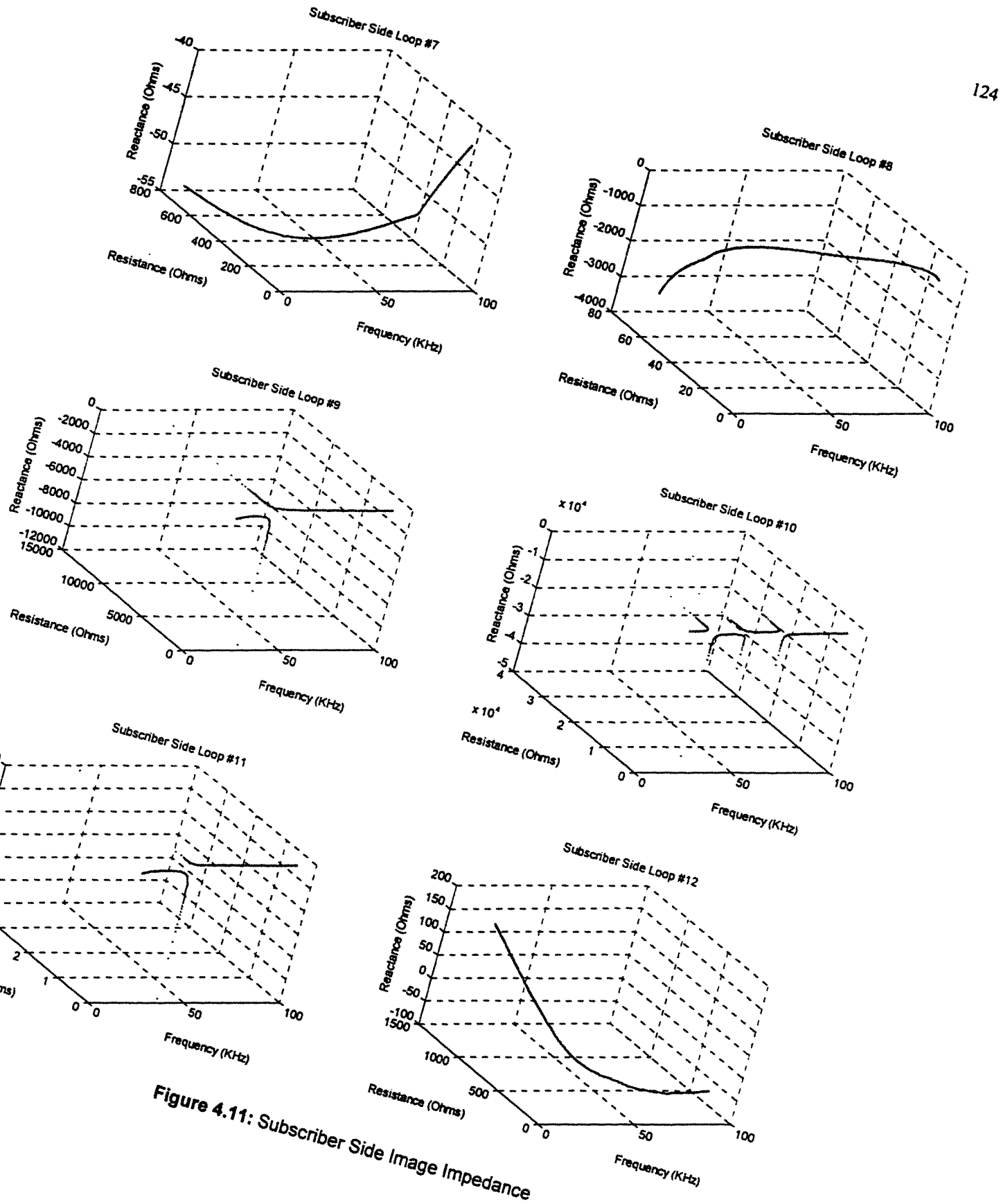

Figure 4.11: Subscriber Side Image Impedance

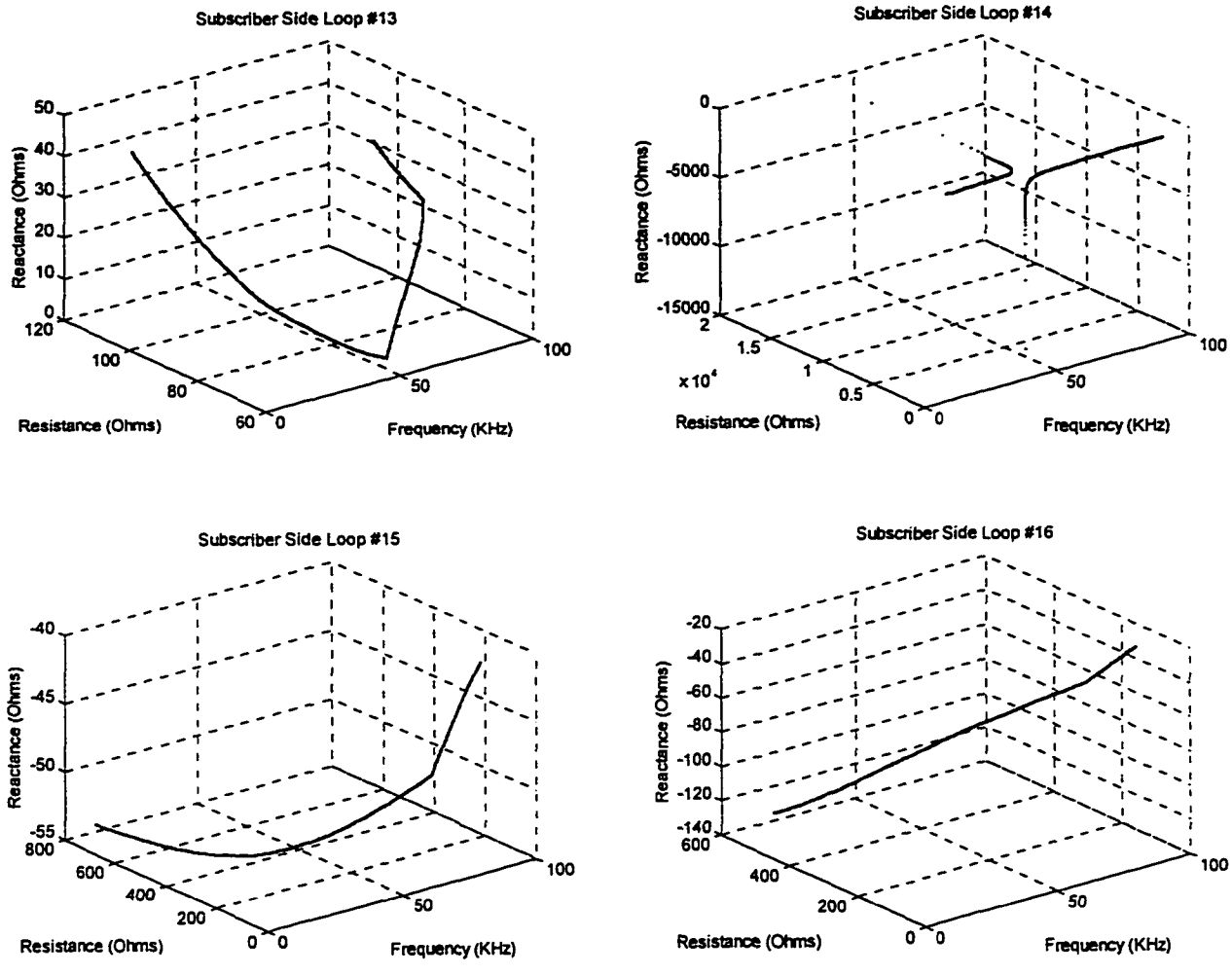

Figure 4.11: Subscriber Side Image Impedance

the plots in the figure 4.8. However for loop 9 the plot is not smooth unlike the others but is of oscillatory nature with the impedance's varying from 122 ohm to 98 ohm between the frequency range of 100 - 1350 kHz which is mainly due to the presence of three bridged taps and each of the bridged taps being of 1500' in length. The high impedance peak between 100kHz to 1350 kHz could be mainly attributed due to the presence of a bridged tap at a distance of 3000' from the Central Office side and also the gauge of the wire used is 26 AWG. A close observation of the loop also indicates the presence of a bridged tap at the distance of 3000' from the CO side of length 1500' also having a wire gauge of 26. The effect could however be reduced by reducing the length of the bridged taps specially the one closer to the CO side. In order to study the effect of the loop 9 a three dimensional plot of resistance, reactance and frequency in figure 4.10 indicates that the effect of the oscillatory nature of the plot is both due to varying resistance and reactance. The upstream channel or the reverse channel has an operating frequency range of 10 kHz to 90 kHz. From the plots of figure 4.9 which gives the plots of the image impedance of the loops v/s the frequency shows that there are at least six loops, that is loops 2,5,9,10,11 and 14 showing very high impedance's between the operating frequency range of 20 - 65 kHz. A closer look at the figure 4.11 for these loops shows that the high impedance's exhibited by these loops at certain frequencies are either due the high reactive component build up or resistive build up at that particular frequency by these heterogeneous loops, which indicates the presence of a high inductive component and

therefore a clear phase lag at some of these frequencies. In the case of loop 2 the fist peak at close to between 20 kHz and 25 kHz region is mainly due the resistive build up and when the impedance reaches its peak value the resistance falls to a very low value but the reactance which mainly the inductive component goes high and gradually decreases thereby the impedance also falls. The second peak which occurs between 60 - 65 kHz is mainly due to the resistive component buildup, that is the rise in the impedance value is due the resistance going high and when the impedance reaches its peak value starts to fall at this point the resistive component becomes very low and the reactive component goes high and then gradually decreases as shown in the loop 2 of the figure 4.11. When the reactive component is maximum the signal undergoes maximum phase lag, in addition to the signal loss. Loop 5 indicates an impedance peak between the 30 - 35 kHz region which is clearly due to the resistive component build up and once the maximum impedance is reached the resistive component value drops and the reactive component becomes large and then gradually falls which leads to the fall in the image impedance. Loop 9 between the frequency range 25 - 30 kHz and the loop 11 between the frequency range 32 - 38 kHz exhibit the same characteristics as loop 5. Loop 14 has an impedance peak between the frequency range 35 - 40 kHz, the rise in the image impedance is mainly due to the resistive component, when the impedance attains a peak value the resistive component becomes low and the reactive component goes high which then falls leading to the fall of the impedance of the loop. However the loop 10 which only has

one bridged tap has three peaks, the first peak value of the impedance lies between 20 - 25 kHz and the third peak value of the impedance lies between 55 - 60 kHz which mainly due the resistive build up and then upon the impedance attaining a high value the resistive component drops and the reactive component picks up and then falls leading to the fall of the impedance also. The second impedance peak is mainly due the reactive component build up at the frequency range 35 - 40 kHz and once the impedance attains a high value the resistive component becomes high and the reactive component falls at the impedance peak and there after the resistive component falls too with the fall in the image impedance.

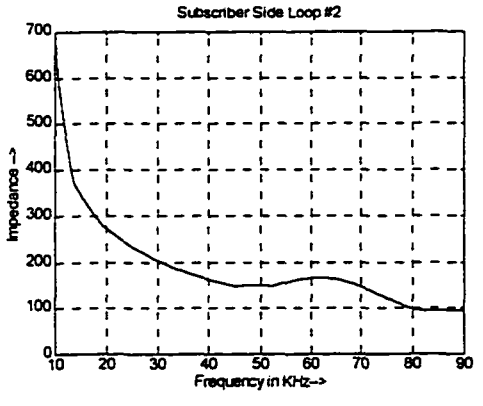

Figure 4.12 (a): Subscriber Side Image Impedance of Loop #2 with Bridged Tap moved away by 3000' from the Subscriber end

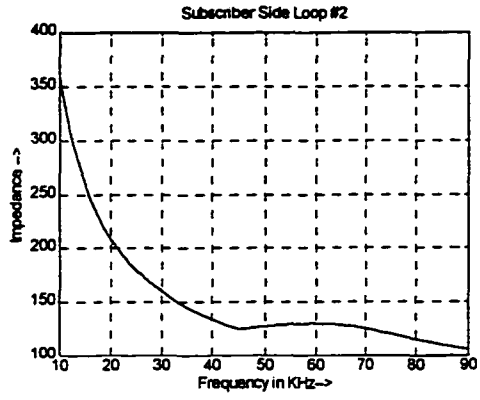

Figure 4.12 (b): Subscriber Side Image Impedance of Loop #2 with Bridged Tap moved away by 3000' from the Subscriber end and Bridged Tap length reduced by 500'

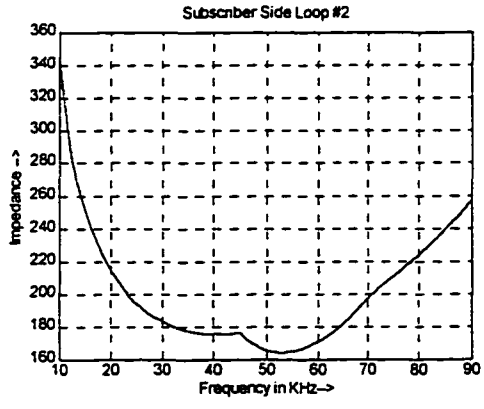

Figure 4.12 (c): Subscriber Side Image Impedance of Loop #2 with Bridged Tap length reduced by 500'

These are clearly seen from the three dimensional plots in figures 4.10 and 4.11. This high impedance phenomenon is mainly due to the presence of bridged taps at the Subscriber Side (SUB) each of length greater than 1000'.

Consider loop 2 which shows a very large impedance peak at 20 kHz and a small impedance peak at 65 kHz. These peaks could be eliminated by moving the bridged tap away from the Subscriber end. Figure 4.12 (a) shows that the image impedance for the loop 2, in which case the bridged tap is moved away from the Subscriber end by a distance of 3000' everything else being the same. Now when the bridged tap length was reduced to 500' we get the image impedance plot as shown in the figure 4.12 (b). The image loop impedance can also be reduced by reducing the length of the bridged tap only. Figure 4.12 (c) indicates that the bridged tap length of the loop 2 was reduced to 500', whereby the peak impedance occurring at 20 kHz and 65 kHz has been eliminated. From the plots discussed it can be said that in order to reduce or eliminate in most cases the impedance peaks occurring at certain frequencies the bridged tap lengths should be reduced to less than 1000' preferably to 500' at the operating frequencies ranges discussed. For the Subscriber side the other alternative is to keep the loops fixed as they are but the operating frequencies to be shifted from 10 kHz to 70 kHz and the upper limit to be shifted from 90 kHz to 150 kHz which means that the downstream channel's operating frequency range should also be shifted

accordingly to carry the same information rate using the same transmitter and receiver structures.

References

[1] G.S. Moschytz and S.V. Ahamed, "Transhybrid loss with RC Balance Circuits for Primary Rate ISDN Transmission Systems", IEEE JSAC, August 1991, Vol. 9, no. 6, pp. 951-959.

[2] S.V.Ahamed, P.P.Bohn and N.L.Gottfried, "A Tutorial on Two Wire Digital Transmission in the Loop Plant", IEEE Transactions on Communications, Vol. COM 11, Nov. 1981, pp. 1554-1564.

[3] Bellcore, "Generic Requirements for High-Bit-Rate Digital Subscriber Lines", Technical Advisory TA-NWT-001210, issue 1, Oct. 1991.

Chapter 5

Matching Function and Relaxation Methods

5.1 Matching Function

One of the primary concerns in high speed digital subscriber lines is the near-end echo. Increase of the transhybrid loss or the echo return loss of the balancing hybrid network is essential in order to reduce the near end echo in the ANSI standard loops for the ADSL environment. With the development of the services like multimedia, distance learning and video on demand, there is a need to support high speed data on the digital subscriber lines. One such technology is ADSL which has been accepted as the transitional transport access technology for the support of these services over the existing loop environment where the media is copper. The increase of the data rate over these copper loops also demands better equalization methods, spectral shaping filters, echo cancellers and matching hybrid circuits.One of the loop impairments due to the impedance mismatch of the hybrid transformer and also due to the bridge taps in the subscriber lines is the echo. Active hybrids are used to reduce the near end echo in the digital subscriber lines transmitting at higher speeds. The echo will only be reduced and needs additional digital echo cancellation circuitry for removal of the echo. The active hybrid circuitry also referred to as the balancing circuitry increases the transhybrid loss (THL) or echo return loss (ERL) which reduces the demands on

the digital echo cancellers and also on the dynamic range of the preceding A/D converter [1] [2]. The line impedance of the ANSI standard loops would be balanced by an electronic hybrid circuit consisting of RC circuits. Consider the network as shown in figure 5.1. The matching function H(s) is the transfer function of the electronic hybrid circuit also referred to as the matching network $Z_{bal}(s)$. In figure 5.1, it is shown that the signal to be transmitted V_T is fed to the input terminals of the wide band differential operational amplifier DA_1.

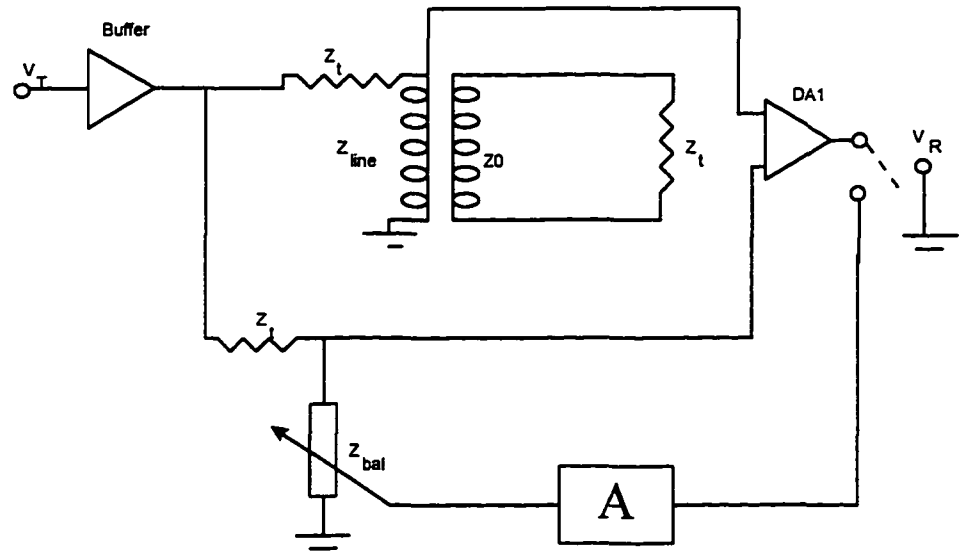

Figure 5.1: General Balancing Hybrid Circuit

The transhybrid loss (THL) or echo return loss (ERL) is the difference between the two signals $Z_{line}(s)$ and $Z_{bal}(s)$ which results due to mismatch between them. It has been shown [1][2] that for most CSA loops at T1 rates for full duplex transmission a

second order RC network would be sufficient to obtain a minimum transhybrid loss of about 20dB.

5.2 Coefficient Relaxation Method

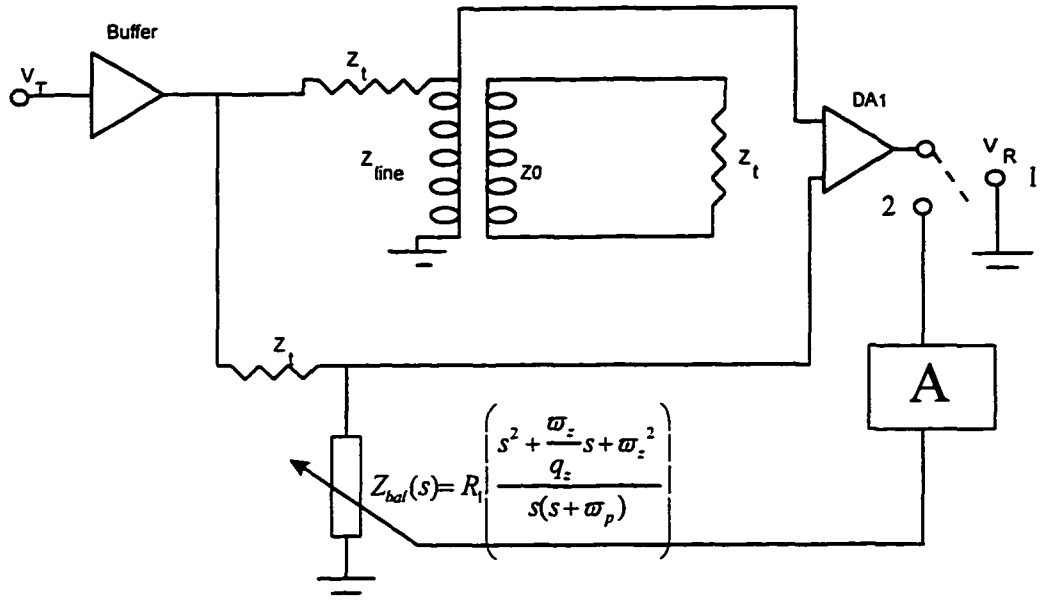

Figure 5.2: Coefficient Relaxed Balancing Hybrid Circuit

At the terminals as shown in the figure 5.2 the incoming signal across the line impedance $Z_{line}(s)$ and $Z_{bal}(s)$ are subtracted. During the initial training period the $Z_{bal}(s)$ is adjusted to match the line impedance $Z_{line}(s)$ and with the switch at position 1, only the far end receive signal V_R should ideally appear at the output of DA_1. The transhybrid loss (THL) or echo return loss (ERL) is the difference between the two signals $Z_{line}(s)$ and $Z_{bal}(s)$ which results due to mismatch between them. The balancing

of the matching circuit $Z_{bal}(s)$ takes place when the switch moves to position 2, where $Z_{bal}(s)$ tries to adjust itself to match the line impedance $Z_{line}(s)$ according to the defined adaptation algorithm. The mismatch signal also called as the error signal ER(s) from the output of the DA1 helps in the adjustment of the coefficients which are variable which form the integral part of the matching network impedance $Z_{bal}(s)$. Assuming that a second order RC circuit comprising of 2 resistors and 2 capacitors would be sufficient to attain maximum transhybrid loss for most of the CSA loops, the second order transfer function H(s) transfer function for the matching network is obtained from the figure 5.2.

$$H(s)=\frac{Z_{bal}(s)}{Z_{bal}(s)+Z_0(s)}$$

from the voltage divider function where

$$Z_{bal}(s)=R_1\left(\frac{s^2+\frac{\omega_z}{q_z}s+\omega_z{}^2}{s(s+\omega_p)}\right)$$

and

$$Z_0(s)=R_p\frac{(s+\omega_{zx})}{(s+\omega_{px})}$$

$$R_p = R_0$$

$$\omega_z^2 = \frac{1}{R_1 R_2 C_1 C_2}$$

$$\frac{\omega_z}{q_z} = \frac{R_1 C_1 + R_2 C_2 + R_2 C_1}{R_1 R_2 C_1 C_2}$$

$$\omega_p = \frac{1}{R_2 C_2}$$

$$\omega_{px} = \frac{1}{R_0}$$

$$\omega_{zx} = 1$$

From the above equations we get

$$H(s) = k\frac{b_2 s^2 + b_1 s + b_0}{a_2 s^2 + a_1 s + a_0}$$

where

$$k = \frac{R_1}{R_1 + R_p}$$

(a_0,a_1,a_2,b_0,b_1 and b_2 are coefficients).

Solving for these coefficients in terms of their RC values used in the matching circuit we obtain

$$b_2 = \omega_{px} + \frac{\omega_z}{q_z} = \frac{1}{R_0} + \frac{R_1 C_1 + R_2 C_2 + R_2 C_1}{R_1 R_2 C_1 C_2}$$

$$b_1 = \frac{\omega_{px}\omega_z}{q_z} + \omega_z^2 = \frac{1}{R_1R_2C_1C_2} + \left(1 + \frac{R_1C_1 + R_2C_2 + R_2C_1}{R_1R_2C_1C_2}\right)$$

$$b_0 = \omega_z^2\omega_{px} = \frac{1}{R_1R_2C_1C_2} + \frac{1}{R_0}$$

$$a_2 = k\left(\omega_{px} + \frac{\omega_z}{q_z} - \omega_p - \omega_{zx}\right) + \omega_p + \omega_{zx}$$

$$= \left(\frac{\omega_z}{q_z} + \omega_{px}\right)k + (\omega_{zx} + \omega_p)\frac{R_p}{(R_1 + R_p)}$$

$$= \frac{R_1}{R_1 + R_p}\left(\frac{1}{R_0} + \frac{R_1C_1 + R_2C_2 + R_2C_1}{R_1R_2C_1C_2}\right) + \frac{R_p}{R_1 + R_p}\left(\frac{1}{R_2C_2}\right)$$

$$a_1 = k\left(\omega_{px}\frac{\omega_z}{q_z} + \omega_z^2 - \omega_p\omega_{zx}\right) + \omega_p\omega_{zx}$$

$$= \frac{R_1}{R_1 + R_p} * \frac{1}{R_1R_2C_1C_2}\left(1 + \frac{R_1C_1 + R_2C_2 + R_2C_1}{R_0}\right) + \frac{R_p}{R_1 + R_p}\left(\frac{1}{R_2C_2}\right)$$

$$a_0 = k\omega_z^2\omega_{px} = \frac{R_1}{R_1 + R_p} * \frac{1}{R_1R_2C_1C_2} * \frac{1}{R_0}$$

The balancing algorithm is nothing but the determination of optimum coefficients k,a_i and b_i for i=0,1 and 2 such that

$$| H(s)| = |T(s)|$$

where

$$T(s) = Z_{line}(s)/(Z_t + Z_{line}(s)) \qquad (s=j\omega)$$

During the course of the adjustment of the coefficients for the maximum transhybrid loss the step size of the coefficients are increased or decreased according to the Least Mean Squared (LMS) algorithm or the Steepest Descent (SD) algorithm so that H(s) is brought as close as possible to T(s).

$Z_{line}(s)$ is the line impedance of a given CSA subscriber loop that is being balanced in the bridge. H(s) is the voltage transfer function of the RC voltage divider consisting of a series RC impedance $Z_0(s)$ and a parallel RC impedance $Z_{bal}(s)$. This makes it the transfer function of a rudimentary RC ladder network and as is well known the poles and zeros of H(s) must therefore lie on the negative real axis in the complex frequency plane. Whereas the question of negative real zeros is of lesser importance the fact that the poles are negative real is quite significant.

5.3 Component Relaxation Method

In this method the line response over the spectral band of interest is first determined as given by the following equation

$$T(s) = Z_{line}(s)/(Z_L + Z_{line}(s)) \qquad (s=j\omega)$$

$Z_{line}(s)$ is the line impedance of a given ANSI standard loop that is being balanced in the bridge that is $Z_{bal}(s)$.

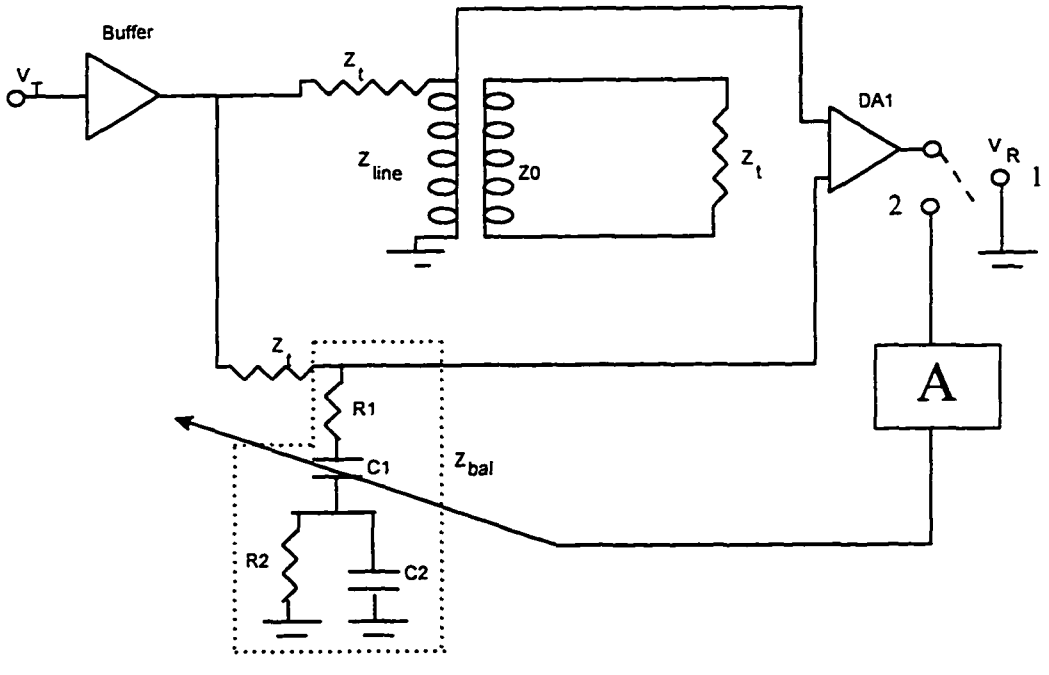

Figure 5.3: Component Relaxed Balancing Hybrid Circuit

The $Z_{bal}(s)$ network consists of the resistors R_1, R_2 and the capacitors C_1 and C_2. In figure 5.3, it is shown that the signal to be transmitted V_T is fed to the input terminals of the wide band differential operational amplifier DA_1, V_R is the received signal.

H(s) is the voltage transfer function of the RC voltage divider consisting of a series RC impedance $Z_L(s)$ and a series parallel RC impedance $Z_{bal}(s)$ and H(s) is given by

$$H(s)=\frac{Z_{bal}(s)}{Z_{bal}(s)+Z_t(s)}$$

where $Z_{bal}(s) = A + jB$. From the electronic hybrid circuit it can be shown that

$$A=R_1 + R_2/(1 + \omega^2 R_2^2 C_2^2)$$

and

$$B=1/\omega C_1 + \omega R_2^2 C_2 / (1+ \omega^2 R_2^2 C_2^2).$$

The line input response not only depends on the balancing impedance $Z_{bal}(s)$ but also on the line terminating impedance Z_L. The resistive part of the impedance is held constant at a suitable value equal to the mean of the image impedance and the reactance is computed over the entire spectral band of interest by choosing a suitable capacitance value. The line input impedance from the central office to the subscriber side is given as

$$Z_1 = (Z_L A + B) / (Z_L C + D)$$

and line input impedance from the subscriber side to the central office side is given as

$$Z_2 = (Z_L D + B) / (Z_L C + A)$$

where A, B, C and D represent the four the elements of the reduced loop matrix of the loop under consideration. The derivation of these elements and the reduction of the loop matrices and the characteristic loop impedance Z_0 and the propagation constant γ is discussed in appendix A and chap. 4.

$Z_{line}(s)$ is equal to Z_1 if the data is transmitted from the central office side to the subscriber side, and it is equal to Z_2 if the data is being transmitted from the subscriber side to the central office side. Assuming suitable initial values for the components the voltage transfer function or the matching function H(s) is computed. For these computations the value of Z_L is kept fixed at either ends. The difference in the error

$$Er(s) = | \, |H(s)| - |T(s)| \, |$$

is computed for the chosen values of the components over the spectral band of interest. From the error function the transhybrid loss is given as

$$THL = -20*\log (\text{abs} (Er(s)))$$

The curve obtained when the transhybrid loss loss obtained in dB is plotted versus the frequency in kHz has crests and troughs. The minimum point of the trough is taken as the loss for that particular iteration. The values of the components are then relaxed by the Least Mean Squared (LMS) method or by the Steepest Descent (SD) method and the process of finding the minimum point in the trough of the curve is continued for several iterations until a point of convergence is reached. The set of different values of THL obtained over the entire spectral band of interest for several iterations is taken and the maximum value obtained from these set of values is taken to be the transhybrid loss for that particular loop.

5.4 Steepest Descent Method

In the steepest descent also known as Cauchy's search method, at every iteration the derivative is computed at the current point and a unidirectional search is performed in the negative to this derivative direction to find the minimum point along the direction. The minimum point becomes the current point and the search is continued from this point. The algorithm continues until a point having a small enough gradient vector is found. This algorithm guarantees improvement in the function value at every iteration.

Algorithm

Step1 Set M equal to the maximum number of iterations to be performed, an initial point $x_{(0)}$, set k=0 and select two termination parameters ε_1, ε_2

Step 2 Calculate $\nabla f(x_{(k)})$, the first derivative at the point $x_{(k)}$.

Step 3 If $\| \nabla f(x_{(k)}) \| \leq \in_1$, Stop;

else if $k \geq M$; Stop;

else goto *Step 4*.

Step 4 Conduct a search in unidirection to find $\alpha_{(k)}$ using ε_2 such that

$f(x_{(k+1)}) = f(x_{(k)} - \alpha_{(k)} \nabla f(x_{(k)}))$ is minimum. One criterion for termination is when

$|\nabla f(x_{(k+1)}) \nabla f(x_{(k)}))| \leq \varepsilon_2$.

Step 5 Is $\frac{\| x_{(k+1)} - x_{(k)} \|}{\| x_{(k)} \|} \leq \varepsilon_1$.

else set k = k+1 and goto *Step 2.*

Since the direction $s_{(k)} = -\nabla f(x_{(k)})$ is a descent direction, the function value $f(x_{(k+1)})$ is always smaller than $f(x_{(k)})$ for positive values of $\alpha_{(k)}$. Cauchy's method works well when $x_{(0)}$ is far away for x*. When the current point is very close to the minimum, the change in the gradient vector is small. Thus, the new point created by the unidirectional search is also close to the current point. This slows the convergence process near the true minimum. Convergence can be made faster by using second-order derivatives and global convergence is achieved in this case of multivariable optimization by selectively choosing the initial values of the components in the component relaxation method and the values of the coefficients in the case of the coefficient relaxation method.

5.5 Least Mean Squared Algorithm

The Least Mean Squared (LMS) method is based on the steepest descent method.. In this method the coefficients are updated as follows

$$\mathbf{B}_{k+1} = \mathbf{B}_k - \mu\nabla_k$$

where the coefficient vector B_k is $[b_0(k), \ldots, b_l(k)]^T$ and the gradient vector

$$\nabla_k = \partial E[\varepsilon^2_k]/\partial \mathbf{B}_k$$

$$= [\partial E[\varepsilon^2_k]/\partial b_0(k) \ldots \partial E[\varepsilon^2_k]/\partial b_l(k)]^T$$

and μ is a parameter that controls the rate of convergence.. When ∇_k is known at each step of the adaptive process, the mean square error (MSE) decreases from step k to k+1. In addition once the MMSE solution is found, the gradient reaches zero so the coefficients remain at their optimal values. The approach taken in the LMS method is to use a gradient estimate on the instantaneous squared error, $\nabla_k' = \partial\varepsilon^2_k/\partial \mathbf{B}_k = 2\varepsilon_k\partial(d_k - y_k)/\partial \mathbf{B}_k$ where ε_k is the error, d_k the desired response and y_k the out response. Since the output response y_k can be expressed in terms of the input since it is dependent on it $\nabla_k' = -2\ \varepsilon_k \mathbf{X}_k$ where $\mathbf{X}_k$ is the input vector which is equal to $\mathbf{X}_k = [x_k x_{k-1} \ldots x_{k-L}]^T$. Combining all the above the LMS algorithm can be written as $\mathbf{B}_{k+1} = \mathbf{B}_k - 2\mu\varepsilon_k \nabla_k$ where μ is the convergence parameter. The convergence parameter plays an important in convergence. If μ is too small then the coefficient vector adaptation is very slow. If μ is very large then it could result in an adaptive process that never converges to the MMSE solution. Choosing an optimal value, that is choosing μ which is neither too small nor too large depending upon the process being stationary or non-stationary convergence can be obtained.

Algorithm

Step 1 Set the value of M the maximum number of iterations, the value of μ to a suitable optimal value and initialize all other variables.

Step 2 Compute the output response $y_k = \mathbf{B}_k^T \mathbf{X}_k$

If (k > M) then stop

else if ((error = $d_k - y_k$) < ε) then stop

else goto *step 3*

Step 3 $\alpha_{nk} = x_{k-n} + \sum_{l=1}^{L} b_{lk} \alpha_{n,k-l}$, $0 \le n \le L$

Step 4 $\nabla_k' = -2(d_k - y_k)\ [\alpha_{0k}, \alpha_{1k}, \ldots, \alpha_{Lk}]$

Step 5 $\mathbf{B}_{k+1} = \mathbf{B}_k - \mu \nabla_k'$ goto step 2

5.6 Mathematical Model

In the implementation and the design of the matching hybrids which are implemented in the form active filters one such problem in the incorporation as a design parameter of the sensitivity of the filter characteristics the variations in the filter components from the designed values. Hence a mathematical model is desired for the above problem and a second order filter is realized using an operational amplifier as the active device with RC components. Using the relaxation methods discussed above the values of the coefficients or the components are varied such that the error obtained is minimum and the echo return loss or the transhybrid loss in ADSL is maximum. Filter response characteristics are frequently specified in terms of gain at one or more critical frequencies and perhaps a bandwidth. These design specifications are related to the values of the coefficients of the polynomials of the transfer function,

$$H(s) = K\frac{N(s)}{D(s)} = K\frac{a_m s^m + a_{m-1}s^{m-1} + \ldots + a_0}{b_m s^m + b_{m-1}s^{m-1} + \ldots + b_0}$$

of the filter. Proper adjustments of the coefficients or the components produces the desired response. Any changes brought about by varying the values of the coefficients or the components could be used to change the filter response as a function of frequency.

The sensitivity function is defined as $S_{X_k}^{H(s)} = \frac{dH(s)/H(s)}{dX_k/X_k}$ [1][2]. Magnitude and phase sensitivities can be determined from $S_{X_k}^{H(s)}$ as

Magnitude $S_{X_k}^{|H(s)|} = \frac{dH(s)/H(s)}{dX_k/X_k} = \mathrm{Re}\{ S_{X_k}^{H(s)} \mid s = j\omega \}$

and Phase $S_{X_k}^{\arg\{H(s)\}} = \frac{dH(s)/H(s)}{dX_k/X_k} = \mathrm{Im}\{ S_{X_k}^{H(s)} \mid s = j\omega \}$ respectively.

Variation in component values also brings about changes in the poles, zeros of H(s) and also the gain constant, H(s) can be expressed as either

$$H(s) = K\frac{\sum_{i=0}^{m} a_i s^m}{\sum_{j=0}^{n} b_j s^n}$$

or in the factored form as

$$H(s) = K\frac{\prod_{i=0}^{m}(s - z_i)}{\prod_{j=0}^{n}(s - p_j)}$$

where z_i are the zeros and p_j are the poles and K is the gain constant. The zero, pole and gain constant sensitivities are defined as [1][2] are defined as

$$S_{X_k}^{z_i} = \frac{dz_i}{dX_k / X_k}$$

$$S_{X_k}^{p_j} = \frac{dp_j}{dX_k / X_k}$$

$$S_{X_k}^{K} = \frac{dK}{dX_k / X_k}$$

These root sensitivities are related to classical sensitivity by

$$S_{X_k}^{H(s)} = S_{X_k}^{G} + \sum_{i=0}^{m}\frac{S_{X_k}^{z_i}}{(s - z_i)} + \sum_{j=0}^{n}\frac{S_{X_k}^{p_j}}{(s - p_j)}$$

From the above sensitivity equation it is obvious that by knowing the poles, zeros and gain the necessary information about filter sensitivity is obtained. Utilization of root sensitivities is one of the practical way of dealing with simultaneous variations in a number of filter components. Practical considerations dictate that is realistic to assume that component variations about their design values will in general be small enough that only first order effects need be considered. Thus from the sensitivity theory for the coefficient relaxation method the sensitivity function is given by

$$\frac{\Delta H(s)}{H(s)} = S_K^{H(s)} \frac{\Delta K}{K} + \sum_{i=0}^{m} S_{A_i}^{H(s)} \frac{\Delta A_i}{A_i} + \sum_{j=0}^{n} S_{B_j}^{H(s)} \frac{\Delta B_j}{B_j}$$

where

$$S_{A_k}^{H(s)} = -\frac{A_i s^i}{D(s)}$$

$$S_{B_j}^{H(s)} = -\frac{B_j s^j}{N(s)}$$

and

$$S_K^{H(s)} = 1.$$

For the component relaxation method the sensitivity function in terms of the components is as follows

$$\frac{\Delta H(s)}{H(s)} = \sum_{i=1}^{n} S_{R_i}^{H(s)} \frac{\Delta R_i}{R_i} + \sum_{j=1}^{m} S_{C_j}^{H(s)} \frac{\Delta C_j}{C_j}$$

5.7 Simulation Setup

In this simulation setup, input databases were used to store the loop information such as the wire length and gauge information including the bridge tap information, cable parameters at different frequencies, etc. The intermediate databases hold intermediate results which are used by various other routines for further computation and analysis. The output databases hold the final results for which the simulation was carried out. These results are used for analysis and visual plots such the waveforms, constellation

plots at different bit rates. The organization of the various modules in the software is as shown in the figure 5.4. The transmission matrix method was used to model the subscriber lines. The ABCD matrices for each uniform section of the transmission line (including bridge taps) were obtained from the values of the sections primary parameters (R,L,G,C) at all the necessary frequencies. The composite matrix for the entire loop is obtained by multiplying the appropriate matrices together [Chap. 4], which includes the normal sections of the loop and the bridged taps sections of the loop.

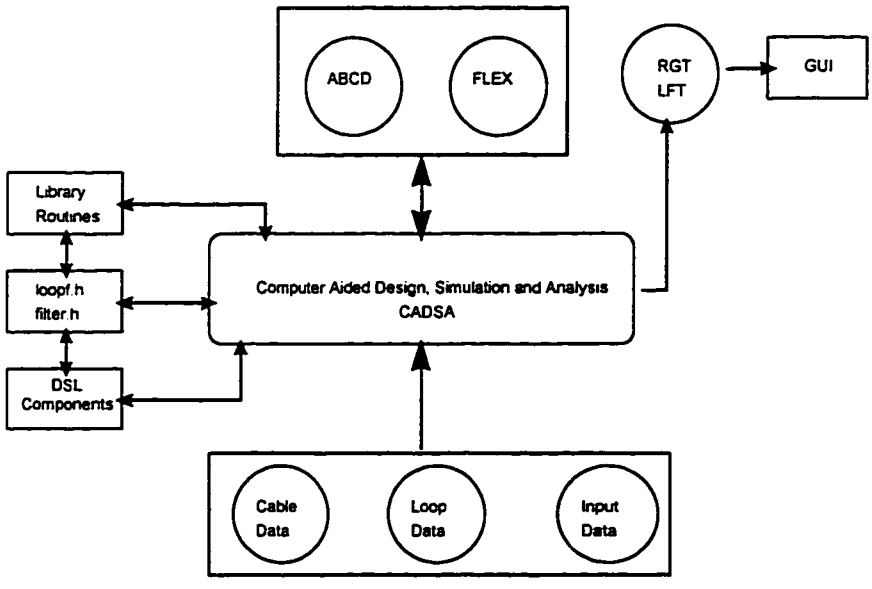

Figure 5.4: Simulation Software Setup

The impulse response of the signal paths (one for each direction of transmission) could be obtained by applying the inverse FFT to the transfer function determined

from the transmission matrix. The ABCD matrix information can easily be converted into a cable input impedance or cable transfer function. The computation of transhybrid loss is based on the accurate computation of the loop input impedance at discrete frequencies which spans the entire spectral band of interest. The bridge termination proposed depends on the line termination impedance and not on the matching impedance Z_B. The line termination impedance is represented by Z_t and is held at a constant. The line input impedance Z_1 from the central office to the subscriber can be computed as follows

$$Z_1=(Z_tA + B) / (Z_tC + D)$$

and Z_2, the line impedance from the subscriber to the central office, as

$$Z_2=(Z_tD + B) / (Z_tC + A)$$

where A, B, C and D represent the four elements of the composite ABCD loop matrix. The loops considered during the course of this simulation are the ANSI standard loops [Chap. 4].

References

[1] G.S. Moschytz and S.V. Ahamed, "Transhybrid loss with RC Balance Circuits for Primary Rate ISDN Transmission Systems", IEEE JSAC, August 1991, vol. 9, no. 6, pp. 951-959.

[2] S.V.Ahamed and G.S.Moschytz, "Optimization of the RC Matching Network in Adaptive Active Hybrids for High-Speed Data Communications", IEEE ISAS, June 1991.

[3] S.V.Ahamed, "Simulation Environments for the High-Speed Digital Subscriber Lines (HDSL)", IEEE ICC May 1993, pp. 811-815.

[4] G.S.Moschytz and Ahamed, "Transhybrid Loss with RC Balance Circuits for High Speed Full Duplex Modems", AT&T Bell Laboratories XGN360000-891214-01-TM, Dec. 1989.

[5] A.Reddy and S.V.Ahamed, "Simulation Study of CAP in High Bit Rate Asymmetrical Digital Subscriber Line (ADSL) Environment", ICCC '95, Aug. 1995, pp. 729-733.

[6] B.Widrow and S.D.Stearns, "Adaptive Signal Processing", Prentice Hall, New York.

Chapter 6

Simulation Results

6.1 Coefficient Relaxation Method

The relaxation of coefficients by this method is discussed in [Chap. 5], the results obtained, that is the transfer function obtained and the maximum transhybrid loss for both the Central Office Side and the Subscriber is presented.

6.1.1 Results at DS1 rates

The results obtained for the transfer function of the impedance matching circuit of the balancing hybrid network for the ADSL, ANSI standard loops at DS1 rates for the forward channel and 218 Kb/s for the reverse channel. The reverse channel is capable of supporting POTS at 64 Kb/s, basic rate ISDN which is 144kb/s and low speed X.25 protocol at data rates of 9.6 Kb/s which is used as the control channel. Adopting bandwidth efficient techniques and therefore using carrier-less amplitude modulation and phase modulation (CAP) which is a multilevel coding technique and using 64 CAP which maps 6 binary bits to a symbol point in the constellation. The spectral band under consideration here is 10 - 47 kHz in the reverse channel and 30 - 300 kHz in the forward channel. Using two capacitors and two resistors in the hybrid matching

circuit we obtain a second order transfer function for the balancing network. The transfer function for each of the ANSI loops is represented as follows

$$H(s)= K\frac{b_2 s^2 + b_1 s + b_0}{a_2 s^2 + a_1 s + a_0}$$

where K is a constant b_2, b_1 and b_0 are the coefficients of the numerator and a_2, a_1 and a_0 are the coefficients of the denominator.

Loop #1

Central office side

$$H(s)_{loop1}=0.8275\frac{s^2 +0.6485s+0.2108}{s^2 +0.1073s+0.2330}$$

Maximum Transhybrid Attenuation in decibels 41.81 dB

Subscriber side

$$H(s)_{loop1}=0.9091\frac{s^2 +0.6573s+0.1895}{s^2 +0.1044s+0.2457}$$

Maximum Transhybrid Attenuation in decibels 25.02 dB

Loop #2

Central Office side

$$H(s)_{loop2}=0.8275\frac{s^2 +0.6485s+0.2108}{s^2 +0.1073s+0.2330}$$

Max Transhybrid Attenuation in decibels 41.81 dB

Subscriber side

$$H(s)_{loop2}=0.8221\frac{s^2+0.6313s+0.1895}{s^2+0.1044s+0.2457}$$

Max Transhybrid Attenuation in decibels 22.13 dB

Loop #3

Central Office side

$$H(s)_{loop3}=0.8275\frac{s^2+0.6485s+0.2108}{s^2+0.1073s+0.2330}$$

Maximum Transhybrid Attenuation in decibels 41.81 dB

Subscriber side

$$H(s)_{loop3}=0.6317\frac{s^2+0.6308s+0.1895}{s^2+0.1044s+0.2457}$$

Maximum Transhybrid Attenuation in decibels 18.82 dB

Loop #4

Central office side

$$H(s)_{loop4}=0.8275\frac{s^2+0.6485s+0.2108}{s^2+0.1073s+0.2330}$$

Maximum Transhybrid Attenuation in decibels 41.81 dB

Subscriber side

$$H(s)_{loop4}=0.9458\frac{s^2+0.6573s+0.1895}{s^2+0.1044s+0.2457}$$

Maximum Transhybrid Attenuation in decibels 35.58 dB

Loop #5

Central office side

$$H(s)_{loop5}=0.8275\frac{s^2+0.6485s+0.2108}{s^2+0.1073s+0.2330}$$

Maximum Transhybrid Attenuation in decibels 41.81 dB

Subscriber side

$$H(s)_{loop5}=0.8056\frac{s^2+0.6573s+0.1895}{s^2+0.1044s+0.2457}$$

Maximum Transhybrid Attenuation in decibels 23.15 dB

Loop #6

Central office side

$$H(s)_{loop6}=0.8275\frac{s^2+0.6485s+0.2108}{s^2+0.1073s+0.2330}$$

Maximum Transhybrid Attenuation in decibels 41.52 dB

Subscriber side

$$H(s)_{loop6}=0.8389\frac{s^2+0.6447s+0.1897}{s^2+0.1045s+0.2459}$$

Maximum Transhybrid Attenuation in decibels 25.01 dB

Loop #7

Central office side

$$H(s)_{loop7}=0.8275\frac{s^2+0.6485s+0.2108}{s^2+0.1073s+0.2330}$$

Maximum Transhybrid Attenuation in decibels 41.81 dB

Subscriber side

$$H(s)_{loop7}=0.9458\frac{s^2+0.6707s+0.1695}{s^2+0.1044s+0.2457}$$

Maximum Transhybrid Attenuation in decibels 27.62 dB

Loop #8

Central office side

$$H(s)_{loop8}=0.7967\frac{s^2+0.6500s+0.1913}{s^2+0.1054s+0.2287}$$

Maximum Transhybrid Attenuation in decibels 43.05 dB

Subscriber side

$$H(s)_{loop8}=0.8644\frac{s^2+0.6000s+0.1914}{s^2+0.1054s+0.2383}$$

Maximum Transhybrid Attenuation in decibels 24.63 dB

Loop #9

Central office side

$$H(s)_{loop9}=0.8464\frac{s^2+0.6243s+0.2113}{s^2+0.1054s+0.2331}$$

Maximum Transhybrid Attenuation in decibels 33.73 dB

Subscriber side

$$H(s)_{loop9}=0.8221\frac{s^2+0.6063s+0.1895}{s^2+0.1044s+0.2457}$$

Maximum Transhybrid Attenuation in decibels 22.94 dB

Loop #10

Central office side

$$H(s)_{loop10}=0.8275\frac{s^2+0.6485s+0.2151}{s^2+0.1073s+0.2426}$$

Maximum Transhybrid Attenuation in decibels 41.49 dB

Subscriber side

$$H(s)_{loop10}=0.8056\frac{s^2+0.6707s+0.1895}{s^2+0.1044s+0.2459}$$

Maximum Transhybrid Attenuation in decibels 23.54 dB

Loop #11

Central office side

$$H(s)_{loop11}=0.8275\frac{s^2+0.6485s+0.2108}{s^2+0.1073s+0.2330}$$

Maximum Transhybrid Attenuation in decibels 41.81 dB

Subscriber side

$$H(s)_{loop11}=0.8735\frac{s^2+0.6187s+0.1895}{s^2+0.1044s+0.2457}$$

Maximum Transhybrid Attenuation in decibels 23.00 dB

Loop #12

Central office side

$$H(s)_{loop12}=0.8275\frac{s^2+0.6485s+0.2108}{s^2+0.1073s+0.2330}$$

Maximum Transhybrid Attenuation in decibels 41.81 dB

Subscriber side

$$H(s)_{loop12}=0.9273\frac{s^2+0.6573s+0.1897}{s^2+0.1045s+0.2459}$$

Maximum Transhybrid Attenuation in decibels 31.67 dB

Loop #13

Central office side

$$H(s)_{loop13}=0.8275\frac{s^2+0.6485s+0.2108}{s^2+0.1073s+0.2330}$$

Maximum Transhybrid Attenuation in decibels 41.80 dB

Subscriber side

$$H(s)_{loop13}=0.7137\frac{s^2+0.6573s+0.1895}{s^2+0.1044s+0.2457}$$

Maximum Transhybrid Attenuation in decibels 19.95 dB

Loop #14

Central office side

$$H(s)_{loop14}=0.8458\frac{s^2+0.6365s+0.2112}{s^2+0.1075s+0.2287}$$

Maximum Transhybrid Attenuation in decibels 40.87 dB

Subscriber side

$$H(s)_{loop14}=0.7431\frac{s^2+0.6447s+0.1897}{s^2+0.1045s+0.2459}$$

Maximum Transhybrid Attenuation in decibels 25.87 dB

Loop #15

Central office side

$$H(s)_{loop15}=0.8275\frac{s^2+0.6485s+0.2108}{s^2+0.1073s+0.2330}$$

Maximum Transhybrid Attenuation in decibels 41.81 dB

Subscriber side

$$H(s)_{loop15}=0.9458\frac{s^2+0.6707s+0.1859}{s^2+0.1044s+0.2457}$$

Maximum Transhybrid Attenuation in decibels 27.06 dB

Loop #16

Central office side

$$H(s)_{loop16}=0.8275\frac{s^2+0.6485s+0.2108}{s^2+0.1073s+0.2330}$$

Maximum Transhybrid Attenuation in decibels 41.81 dB

Subscriber side

$$H(s)_{loop16}=0.9273\frac{s^2+0.6447s+0.1897}{s^2+0.1045s+0.2459}$$

Maximum Transhybrid Attenuation in decibels 25.14 dB

6.1.2 Results of the DS1C rates

The following results are for the ADSL transport model which supports 3.152Mb/s in the forward channel and supports a low speed data rate of 9.6Kb/s for control purposes in the reverse channel, in addition to the basic rate ISDN of 144Kb/s and POTS as shown in figure 6.1. The spectral band for the forward channel is 40 - 645 KHz and in the reverse it is 10 - 65 KHz. For upstream 16 CAP and for the downstream 64 CAP is used.

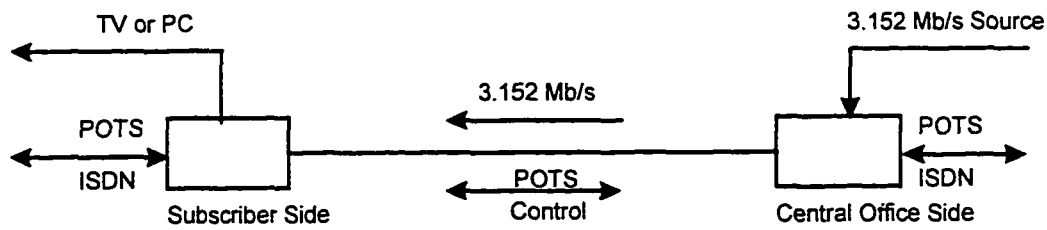

Figure 6.1: ADSL DS1C Rates Transmission Model

Loop #1

Central office side

$$H(s)_{loop1}=0.7820\frac{s^2+0.6385s+0.2739}{s^2+0.1056s+0.2339}$$

Maximum Transhybrid Attenuation in decibels 31.49 dB

Subscriber side

$$H(s)_{loop1}=0.8877\frac{s^2+0.5800s+0.1926}{s^2+0.1083s+0.2350}$$

Maximum Transhybrid Attenuation in decibels 28.35 dB

Loop #2

Central Office side

$$H(s)_{loop2}=0.7820\frac{s^2+0.6385s+0.2739}{s^2+0.1056s+0.2339}$$

Max Transhybrid Attenuation in decibels 31.49 dB

Subscriber side

$$H(s)_{loop2}=0.7498\frac{s^2+0.4168s+0.1952}{s^2+0.1119s+0.2067}$$

Max Transhybrid Attenuation in decibels 31.09 dB

Loop #3

Central Office side

$$H(s)_{loop3}=0.7820\frac{s^2+0.6385s+0.2739}{s^2+0.1056s+0.2339}$$

Maximum Transhybrid Attenuation in decibels 31.49 dB

Subscriber side

$$H(s)_{loop3}=0.5860\frac{s^2+0.5080s+0.1905}{s^2+0.1071s+0.2232}$$

Maximum Transhybrid Attenuation in decibels 19.18 dB

Loop #4

Central office side

$$H(s)_{loop4}=0.7820\frac{s^2+0.6385s+0.2739}{s^2+0.1056s+0.2339}$$

Maximum Transhybrid Attenuation in decibels 31.49 dB

Subscriber side

$$H(s)_{loop4}=0.9228\frac{s^2+0.6157s+0.1964}{s^2+0.1127s+0.2398}$$

Maximum Transhybrid Attenuation in decibels 44.22 dB

Loop #5

Central office side

$$H(s)_{loop5}=0.7820\frac{s^2+0.6385s+0.2739}{s^2+0.1056s+0.2339}$$

Maximum Transhybrid Attenuation in decibels 31.49 dB

Subscriber side

$$H(s)_{loop5}=0.7201\frac{s^2+0.4428s+0.2023}{s^2+0.1214s+0.2067}$$

Maximum Transhybrid Attenuation in decibels 37.34 dB

Loop #6

Central office side

$$H(s)_{loop6}=0.7820\frac{s^2+0.6385s+0.2739}{s^2+0.1056s+0.2339}$$

Maximum Transhybrid Attenuation in decibels 31.49 dB

Subscriber side

$$H(s)_{loop6}=0.8110\frac{s^2+0.5517s+0.1908}{s^2+0.1073s+0.2281}$$

Maximum Transhybrid Attenuation in decibels 29.28 dB

Loop #7

Central office side

$$H(s)_{loop7}=0.7820\frac{s^2+0.6385s+0.2739}{s^2+0.1056s+0.2339}$$

Maximum Transhybrid Attenuation in decibels 31.49 dB

Subscriber side

$$H(s)_{loop7}=0.9451\frac{s^2+0.5818s+0.1934}{s^2+0.1087s+0.2408}$$

Maximum Transhybrid Attenuation in decibels 33.72 dB

Loop #8

Central office side

$$H(s)_{loop8}=0.7571\frac{s^2+0.6432s+0.2549}{s^2+0.1042s+0.2356}$$

Maximum Transhybrid Attenuation in decibels 31.74 dB

Subscriber side

$$H(s)_{loop8}=0.8451\frac{s^2+0.4891s+0.1949}{s^2+0.1118s+0.2149}$$

Maximum Transhybrid Attenuation in decibels 37.05 dB

Loop #9

Central office side

$$H(s)_{loop9}=0.7895\frac{s^2+0.6442s+0.2709}{s^2+0.1065s+0.2313}$$

Maximum Transhybrid Attenuation in decibels 30.05 dB

Subscriber side

$$H(s)_{loop9}=0.7474\frac{s^2+0.4883s+0.2067}{s^2+0.1243s+0.2189}$$

Maximum Transhybrid Attenuation in decibels 32.52 dB

Loop #10

Central office side

$$H(s)_{loop10}=0.7820\frac{s^2+0.6385s+0.2739}{s^2+0.1056s+0.2339}$$

Maximum Transhybrid Attenuation in decibels 31.49 dB

Subscriber side

$$H(s)_{loop10}=0.7876\frac{s^2+0.5358s+0.1930}{s^2+0.1085s+0.2307}$$

Maximum Transhybrid Attenuation in decibels 27.90 dB.

Loop #11

Central office side

$$H(s)_{loop11}=0.7820\frac{s^2+0.6385s+0.2739}{s^2+0.1056s+0.2339}$$

Maximum Transhybrid Attenuation in decibels 31.49 dB

Subscriber side

$$H(s)_{loop11}=0.7633\frac{s^2+0.4243s+0.2027}{s^2+0.1211s+0.2021}$$

Maximum Transhybrid Attenuation in decibels 38.12 dB

Loop #12

Central office side

$$H(s)_{loop12}=0.7820\frac{s^2+0.6385s+0.2739}{s^2+0.1056s+0.2339}$$

Maximum Transhybrid Attenuation in decibels 31.49 dB

Subscriber side

$$H(s)_{loop12}=0.9273\frac{s^2+0.6313s+0.1934}{s^2+0.1109s+0.2457}$$

Maximum Transhybrid Attenuation in decibels 35.66 dB

Loop #13

Central office side

$$H(s)_{loop13}=0.7820\frac{s^2+0.6385s+0.2739}{s^2+0.1056s+0.2339}$$

Maximum Transhybrid Attenuation in decibels 31.49 dB

Subscriber side

$$H(s)_{loop13}=0.6944\frac{s^2+0.6526s+0.1920}{s^2+0.1079s+0.2439}$$

Maximum Transhybrid Attenuation in decibels 19.46 dB

Loop #14

Central office side

$$H(s)_{loop14}=0.7694\frac{s^2+0.6542s+0.2750}{s^2+0.1060s+0.2445}$$

Maximum Transhybrid Attenuation in decibels 31.64 dB

Subscriber side

$$H(s)_{loop14}=0.7431\frac{s^2+0.6447s+0.1897}{s^2+0.1045s+0.2459}$$

Maximum Transhybrid Attenuation in decibels 25.87 dB

Loop #15

Central office side

$$H(s)_{loop15}=0.7820\frac{s^2+0.6385s+0.2739}{s^2+0.1056s+0.2339}$$

Maximum Transhybrid Attenuation in decibels 31.49 dB

Subscriber side

$$H(s)_{loop15}=0.9451\frac{s^2+0.5818s+0.1934}{s^2+0.1087s+0.2408}$$

Maximum Transhybrid Attenuation in decibels 33.72 dB

Loop #16

Central office side

$$H(s)_{loop16}=0.7820\frac{s^2+0.6385s+0.2739}{s^2+0.1056s+0.2339}$$

Maximum Transhybrid Attenuation in decibels 31.49 dB

Subscriber side

$$H(s)_{loop16}=0.8792\frac{s^2+0.5298s+0.1949}{s^2+0.1118s+0.2237}$$

Maximum Transhybrid Attenuation in decibels 33.58 dB

In the above transfer functions the coefficient b_1 is scaled by 10^7, the coefficient b_0 is scaled by 10^{13}, the coefficients a_1 is scaled by 10^8 and the coefficient a_0 is scaled by 10^{13}.

6.1.3 Results of the DS2 rates

The results obtained for the DS2 rates in the forward channel which is 6.312 Mb/s and in the reverse channel data rates at 384 kb/s using the coefficient relaxation method are presented. The modulation considered here for the transmission of data both in the forward and the reverse channel is the 64 carrierless amplitude modulation / phase modulation (CAP). Using 64 CAP at an excess bandwidth of 15 % the band used for the forward channel is 70 kHz to 1320 kHz and in the reverse channel the band utilized assuming the use of the 64 CAP is 10 kHz to 90 kHz. The band 10 - 90 kHz is used as a bi-directional channel having the capacity to handle video telephony. In the following transfer functions the coefficient b_1 is scaled by 10^7, the coefficient b_0 is scaled by 10^{13}, the coefficients a_1 is scaled by 10^8 and the coefficient a_0 is scaled by 10^{13}.

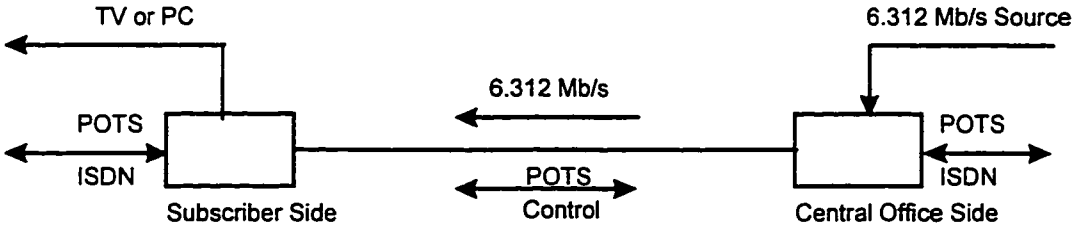

Figure 6.2: ADSL DS2 Rates Transmission Model

Loop #1

Central office side

$$H(s)_{loop1} = 0.7024\frac{s^2 + 0.6474s + 0.5930}{s^2 + 0.1050s + 0.5171}$$

Maximum Transhybrid Attenuation in decibels 23.86 dB

Subscriber side

$$H(s)_{loop1} = 0.8877\frac{s^2 + 0.5800s + 0.1926}{s^2 + 0.1083s + 0.2350}$$

Maximum Transhybrid Attenuation in decibels 28.35 dB

Loop #2

Central Office side

$$H(s)_{loop2} = 0.7029\frac{s^2 + 0.6474s + 0.5930}{s^2 + 0.1050s + 0.5171}$$

Max Transhybrid Attenuation in decibels 23.86 dB

Subscriber side

$$H(s)_{loop2} = 0.6616\frac{s^2 + 0.4500s + 0.2194}{s^2 + 0.1338s + 0.1862}$$

Max Transhybrid Attenuation in decibels 27.69 dB

Loop #3

Central Office side

$$H(s)_{loop3} = 0.7029\frac{s^2 + 0.6606s + 0.5930}{s^2 + 0.1072s + 0.5171}$$

Maximum Transhybrid Attenuation in decibels 24.21 dB

Subscriber side

$$H(s)_{loop3} = 0.5879\frac{s^2 + 0.4995s + 0.1873}{s^2 + 0.1032s + 0.2230}$$

Maximum Transhybrid Attenuation in decibels 18.67 dB

Loop #4

Central office side

$$H(s)_{loop4} = 0.7029\frac{s^2 + 0.6606s + 0.5903}{s^2 + 0.1072s + 0.5171}$$

Maximum Transhybrid Attenuation in decibels 24.21 dB

Subscriber side

$$H(s)_{loop4} = 0.9040\frac{s^2 + 0.6272s + 0.2003}{s^2 + 0.1126s + 0.2396}$$

Maximum Transhybrid Attenuation in decibels 43.85 dB

Loop #5

Central office side

$$H(s)_{loop5} = 0.7029\frac{s^2 + 0.6474s + 0.5930}{s^2 + 0.1050s + 0.2396}$$

Maximum Transhybrid Attenuation in decibels 23.86 dB

Subscriber side

$$H(s)_{loop5} = 0.6751\frac{s^2 + 0.5080s + 0.2149}{s^2 + 0.1338s + 0.2019}$$

Maximum Transhybrid Attenuation in decibels 32.21 dB

Loop #6

Central office side

$$H(s)_{loop6} = 0.7024\frac{s^2 + 0.6606s + 0.5811}{s^2 + 0.1072s + 0.4964}$$

Maximum Transhybrid Attenuation in decibels 24.21 dB

Subscriber side

$$H(s)_{loop6} = 0.8162\frac{s^2 + 0.5666s + 0.1959}{s^2 + 0.1124s + 0.2343}$$

Maximum Transhybrid Attenuation in decibels 30.12 dB

Loop #7

Central office side

$$H(s)_{loop7} = 0.7029\frac{s^2 + 0.6474s + 0.5903}{s^2 + 0.1050s + 0.5171}$$

Maximum Transhybrid Attenuation in decibels 23.86 dB

Subscriber side

$$H(s)_{loop7} = 0.9258\frac{s^2 + 0.5814s + 0.1931}{s^2 + 0.1064s + 0.2356}$$

Maximum Transhybrid Attenuation in decibels 33.64 dB

Loop #8

Central office side

$$H(s)_{loop8} = 0.6933\frac{s^2 + 0.6391s + 0.4323}{s^2 + 0.1036s + 0.2437}$$

Maximum Transhybrid Attenuation in decibels 24.10 dB

Subscriber side

$$H(s)_{loop8} = 0.7801\frac{s^2 + 0.5753s + 0.2114}{s^2 + 0.1288s + 0.2024}$$

Maximum Transhybrid Attenuation in decibels 30.97 dB

Loop #9

Central office side

$$H(s)_{loop9} = 0.7052\frac{s^2 + 0.5097s + 0.2201}{s^2 + 0.1315s + 0.2125}$$

Maximum Transhybrid Attenuation in decibels 34.60 dB

Subscriber side

$$H(s)_{loop9} = 0.7052\frac{s^2 + 0.5097s + 0.2201}{s^2 + 0.1315s + 0.2152}$$

Maximum Transhybrid Attenuation in decibels 34.60 dB

Loop #10

Central office side

$$H(s)_{loop10} = 0.7029\frac{s^2 + 0.6474s + 0.5930}{s^2 + 0.1050s + 0.5175}$$

Maximum Transhybrid Attenuation in decibels 23.86 dB

Subscriber side

$$H(s)_{loop10} = 0.7331\frac{s^2 + 0.5744s + 0.2070}{s^2 + 0.1236s + 0.2193}$$

Maximum Transhybrid Attenuation in decibels 34.24 dB.

Loop #11

Central office side

$$H(s)_{loop11} = 0.7029\frac{s^2 + 0.6474s + 0.5930}{s^2 + 0.1050s + 0.5171}$$

Maximum Transhybrid Attenuation in decibels 23.86 dB

Subscriber side

$$H(s)_{loop11} = 0.7172\frac{s^2 + 0.4782s + 0.2150}{s^2 + 0.1312s + 0.2019}$$

Maximum Transhybrid Attenuation in decibels 30.76 dB

Loop #12

Central office side

$$H(s)_{loop12} = 0.7029\frac{s^2 + 0.6606s + 0.5930}{s^2 + 0.1072s + 0.6171}$$

Maximum Transhybrid Attenuation in decibels 24.21 dB

Subscriber side

$$H(s)_{loop12} = 0.8968\frac{s^2 + 0.6617s + 0.1949}{s^2 + 0.1140s + 0.2377}$$

Maximum Transhybrid Attenuation in decibels 37.23db

Loop #13

Central office side

$$H(s)_{loop13} = 0.7029\frac{s^2 + 0.6474s + 0.5930}{s^2 + 0.1050s + 0.5171}$$

Maximum Transhybrid Attenuation in decibels 23.86 dB

Subscriber side

$$H(s)_{loop13} = 0.6905\frac{s^2 + 0.5986s + 0.1871}{s^2 + 0.1031s + 0.2439}$$

Maximum Transhybrid Attenuation in decibels 20.01 dB

Loop #14

Central office side

$$H(s)_{loop14} = 0.7029\frac{s^2 + 0.6606s + 0.5566}{s^2 + 0.1072s + 0.4586}$$

Maximum Transhybrid Attenuation in decibels 24.20 dB

Subscriber side

$$H(s)_{loop14} = 0.7213\frac{s^2 + 0.6380s + 0.1956}{s^2 + 0.1078s + 0.2436}$$

Maximum Transhybrid Attenuation in decibels 23.86 dB

Loop #15

Central office side

$$H(s)_{loop15} = 0.7029\frac{s^2 + 0.6474s + 0.5930}{s^2 + 0.1050s + 0.5171}$$

Maximum Transhybrid Attenuation in decibels 23.86 dB

Subscriber side

$$H(s)_{loop15} = 0.9258\frac{s^2 + 0.5814s + 0.1931}{s^2 + 0.1064s + 0.2356}$$

Maximum Transhybrid Attenuation in decibels 33.61 dB

Loop #16

Central office side

$$H(s)_{loop16} = 0.7029\frac{s^2 + 0.6606s + 0.5811}{s^2 + 0.1072s + 0.4968}$$

Maximum Transhybrid Attenuation in decibels 24.21 dB

Subscriber side

$$H(s)_{loop16} = 0.8672\frac{s^2 + 0.5226s + 0.2001}{s^2 + 0.1148s + 0.2252}$$

Maximum Transhybrid Attenuation in decibels 34.61 dB

6.2 Component Relaxation Method

The results obtained from the component relaxation method give the best values for the RC components used in the matching circuit which results in the maximum transhybrid loss for the loop under study. In determining the maximum transhybrid loss a second order transfer function is assumed to be sufficient for the matching hybrid circuit for each of the loops. The technique used in order to relax the values of the components is as discussed in chapter 5.

6.2.1 Results of DS1 rates

The data rates are 1.544 Mbps in the forward channel and a very speed 9.6 Kbps reverse channel. The spectral band of interest is therefore 10 - 47 KHz in the reverse channel and 30 - 300 KHz in the forward channel using 64 CAP. The component values along with the maximum THL both at the Central Office (CO) side and the subscriber (SUBS) is given for all the sixteen loops.

Loop # 1

Side	*R1*	*C1*	*R2*	*C2*	*THL*
CO	109.9	0.150	80	0.08	34.48
SUBS	112.7	0.150	80	0.08	29.10

Loop # 2

Side	*R1*	*C1*	*R2*	*C2*	*THL*
CO	109.	0.150	80	0.08	34.48
SUBS	112.7	0.150	80	0.08	17.61

Loop # 3

Side	R1	C1	R2	C2	THL
CO	109.9	0.150	80	0.08	34.35
SUBS	112.7	0.150	80	0.08	10.07

Loop # 4

Side	R1	C1	R2	C2	THL
CO	109.9	0.150	80	0.08	34.34
SUBS	143.5	0.1101	68.47	0.0994	26.73

Loop # 5

Side	R1	C1	R2	C2	THL
CO	109.9	0.150	80	0.08	34.52
SUBS	112.7	0.150	80	0.08	17.76

Loop # 6

Side	R1	C1	R2	C2	THL
CO	109.9	0.150	80	0.08	35.53
SUBS	112.7	0.150	80	0.08	213

Loop # 7

Side	R1	C1	R2	C2	THL
CO	109.9	0.150	80	0.08	34.48
SUBS	140.3	0.0900	63.46	0.1483	24.18

Loop # 8

Side	R1	C1	R2	C2	THL
CO	112.7	0.150	80	0.08	33.90
SUBS	109.9	0.150	80	0.08	26.10

Loop # 9

Side	R1	C1	R2	C2	THL
CO	109.9	0.150	80	0.08	26.57
SUBS	112.7	0.150	80	0.08	18.10

Loop # 10

Side	R1	C1	R2	C2	THL
CO	109.9	0.150	80	0.08	34.34
SUBS	112.7	0.150	80	0.08	19.57

Loop # 11

Side	R1	C1	R2	C2	THL
CO	109.9	0.150	80	0.08	34.46
SUBS	112.7	0.150	80	0.08	19.45

Loop # 12

Side	*R1*	*C1*	*R2*	*C2*	*THL*
CO	109.9	0.150	80	0.08	34.37
SUBS	133.4	0.1074	58.75	0.0947	30.07

Loop # 13

Side	*R1*	*C1*	*R2*	*C2*	*THL*
CO	109.9	0.150	80	0.08	34.45
SUBS	115.6	0.15076	80	0.08	24.43

Loop # 14

Side	*R1*	*C1*	*R2*	*C2*	*THL*
CO	109.9	0.150	80	0.08	31.65
SUBS	112.7	0.150	80	0.08	17.17

Loop # 15

Side	*R1*	*C1*	*R2*	*C2*	*THL*
CO	109.9	0.150	80	0.08	34.46
SUBS	140.3	0.0900	63.46	0.1483	24.17

Loop # 16

Side	*R1*	*C1*	*R2*	*C2*	*THL*
CO	109.9	0.150	80	0.08	34.45
SUBS	115.6	0.15076	80	0.08	24.43

The values of the resistors R1 and R2 are in ohms and the capacitors C1 and C2 are in micro farads. The THL is in decibels.

6.2.2 Results of DS1C Rates

The data rates at which simulation was carried are the same as explained in section 6.1.1 both for the forward and reverse channel.

Loop # 1

Side	*R1*	*C1*	*R2*	*C2*	*THL*
CO	112.7	0.150	80	0.08	36.09
SUBS	109.9	0.150	80	0.08	26.45

Loop # 2

Side	*R1*	*C1*	*R2*	*C2*	*THL*
CO	112.7	0.150	80	0.08	36.09
SUBS	112.7	0.150	80	0.08	14.39

Loop # 3

Side	*R1*	*C1*	*R2*	*C2*	*THL*
CO	112.7	0.150	80	0.08	36.09
SUBS	112.7	0.150	80	0.08	9.98

Loop # 4

Side	*R1*	*C1*	*R2*	*C2*	*THL*
CO	112.7	0.150	80	0.08	36.09
SUBS	126.9	0.097	75.83	0.0994	26.73

Loop # 5

Side	*R1*	*C1*	*R2*	*C2*	*THL*
CO	112.7	0.150	80	0.08	36.09
SUBS	112.7	0.150	80	0.08	14.29

Loop # 6

Side	*R1*	*C1*	*R2*	*C2*	*THL*
CO	112.7	0.150	80	0.08	36.08
SUBS	112.7	0.150	80	0.08	20.86

Loop # 7

Side	*R1*	*C1*	*R2*	*C2*	*THL*
CO	112.7	0.150	80	0.08	36.09
SUBS	123.9	0.0900	73.69	0.1126	24.18

Loop # 8

Side	*R1*	*C1*	*R2*	*C2*	*THL*
CO	112.7	0.150	80	0.08	33.64
SUBS	112.7	0.150	80	0.08	21.15

Loop # 9

Side	*R1*	*C1*	*R2*	*C2*	*THL*
CO	109.9	0.149	80	0.08	31.81
SUBS	112.7	0.150	80	0.08	15.60

Loop # 10

Side	*R1*	*C1*	*R2*	*C2*	*THL*
CO	112.7	0.150	80	0.08	36.09
SUBS	112.7	0.150	80	0.08	18.62

Loop # 11

Side	*R1*	*C1*	*R2*	*C2*	*THL*
CO	112.7	0.150	80	0.08	36.09
SUBS	112.7	0.150	80	0.08	14.86

Loop # 12

Side	*R1*	*C1*	*R2*	*C2*	*THL*
CO	112.7	0.150	80 Ω	0.08	34.37
SUBS	133.4	0.1074	58.75	0.0947	30.07

Loop # 13

Side	*R1*	*C1*	*R2*	*C2*	*THL*
CO	112.7	0.150	80	0.08	36.09
SUBS	112.7	0.150	80	0.08	13.46

Loop # 14

Side	*R1*	*C1*	*R2*	*C2*	*THL*
CO	112.7	0.150	80	0.08	36.16
SUBS	112.7	0.150	80	0.08	17.17

Loop # 15

Side	*R1*	*C1*	*R2*	*C2*	*THL*
CO	112.7	0.150	80	0.08	36.09
SUBS	123.9	0.0900	73.69	0.112	24.17

Loop # 16

Side	*R1*	*C1*	*R2*	*C2*	*THL*
CO	112.7	0.150	80	0.08	36.09
SUBS	109.9	0.150	80	0.08	24.43

The values of the resistors R1 and R2 are in ohms and the capacitors C1 and C2 are in micro farads. The THL is in decibels.

6.2.3 Results of DS2 rates

In this case the spectral band of interest is 10 - 90 kHz for the reverse channel and 70 - 1320 kHz for the forward channel. Since 64 CAP is used with an excess bandwitdh of 15% the total data rate is 6.312 Mbps for the forward channel and 384 Kbps for the reverse channel. The band between 10 - 95 kHz is a bi-directional channel.

Loop # 1

Side	*R1*	*C1*	*R2*	*C2*	*THL*
CO	112.7	0.150	80	0.08	32.69
SUBS	109.0	0.150	80	0.08	26.45

Loop # 2

Side	*R1*	*C1*	*R2*	*C2*	*THL*
CO	112.7	0.150	80	0.08	32.69
SUBS	112.7	0.150	80	0.08	12.72

Loop # 3

Side	*R1*	*C1*	*R2*	*C2*	*THL*
CO	112.7	0.150	80	0.08	32.69
SUBS	112.7	0.150	80	0.08	9.98

Loop # 4

Side	*R1*	*C1*	*R2*	*C2*	*THL*
CO	112.7	0.150	80	0.08	32.68
SUBS	120.7	0.097	77.51	0.7175	27.23

Loop # 5

Side	*R1*	*C1*	*R2*	*C2*	*THL*
CO	112.7	0.150	80	0.08	32.69
SUBS	112.7	0.150	80	0.08	13.11

Loop # 6

Side	*R1*	*C1*	*R2*	*C2*	*THL*
CO	112.7	0.150	80	0.08	32.69
SUBS	112.7	0.150	80	0.08	20.81

Loop # 7

Side	R1	C1	R2	C2	THL
CO	112.7	0.150	80	0.08	32.69
SUBS	117.9	0.087	73.73	0.104	24.18

Loop # 8

Side	R1	C1	R2	C2	THL
CO	112.7	0.150	80	0.08	31.33
SUBS	112.7	0.150	80	0.08	18.98

Loop # 9

Side	R1	C1	R2	C2	THL
CO	112.7	0.150	80	0.08	32.74
SUBS	112.7	0.150	80	0.08	14.30

Loop # 10

Side	R1	C1	R2	C2	THL
CO	112.7	0.150	80	0.08	32.69
SUBS	112.7	0.150	80	0.08	17.96

Loop # 11

Side	R1	C1	R2	C2	THL
CO	112.7	0.150	80	0.08	32.69
SUBS	112.7	0.150	80	0.08	13.44

Loop # 12

Side	R1	C1	R2	C2	THL
CO	112.7	0.150	80 Ω	0.08	32.69
SUBS	120.7	0.1074	58.75	0.0947	30.07

Loop # 13

Side	R1	C1	R2	C2	THL
CO	112.7	0.150	80	0.08	32.69
SUBS	112.7	0.150	80	0.08	13.76

Loop # 14

Side	R1	C1	R2	C2	THL
CO	112.7	0.150	80	0.08	32.69
SUBS	112.7	0.150	80	0.08	17.59

Loop # 15

Side	R1	C1	R2	C2	THL
CO	112.7	0.150	80	0.08	32.69
SUBS	117.9	0.8781	73.69	0.112	24.17

Loop # 16

Side	*R1*	*C1*	*R2*	*C2*	*THL*
CO	112.7	0.150	80	0.08	32.69
SUBS	112.7	0.150	80	0.08	24.43

The values of the resistors R1 and R2 are in ohms and the capacitors C1 and C2 are in micro farads. The THL is in decibels.

6.3 Discussion

We compare the results obtained by the component relaxation method with that of the coefficient relaxation method [1][2][5].

6.3.1 DS1 Rates

Figure 6.3(a) indicates the THL obtained by the two methods at the Central Office side. Both the methods indicate an approximate THL of about 35 dB for most of the loops except for loops 8, 9 and 14.

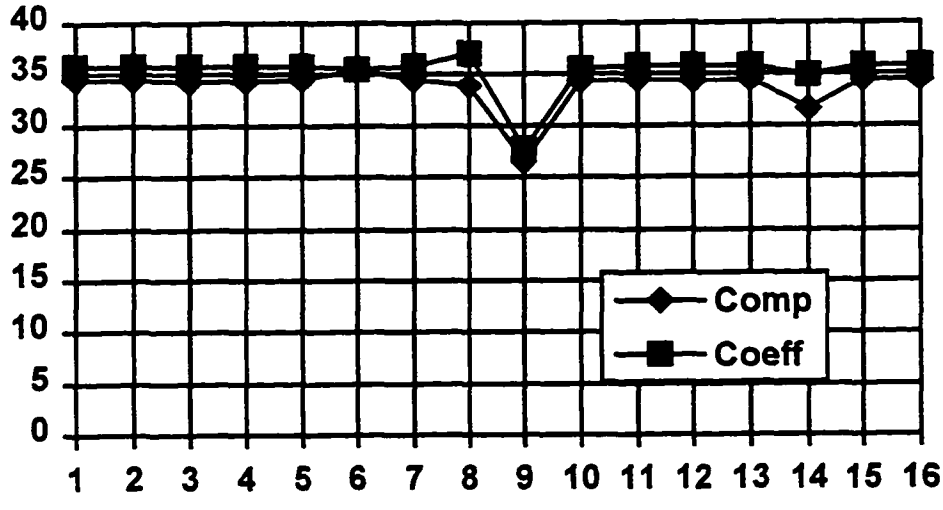

Figure 6.3(a): Central Office Side Comparison at DS1 Rates

For the Subscriber side figure 6.3(b) shows the THL obtained by the two methods.

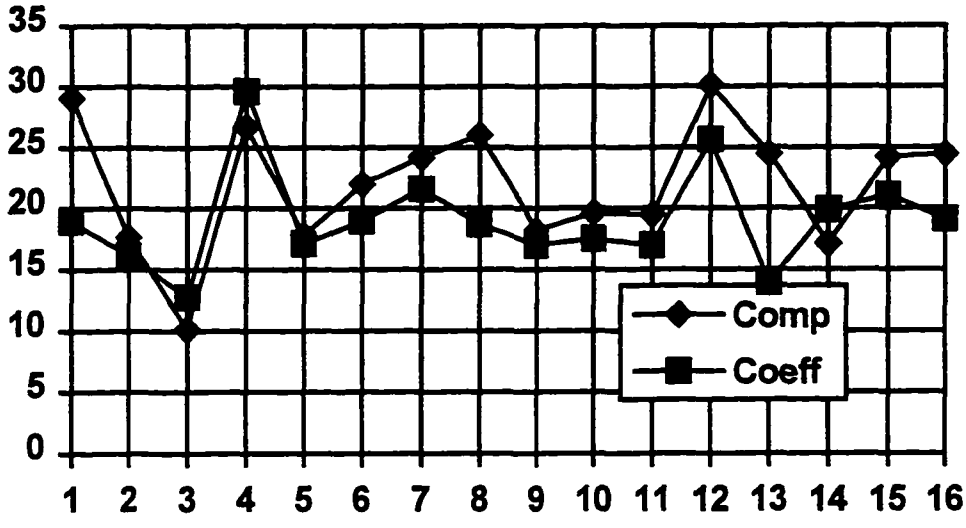

Figure 6.3(b): Subscriber Side Comparison at DS1 Rates

From figure 6.3 the two methods show that the THL obtained for the different loops is quite close that is less than ± 3 dB except for the loops 1, 8, 13 and 16.

6.3.3 DS1C Rates

Figure 6.4(a) indicates the THL obtained by the two methods at the Central Office side. At higher frequencies the component relaxation method indicates an approximate THL of about 35 dB for most of the loops except for loops 8 and 9 which gives better results than the coefficient relaxation method.

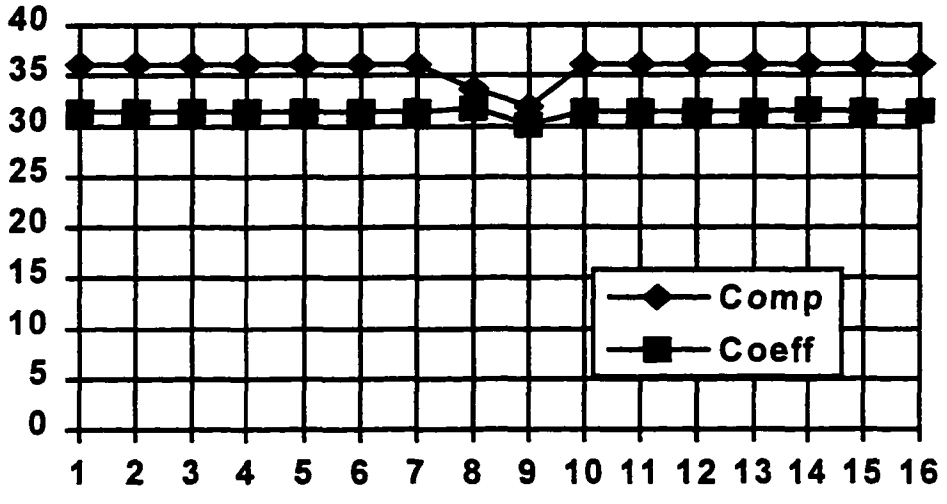

Figure 6.4(a): Central Office Side Comparison at DS1C Rates

For the Subscriber side figure 6.4(b) shows the THL obtained by the two methods.

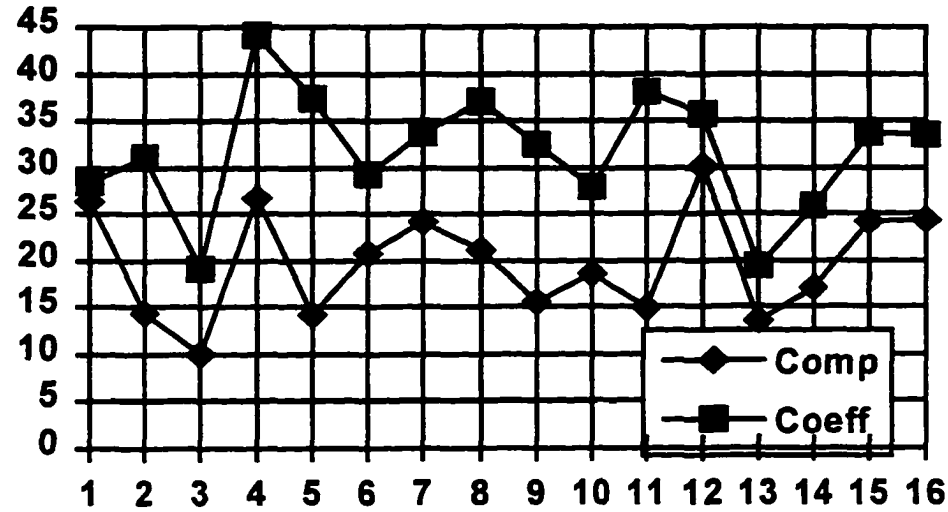

Figure 6.4(b): Subscriber Side Comparison at DS1C Rates

From figure 6.4 the two methods show that the THL obtained for the different loops is quite different, that is the component relaxation although gives better results for higher frequencies it does not perform that well for lower frequencies.

6.3.3 DS2 Rates

Figure 6.5(a) indicates the THL obtained by the two methods at the Central Office side. At higher frequencies the component relaxation method indicates an approximate THL of about 35 dB for most of the loops except for loop 9 which gives better results than the coefficient relaxation method.

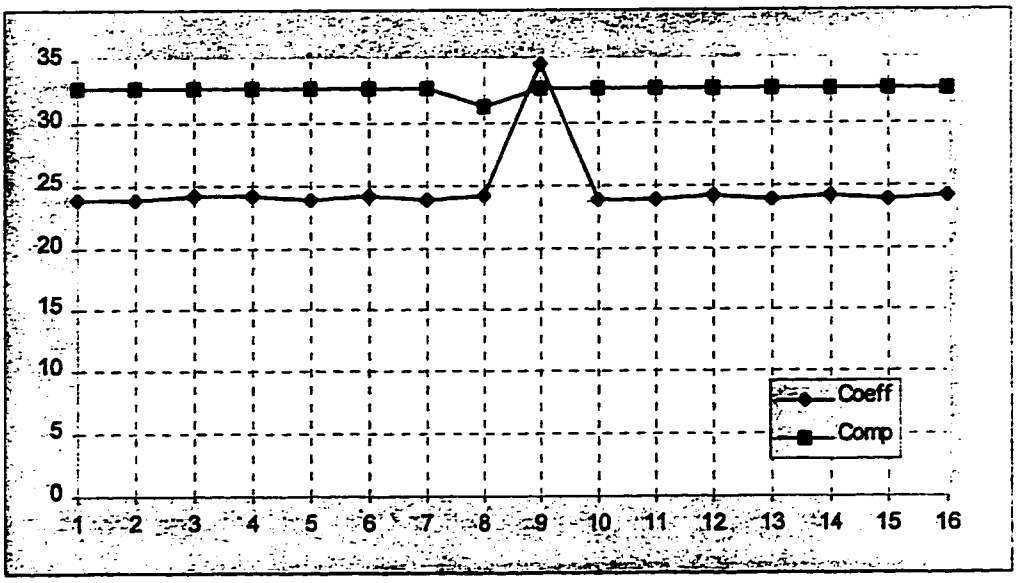

Figure 6.5 (a): Central Office Side Comparison at DS2 Rates

For the Subscriber side figure 6.5 (b) shows the THL obtained by the two methods.

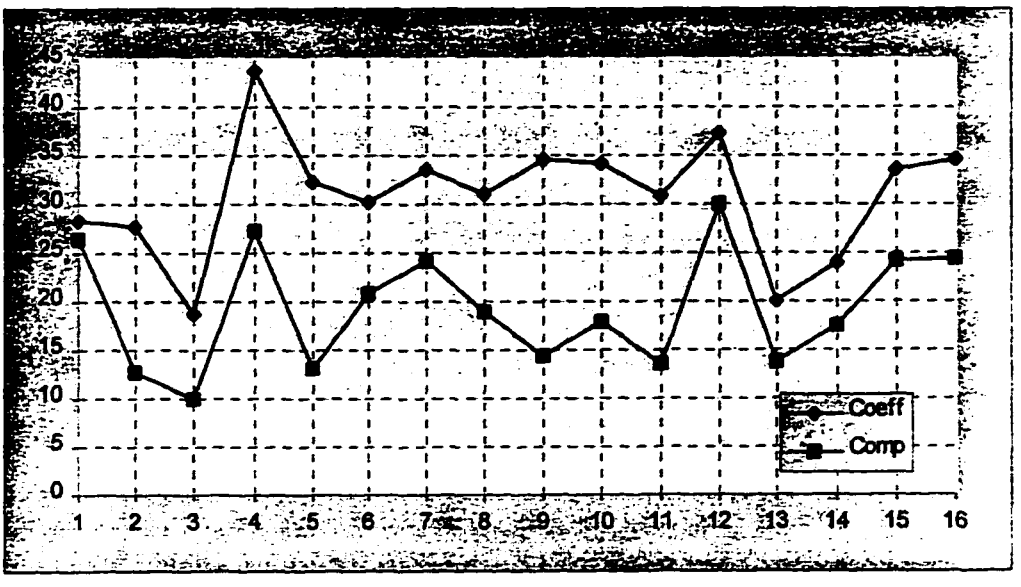

Figure 6.5 (b): Subscriber Side Comparison at DS2 Rates

From figure 6.5 it is clear that the THL obtained for the different loops using the two methods indicate that in the case of the above mentioned rates the values of THL obtained by using component relaxation method seems to perform better except for the loop 9, both the forward and the reverse channel the coefficient relaxation method seems to perform better as is seem for the charts 6.5 (a) and 6.5 (b).

6.4 Conclusion

From the above charts it is quite clear that coefficient relaxation method seems to perform better at certain frequency bands whereas at certain other bands for certain loops the component relaxation method seems to perform better. However one must realize that the coefficient relaxation method although it gives better results in terms

of the THL at certain frequency bands it is difficult to obtain the exact values of the components which is not the case with regards to the component relaxation method. More study needs to be done with regards to saying that component relaxation method is definitely better than the coefficient relaxation at higher frequencies, although it seems to perform better at higher frequencies than the coefficient relaxation method for the spectral bands for which simulations were conducted. However still for higher frequencies there is a possibility that coefficient relaxation method could give better results. From the results obtained so far for the different spectral bands it is seen that for different spectral bands one of the two methods gives better results in terms of the THL. Combining the two methods (Hybrid Method) it is possible to obtain better results (THL) but maintaining the argument that it is not so easy to obtain the values of the RC components from the coefficient relaxation method.

Further the investigations show that it is possible to obtain about 20 dB to 25 dB of THL on an average using second order matching function for loops with bridged taps, and it is possible to obtain as high as 40 dB for certain without bridged taps for both the sides. Depending on the loop characteristics and choosing suitable line codes for data rates specified it is possible to increase the THL by at least 3dB to 6dB even for the worst case loops.

References

[1] G.S.Moschytz and S.V.Ahamed, "Transhybrid loss with RC Balance Circuits for Primary Rate ISDN Transmission Systems", IEEE JSAC, August 1991, Vol. 9, No. 6, pp. 951-959.

[2] S.V.Ahamed and G.S.Moschytz, "Optimization of the RC Matching Network in Adaptive Active Hybrids for High-Speed Data Communications", IEEE, ISCAS, June 1991.

[3] S.V.Ahamed, "Simulation Environments for the High-Speed Digital Subscriber Lines (HDSL)", IEEE ICC May 1993, pp. 811-815.

[4] G.S.Moschytz and S.V.Ahamed, "Transhybrid Loss with RC Balance Circuits for High Speed Full Duplex Modems", AT & T Bell Laboratories XGN360000-891214-01-TM, Dec. 1989

[5] A.Reddy and S.V.Ahamed, "Matching Functions by Component Relaxation Method for Asymmetrical Digital Subscriber Line (ADSL)", AEIC' 95, Dec. 1995, pp. 306 - 310.

Chapter 7

Time Domain Transhybrid Attenuation

In two wire transmission, both the transmitter and receiver are coupled to the line through a hybrid which is built so that the signal leakage from the transmitter to the receiver side is theoretically zero assuming 100% matching of the line impedance and matching impedance. In practice, however the line impedance is different for each connection and can even change during a connection resulting in leakage, known as near-end reflection, between the transmitter and receiver. Impedance changes in the line caused by different diameter wires, bridged taps, and imperfect matching of the far-end hybrid produce a second type of reflection known as far-end reflection. In one or two way half duplex connections the reflection problem can be overcome by path switching, the technique used by reflection suppressers. However path switching cannot be used in full-duplex connections instead reflection attenuators are employed, which rely on local simulation of the reflection path. This estimated reflected signal is subtracted from the incoming signal resulting in clean attenuated version of the transmitted signal. Unfortunately the realization of the attenuator is not straightforward because the echo path is unknown and can change from one connection to another and even during a call. Fixed characteristics based on the

expected average for each of the loops is determined and checked to find out as to how it perform compared to the adaptive filter implementation of the attenuator.

7.1 Digital Filters

The adaptive filter used would be of the infinite impulse response (IIR) type. The reason for the use of the IIR filter in the implementation both for the fixed coefficient and the adaptive type is its main advantage of it having a longer impulse response than that of an Finite Impulse Response (FIR) type of filter for any fixed number of coefficients. For strong undelayed reflection FIR filters would be used but for the far end reflection with longer delays there is a need for the IIR filter which is considered suitable to cancel the far-end reflection.

7.1.1 Infinite Impulse Response (IIR) Filters

The reason for using IIR filters is that compared to the FIR filters, IIR filters can often be much more efficient in terms of attaining better magnitude response with a given filter order. This is because IIR filters incorporate feedback and are capable of realizing both poles and zeros. This means that IIR filters can run faster and hence must be considered in applications where speed is important, however the only disadvantage which goes against using IIR filters is because of its instability and it

also has nonlinear phase characteristics. The system function of the IIR filter is given by

$$H(z) = \frac{Y(z)}{X(z)} = \frac{\sum_{n=0}^{N} b_n z^{-n}}{\sum_{n=0}^{N} a_n z^{-n}} = \frac{b_0 + b_1 z^{-1} + \ldots + b_N z^{-N}}{1 - a_1 z^{-1} - \ldots - a_N z^{-N}}$$

where b_n and a_n are the coefficients of the filter. We have assumed that both the numerator and the denominator polynomials are of the order N. The difference equation of the IIR filter is given by

$$y(n) = \sum_{m=0}^{N} b_m x(n-m) + \sum_{m=1}^{N} a_m y(n-m)$$

The above equation indicates that the output of the IIR filter is a function of not only the present input but also the past inputs and outputs. The IIR filters are also referred to as the recursive filters. The IIR filters could be implemented by using any of the three structures mentioned below.

Direct form In this form the difference equation is implemented directly as given. Since there are two parts to this filter, namely the FIR part and the recursive part, it leads to two version of implementation that direct form I and direct form II.

Consider the difference equation

$$y(n) = b_0x(n) + b_1x(n-1)\ b_2x(n-2) + a_1y(n-1)\ a_2y(n-2)$$

which indicates that N = 2. The implementation for this using direct form I is shown in the figure 7.1.

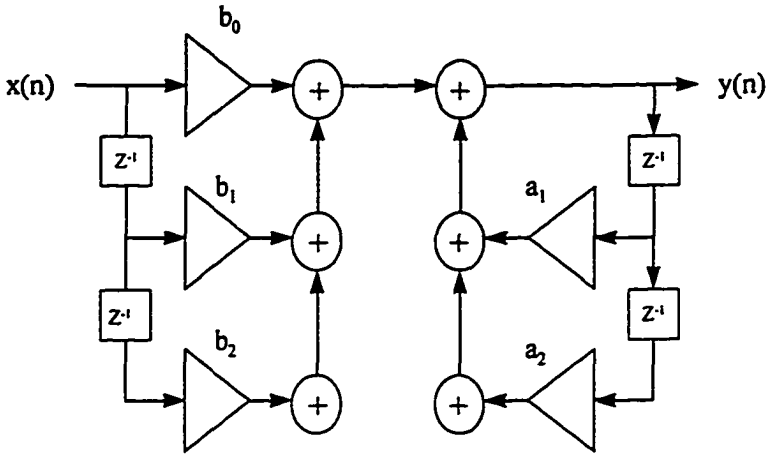

Figure 7.1: Direct Form I

In the direct form I structure each part of the transfer function is implemented separately with a cascade connection between them. The numerator part of the function is a feedforward tapped delay line followed by the recursive part which is the feedback tapped delay line. This structure could be modified and the same difference equation could still be implemented by the elimination of one of the delay lines and the interchanging by the way in which the two parts are connected in cascade. The modified structure is as shown in the figure 7.2 is now called as the direct form II.

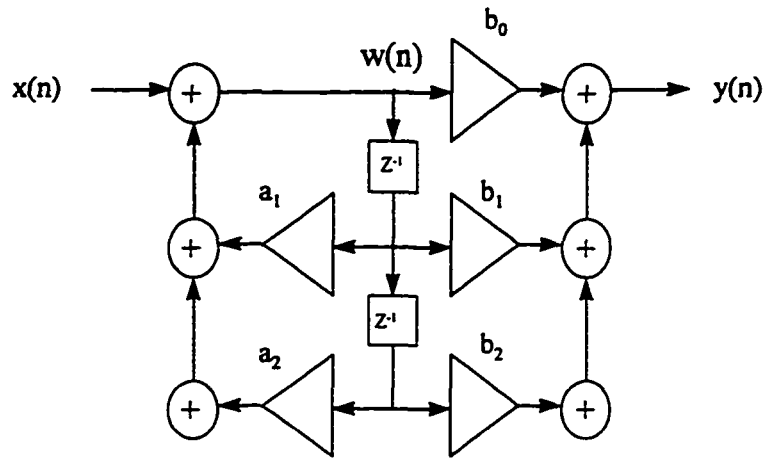

Figure 7.2: Direct Form II

The two structures although they appear to be different in the way they have been connected, a point worth to noting is that for a given input signal the output produced by the two structures are identical, however the internal data flow for the two structures are not the same. The second structure that is the direct form II uses less number of memory elements. In terms of the hardware complexity the second structure is the most suitable one.

Cascade Form In this form the transfer function is implemented by factoring it into smaller second order sections called as biquads. The system function or the transfer function is then represented as the product of these biquads. The structure chosen to implement these biquads is the direct form II and in the process of implementing the entire function each of the biquad so formed are cascaded together and hence the final

structure formed is called as the cascaded form. Now once again lets consider a difference equation where N is of the order 4.

$$y(n) = \sum_{m=0}^{4} b_m x(n-m) + \sum_{m=1}^{4} a_m y(n-m)$$

$$H(z) = \frac{Y(z)}{X(z)} = \frac{\sum_{n=0}^{4} b_n z^{-n}}{\sum_{n=0}^{4} a_n z^{-n}} = \frac{b_0 + b_1 z^{-1} + \ldots + b_4 z^{-4}}{1 - a_1 z^{-1} - \ldots - a_4 z^{-4}}$$

$$= b_0 \frac{1 + \frac{b_1}{b_0} z^{-1} + \ldots + \frac{b_4}{b_0} z^{-4}}{1 - a_1 z^{-1} - \ldots - a_4 z^{-4}}$$

$$= b_0 \prod_{k=1}^{M} \frac{1 + B_{1k} z^{-1} + B_{2k} z^{-2}}{1 - A_{1k} z^{-1} - A_{2k} z^{-2}}$$

In the above equation the value of M is equal to N/2 and the coefficients B_{1k}, B_{2k}, A_{1k} and A_{2k} are real numbers of the second order sections. For the given value of N=4 the difference equation is implemented by using two second order biquad sections. In general if the value of N is large then we would require N/2 biquad sections in order to realize the difference equation, and each of the biquad section which are intermediate would be referred to as the k^{th} biquad section. The output of the first biquad is connected to the input of the second and in general the output of the k^{th} biquad section would be connected to the input of the $(k+1)^{th}$ biquad section. For N=4 the cascaded form structure is shown in the figure 7.3.

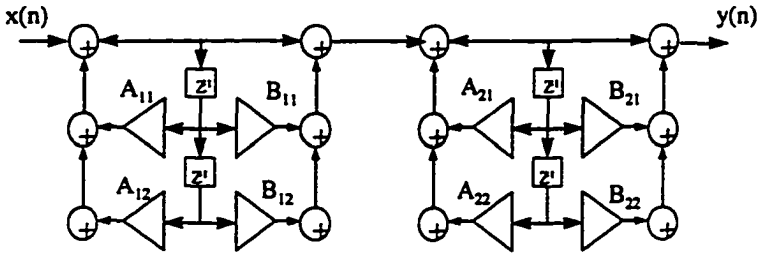

Figure 7.3: Cascade Form Structure

Parallel Form In this form the difference equation is represented in a similar manner as that of the cascaded form but the main difference between the two forms is that after factorization the partial fraction expansion is used to represent H(z) as a sum of smaller second order sections, in which case each of the section is implemented in the direct form II as a parallel network of sections.

7.2 Hybrid Attenuator Requirements

Near end reflection has a short delay and a high signal level. Typical hybrid attenuation can be around 10 dB to 20dB depending on the type of the loop under consideration. Far end echo is a low level signal with a significant delay which depends on the length and hence impulse response of the line in this case the main attenuator requirement is for a long or delayed response rather than a major reduction in the reflection level. In baseband transmission the reflection path can be considered as linear. Nevertheless some non-linearities should be considered such as the

nonlinearity of the A/D converter, asymmetry between transmitted positive and negative pulses and coupling coil saturation. The nonlinearities which occur must be dealt with by the attenuator or additional circuitry. Either the cancellation level is increased or the canceling algorithm is designed to take the nonlinearities into consideration. Reflection compensation, which is only partial produces a residual signal that can be considered as an interfering signal to be added to the incoming signal from the far end. The effect of this is to scatter the constellation points of the CAP. Finite precision arithmetic in the digital IIR part of the attenuator is another point to consider. As well as analog to digital and digital to analog conversion input and output implementation of the detailed algorithm should be considered to determine the most critical steps with regard to the precision requirements, mainly when multipliers are used. A decision regarding the compromise between the computational complexity, speed of convergence and noise around the convergence point have to be made. Continuous advances in technology are making the first factor less critical. In many algorithms higher convergence speed increases the error in steady conditions; a decision has to be made as to the relative importance of each.

Adaptive algorithms use a minimization criterion and error signal related to the degree of adaptation . One of the commonest criteria is the least mean square error as the equations arising from it are of limited complexity and it is sufficiently robust to allow small changes around the optimum point without seriously degrading system

behavior. The following algorithm Least Mean Squared (LMS) algorithm [Chap. 5] is used for the coefficient adjustment using the IIR filter.

7.3 Least Mean Square (LMS) Algorithm for Coefficient Adjustment of IIR Filter

Let us consider an IIR filter with adjustable coefficients {U(k), $0 \leq k \leq L-1$ }. Let {x(k) denote the input sequence to the filter and let {y(k)} be the corresponding output, where y(k) is given by the difference equation

$$y(k) = \sum_{m=0}^{L-1} b_m x(k-m) + \sum_{m=1}^{L-1} a_m y(k-m)$$

During the implementation of the adaptive filters which are recursive in nature care must be taken that the poles remain with the unit circle least the filter become unstable and also during the adaptation process care also should be taken that it does not have local minima by suitably adding filter weights. For the sake of convenience we define the time varying weight vector W(k) and the signal vector U(k).

$$W(k) = [a_{0k} a_{1k} \cdots a_{Lk} b_{1k} \cdots b_{Lk}]^T$$

$$U(k) = [x_k x_{k-1} \cdots x_{k-L} y_{k-1} \cdots y_{k-L}]$$

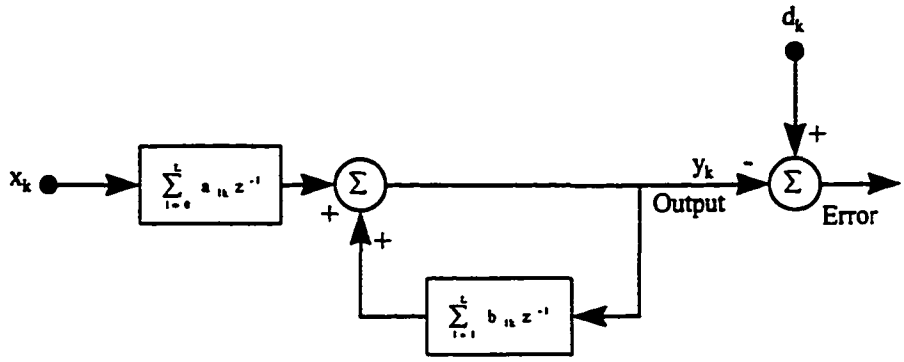

Figure 7.4: Adaptive IIR Filter

From the figure 7.4 we obtain the error

$$\varepsilon(k) = d(k) - y(k)$$

$$= d(k) - \mathbf{W}(k)^T\mathbf{U}(k)$$

The coefficient of the IIR filter will be selected to minimize the sum of squared errors, which leads to the following equation

$$\xi = \sum_{k=0}^{M} e^2(k) = \sum_{k=0}^{M}\left[d(k) - \sum_{n=0}^{L-1} \mathbf{W}(n)\mathbf{U}(k-n) \right]^2$$

$$\varepsilon^2(k) = (d(k) - y(k))^2$$

$$\hat{\nabla}_k = \frac{\partial \varepsilon^2}{\partial W(k)} = 2\frac{\partial \varepsilon}{\partial W(k)}$$

$$= 2\,\varepsilon(k)\left[\frac{\partial \varepsilon(k)}{\partial a(0,k)} \cdots \frac{\partial \varepsilon(k)}{\partial a(L,k)} \frac{\partial \varepsilon(k)}{\partial b(1,k)} \cdots \frac{\partial \varepsilon(k)}{\partial b(L,k)}\right]^T$$

$$= -2\,\varepsilon(k)\left[\frac{\partial y(k)}{\partial a(0,k)} \cdots \frac{\partial y(k)}{\partial a(L,k)} \frac{\partial y(k)}{\partial b(1,k)} \cdots \frac{\partial y(k)}{\partial b(L,k)}\right]^T$$

$$\alpha(n,k) = \frac{\partial y(k)}{\partial a(n)} = x(k-n) + \sum_{l=1}^{L} b_l \frac{\partial y(k-l)}{\partial a(n)}$$

$$x(k-n) + \sum_{l=1}^{L} b_l \alpha(n,k-l)$$

$$\beta(n,k) = \frac{\partial y(k)}{\partial b(n)} = y(k-n) + \sum_{l=1}^{L} b_l \frac{\partial y(k-l)}{\partial b(n)}$$

$$y(k-n) + \sum_{l=1}^{L} b_l \beta(n,k-l)$$

$$\hat{\nabla}_k = -2\,\varepsilon(k)\,[\alpha(0,k) \ldots \alpha(L,k)\ \beta(1,k)\ \beta(L,k)]$$

The coefficient update in the LMS algorithm is written as follows:

$$\mathbf{W}(k+1) = \mathbf{W}(k) - \mathbf{M}\,\hat{\nabla}_k$$

$$\mathbf{M} = \mathrm{diag}[\mu \ldots \mu v_1 \ldots v_L]$$

7.4 Attenuator Convergence

It is hard to analyze the stochastic update method. Convergence in the case of IIR filter is obtained only when the step size is neither too large nor too small. It is observed that when the same step sizes are used for updating the coefficients both in the numerator and denominator and the step sizes are large then the error increases at a very fast rate and the filter becomes unstable and also when the step size is too small then also the convergence fails to occur in which case the filter reaches an

unstable state. So an optimum value of the step size has to selected in order to attain the convergence.

7.5 Simulation Setup

The simulation setup is the same as explained in [Chap. 5]. During the first part of the simulation the coefficients for the biquad is computed for every frequency using the LMS algorithm such that resultant coefficients obtained for biquad results in a minimum error. This procedure is carried out both for the forward and reverse channels over the entire spectral band of interest. Once this is done then the coefficients corresponding to minimum error is searched for by plotting the error against the frequency range and the lowest crest or valley is located and the coefficients corresponding to this error point is taken as the coefficients for the biquad for the loop under study. There are two biquads which correspond to the inphase and the quadrature component of the signal as shown in the figure 7.5. In this modeling a digital-analog hybrid component setup is considered in which the digital IIR filters are used to do the analog cancellation. The model as shown in the figure 7.5 is used to compute the coefficients for the two biquads. To begin with the biquads are set to some initial values and the step size of the LMS algorithm is chosen.

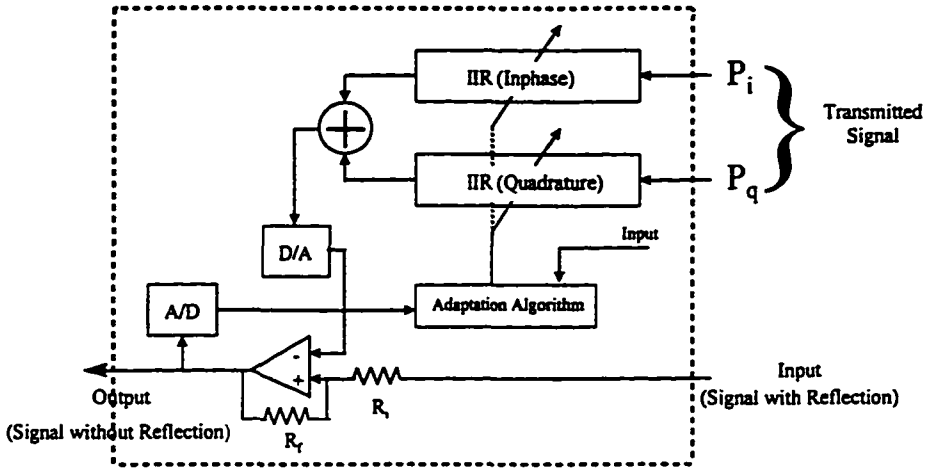

Figure 7.5: Adaptive Attenuator Model

The received signal which is sampled and held is fed to the input of the operational amplifier. The other input of the op-amp is from the D/A which depends on the initial values of the coefficients chosen for IIR filter. The operational amplifier is operated in the differential mode and the output of the operational amplifier if fed to the A/D which is basically the error which serves as the input to the adaptation algorithm along with the input from the memory elements of the biquad it then computes the new set of coefficients and then updates the coefficients of the filter. The update of the coefficients is done for every symbol period. The convergence is obtained by suitably choosing not only the initial coefficients but also the step size. Once this is done the adaptive IIR filters shown in the figure 7.5 are replaced by biquads having fixed set of coefficients, now the model in the figure 7.5 gets modified to the model

shown in figure 7.6 and the set of coefficients obtained for each of the loops both for the forward channel

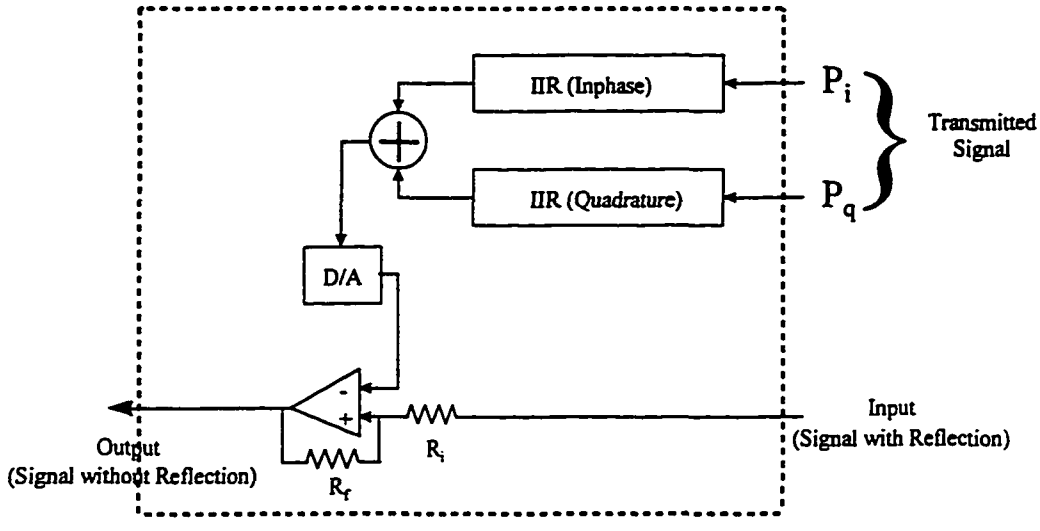

Figure 7.6: Fixed Attenuator Model

and the reverse channel are as shown in the tables 7.1 and 7.2 for the reflected signals being -26dB and -40dB respectively.

The flow chart shows the various software routines that are used for the simulation in addition to the setup discussed in figure 5.4 [Chap. 5]. The various functions used in the simulation setup are as shown in the figure 7.7 which are

1. Capansi
2. Adapt

3. Biquad
4. PLOT and
5. SNR

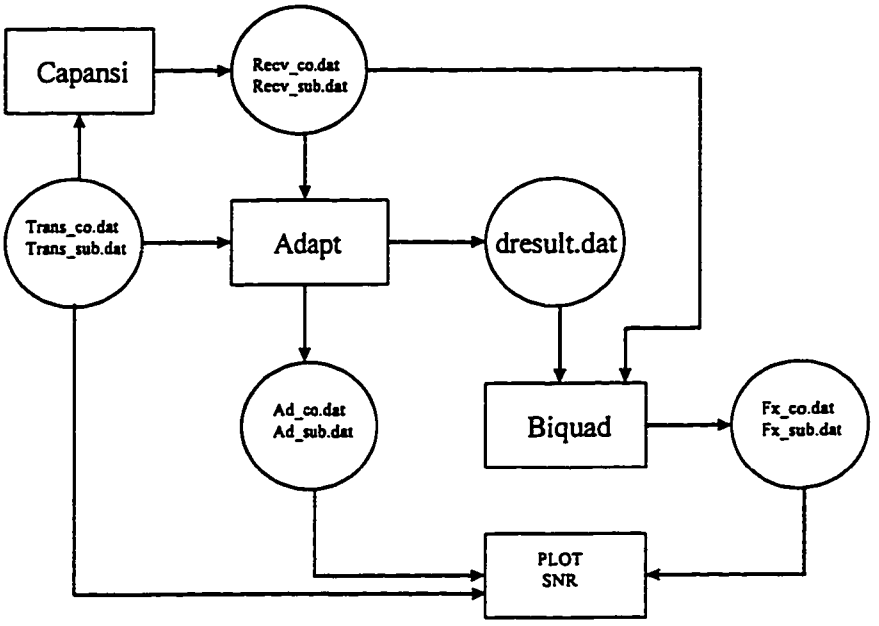

Figure 7.7: Simulation Flow Chart

These are functions which are used in addition to the functions shown in the simulation setup in [Chap. 5].

7.5.1 Function Capansi ( )

Input: Trans_co.dat, Trans_sub.dat (Primary files)

Output: Recv_co.dat, Recv_sub.dat (Intermediate files)

Main:

The Capansi routines takes the primary files Trans_co.dat and Trans_sub.dat which are 64 constellation CAP source for the central office side and the subscriber side and accesing the database of the ANSI standard loops and the twisted wire pair data it computes the equivalent ABCD matrices and thereby the required transfer function of the transmission line over the spectral band of interest. The Recv_co.dat and Recv_sub.dat are the received signals at the central office side and the subscriber side respectively which essentially consists of two components the transmitted signal convolved with the transmission line impulse response plus the reflected signal caused due to the mismatch of the line hybrids and the heterogeneous cable makeup of the transmission line. These files are stored in the intermediate databases for further processing.

7.5.2 Function Adapt ( )

Input: Recv_co.dat, Recv_sub.dat (Intermediate files)

Trans_co.dat, Trans_sub.dat (Secondary files)

Output: dresult.dat , Ad_co.dat, Ad_sub.dat (Secondary files)

Main:

The Adapt function takes Recv_co.dat and Recv_sub.dat as the input and the information of the original transmitted signal, processes these signals which is contaminated with noise and reflected signals, and using the LMS algorithm computes the coefficients of the IIR filter using the model shown in the figure 7.5 over the entire spectral band under study such that it results in a minimum error for each frequency of the band under consideration. The results of the coefficients so obtained are stored in the file dresult.dat. It also processes the files Recv_co.dat and Recv_sub.dat which is contaminated with reflected signal and noise and the adaptation process is carried out by continuously updating the filter coefficients of the biquad until the convergence occurs and the output files obtained Ad_co.dat and Ad_sub.dat are stored as the secondary files.

7.5.3 Function Biquad ( )

Input: Recv_co.dat, Recv_sub.dat (Intermediate files)

dresult.dat (Secondary file)

Output: Fx_co.dat, Fx_sub.dat (Secondary file)

Main:

The biquad routine takes the input file dresult.dat and the coefficients contained in the file are read into the memory elements of the biquads the inphase and the quadrature filters as shown in the figure 7.6. The biquad routine also needs the files Recv_co.dat and Recv_sub.dat as the input and using the fixed coefficients in the IIR filter the signals are processed and the processed signals are stored as Fx_co.dat and Fx_sub.dat which are secondary files.

7.5.4 Function PLOT ( )

Input: Ad_co.dat, Ad_sub.dat, Fx_co.dat, Fx_sub.dat (Secondary files)

Output: Display, Printer

Main:

The plot routine takes the input files which are the secondary files and plots the points in order to obtain the constellation plots for different types of signals both one dimensional and two dimensional signals.

The plots are displayed on the window screen and the plots could also be printed. The plots thus obtained can also be saved as a file for future reference.

7.5.5 Function SNR ( )

Input: Trans_co.dat, Trans_sub.dat, Fx_co.dat, Fx_sub.dat Ad_co.dat, Ad_sub.dat (Secondary files)

Output: Display, Printer

Main:

The SNR function takes the input files and finds out the energy of the actual transmitted signal and by knowing the received signal which is processed by the biquads it computes the noise energy which is due to the impairments in the received signal and also the received signal containing the reflected component of the transmitted signal due to the imperfect matching of the hybrids and the heterogeneous makeup of the cable including bridged taps. Once the signal and the noise energy is determined then the signal to noise ratio is computed and the results displayed on the screen or sent to the printer and for further analysis of the signal the computed values could be stored in the file.

For the second part of the simulation the Adapt routine instead of computing the set of fixed coefficients used by the biquad it continuously adapts using the LMS

algorithm and updates the set of coefficients withing the biquad as per the model shown in figure 7.5 and processes the files Recv_co.dat and Recv_sub.dat and stores the output in the secondary database as the files Ad_co.dat and Ad_sub.dat which are then plotted and analyzed.

The major part of the consideration in the simulation setup is the complexity involved in the computation of the Fast Fourier Transform (FFT), convolution, computation of the ABCD matrices which are complex numbers and hence the use of a complex routine math library.

The adaptation process is a very complex process for the IIR filters due to the recursive nature of the structure. The step size has to properly selected else the error tends to grow which takes the process into a state of no return or instability. For convergence to occur with better accuracy the step size chosen should be small not so small as to once again create instability but small enough so that convergence could be achieved within the reasonable amount of time. If the step is small the number of iterations required to converge is quite large and therefore takes a lot of CPU time. The size of the input data files used are also considerably large which means that care should be taken such that sufficient amount of secondary storage is available before the simulation is carried out. The output files so obtained after processing are also large which are also stored in the secondary storage devices for plot and further analysis. The intermediate data files are temporary files which are held in the database

only for the time the processing is going on and once it is over then these files get erased but could also be stored as separate files only if further analysis needs to be done.

The entire simulation package has been developed in C with flexibility as one of the other major consideration such that this software can easily be enhanced by the addition of the other library functions and any other type of simulation could be carried out with little or no changes to the software routines. Most the routines developed can be used on any platform with little modifications. The software could be easily interfaced to other types of commercially available tools which are used for simulations. The files are stored in the regular ASCII format with no compression and hence can be easily used as input files by the other existing simulation software like MATLAB for plotting and further analysis of the signal using functions which are readily available in such packages. The speed of computation during the processing of complex transmission signals not only depends on the CPU but also on the I/O bus that are used by the different platforms.

In table 7.1 and table 7.2 the numbers in each of the row indicate error, and the coefficients b0, b1, b2, a0 and a1 of the biquad respectively.

Loop #1
Subscriber Side
In Phase Filter Coefficients
0.000000, 0.999839, -0.004185, 0.013535, 0.004414, -0.013264
Quadrature Filter Coefficients
0.000008, 1.000931, 0.014619, -0.015806, -0.012160, 0.016421
Central Office Side
In Phase Filter Coefficients
0.000005, 0.995912, -0.010658, -0.005157, -0.000507, -0.002005
Quadrature Filter Coefficients
0.000000, 0.997322, -0.000918, -0.048624, 0.005845, 0.050066

Loop #2
Subscriber Side
In Phase Filter Coefficients
0.000006, 1.000239, -0.005844, 0.002134, 0.005165, -0.000658
Quadrature Filter Coefficients
0.000000, 1.001725, 0.012240, -0.018165, -0.013658, 0.018938
Central Office Side
In Phase Filter Coefficients
0.000005, 0.995646, -0.009011, 0.006431, 0.002708, -0.006419
Quadrature Filter Coefficients
0.000006, 0.999587, 0.011597, -0.048377, -0.004384, 0.055187

Loop #3
Subscriber Side
In Phase Filter Coefficients
0.000001, 1.001464, -0.002201, 0.002196, 0.002518, -0.000135
Quadrature Filter Coefficients
0.000003, 0.997867, 0.014421, -0.013961, -0.014236, 0.015601
Central Office Side
In Phase Filter Coefficients
0.000018, 1.001998, -0.008124, -0.035550, 0.011435, 0.038193
Quadrature Filter Coefficients
0.000007, 0.983081, -0.022291, -0.055024, 0.001016, 0.032751

Table 7.1: Coefficients of the Biquad at DS2 Rates with Reflected Signal = -26dB

Loop # 4
Subscriber Side
In Phase Filter Coefficients
0.000000, 1.000143, -0.002306, 0.001545, 0.002538, -0.001476
Quadrature Filter Coefficients
0.000002, 1.000353, 0.012733, -0.015660, -0.012958, 0.015597
Central Office Side
In Phase Filter Coefficients
0.000013, 1.005382, -0.006207, 0.001077, 0.005559, 0.003202
Quadrature Filter Coefficients
0.000001, 0.998117, 0.006971, -0.048426, -0.006567, 0.049176

Loop #5
Subscriber Side
In Phase Filter Coefficients
0.000005, 1.000619, -0.010109, -0.000912, 0.000783, -0.003605
Quadrature Filter Coefficients
0.000007, 0.994227, 0.008467, -0.022611, -0.015465, 0.013769
Central Office Side
In Phase Filter Coefficients
0.000005, 0.998604, -0.013536, -0.016409, 0.011509, 0.010205
Quadrature Filter Coefficients
0.000002, 0.998386, -0.012225, -0.050599, 0.005734, 0.051140

Loop # 6
Subscriber Side
In Phase Filter Coefficients
0.000004 , 0.995835, -0.002381, 0.001759, 0.009250, 0.000583
Quadrature Filter Coefficients
0.000005 1.000374 0.013293 -0.018605 -0.013473 0.017474
Central Office Side
In Phase Filter Coefficients
0.000001 1.002544 -0.018029 -0.027956 0.017657 0.024131
Quadrature Filter Coefficients
0.000009 0.998863 -0.017229 -0.045764 0.018966 0.043710

Table 7.1: Coefficients of the Biquad at DS2 Rates with Reflected Signal = -26dB

Loop #7
Subscriber Side
In Phase Filter Coefficients
0.000000, 0.999972, -0.002468, 0.001441, 0.002402, -0.001629
Quadrature Filter Coefficients
0.000015, 0.996316, 0.012315, -0.016721, -0.014799, 0.014732
Central Office Side
In Phase Filter Coefficients
0.000003, 1.006050, -0.003704, -0.005451, 0.011632, 0.012592
Quadrature Filter Coefficients
0.000008, 1.006594, 0.009191, -0.039345, 0.008754, 0.061340

Loop # 8
Subscriber Side
In Phase Filter Coefficients
0.000000, 0.995626, -0.003213, 0.003141, 0.007567, -0.000369
Quadrature Filter Coefficients
0.000004, 1.014160, 0.015219, -0.013179, -0.008036, 0.023205
Central Office Side
In Phase Filter Coefficients
0.000005, 0.999745, -0.006053, 0.019554, 0.001710, -0.018574
Quadrature Filter Coefficients
0.000006, 0.999837, 0.007390, -0.056349, -0.014056, 0.055274

Loop # 9
Subscriber Side
In Phase Filter Coefficients
0.000004, 1.002768, -0.004782, -0.001138, 0.006094, -0.003939
Quadrature Filter Coefficients
0.000014, 0.998875, 0.011056, -0.018186, -0.012329, 0.017027
Central Office Side
In Phase Filter Coefficients
0.000003, 0.995121, -0.001671, -0.009069, -0.006141, 0.007187
Quadrature Filter Coefficients
0.000007, 1.004272, 0.024732, -0.050524, -0.020370, 0.056300

Table 7.1: Coefficients of the Biquad at DS2 Rates with Reflected Signal = -26dB

Loop #10
Subscriber Side
In Phase Filter Coefficients
0.000005, 0.997730, -0.004626, 0.003168, 0.006367, -0.000431
Quadrature Filter Coefficients
0.000007, 0.998905, 0.006492, -0.018337, -0.016317, 0.017655
Central Office Side
In Phase Filter Coefficients
0.000013, 0.993131, -0.000555, 0.019304, -0.000899, -0.018522
Quadrature Filter Coefficients
0.000007, 0.997329, 0.011735, -0.050115, -0.010087, 0.052925

Loop #11
Subscriber Side
In Phase Filter Coefficients
0.000008, 0.999775, -0.003845, 0.001563, 0.006917, -0.001029
Quadrature Filter Coefficients
0.000008, 1.001332, 0.016444, -0.011849, -0.007687, 0.024157
Central Office Side
In Phase Filter Coefficients
0.000005, 0.999266, -0.014248, -0.016400, 0.015547, 0.015726
Quadrature Filter Coefficients
0.000001, 1.000061, -0.012306, -0.049855, 0.012609, 0.048298

Loop #12
Subscriber Side
In Phase Filter Coefficients
0.000000, 1.000430, -0.002218, 0.001528, 0.002570, -0.001414
Quadrature Filter Coefficients
0.000000, 1.000440, 0.013843, -0.015492, -0.013050, 0.015767
Central Office Side
In Phase Filter Coefficients
0.000018, 1.001182, -0.009726, -0.003019, 0.010751, -0.002357
Quadrature Filter Coefficients
0.000012, 1.000023, 0.004633, -0.047590, 0.001753, 0.057144

Table 7.1: Coefficients of the Biquad at DS2 Rates with Reflected Signal = -26dB

Loop #13
Subscriber Side
In Phase Filter Coefficients
0.000001, 0.999807, -0.000347, 0.001351, 0.002407, -0.001162
Quadrature Filter Coefficients
0.000006, 1.000229, 0.012894, -0.015598, -0.012118, 0.013877
Central Office Side
In Phase Filter Coefficients
0.000003, 1.042066, 0.063740, -0.037449, -0.022627, 0.066996
Quadrature Filter Coefficients
0.000001, 0.995426, 0.433053, -0.175028, -0.455761, 0.170945

Loop #14
Subscriber Side
In Phase Filter Coefficients
0.000000, 1.003465, -0.006734, 0.002031, 0.004184, -0.001701
Quadrature Filter Coefficients
0.000009, 1.002143, 0.011201, -0.018038, -0.012178, 0.018024
Central Office Side
In Phase Filter Coefficients
0.000001, 0.992322, -0.006195, 0.000496, 0.001352, -0.006279
Quadrature Filter Coefficients
0.000003, 1.003190, 0.004818, -0.052100, -0.007857, 0.053277

Loop #15
Subscriber Side
In Phase Filter Coefficients
0.000000, 1.000179, -0.002389, 0.001644, 0.002366, -0.001240
Quadrature Filter Coefficients
0.000004, 0.999060, 0.013063, -0.015632, -0.013025, 0.015531
Central Office Side
In Phase Filter Coefficients
0.000001, 0.995120, -0.016007, -0.010641, 0.008468, 0.007875
Quadrature Filter Coefficients
0.000008, 1.000861, -0.005047, -0.050507, 0.003827, 0.051316

Table 7.1: *Coefficients of the Biquad at DS2 Rates with Reflected Signal = -26dB*

Loop #16
Subscriber Side
In Phase Filter Coefficients
0.000002, 0.999495, -0.000348, 0.001380, 0.002390, -0.002462
Quadrature Filter Coefficients
0.000009, 1.002531, 0.011961, -0.016356, -0.011779, 0.013294
Central Office Side
In Phase Filter Coefficients
0.000002, 0.997743, -0.019811, -0.026107, 0.014225, 0.023884
Quadrature Filter Coefficients
0.000021, 1.004866, -0.012564, -0.043559, 0.025988, 0.051730

Table 7.1: Coefficients of the Biquad at DS2 Rates with Reflected Signal = -26dB

7.6 Discussion

Using the coefficients in the biquads as shown in the tables 7.1 and 7.2 for the various loops the constellation points obtained for these loops in the forward and the reverse channel is as shown in the figure 7.8(a), 7.8(b), 7.8(c) and 7.8(d). Figures 7.81(a), 7.81(b), 7.81(c) and 7.81(d) are the enhanced view of the best and the worst case loops for the Central Office Side and Subscriber Side with the reflected signal being -26dB. Figure 7.8(a) is the constellation points of the Central Office side for 64 CAP used in the simulation where the reflection signal used is -26 dB, and the figure 7.8(b) shows the constellation points for the Subscriber Side where the reflection signal is also the same that is -26 dB.

Loop #1
Subscriber Side
In Phase Filter Coefficients
0.000000,0.999977,-0.004246,0.013437,0.004259,-0.013441
Quadrature Filter Coefficients
0.000001,1.000458,0.013373,-0.015146,-0.012902,0.015250
Central Office Side
In Phase Filter Coefficients
0.000001,0.999979,-0.014933,-0.008015,0.015124,0.007678
Quadrature Filter Coefficients
0.000001,0.999525,-0.001116,-0.032289,-0.000271,0.031389

Loop #2
Subscriber Side
In Phase Filter Coefficients
0.000002,1.001025,-0.002590,0.001734,0.003222,-0.001210
Quadrature Filter Coefficients
0.000000,1.000472,0.012466,-0.016388,-0.013192,0.014872
Central Office Side
In Phase Filter Coefficients
0.000001,1.000246,-0.018605,-0.012633,0.018475,0.012660
Quadrature Filter Coefficients
0.000001,1.000262,0.004252,-0.034719,-0.004536,0.034138

Loop #3
Subscriber Side
In Phase Filter Coefficients
0.000000,0.999798,-0.002738,0.001015,0.001828,-0.001800
Quadrature Filter Coefficients
0.000001,1.000523,0.013607,-0.015059,-0.013311,0.014855
Central Office Side
In Phase Filter Coefficients
0.000003,1.000700,-0.023524,-0.023416,0.019366,0.021850
Quadrature Filter Coefficients
0.000000,0.997499,-0.011123,-0.029442,0.006916,0.026341

Table 7.2: Coefficients of the Biquad at DS2 Rates with Reflected Signal = -40dB

Loop #4
Subscriber Side
In Phase Filter Coefficients
0.000000,1.000006,-0.002273,0.001508,0.002303,-0.001441
Quadrature Filter Coefficients
0.000000,0.999475,0.012662,-0.015659,-0.013575,0.014622
Central Office Side
In Phase Filter Coefficients
0.000000,1.001036,-0.018623,-0.014084,0.019042,0.014281
Quadrature Filter Coefficients
0.000003,1.000515,0.002645,-0.033261,-0.002737,0.032774

Loop #5
Subscriber Side
In Phase Filter Coefficients
0.000000,1.000485,-0.002753,0.000947,0.003035,-0.001970
Quadrature Filter Coefficients
0.000000,0.999889,0.012711,-0.015581,-0.012971,0.015578
Central Office Side
In Phase Filter Coefficients
0.000000,0.999745,-0.020276,-0.016237,0.019492,0.016536
Quadrature Filter Coefficients
0.000000,1.000954,0.000943,-0.031373,0.001917,0.032638

Loop #6
Subscriber Side
In Phase Filter Coefficients
0.000000,0.999978,-0.002767,0.001682,0.003187,-0.001175
Quadrature Filter Coefficients
0.000000,0.999481,0.013043,-0.015678,-0.013148,0.015465
Central Office Side
In Phase Filter Coefficients
0.000000,1.000809,-0.020851,-0.018719,0.020753,0.019007
Quadrature Filter Coefficients
0.000002,0.998505,-0.003842,-0.030144,0.003261,0.029473

Table 7.2: Coefficients of the Biquad at DS2 Rates with Reflected Signal = -40dB

Loop #7
Subscriber Side
In Phase Filter Coefficients
0.000000,1.000090,-0.002273,0.001536,0.002301,-0.001426
Quadrature Filter Coefficients
0.000000,0.999945,0.013376,-0.015065,-0.012950,0.015194
Central Office Side
In Phase Filter Coefficients
0.000000,0.999995,-0.019686,-0.015393,0.018533,0.015663
Quadrature Filter Coefficients
0.000001,0.999158,0.000465,-0.032461,-0.001073,0.032245

Loop #8
Subscriber Side
In Phase Filter Coefficients
0.000000,0.999424,-0.003351,0.001201,0.002402,-0.001782
Quadrature Filter Coefficients
0.000001,0.998484,0.012025,-0.016200,-0.013519,0.015002
Central Office Side
In Phase Filter Coefficients
0.000001,0.998202,-0.016898,-0.010377,0.019524,0.010417
Quadrature Filter Coefficients
0.000000,1.000588,0.007181,-0.036436,-0.007878,0.035928

Loop #9
Subscriber Side
In Phase Filter Coefficients
0.000000,1.000007,-0.002809,0.001400,0.002961,-0.001501
Quadrature Filter Coefficients
0.000000,0.999801,0.013371,-0.015366,-0.012347,0.015709
Central Office Side
In Phase Filter Coefficients
0.000003,0.999873,-0.016099,-0.014544,0.017954,0.015126
Quadrature Filter Coefficients
0.000003,0.998175,0.001328,-0.033478,-0.000864,0.033472

Table 7.2: Coefficients of the Biquad at DS2 Rates with Reflected Signal = -40dB

Loop #10
Subscriber Side
In Phase Filter Coefficients
0.000001,1.000926,-0.002973,0.001990,0.002830,-0.001034
Quadrature Filter Coefficients
0.000000,1.000001,0.012277,-0.016063,-0.013120,0.015100
Central Office Side
In Phase Filter Coefficients
0.000001,1.000302,-0.018098,-0.010848,0.017021,0.009981
Quadrature Filter Coefficients
0.000001,0.998728,0.007326,-0.035956,-0.006321,0.036250

Loop #11
Subscriber Side
In Phase Filter Coefficients
0.000000,1.001278,-0.003013,0.001140,0.002762,-0.001783
Quadrature Filter Coefficients
0.000000,0.999432,0.011269,-0.015962,-0.014431,0.015154
Central Office Side
In Phase Filter Coefficients
0.000000,1.000430,-0.020317,-0.017020,0.020096,0.016733
Quadrature Filter Coefficients
0.000003,1.001823,0.000225,-0.030059,0.002596,0.032876

Loop #12
Subscriber Side
In Phase Filter Coefficients
0.000000,0.999992,-0.002269,0.001464,0.002293,-0.001469
Quadrature Filter Coefficients
0.000001,0.999465,0.012861,-0.015434,-0.013467,0.014799
Central Office Side
In Phase Filter Coefficients
0.000000,1.000619,-0.018851,-0.013808,0.019916,0.014042
Quadrature Filter Coefficients
0.000000,0.999856,0.002577,-0.033828,-0.003035,0.033549

Table 7.2: Coefficients of the Biquad at DS2 Rates with Reflected Signal = -40dB

Loop #13
Subscriber Side
In Phase Filter Coefficients
0.000001,1.000198,-0.001975,0.001548,0.002217,-0.001311
Quadrature Filter Coefficients
0.000001,1.000325,0.012688,-0.015335,-0.013438,0.014545
Central Office Side
In Phase Filter Coefficients
0.000011,0.986196,-0.025756,-0.035259,0.017855,0.028169
Quadrature Filter Coefficients
0.000003,0.998535,-0.022479,-0.027065,0.020358,0.024753

Loop #14
Subscriber Side
In Phase Filter Coefficients
0.000001,1.000629,-0.003158,0.001564,0.002615,-0.001424
Quadrature Filter Coefficients
0.000002,0.999225,0.012276,-0.015247,-0.013246,0.015898
Central Office Side
In Phase Filter Coefficients
0.000000,0.999028,-0.017268,-0.013002,0.019165,0.013677
Quadrature Filter Coefficients
0.000000,0.999589,0.003284,-0.035086,-0.003299,0.033762

Loop #15
Subscriber Side
In Phase Filter Coefficients
0.000000,1.000000,-0.002282,0.001478,0.002274,-0.001444
Quadrature Filter Coefficients
0.000000,1.000562,0.013742,-0.014519,-0.012609,0.015700
Central Office Side
In Phase Filter Coefficients
0.000000,0.999436,-0.019539,-0.015827,0.019752,0.015190
Quadrature Filter Coefficients
0.000002,0.999922,0.000167,-0.033011,-0.000985,0.032384

Table 7.2: Coefficients of the Biquad at DS2 Rates with Reflected Signal = -40dB

Loop #16
Subscriber Side
In Phase Filter Coefficients
0.000000,0.999962,-0.002053,0.001379,0.002115,-0.001757
Quadrature Filter Coefficients
0.000000,1.000156,0.013764,-0.014283,-0.011916,0.015625
Central Office Side
In Phase Filter Coefficients
0.000000,1.001311,-0.020126,-0.017705,0.021256,0.019729
Quadrature Filter Coefficients
0.000001,1.000487,-0.004054,-0.030908,0.003682,0.030275

Table 7.2: Coefficients of the Biquad at DS2 Rates with Reflected Signal = -40dB

Figures 7.8(c) and 7.8(d) are the constellation points for the reflected signal being -40 dB for the Central Office Side and the Subscriber Side respectively. Tables 7.3 and 7.4 indicate the signal to noise ratio obtained for the reflected signal being -26 dB and -40 dB respectively.

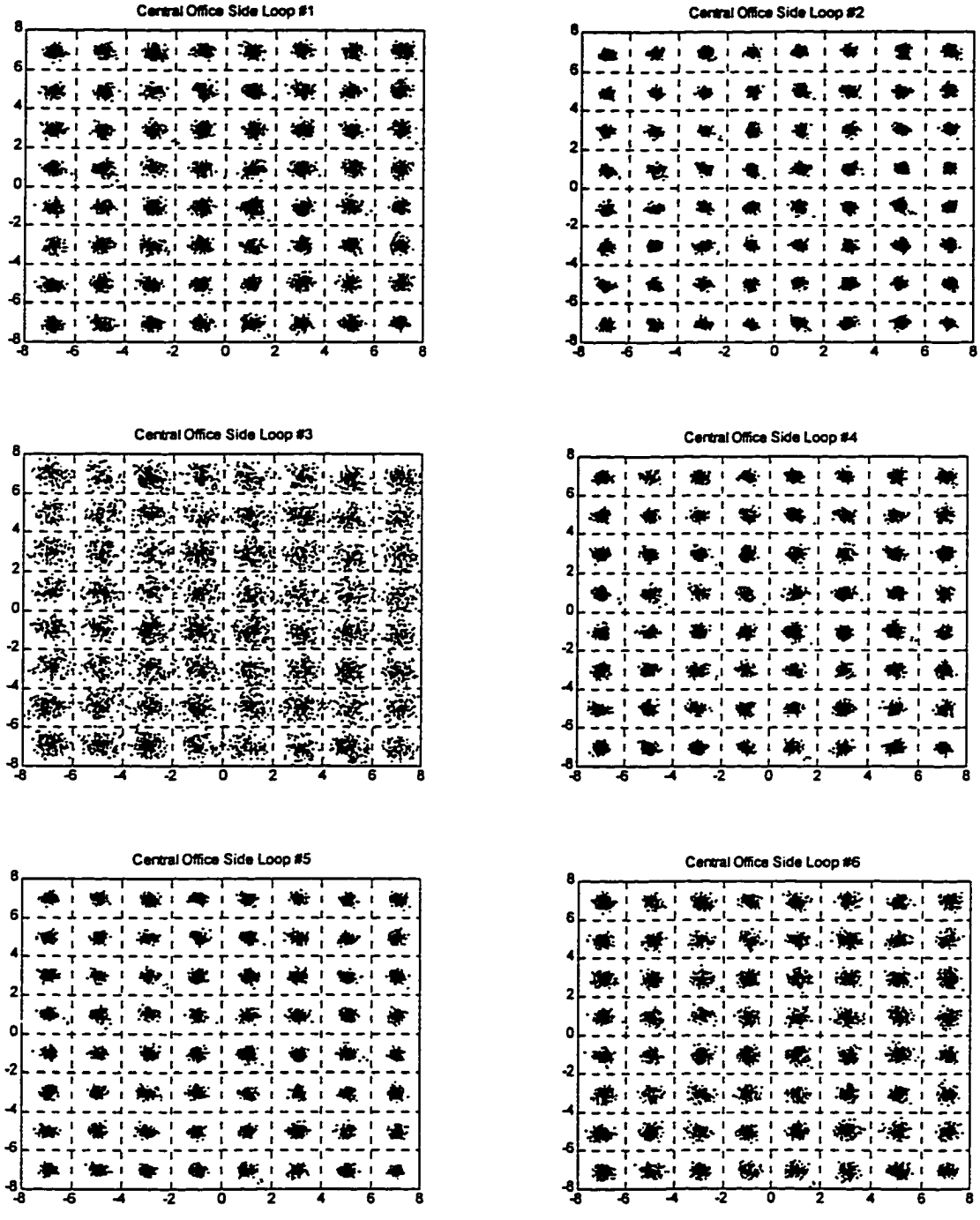

Figure 7.8(a): Central Office Side 64 CAP Constellation Reflected Signal = -26dB

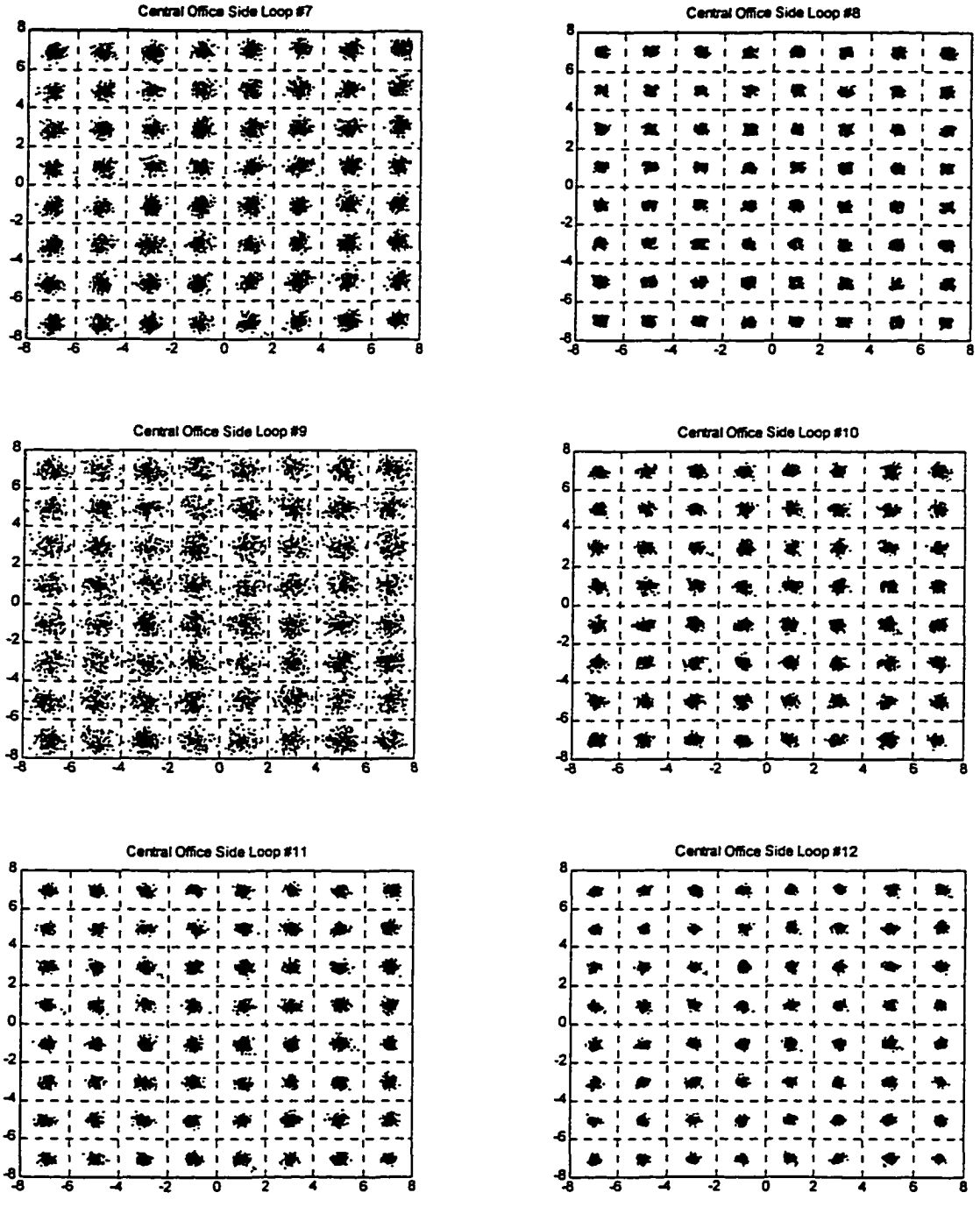

Figure 7.8(a): Central Office Side 64 CAP Constellation Reflected Signal = -26dB

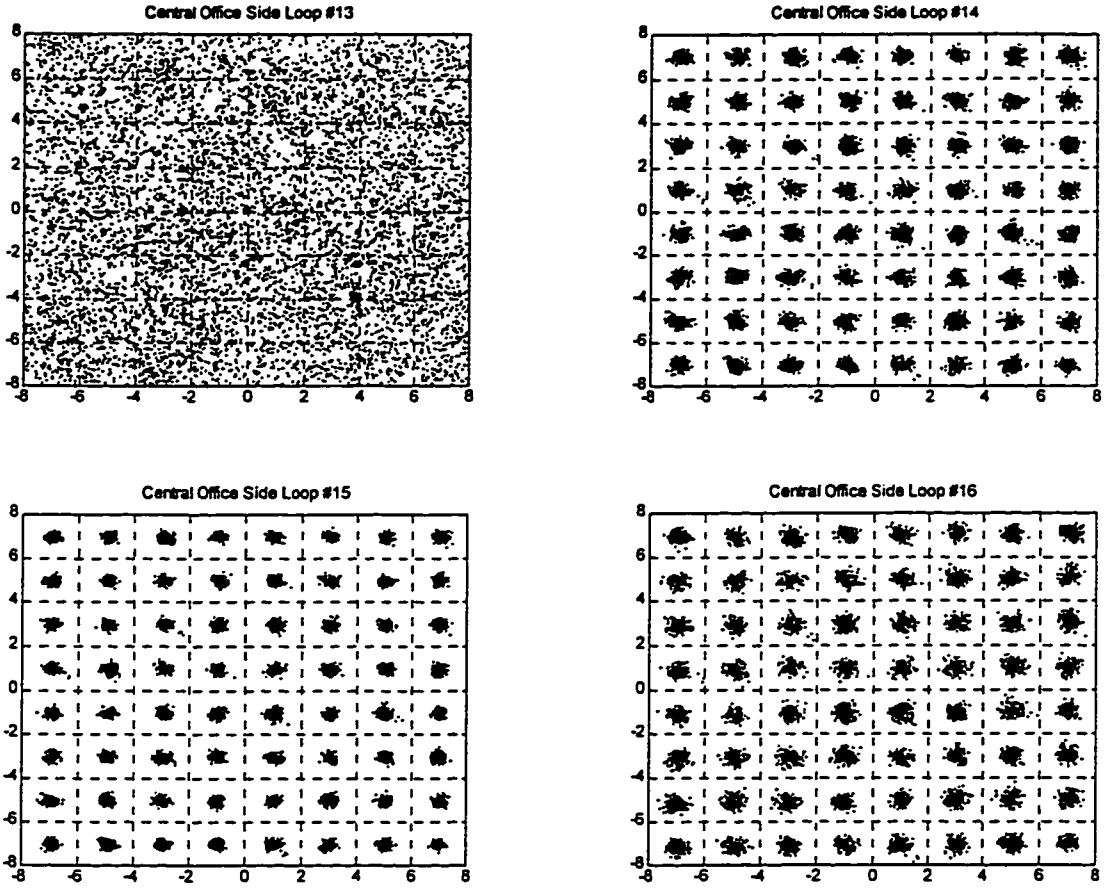

Figure 7.8(a): Central Office Side 64 CAP Constellation Reflected Signal = -26dB

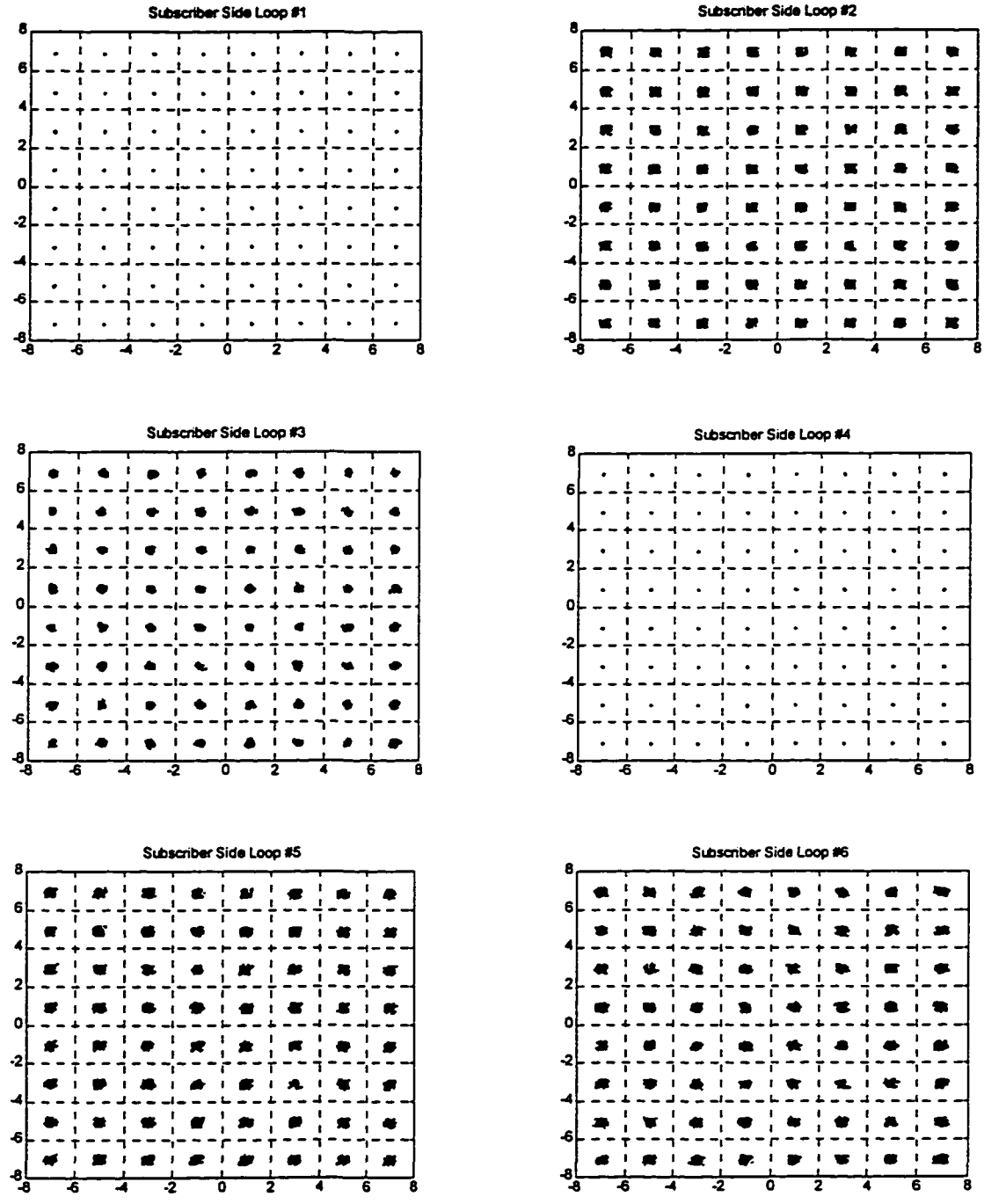

Figure 7.8(b): Subscriber Side 64 CAP Constellation Reflected Signal =-26dB

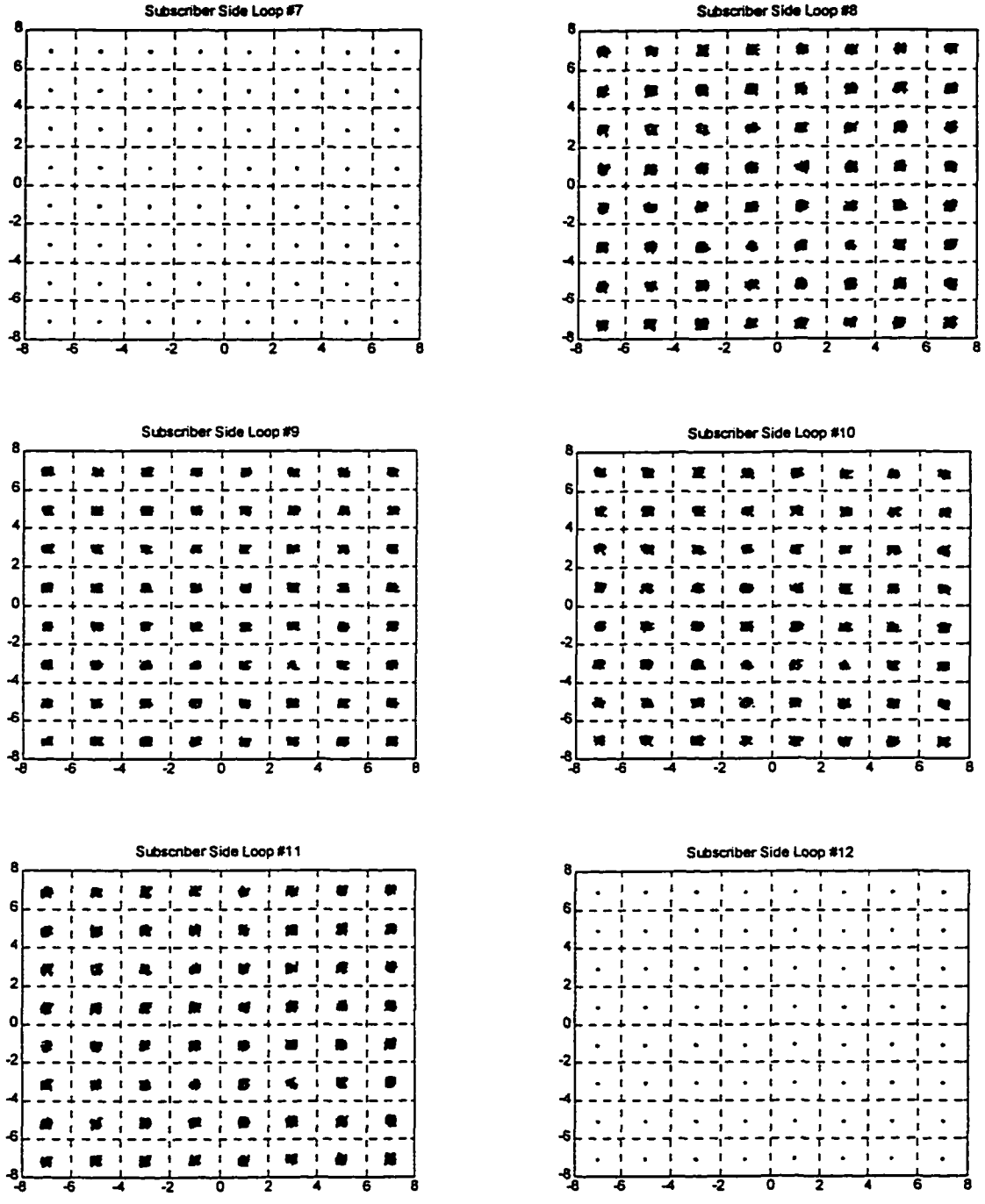

Figure 7.8(b): Subscriber Side 64 CAP Constellation Reflected Signal =-26dB

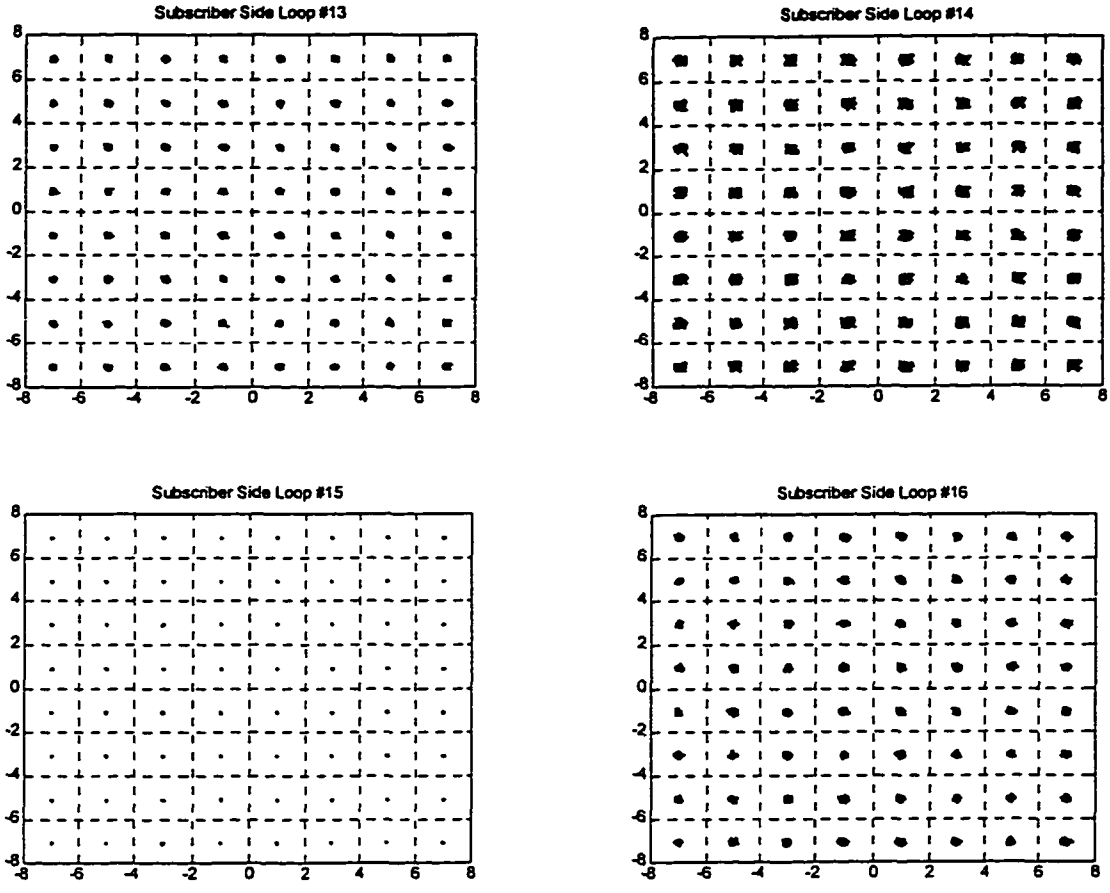

Figure 7.8(b): Subscriber Side 64 CAP Constellation Reflected Signal =-26dB

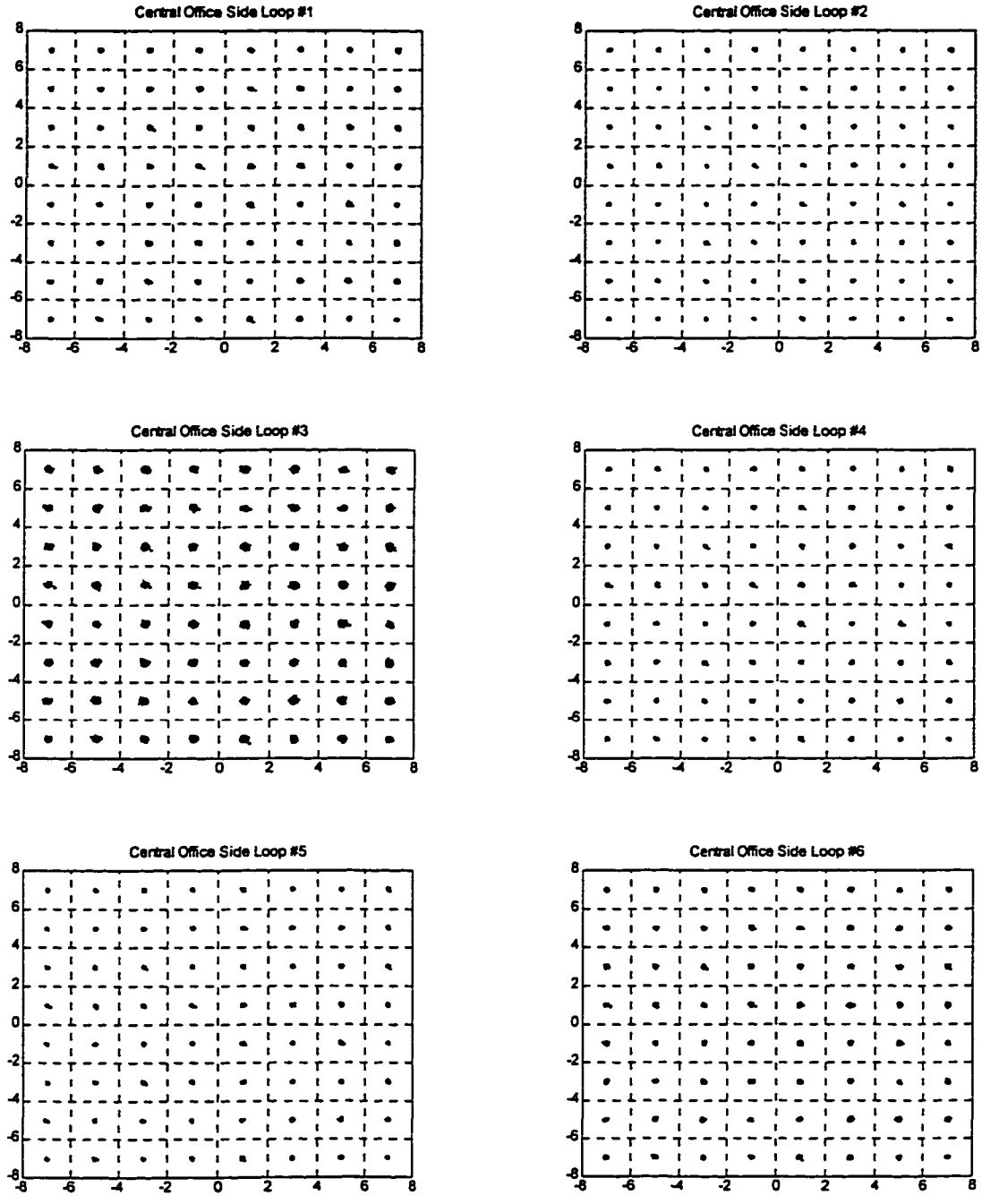

Figure 7.8(c): Central Office Side 64 CAP Constellation Reflected Signal =-40dB

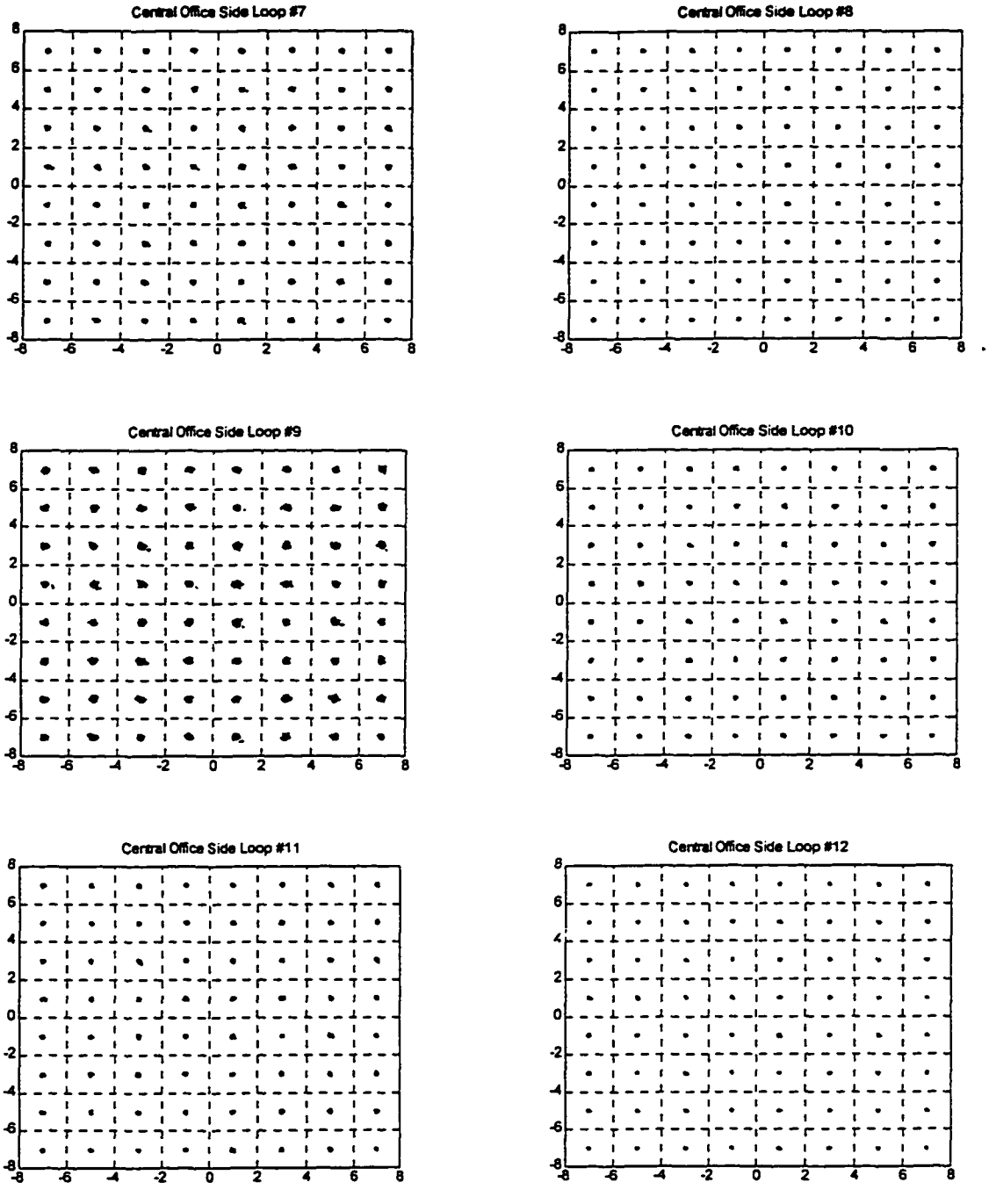

Figure 7.8(c): Central Office Side 64 CAP Constellation Reflected Signal =-40dB

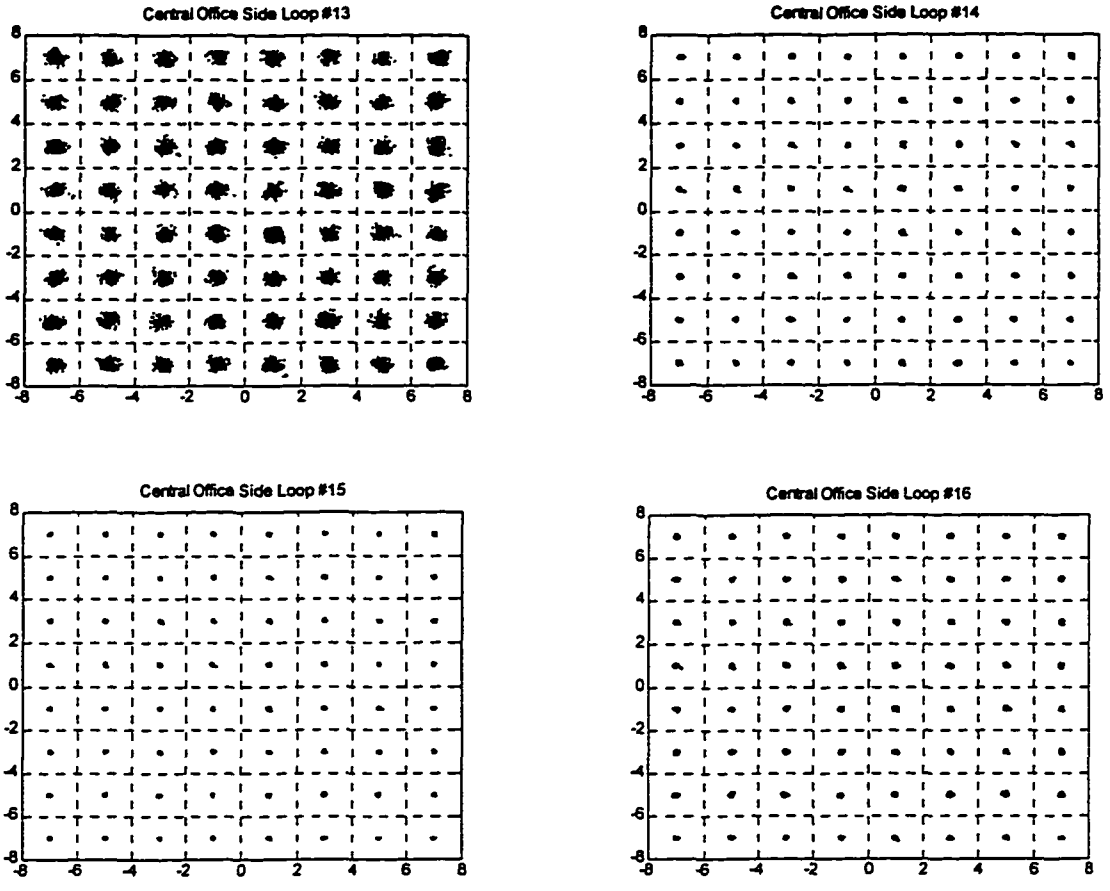

Figure 7.8(c): Central Office Side 64 CAP Constellation Reflected Signal =-40dB

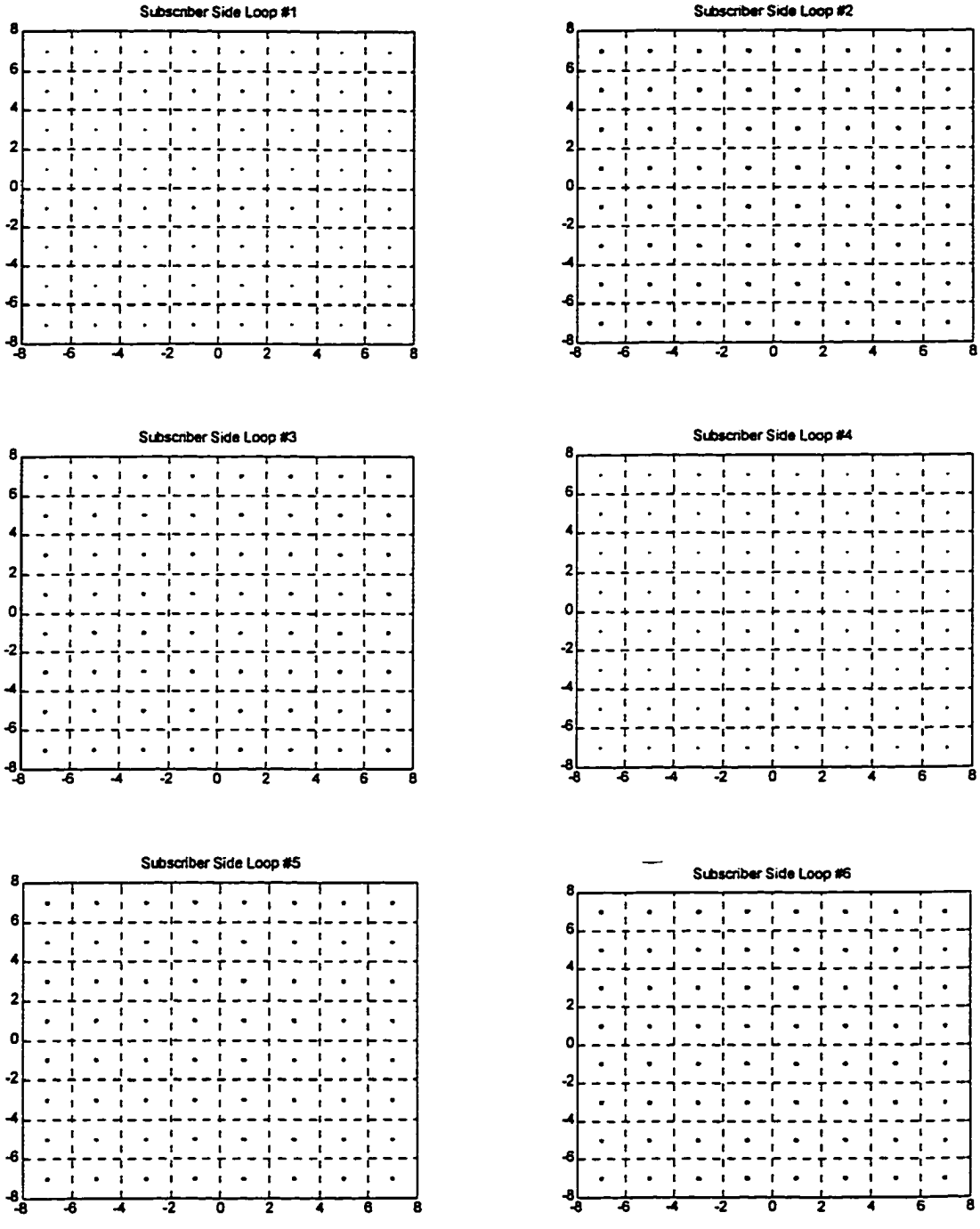

Figure 7.8(d): Subscriber Side 64 CAP Constellation Reflected Signal = -40dB

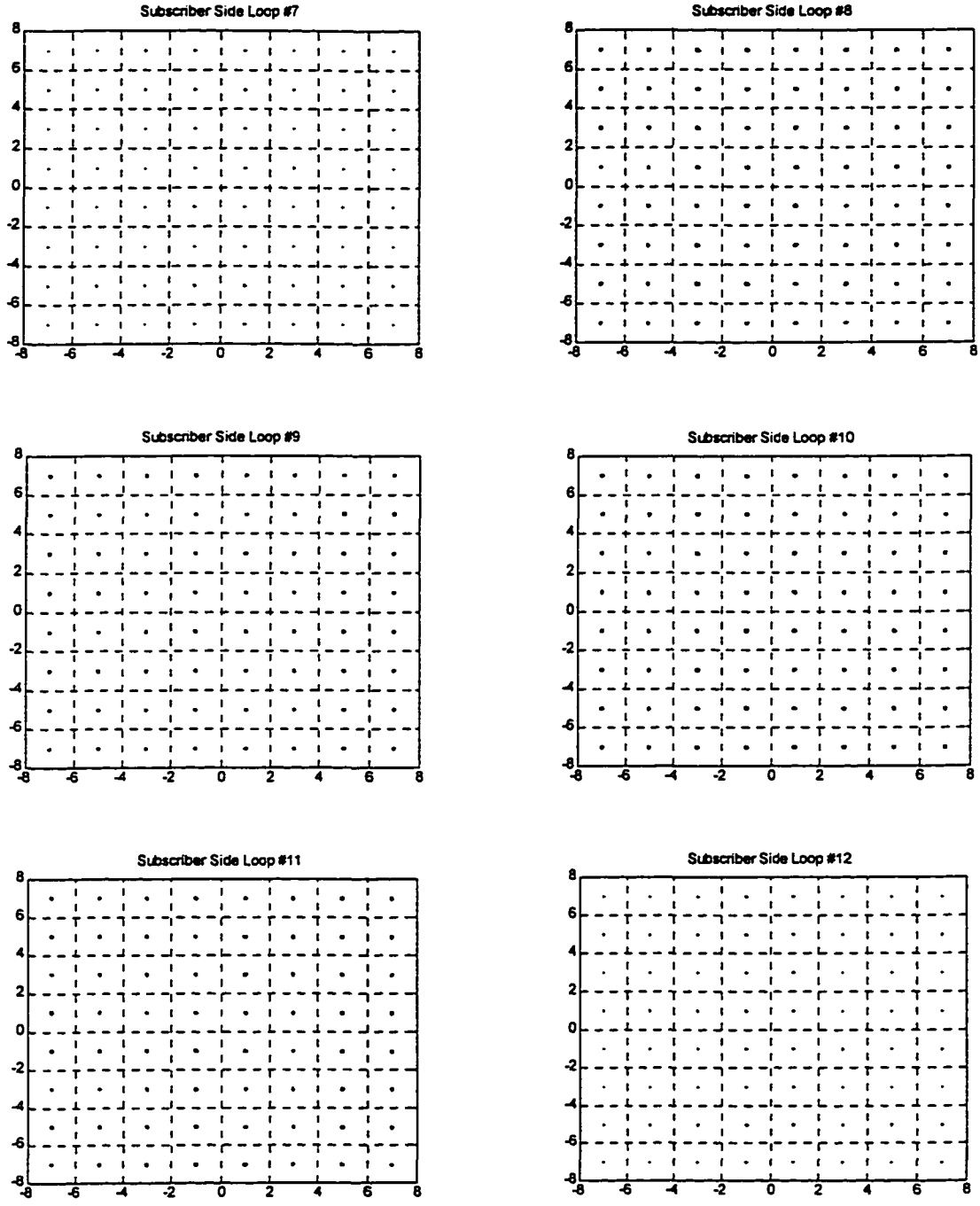

Figure 7.8(d): Subscriber Side 64 CAP Constellation Reflected Signal = -40dB

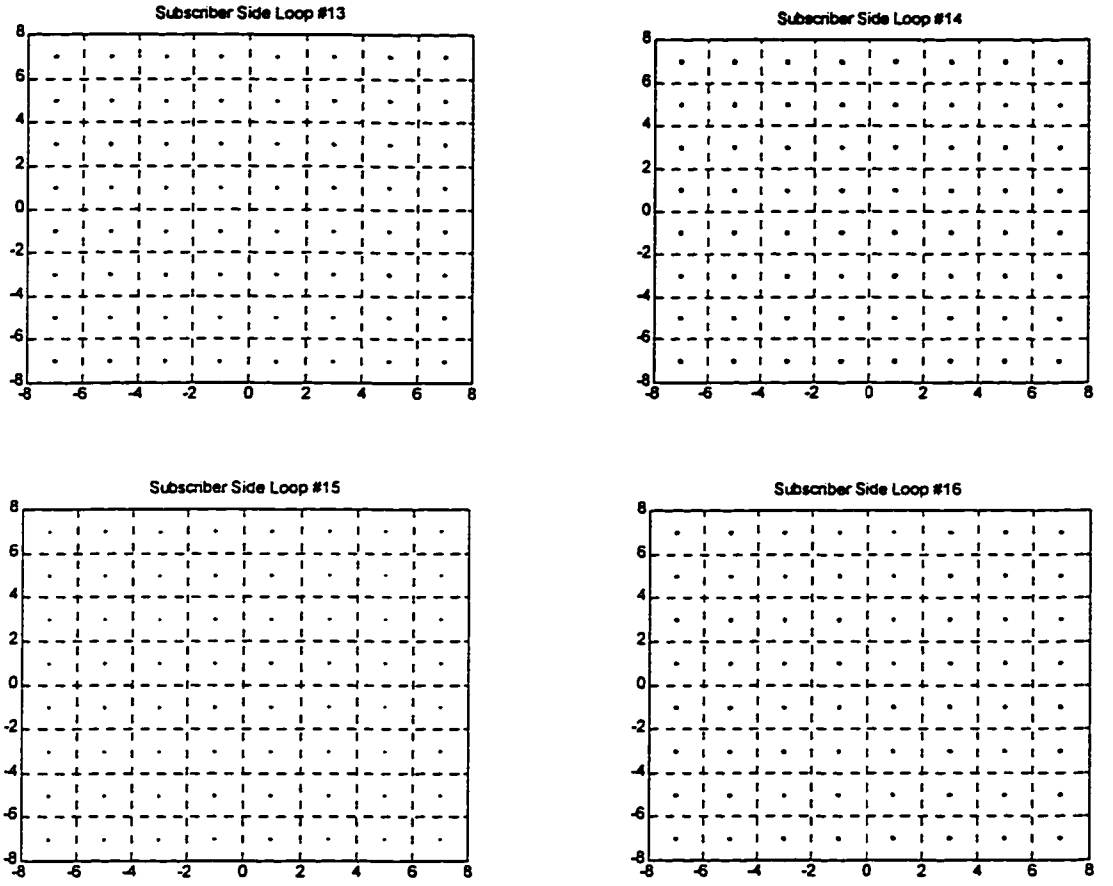

Figure 7.8(d): Subscriber Side 64 CAP Constellation Reflected Signal = -40dB

The signal to noise ratio is presented for the above constellations for both the reflected signals of -26dB and -40dB.

Loop #	SNR at SUB Side in dB	SNR at CO Side in dB
1	52.026194	25.585335
2	33.080543	27.854953
3	36.604254	20.213546
4	51.698812	26.949577
5	33.506317	26.921958
6	33.758717	24.761419
7	51.983024	25.701253
8	33.465671	26.610219
9	33.922607	21.805605
10	33.224761	26.277449
11	33.710060	27.183372
12	52.366499	29.618196
13	39.559931	13.309741
14	33.567065	26.396763
15	52.026998	28.322386
16	38.409177	25.195626

Table 7.3: SNR with the reflected signal being 26 dB down

When the signal is received on the Subscriber Side with a reflection component of -26dB in it, loops 1, 4, 7, 12 and 15 have SNR of above 50dB while the other loops have a SNR of about 33 dB and with loop 3 having 36 dB and the loops 13 and 16 coming close to 40dB. On the Central Office Side most of the loops have a SNR of greater than 20dB with average being for all the loops of about 25 dB. Loop 13 seems

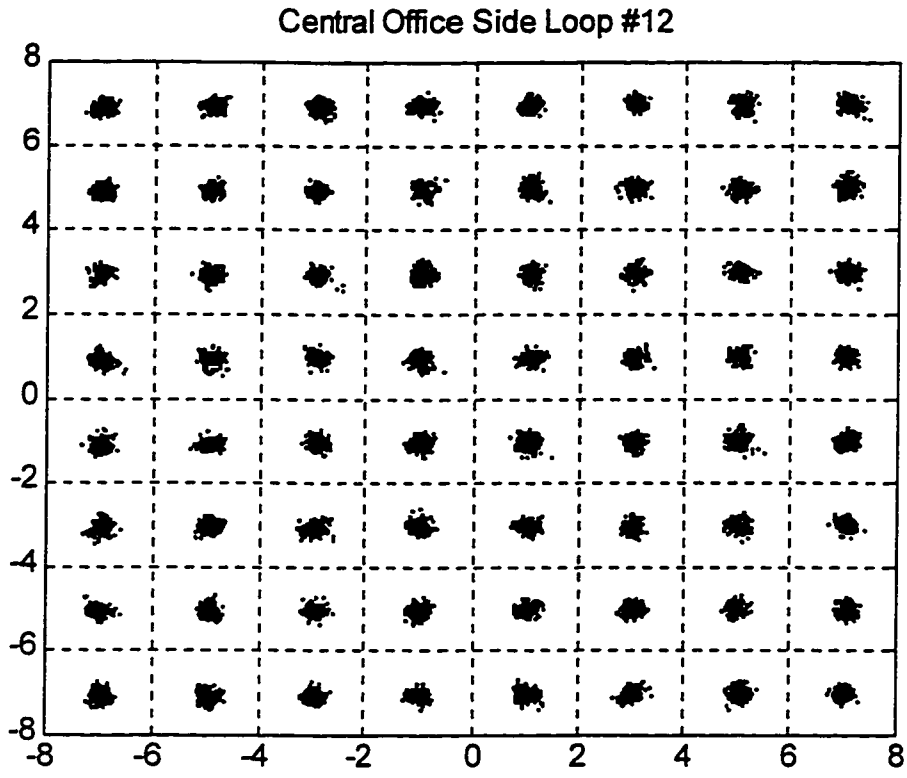

Figure 7.81(a): Best Case loop of the Central Office Side with the Reflected Signal = -26dB and SNR = 29.61dB

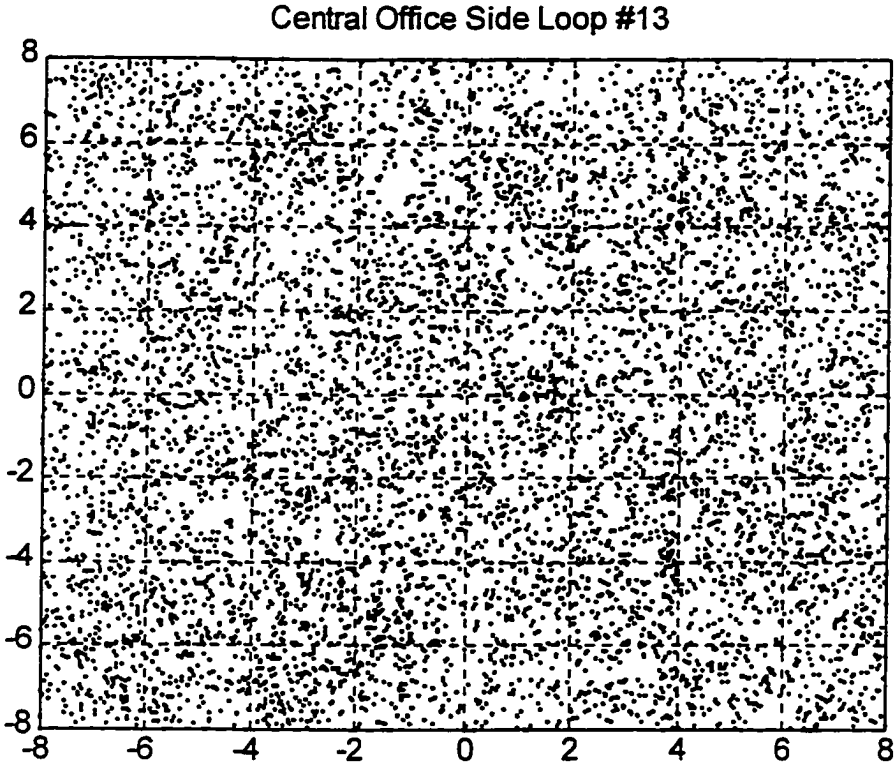

Figure 7.81(b): Worst Case loop of the Central Office Side with the Reflected Signal = -26dB and SNR = 13.30dB

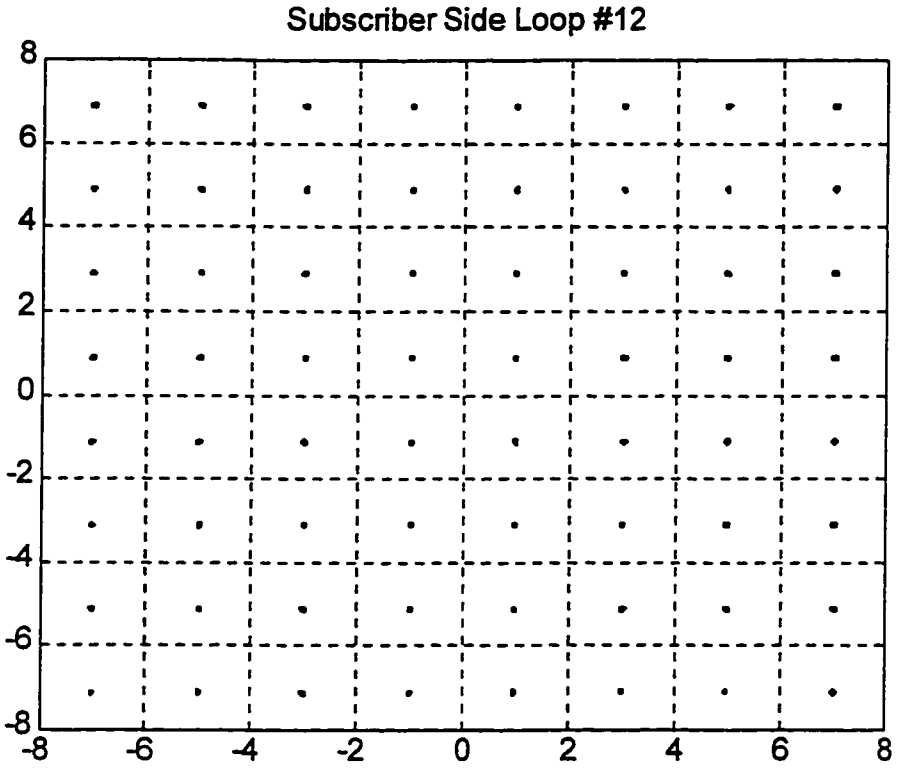

Figure 7.81(c): Best Case loop of the Subscriber Side with the Reflected Signal = -26dB and SNR = 52.36dB

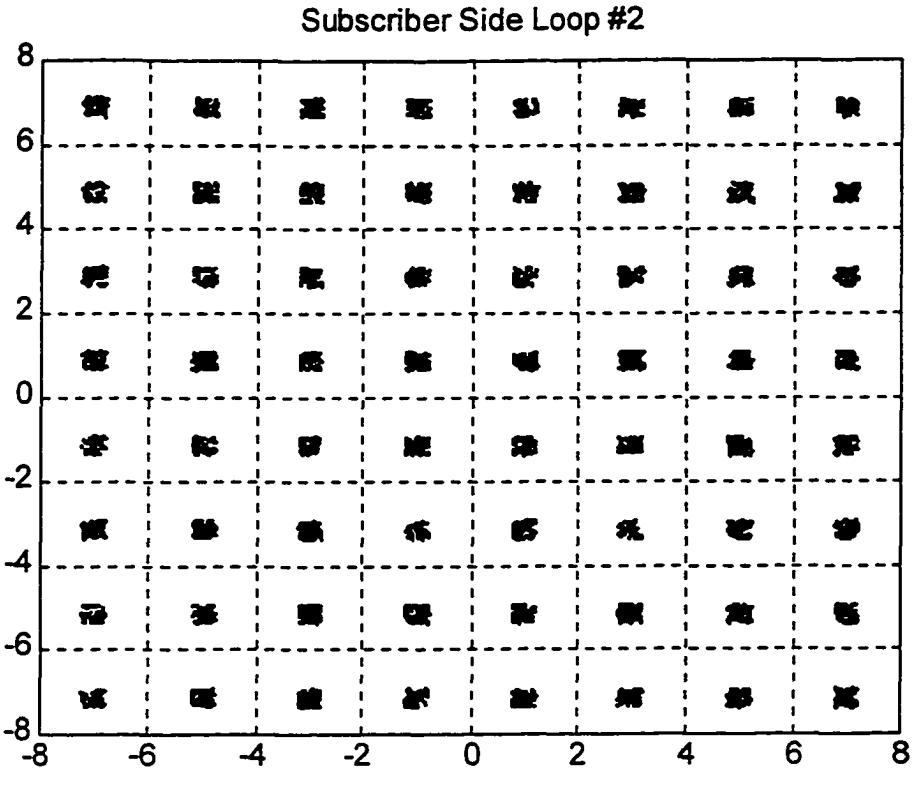

Figure 7.81(d): Worst Case loop of the Subscriber Side with the Reflected Signal = -26dB and SNR = 33.08dB

to behave badly with a SNR of 13 dB, loops 3 and 9 are also equally bad with SNR of 20 dB which as seen from the table and the constellation plot.

Loop #	SNR at SUB Side in dB	SNR at CO Side in dB
1	66.005500	39.564732
2	47.059937	41.834345
3	50.583634	34.192952
4	65.678105	40.928978
5	47.485716	40.901344
6	47.738121	38.740817
7	65.962349	39.680651
8	47.445068	40.589616
9	47.902006	35.785004
10	47.204168	40.256842
11	47.689456	41.162773
12	66.345800	43.597581
13	53.539286	27.289144
14	47.546473	40.376156
15	66.006359	42.301786
16	52.388563	39.175023

Table 7.4: SNR with the reflected signal being 40 dB down

With the reflection signal being -40dB the Subscriber Side loops have SNR of 47 dB and greater with loop 3, 13 and 16 having SNR of 50 dB and above and the loops 1, 4, 7 and 15 doing well with SNR of about 66 dB.

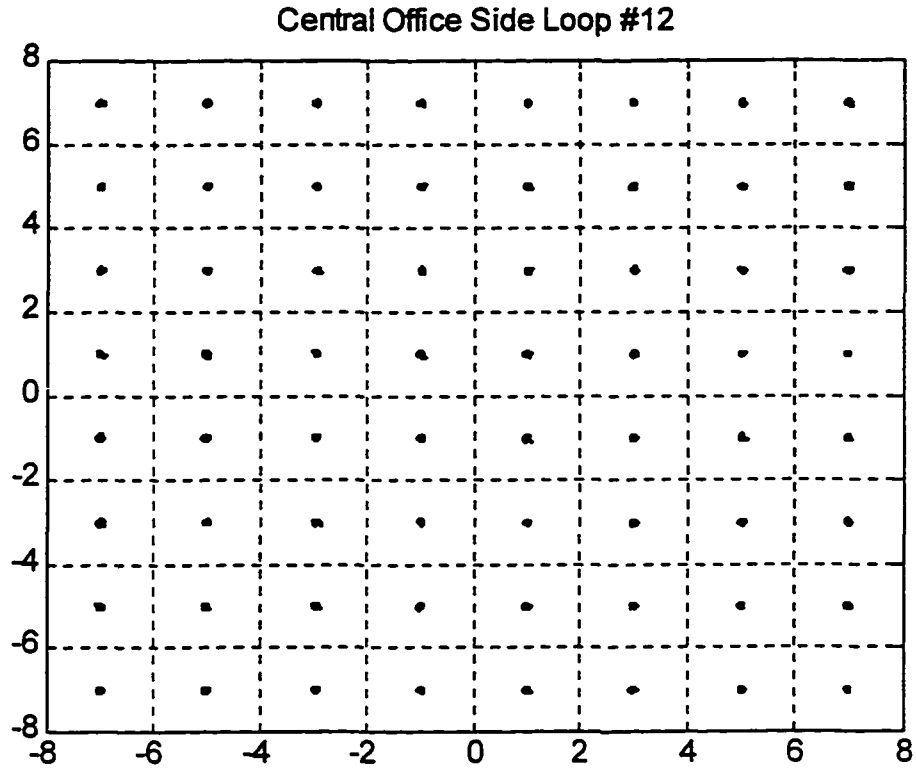

Figure 7.82(a): Best Case loop of the Central Office Side with the Reflected Signal = -40dB and SNR = 43.59dB

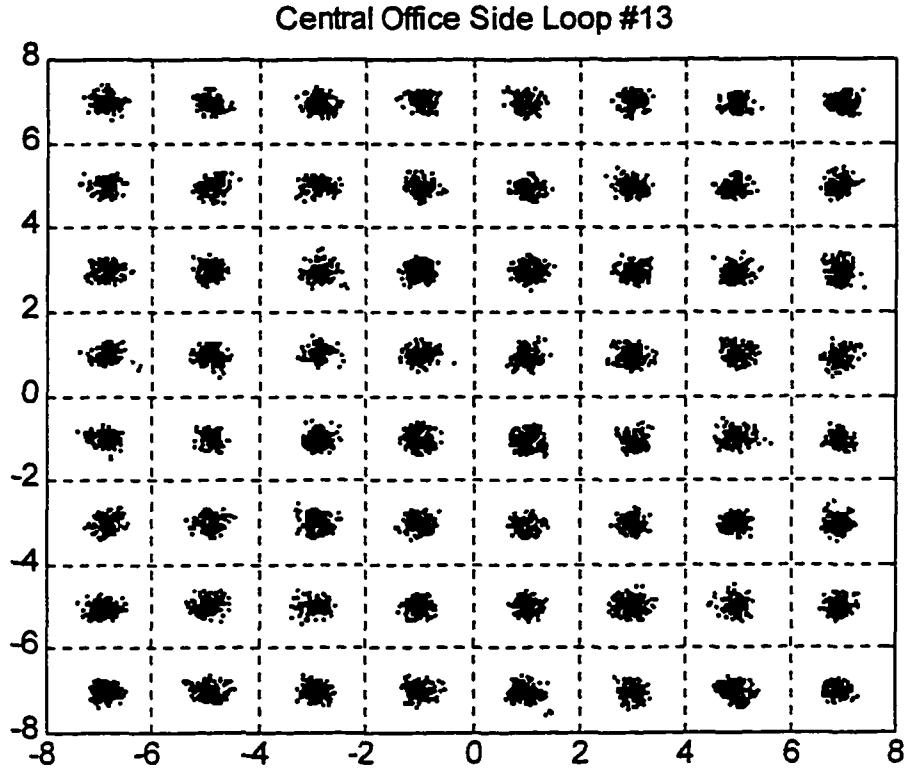

Figure 7.82(b): Worst Case loop of the Central Office Side with the Reflected Signal = -40dB and SNR = 27.28dB

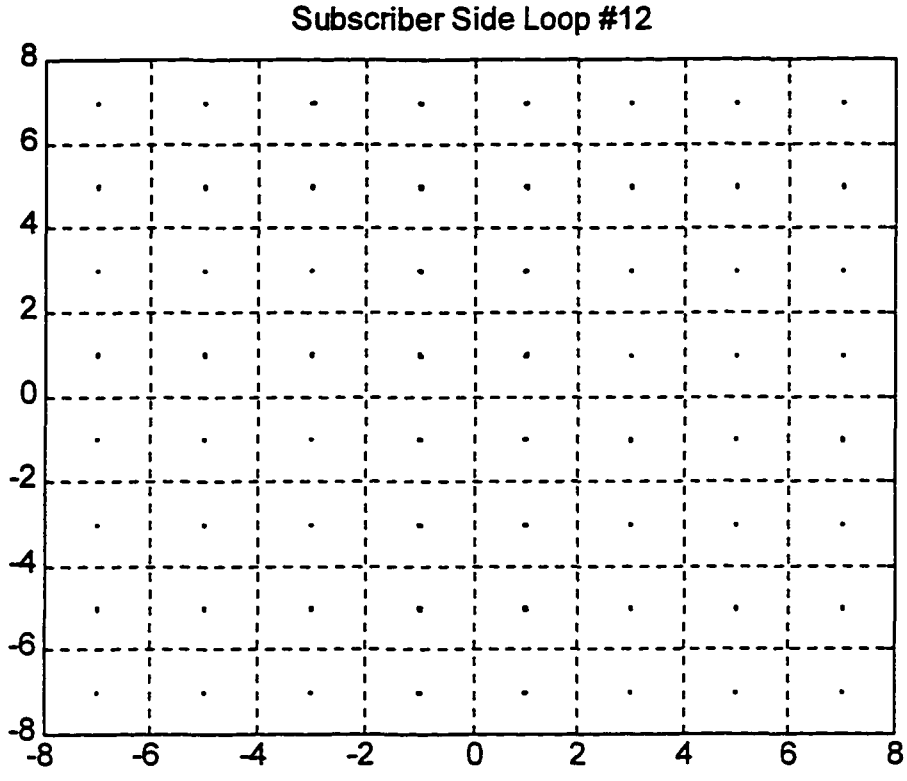

Figure 7.82(c): Best Case loop of the Subscriber Side with the Reflected Signal = -40dB and SNR = 66.34dB

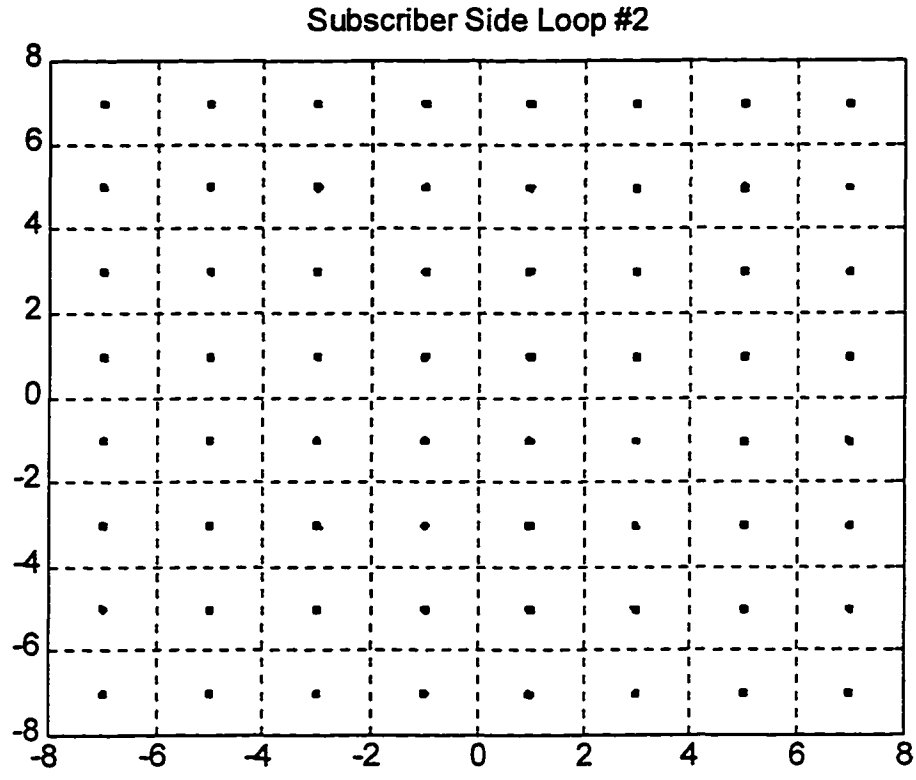

Figure 7.82(d): Worst Case loop of the Subscriber Side with the Reflected Signal = -40dB and SNR = 47.05dB

In the second part of the simulation the biquads were used but instead of using fixed coefficients the coefficients were adapted continuously, that is the update of the coefficients were done for every symbol update. The training was carried for 3200 symbol period and the constellation plots are as shown in the figure 7.9(a), 7.9(b), 7.9(c) and 7.9(d). Figure 7.9(a) indicates the plot for the Central Office Side with the reflected component being -26dB and figure 7.9(b) shows the plot for the Subscriber Side with the reflected signal also being -26dB. For the reflected signal being -40dB the Central Office Side and the Subscriber Side plots are as shown in the figures 7.9(c) and 7.9(d) respectively. The signal to noise ratio for these constellation plots are as shown in the tables 7.5 and 7.6, with table 7.5 representing the loops with reflected signal of -26dB both for the CO and the SUB side and the table 7.6 representing the loops with the reflected signal of -40dB. The model used for this simulation is the same as the model shown in the figure 7.5. The constellation points in the figures 7.82(a), 7.82(b), 7.82(c) and 7.82(d) represent the enhanced view of the constellation plots for the best case and the worst case loops at the Central Office side and Subscriber side with the reflected component being -40dB.

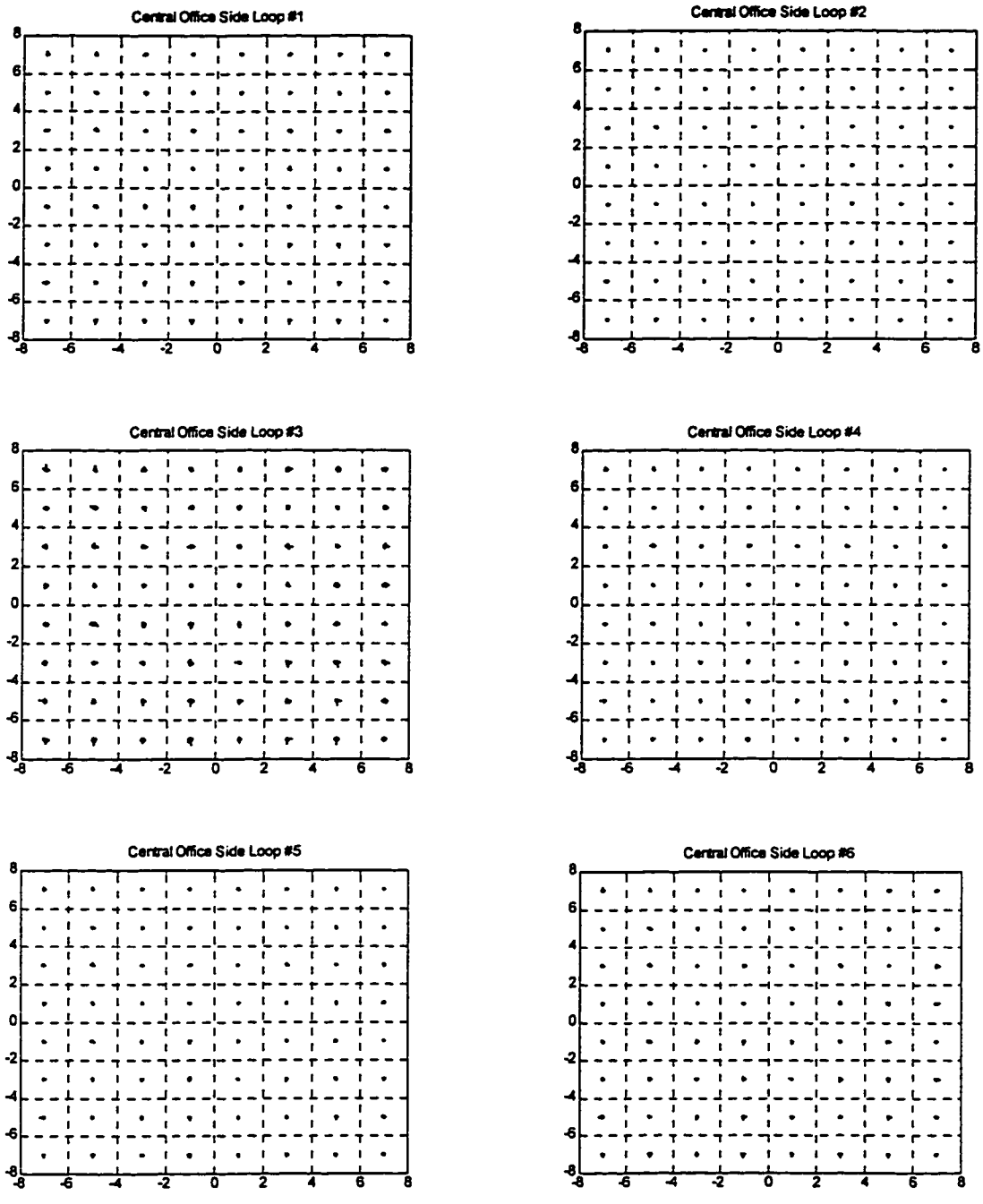

Figure 7.9(a): Central Office Side 64 CAP Constellation after Adaptation with Reflected Signal =- 26 dB

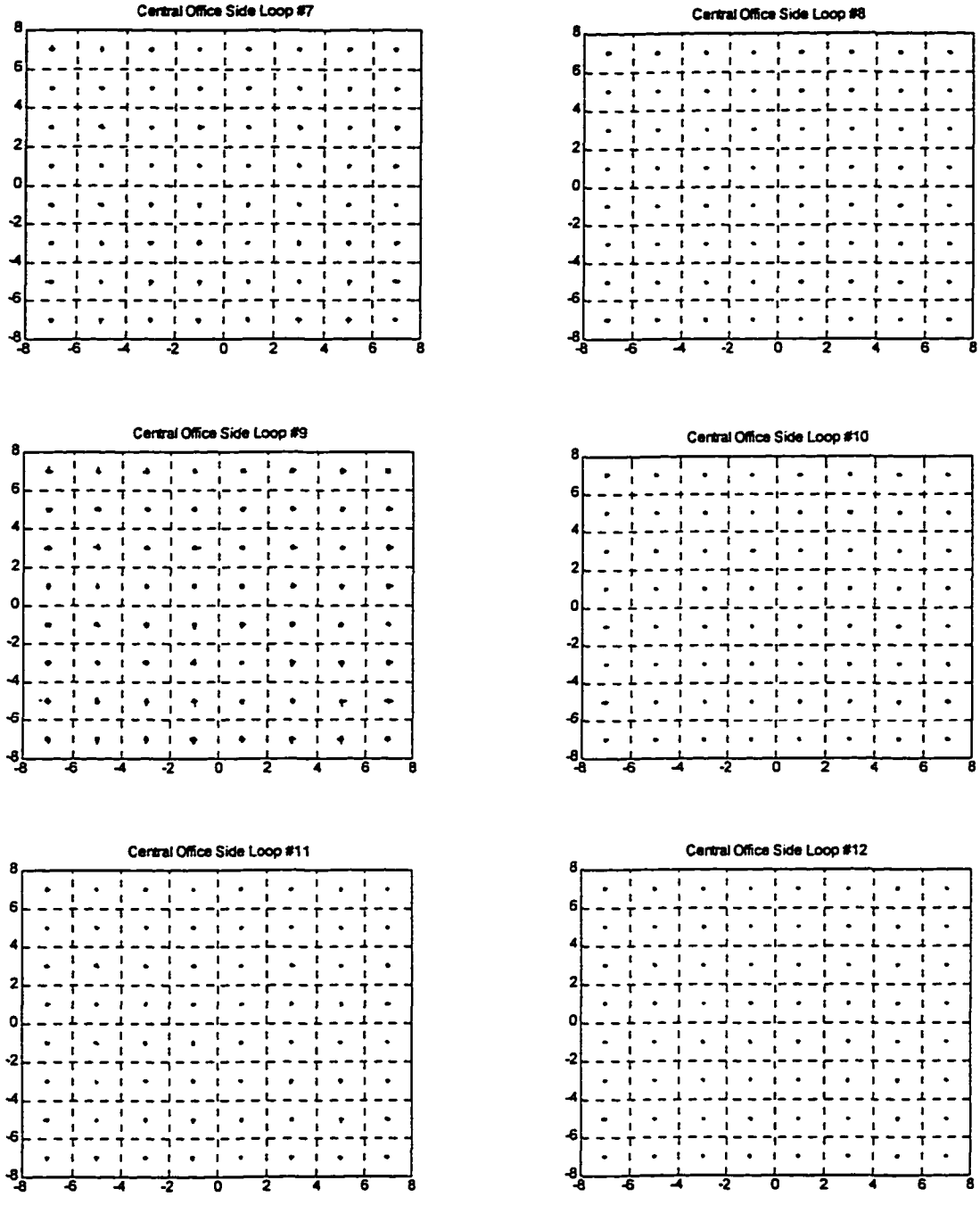

Figure 7.9(a): Central Office Side 64 CAP Constellation after Adaptation with Reflected Signal =- 26 dB

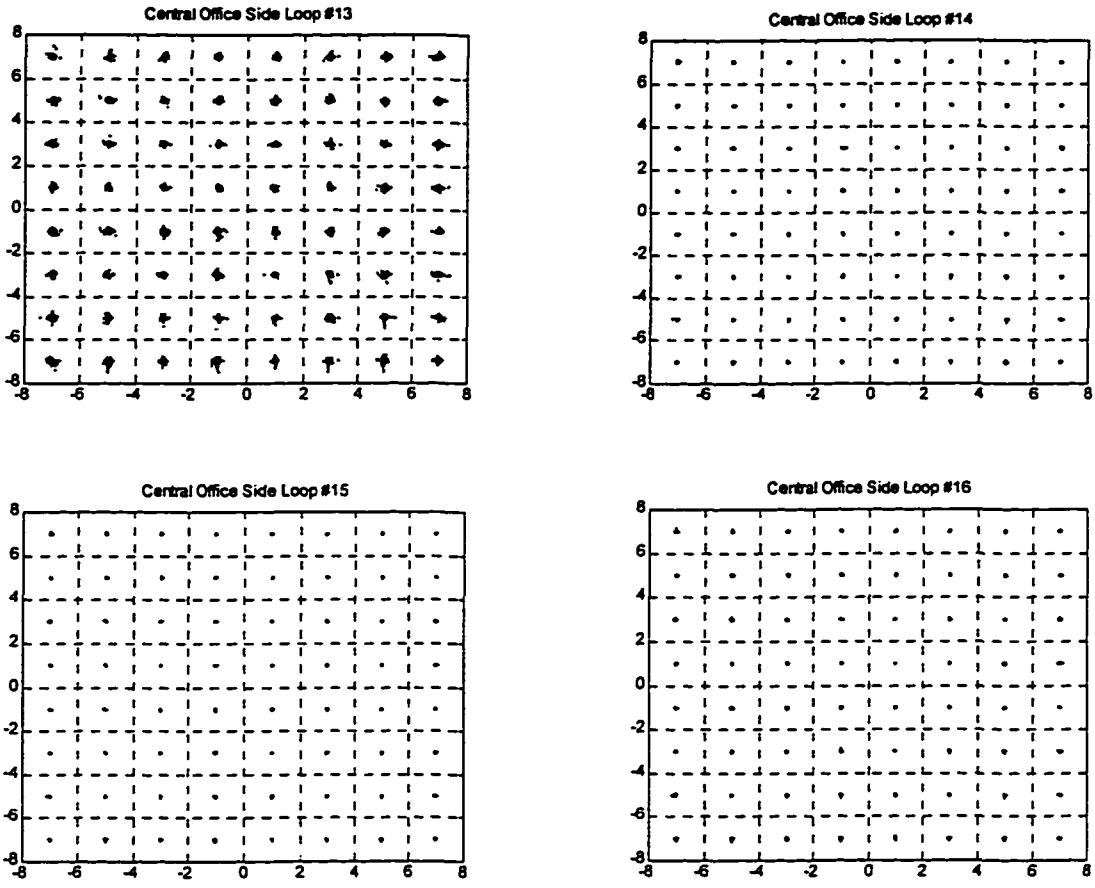

Figure 7.9(a): Central Office Side 64 CAP Constellation after Adaptation with Reflected Signal =- 26 dB

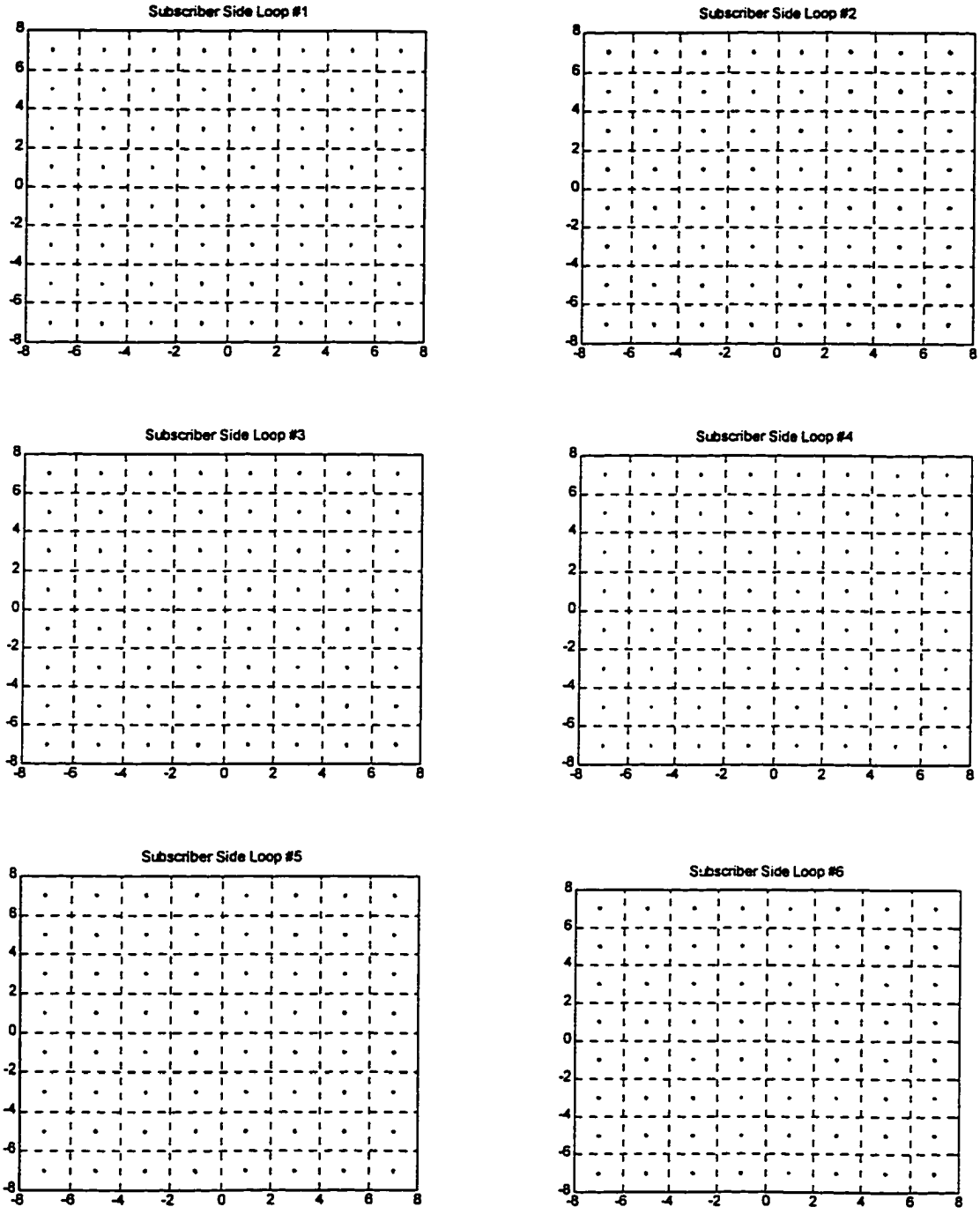

Figure 7.9(b): Subscriber Side 64 CAP Constellation after Adaptation with Reflected Signal =-26 dB

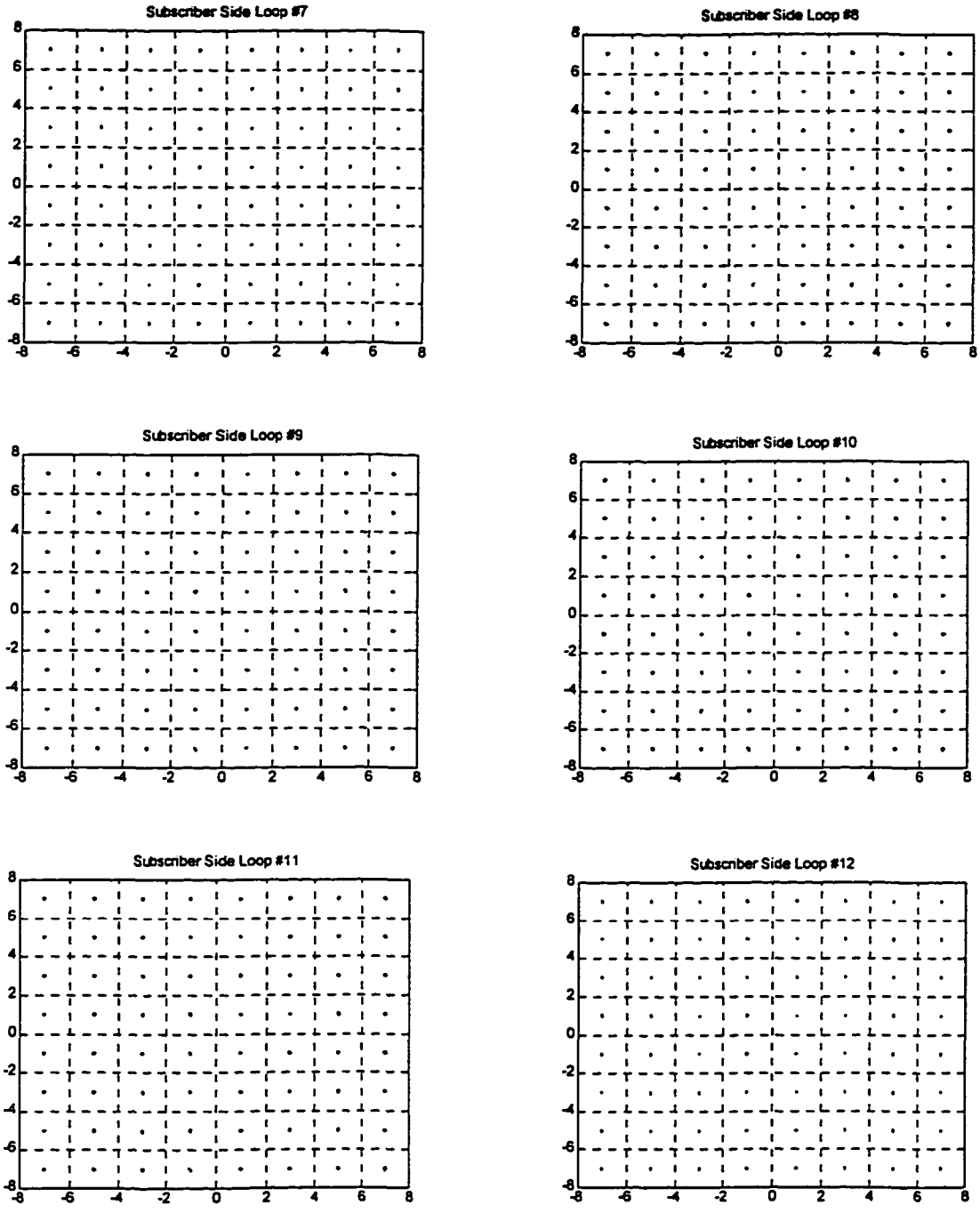

Figure 7.9(b): Subscriber Side 64 CAP Constellation after Adaptation with Reflected Signal =-26 dB

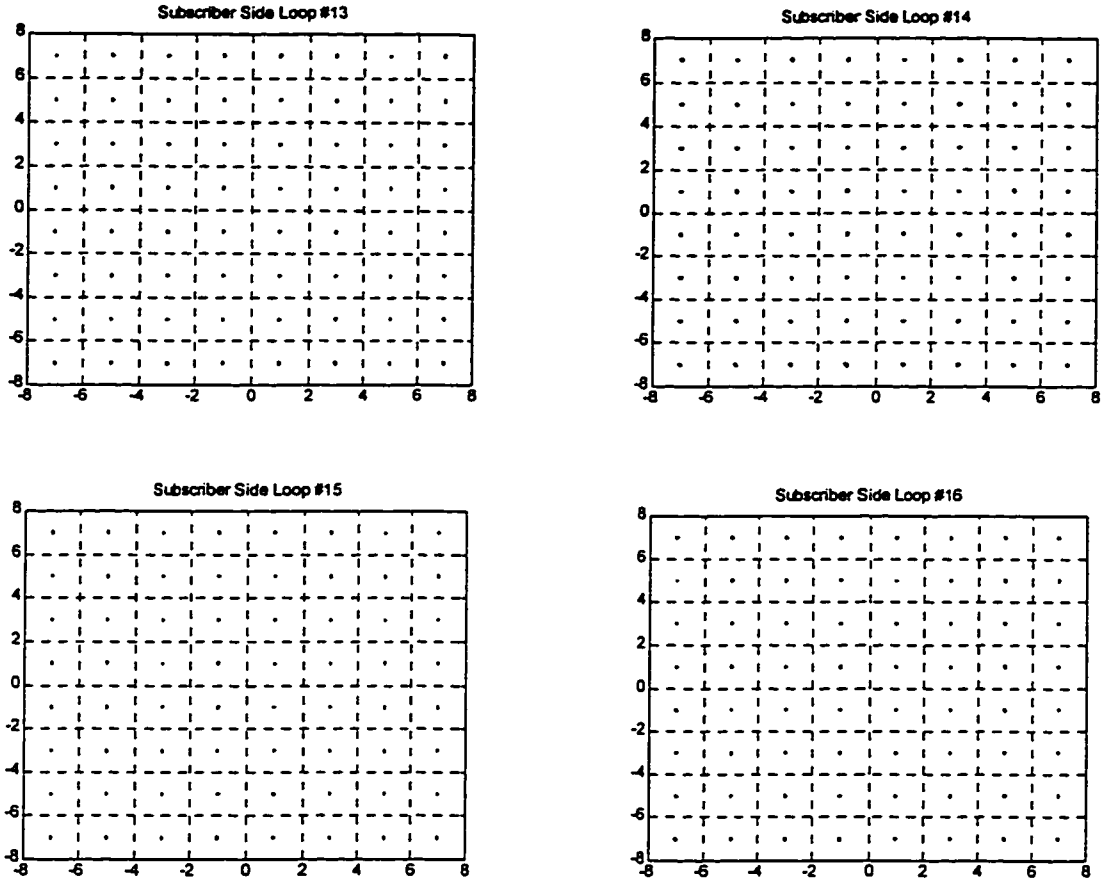

Figure 7.9(b): Subscriber Side 64 CAP Constellation after Adaptation with Reflected Signal =-26 dB

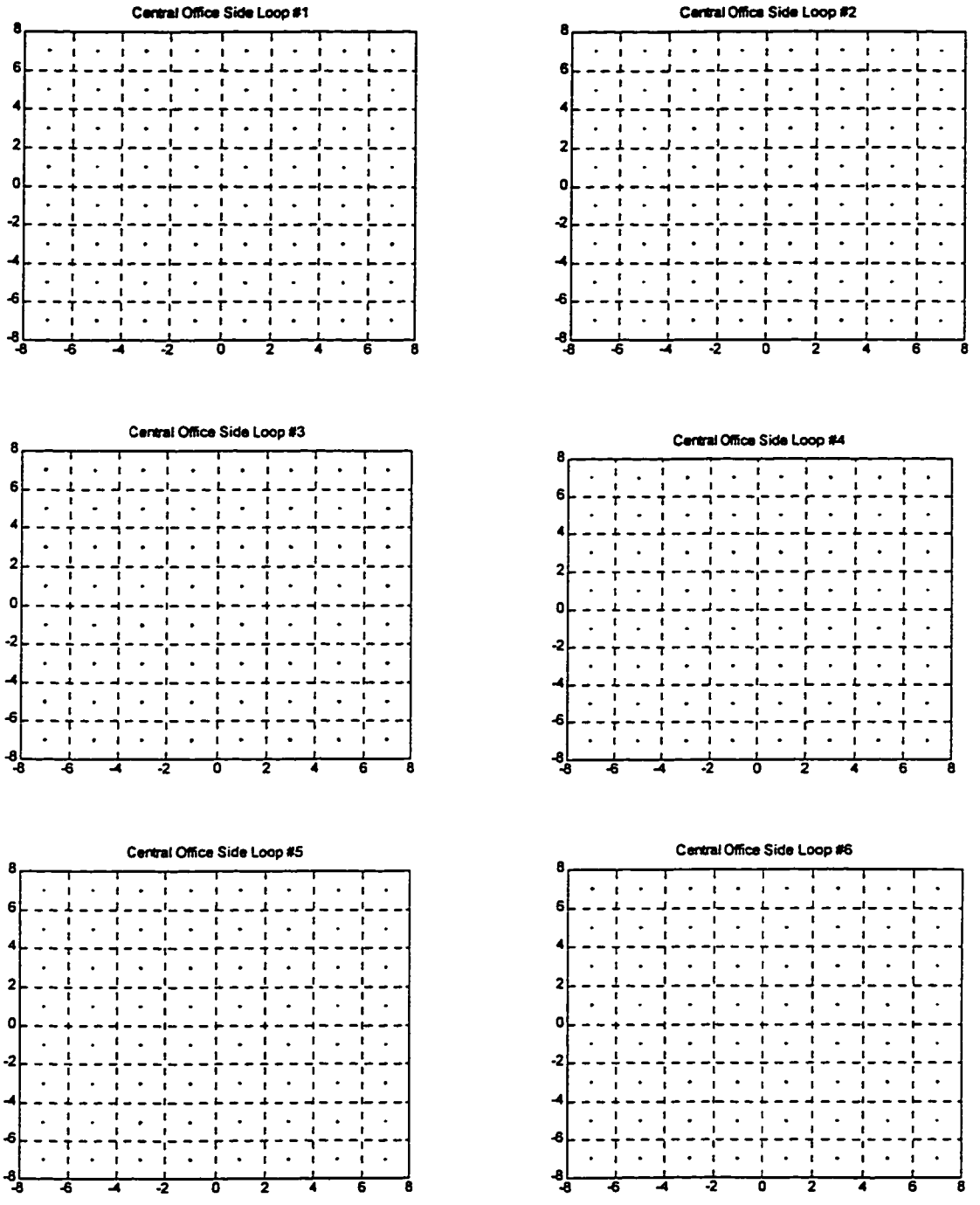

Figure 7.9(c): Central Office Side 64 Constellation After Adaptation with Reflected Signal =-40dB

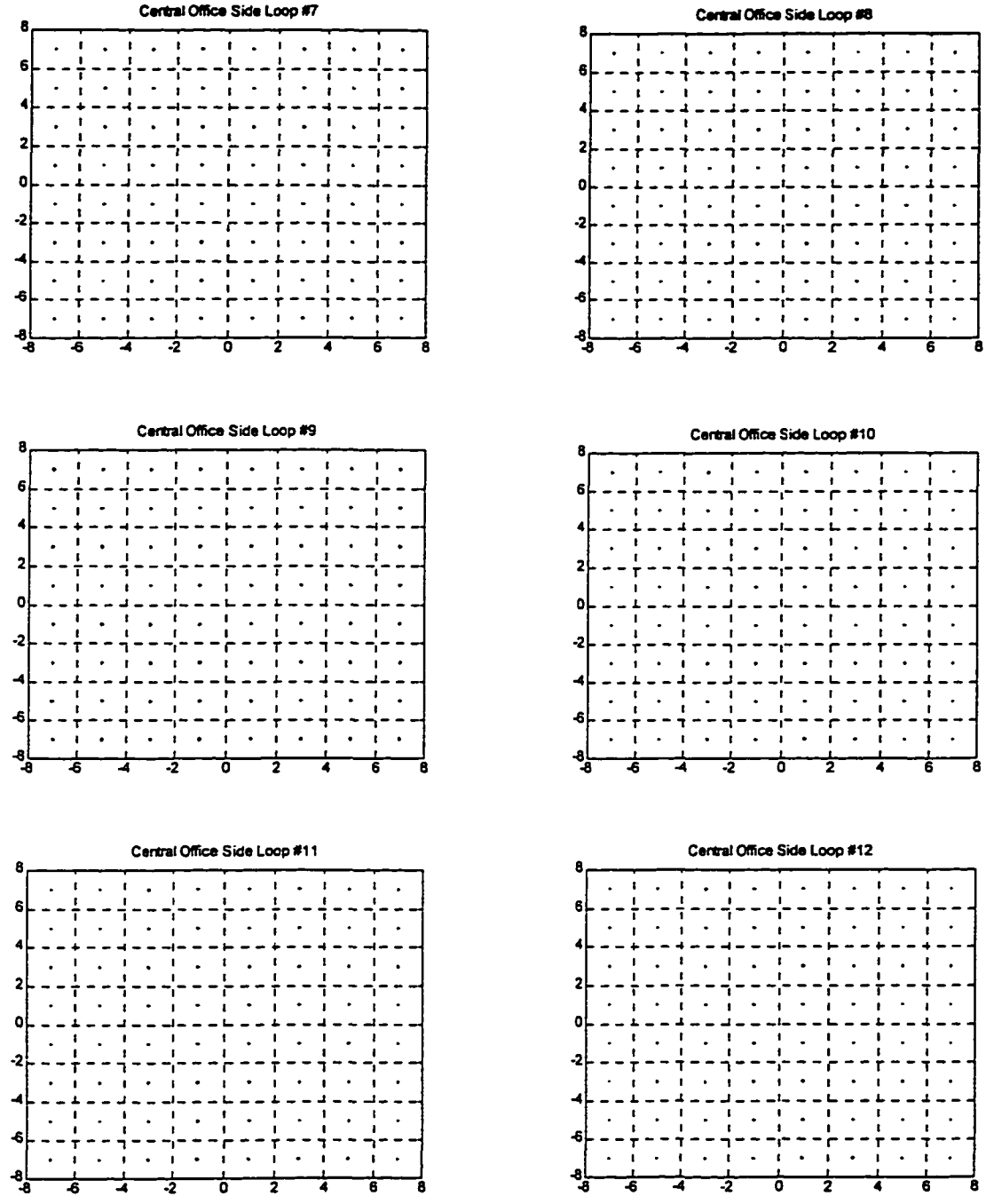

Figure 7.9(c): Central Office Side 64 Constellation After Adaptation with Reflected Signal =-40dB

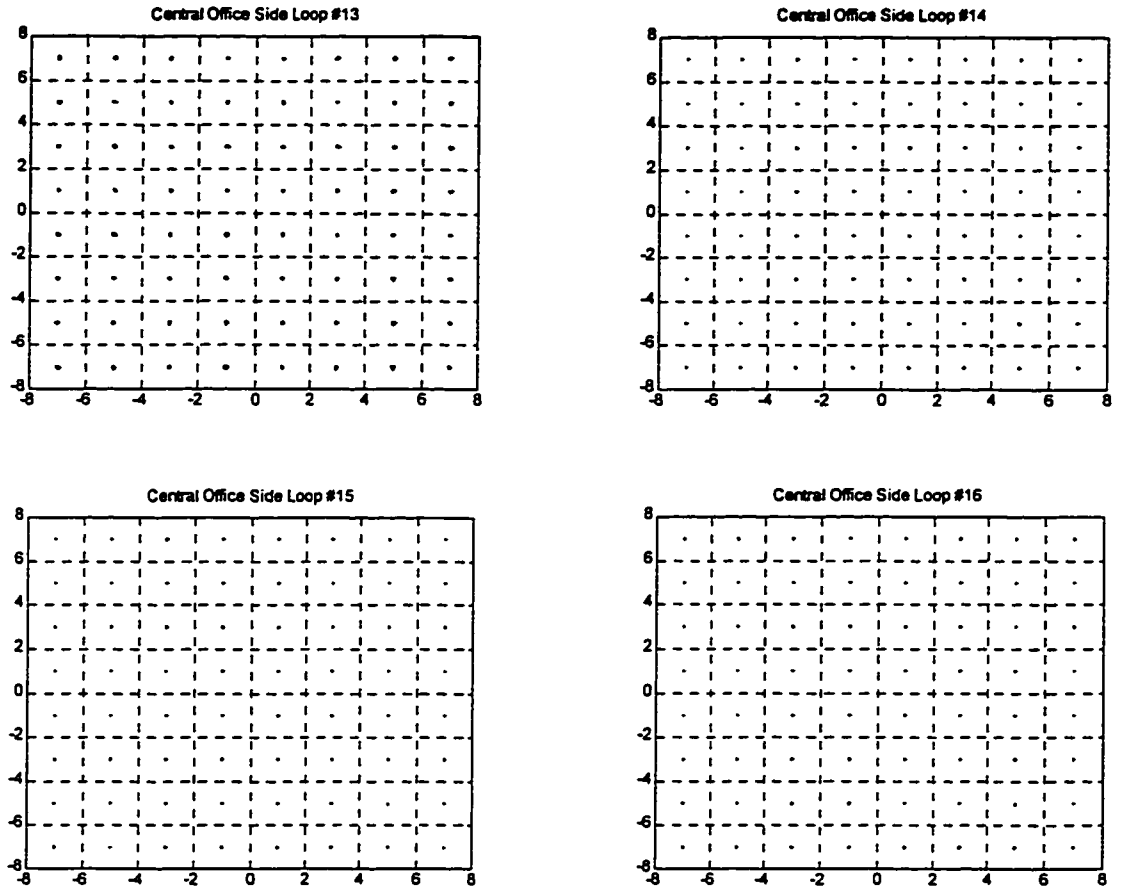

Figure 7.9(c): Central Office Side 64 Constellation After Adaptation with Reflected Signal =-40dB

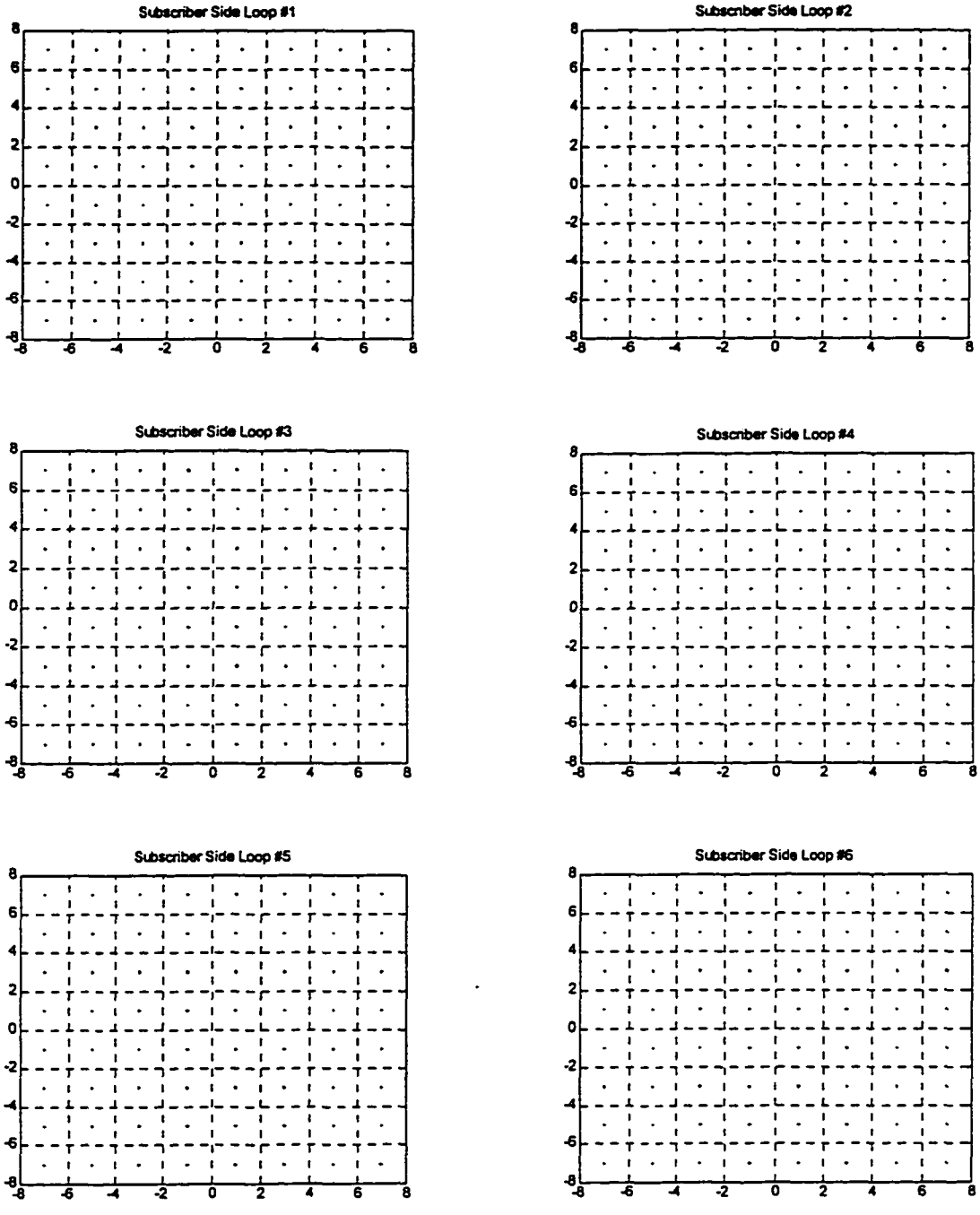

Figure 7.9(d): Subscriber Side 64 CAP Constellation After Adaptation with Reflected Signal =-40dB

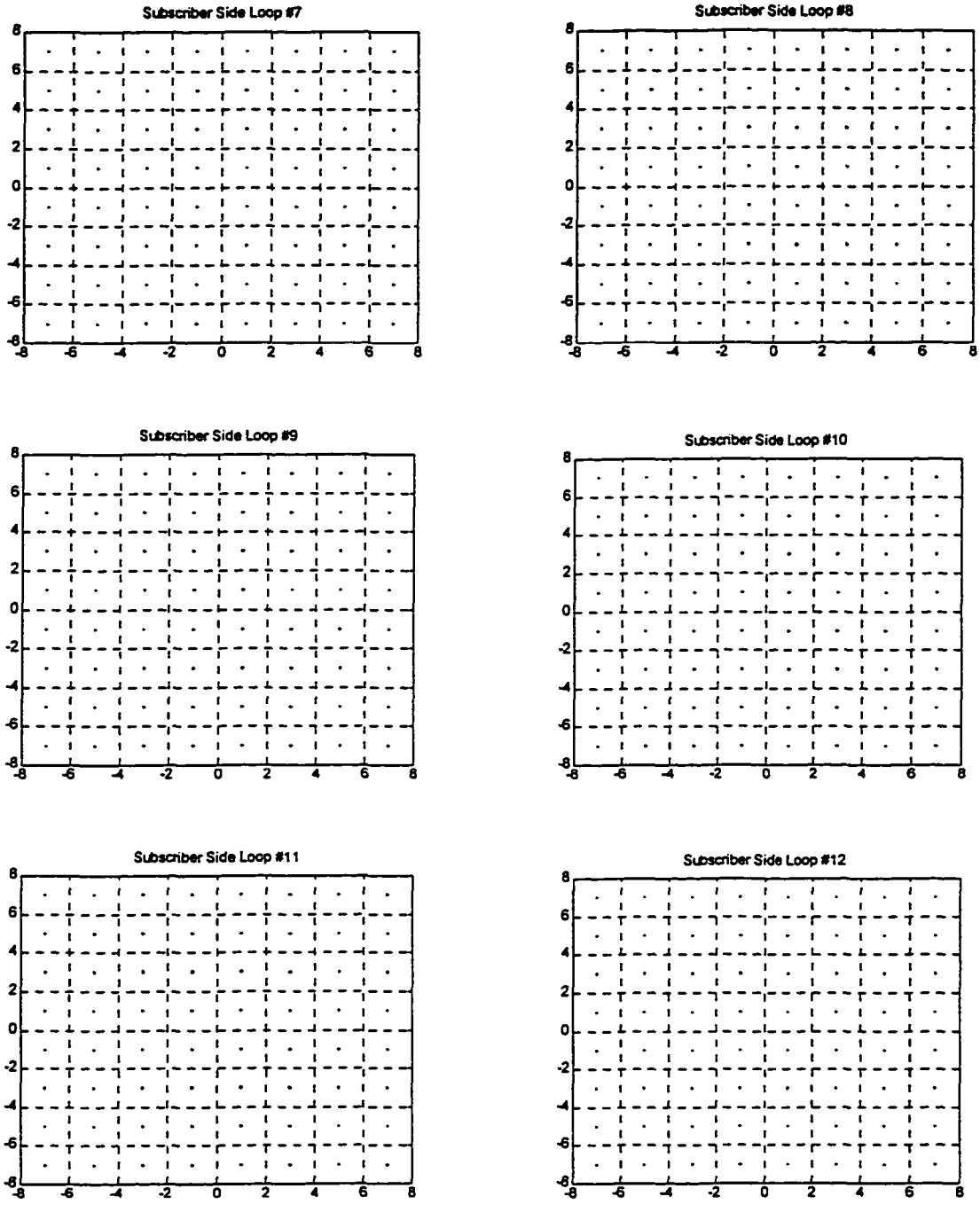

Figure 7.9(d): Subscriber Side 64 CAP Constellation After Adaptation with Reflected Signal =-40dB

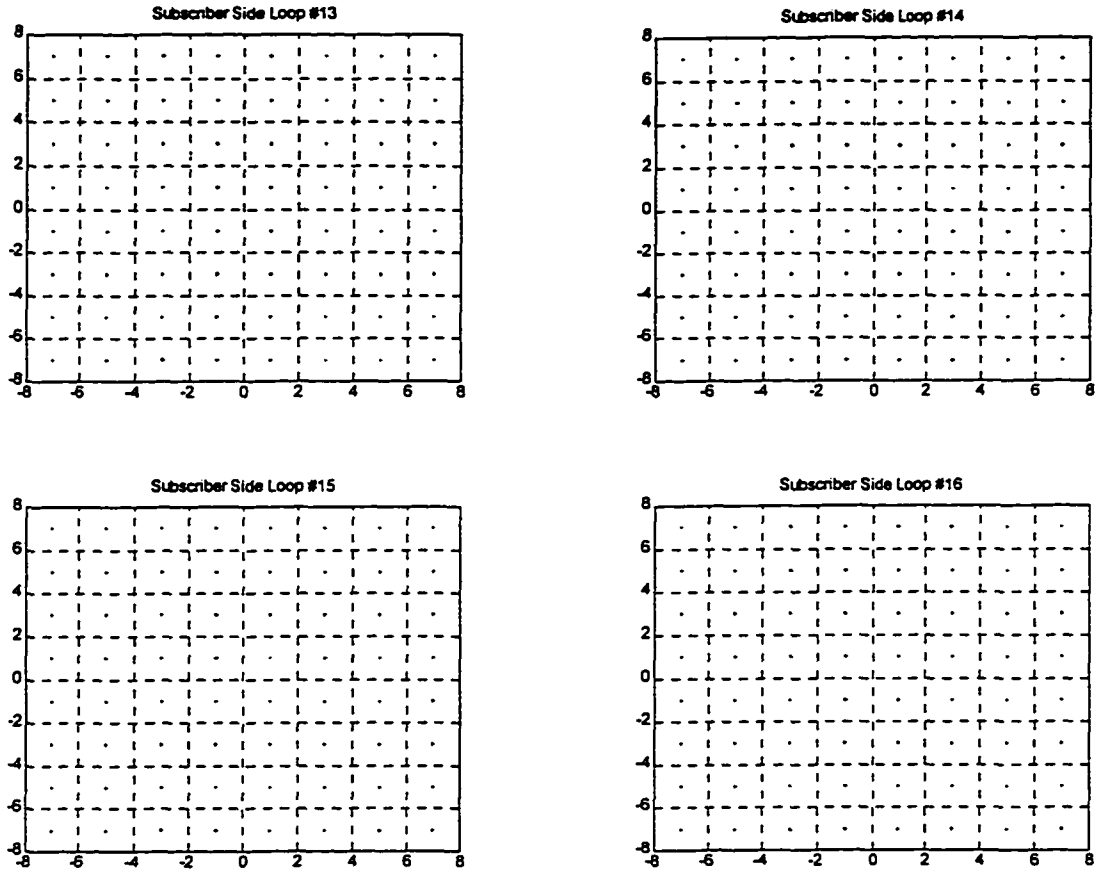

Figure 7.9(d): Subscriber Side 64 CAP Constellation After Adaptation with Reflected Signal =-40dB

The SNR for the above constellations is presented for the reflected signal of -26dB and -40 dB both for the CO and SUB Side.

Loop #	SNR at SUB Side in dB	SNR at CO Side in dB
1	67.216282	50.261018
2	52.319350	52.785229
3	57.531274	46.097752
4	67.628302	51.568351
5	52.961885	52.080420
6	53.190540	50.149729
7	67.729104	50.564291
8	53.058631	53.011516
9	53.651695	46.797351
10	52.879796	51.985147
11	53.244155	52.516787
12	67.829040	54.635250
13	59.010759	39.264877
14	53.464837	51.466099
15	67.728409	53.459615
16	57.987320	51.437709

Table 7.5: Adaptive 3200 symbol period training with Reflected Signal at 26 dB down

With the reflected signal at -26dB the SUB Side loops have an SNR of greater than 52 dB. Loops 3 and 16 having a SNR of 57 dB, loop 13 at 59 dB and the loops 1, 4, 7, 12 and 15 at 67 dB. The Central Office Side also does well with most of the loops having a SNR at above 50 dB with exception of the loops 3 and 9 at 46 dB and the loop 13 with 39 dB. The figures 7.91(a), 7.91(b) 7.91(c) and 7.91(d) indicate the

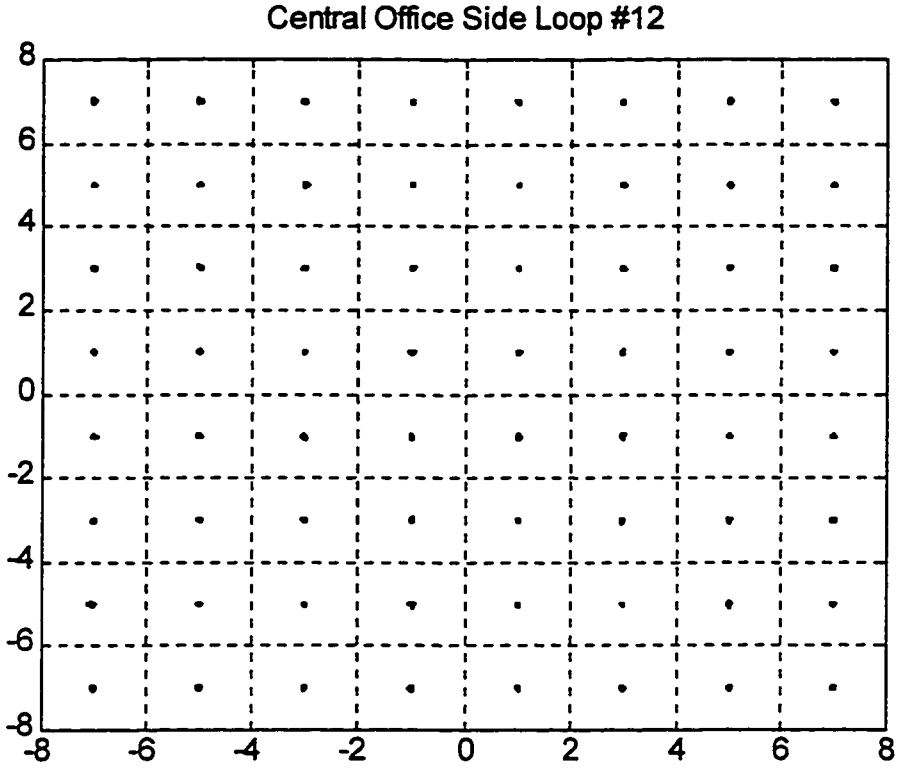

Figure 7.91(a): Best Case loop of the Central Office Side after adaptation with the Reflected Signal = -26dB and SNR = 54.63dB

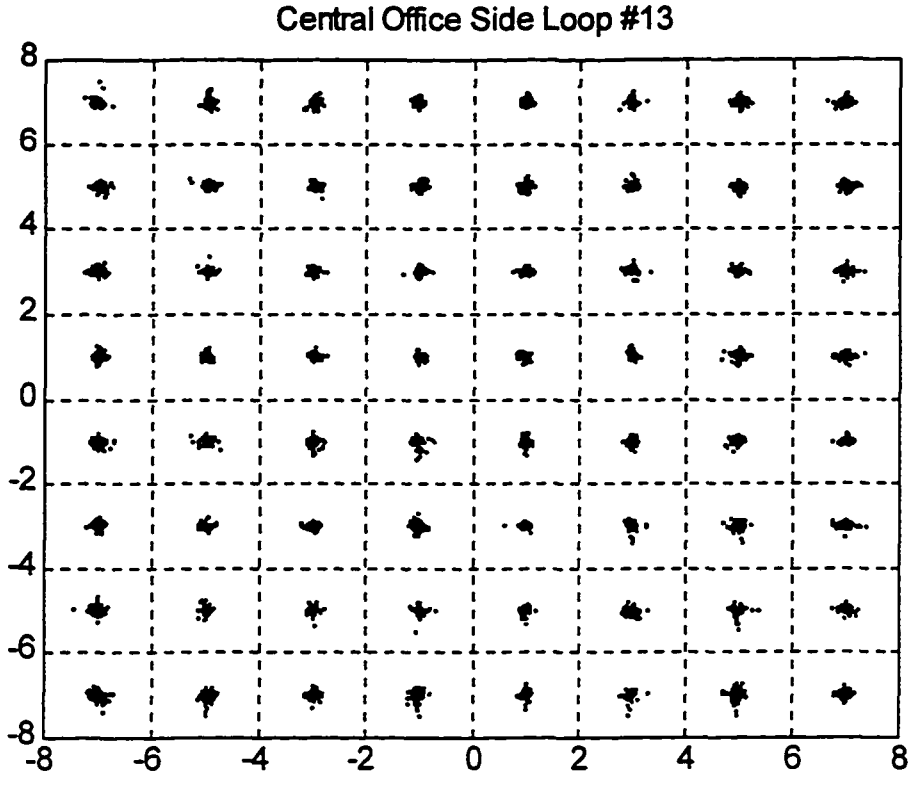

Figure 7.91(b): Worst Case loop of the Central Office Side after adaptation with the Reflected Signal = -26dB and SNR = 39.26dB

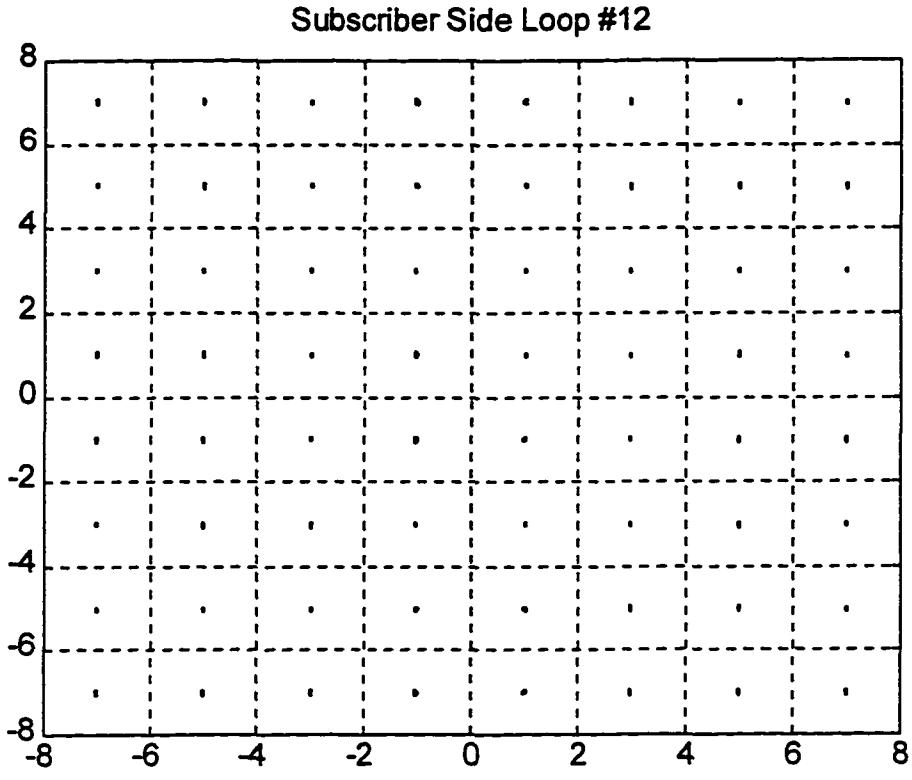

Figure 7.91(c): Best Case loop of the Subscriber Side after adaptation with the Reflected Signal = -26dB and SNR = 67.82dB

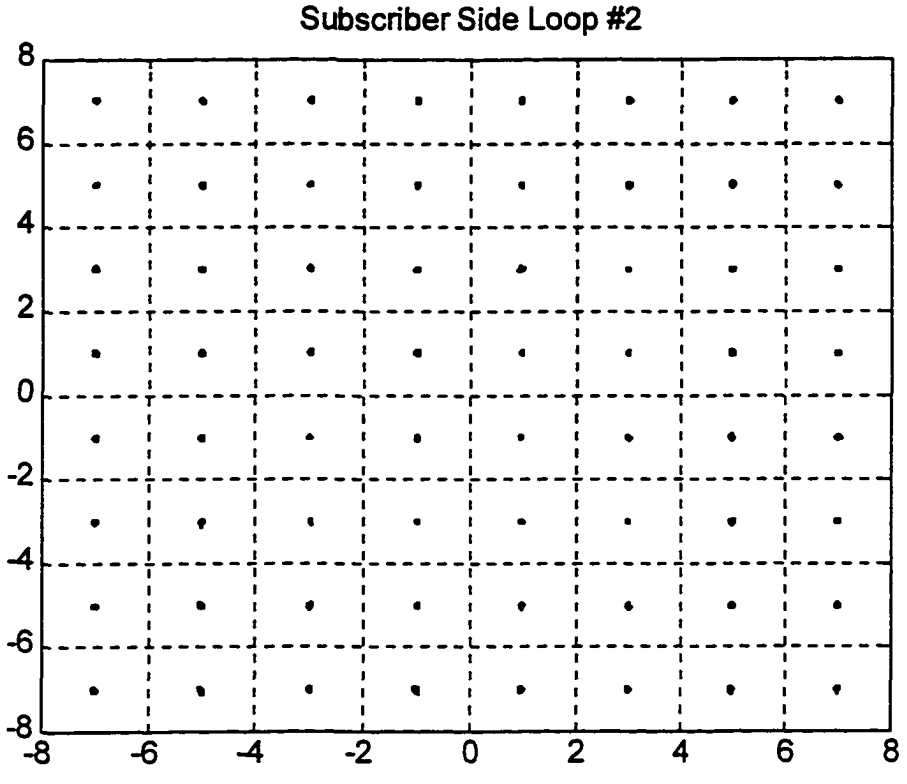

Figure 7.91(d): Worst Case loop of the Subscriber Side after adaptation with the Reflected Signal = -26dB and SNR = 52.31dB

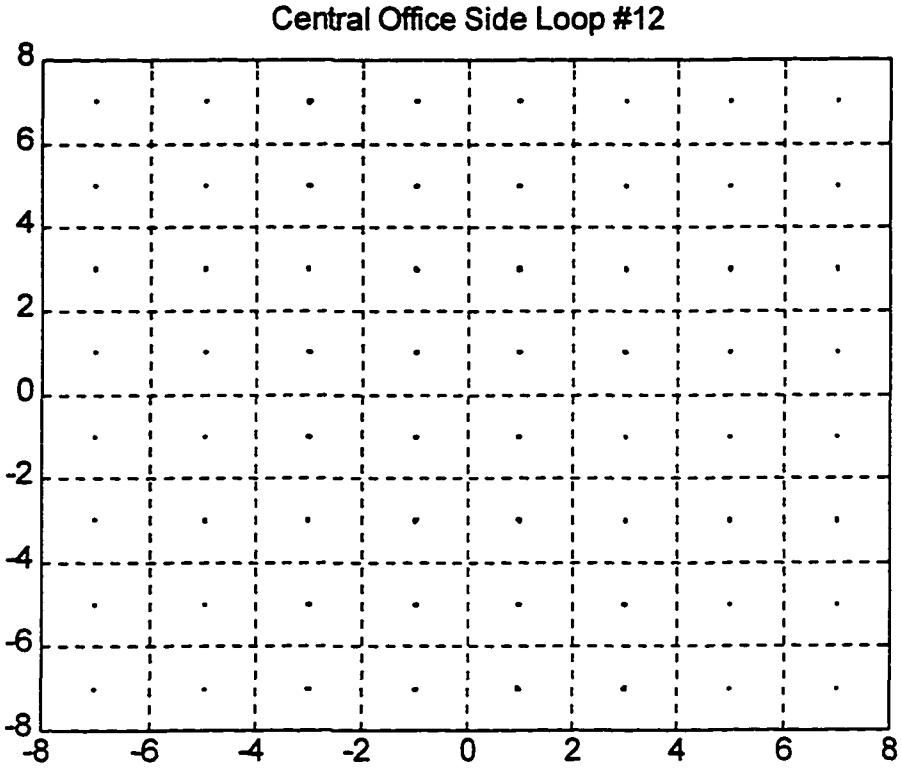

Figure 7.92(a): Best Case loop of the Central Office Side after adaptation with the Reflected Signal = -40dB and SNR = 67.82dB

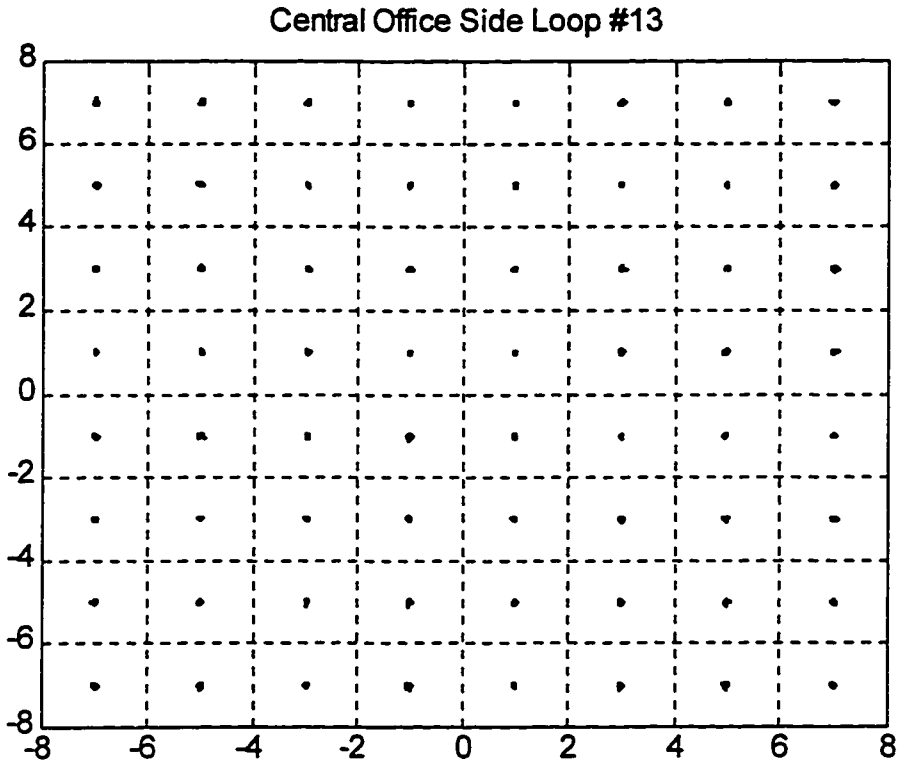

Figure 7.92(b): Worst Case loop of the Central Office Side after adaptation with the Reflected Signal = -40dB and SNR = 53.34dB

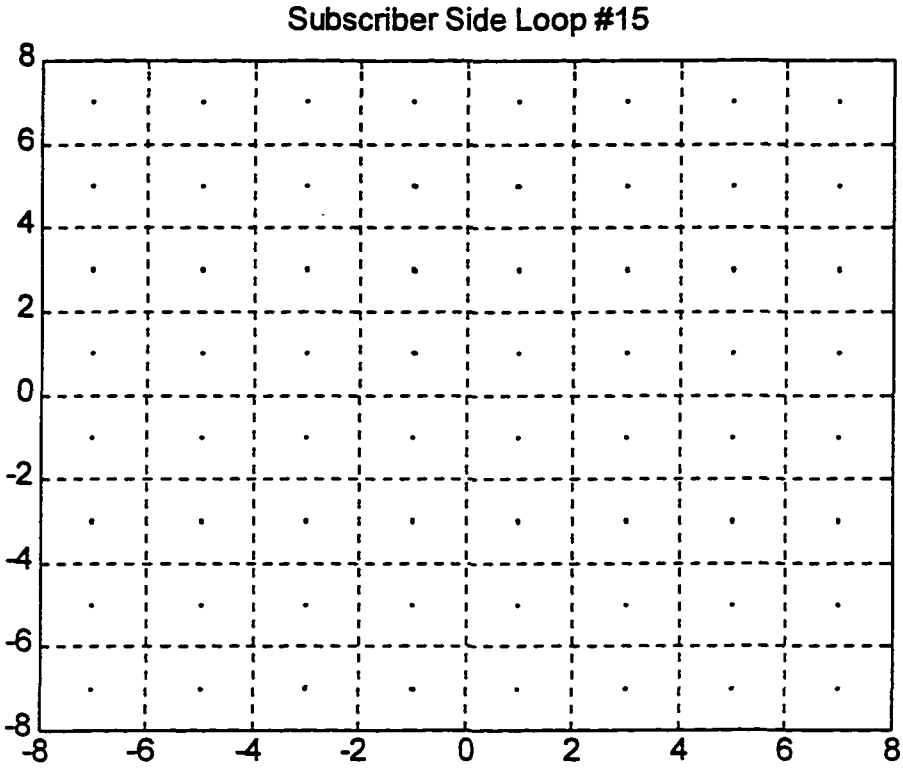

Figure 7.92(c): Best Case loop of the Subscriber Side after adaptation with the Reflected Signal = -40dB and SNR = 70.28dB

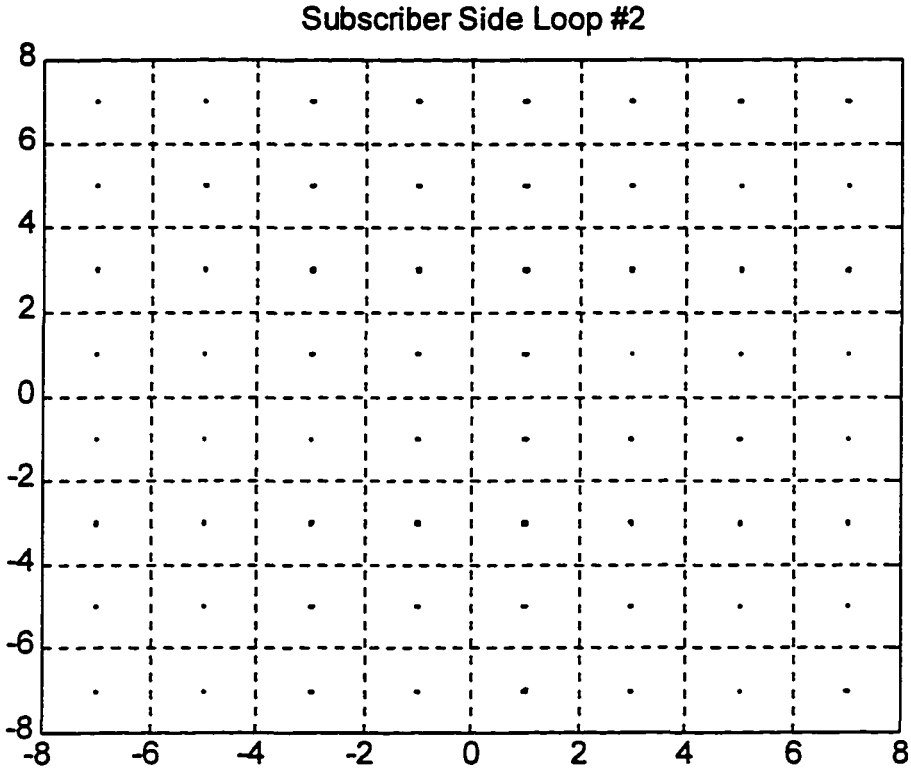

Figure 7.92(d): Worst Case loop of the Subscriber Side after adaptation with the Reflected Signal = -40dB and SNR = 65.33dB

best and the worst case loops for the Central Office side and Subscriber side for the reflected signal component being -26dB after adaptation.

When the training period is reduced the constellation point for certain loops just fails to converge and the SNR is also bad. For the given step size which is optimal and convergence is also guaranteed the training period could increase depending on the characteristics of the loop.

Loop #	SNR at SUB Side in dB	SNR at CO Side in dB
1	69.541747	63.920154
2	65.336431	66.186121
3	68.241840	60.032642
4	69.884051	65.035502
5	66.007820	65.556880
6	66.080598	63.865287
7	70.039677	64.130496
8	66.164901	66.571675
9	66.778537	60.545328
10	66.075948	65.483203
11	66.319939	65.972341
12	70.278417	67.820026
13	69.034455	53.341784
14	66.725532	64.888952
15	70.280642	66.762880
16	69.219978	65.003878

Table 7.6: Adaptive 3200 symbol period training with Reflected Signal at 40 dB down

Faster convergence could be obtained by going in for an increase in step size but the problem of convergence becomes a critical issue. For obtaining better SNR in the case of the adaptive method used the factors which come into play are the number of taps of the IIR filter, step size used in the LMS algorithm and training period. From the above table it is clear that most of the loops for the SUB Side have SNR of 66dB with certain loops like 1, 3, 4, 7, 12, 13, 15 and 16 performing even better with SNR of 68dB to 70 dB. On the Central Office Side most of the loops have SNR of above 60 dB with exception of loop 13 with 53 dB and the loops in general averaging to a SNR of about 65 dB. It can be clearly seen from the SNR best case at the Central Office side is loop number 12 and the worst case loop being loop number 13 for the reflected signal being -26dB and -40dB whether fixed coefficients or adaptive coefficients are used for the spectral band under study, but for Subscriber Side loop number 2 is the worst case loop whereas the loop number 12 is still generally the best case loop with loop number 15 also doing as the best case loop when adaptive coefficients are used.

Conclusion

From the results obtained above in which the results of the two methods that is the fixed coefficient method for the biquad versus the adaptive coefficient method for every symbol period in the biquad are discussed and it clear that the adaptive coefficient method obviously gives better results in terms of the SNR. Comparing the time domain techniques to the frequency domain techniques used it is clear that the

error that occurs in the phase is difficult to correct in the case of the frequency domain methods whereas in the time domain it is not so. In either of the methods discussed it is to be said that continuous adaptation, that is during every symbol period is likely to provide better results whether it is in time domain or frequency domain. However it is to be noted that better matching and circuit realization is possible in the time domain.

References

[1] O.Agazzi, D.A.Hodges & D.G.Messerschmitt, "Large Scale Integration of Hybrid Method Digital Subscriber Loops", IEEE Trans. on Comm., Vol. COM-30, No.9, Sept. '82.

[2] W.Y.Chen, J.L.Dixon & D.L.Waring, "High Bit Rate Digital Subscriber Line Echo Cancellation", IEEE JSAC, Vol. 9, No. 6, August 1991, pp. 848-860.

[3] K.Feher, "Advanced Digital Communications: Systems and Signal Processing Techniques", Prentice Hall, New York.

[4] R.L.Geiger, P.E.Allen & N.R.Strader, "VLSI Design Techniques for Analog and Digital Circuits", McGraw Hill.

[5] S.V. Ahamed, "Simulation and Design of Digital Subscriber Lines", The Bell System Technical Journal, Vol. 61, No. 6, July-August 1982.

[6] S.V.Ahamed, "Simulation Environments for the High-speed Digital Subscriber Line (HDSL)", IEEE International Conference on Communications ICC '93, May 23-26, 1993.

[7] G.S.Moschytz & S.V.Ahamed, "Transhybrid Loss with RC Balance Circuits for Primary-Rate ISDN Transmission Systems", IEEE JSAC Vol. 9, No. 6, August 1991.

[8] S.V.Ahamed & V.B.Lawrence, "Simulation Studies of Higher Rates in Subscriber Loop Plant", ISSSE '89.

[9] B.Widrow and S.D.Stearns, "Adaptive Signal Processing", Prentice Hall , New York, 1985.

Chapter 8

Hardware Implementation

The time domain methods used to obtain the results discussed in [Chap. 7] was based on the model that the reflections was canceled in the analog domain and the adaptation and the updating of the coefficients was done in the digital domain. The hardware model used in order to achieve the attenuation is presented as shown in figure 8.1

8.1 Hardware Structure

In the structure presented in the figure 8.1 the output form the spectral shaping filters both the inphase and the quadrature filters are fed to the corresponding inputs of the biquads. The signal with the reflection from the hybrid contaminated with the reflected portion of the signal is fed to the input of the positive terminal of the differential operation amplifier. The output of the differential amplifier is the error part of the signal which results due to the approximate computation of the filter coefficients. Ideally the computed coefficients should match the reflected signal of the transmitter when the resultant error would be zero. The error is now fed to the adaptation block which computes the coefficients for the biquads. The input to the adaptation block is the input from the memory elements of the biquads. The output from the biquads is real part of the signal consisting of the inphase and quadrature

component which is converted from the digital to the analog domain by R - 2R ladder network technique as shown in the figure 8.1.

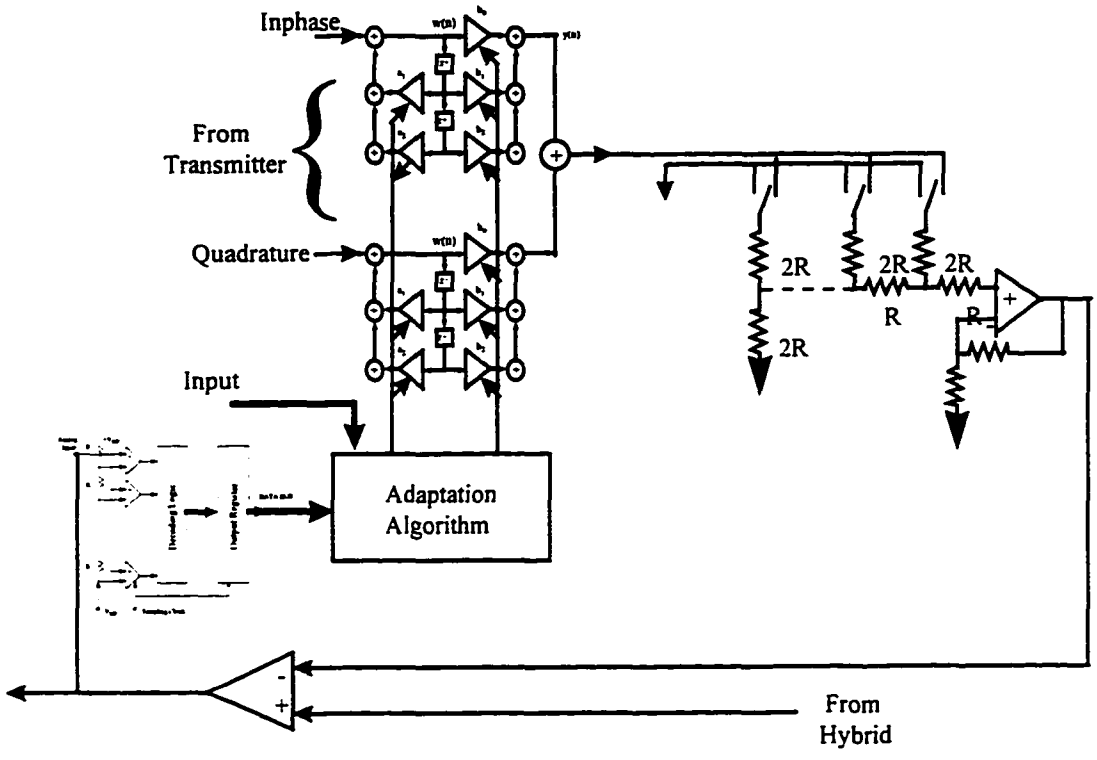

Figure 8.1: Analog Attenuator with Digital Adaption

8.2 Parallel Digital Canceler

This is a parallel structure based on the digital adaptive method and also cancellation of the reflection or the echo in the digital domain. This structure is to be used for high speed digital networks for fine echo cancellation or to be used jointly as a structure cascaded with the analog echo cancelers for fine echo cancellation, that is to remove

any further residual echo that is present at receiver side after the coarse echo cancellation done by the analog echo cancelers.

8.3 Implementation

A parallel adaptive echo canceler for two wire digital transmission is described using the Modified Mesh Architecture. This architecture along with the parallel adaptation algorithm involves simple digital signal processing which is much faster in terms of real time operations for video and high speed digital data transmission over the subscriber loops compared to the existing architectures of the digital signal processors, The feasibility of this architecture for adaptive echo cancellation for higher data rates such as DS2 rates and higher over the existing subscriber loops conforming to the CSA guidelines is discussed.

The adaptive echo cancellation is required in loop applications because of the wide range of different channel characteristics encountered due to different cable makeup's. A cable is typically made up of different sections having different gauge and length, and often includes bridge taps.

8.4 Adaptive Echo Canceler

Adaptive echo canceler consists of an FIR filter whose tap coefficients are changed depending on the line characteristics. The FIR filter is implemented using the parallel architecture based on the Modified Mesh Connected Architecture [1].

8.5 Modified Mesh Architecture

The Mesh Architecture is modified in the following manner. The connections for the 16 processing elements of the Modified Mesh Connected Architecture(MMCA) is the same as any of the conventional Mesh Connected Architecture MCA as shown in the figure 8.2, except that the result is always stored in P(1,1).

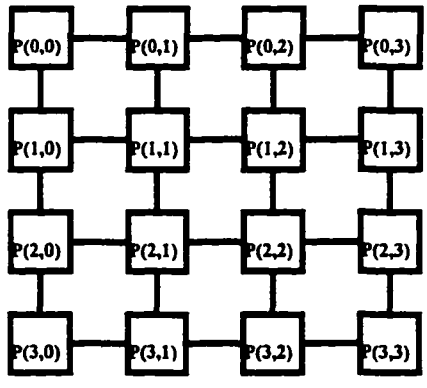

Figure 8.2: 16 PE's Modifed Mesh

The Modified Mesh Connected Architecture is formed of processing elements of the order of $N=2^i$ where i=4,6,8.... For a 64 element Modified Mesh Connected

Architecture the additional connections are as shown in the figure 8.3. P(1,1) is connected to P(1,5) and also to P(5,1). P(1,5) is connected to P(5,5). The extra links are shown in figure 8.3 by dashed lines.

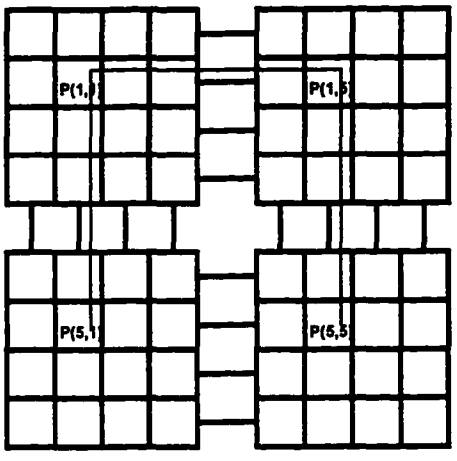

Figure 8.3: 64 PE's Modified Mesh

The FIR filter part of the adaptive echo canceler is implemented by using the Modified Mesh Architecture which uses the linear convolution program. If x(n) is the input and y(n) is the output then its difference equation is given by

$$y(n) = b_0x(n) + b_1x(n-1) + \ldots + b_{M-1}x(n-N+1)$$

where b_n, $0 \leq n \leq N-1$ are filter tap weights, h(n) is the impulse response, and

$$h(n) = \begin{cases} b_n, & 0 \le n \le N-1 \\ 0, & \text{otherwise} \end{cases}$$

If x(n) is an M-point sequence then y(n) will be M+N-1 point sequence (N represents the number of taps of the filter) after filtering is completed. Here h(i) is the filter coefficients, where i takes a value 0 to N-1 and is stored in the register *b* of the PE's. The filter coefficients are stored in the reverse order in the processing elements that is for a 16 processing element Modified Mesh Architecture h(N-1) is stored in the register *b* of the processing element P1 or P(0,0) and h(0) is stored in the register *b* of the processing element P(3,3). The number N in the equation represents the number of taps in the filter, which then corresponds to the number of processing elements used. We now discuss the implementation of a 16 tap FIR filter using the above proposed architecture that is the Modified Mesh Architecture. The coefficients h(N-1) to h(0) are stored in the register *b* of the processing elements P(0,0) to P(3,3).

The associated data points circulate through the memory and new samples, replace the oldest sample each time a filter output is computed. We make use of a circular buffer in which the oldest sample is replaced by the new sample after each convolution. The history of the N recent samples is kept in the circular buffer at any given time. The way the memory is addressed is as follows, old values are read from

the memory starting with the value one location immediately after the location into which the current or the new sample was just written. These values read from the memory are placed into the register *a* of the PE's. FIR filter design requires that all N coefficients be determined and placed in the respective *b* registers of the different PE's of the Modified Mesh Connected Architecture.

In the figure 8.4, n is equivalent to the number of data points. The circular buffer length is equal to N.

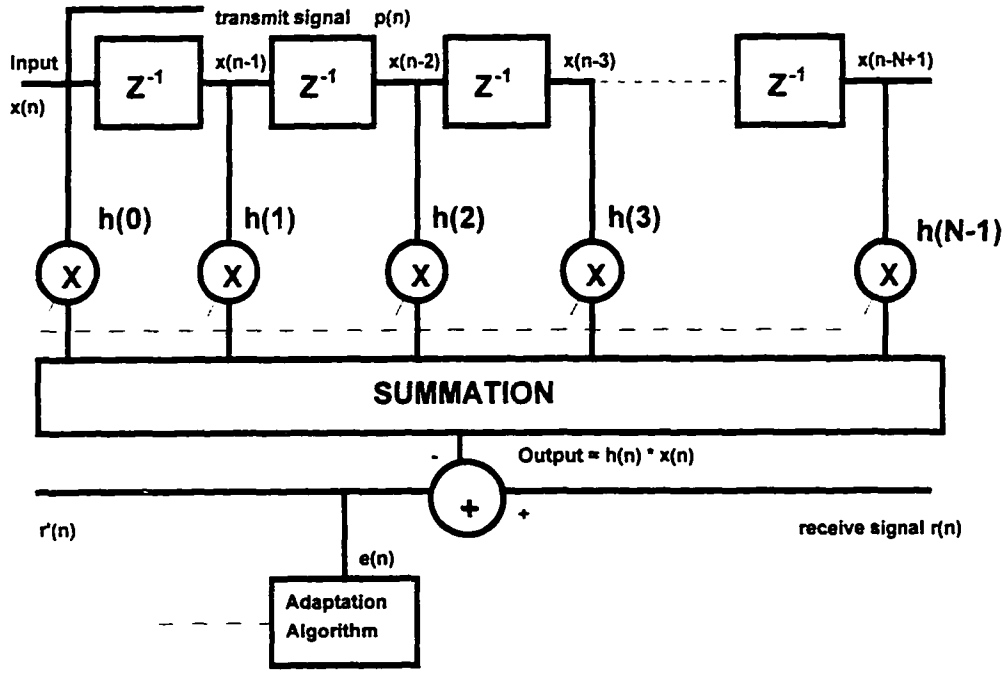

Figure 8.4: FIR Filter

For the Modified Mesh Connected Computer to perform the convolution operation we assume that each of the processing elements has at least four registers *a*, *b*, *c* and *d*. Registers *b* are used to store the coefficients h(i) as discussed before, registers *a* are used to hold the input data x(n) from the memory and finally registers *c* are used to hold the computed results.

Figure 8.5, shows the multiplication stage of the computation of each point of the output y(n). After the multiplication stage the summation is performed as discussed in [1].

a = x(n-N+1) b = h(N-1) c = a * b	a = x(n-N+2) b = h(N-2) c = a * b	a = x(n-N+3) b = h(N-3) c = a * b	a = x(n-N+4) b = h(N-4) c = a * b
a = x(n-N+5) b = h(N-5) c = a * b	a = x(n-N+6) b = h(N-6) c = a * b	a = x(n-N+7) b = h(N-7) c = a * b	a = x(n-N+8) b = h(N-8) c = a * b
a = x(n-N+9) b = h(N-9) c = a * b	a = x(n-N+10) b = h(N-10) c = a * b	a = x(n-N+11) b = h(N-11) c = a * b	a = x(n-N+12) b = h(N-12) c = a * b
a = x(n-N+13) b = h(N-13) c = a * b	a = x(n-N+14) b = h(N-14) c = a * b	a = x(n-N+15) b = h(N-15) c = a * b	a = x(n-N+16) b = h(N-16) c = a * b

Figure 8.5: Computation Stage

8.6 Data Memory Addressing

The data memory addressing for a 16 tap FIR filter is considered. The input buffer is at first initialized. The first incoming sample x(0) from the A/D converter is stored in the location (0) of the input circular buffer. The data from the circular buffer is then loaded into the registers *a* of the MMCC. The loading of the data from the circular buffer to the registers *a* of the processing is done in the following manner, the data from the location (1) of the circular buffer is placed in the register *a* of the PE, P(0,0), then the data from the location (2) is placed in the register *a* of the PE, P(0,1) and so on till all the PE's have the data from all the locations of the circular buffer.

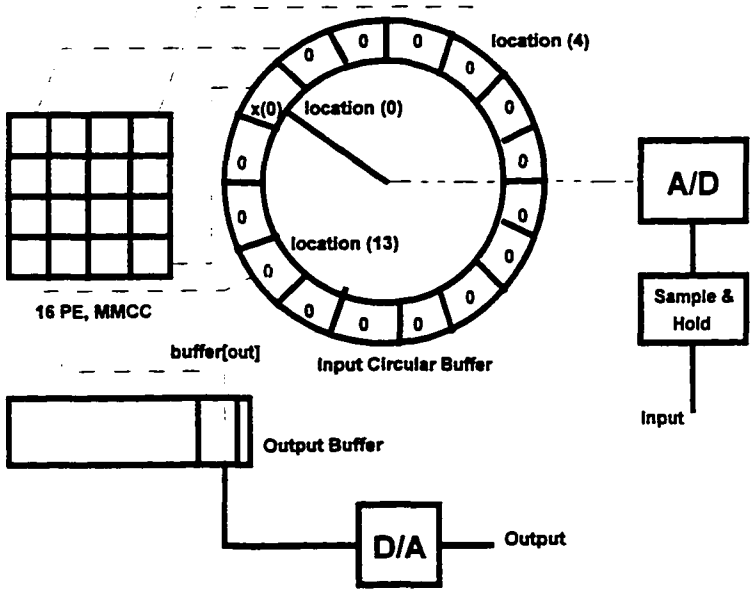

Figure 8.6: Data Memory Addressing

The PE, P(3,3) holds the data from the location (0) and in this case it happens to be the first sample x(0) of the N point sequence. In figure 8.6, the dashed lines show the data lines on which data transfers take place between the processing elements and the memory, the memory in this case being the circular buffer. Similarly such data lines exists between the other PE's of the MMCC and each of the other locations of the circular buffer. The input signal is sampled and held by the sample and hold device which is then converted into digital information by the analog to digital (A/D) converter. The digital input is stored in the circular buffer starting from location (0) of the buffer. Once the buffer is full the next incoming signal data in the case when 'n' is greater than the buffer length is written into the location (n mod N) where 'n' is the number of points of the input sequence x(n) and N is the length of the circular buffer.

Here memory interleaving is used so that all the 16 different values could be loaded into the 16 different processing elements of the MMCA at the same time. This can be implemented by the use of a 'Crossbar Switch' or the 'Benes Switch'. The computation is then performed for the first sample x(0) which includes multiplication and the summation operations and the result y(n) stored in the PE, P(1,1) is then written back to one of the memory locations in the output buffer.

We know that the difference equation for the FIR filter is

$$y(n) = h(N-1)\,x(n-N+1) + h(n-2)\,x(n-N+2) \ldots h(1)\,x(n-1) + \quad h(0)x(0)$$

After the first sample x(0) is processed and computed the value of

$$y(0) = h(15)x(1) + h(14)x(2) + h(13)x(3) + h(12)x(4) + h(11)x(5) + h(10)x(6) + h(9)x(7) + h(8)x(8) + h(7)x(9) + h(6)x(10) + h(5)x(11) + h(4)\,x(12) + h(3)x(13) + h(2)x(14) + h(1)x(15) + h(0)x(0).$$

In the above equation y(0) has been computed assuming that n=16 , which is the number of points of the input sequence x(n) and N=16 which is equal to the number of taps of the FIR filter and hence is equivalent to the number of processing elements.

When the second sample arrives it is placed in the location (1) of the circular buffer. The data present in the circular buffer is then loaded into the registers *a* of the processing elements of the MMCC. The data from location (2) of the buffer is placed in the PE, P(0,0), location (0) which holds the sample x(0) is placed in the register *a*of the PE, P(3,2), the other locations of the buffer which holds the zero values are placed in the registers *a* of the other PE's from P(0,1) to P(3,1). P(3,3) now holds the recent data, that is the sample x(1). the computation is once again performed using the multipliers and adders resident in the respective processing elements and the final

result is stored in the PE, P(1,1), The PE, P(1,1) the writes back the data into output memory buffer which now holds the value of y(1).

$$y(1)=h(15)x(2)+h(14)x(3)+ ...+h(1)x(0)+h(0)x(1).$$

The n+N-1 values of 'y' are computed and stored in the successive locations of the output buffer. When n=15 the input circular buffer is full and

$$y(15)=h(15)x(0)+h(14)x(1) + ... + h(0)x(15).$$

8.7 Echo Cancellation Algorithm

A parallel algorithm for the Modified Mesh Architecture is presented based on the stochastic gradient least mean square (LMS) algorithm.

If the near end device is transmitting a signal p(n) and the far end device is transmitting a signal q(n) then the near end received signal

$$r(n) = q(n) + p_{ne}(n) + p_{fe}(n) + w(n)$$

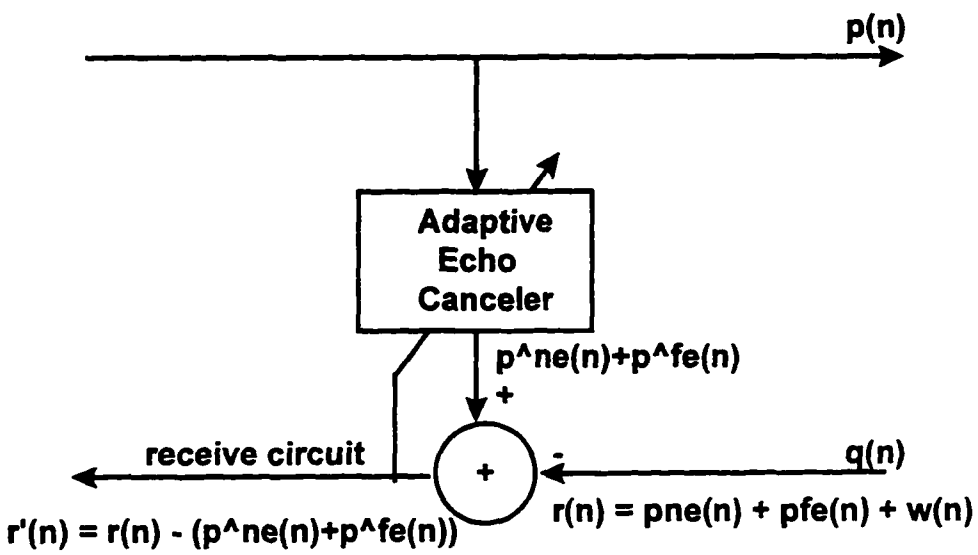

Figure 8.7: Adaptive Digital Echo Canceler Model

where $p_{ne}(n)$ and $p_{fe}(n)$ are the near end and the far end echo respectively and w(n) is the noise introduced in by the system. Echo cancellation is achieved by subtracting the echo return signal from the actual signal. The received signal after echo cancellation is

$$r'(n) = r(n) - (p\hat{}_{ne}(n)+p\hat{}_{fe}(n))$$

where $p\hat{}_{ne}(n)$ = estimate of the near end echo and $p\hat{}_{fe}(n)$ = estimate of the far end echo. The echo is estimated by feeding the transmitted signal into adaptive FIR filter whose transfer function tries to model the telephone channel. The filter coefficients

are determined using the stochastic gradient least mean square (LMS) algorithm [2]. The dashed line in figure 8.7 represents the feedback to the adaptive echo canceler.

8.8 Training method

Before communications is established in full duplex mode a training sequence is used and the LMS algorithm attempts to minimize the mean squared error | $E(n)^2$ |. During the training period, a sequence long enough is used so that the convergence of the filter is forced for the unknown system and during this time, since the far end device is not transmitting the signal received at the near end only consists of echo $r(n) = p_{ne}(n) + p_{fe}(n)$. The output of the filter is $y(n) = p\hat{}_{ne}(n) + p\hat{}_{fe}(n)$. The ouput y(n) from the filter is now equal to the signal fed to the receive circuit as shown in the figure 8.7, r'(n) = y(n), the error e(n) is obtained by taking the difference of r(n) and r'(n).

The equation for the updating of the FIR filter coefficients using the LMS algorithm is

$$h_{k+1}(n) = h_k(n) + \beta * e(n) * p(n)$$

where p(n) is the sample transmitted at the sample time n, e(n) is the residual error and β is the adaptation constant.

The Echo Canceler generally keeps track of the slowly changing telephone channel and updates the tap coefficients of the FIR filter whenever such changes occur. In a communication system which uses two dimensional line codes the echo canceler should be capable of handling complex data and therefore the taps of the FIR filter have complex coefficients.

8.9 Parallel Algorithm

The parallel algorithm for the 16 PE MMCA is as follows

```
procedure echo_canceler;

received_data, transmitted _data, out:link;
beta:const;

X[0..15]:input circular buffer  /complex / ;
h[0..15]:coefficients  /complex/ ;

k,i,j:variables  /integer/;
p,q:variables  /complex/;
a_ij,b_ij,c_ij,d_ij:registers;


begin
for i=0 to 3 do in parallel
   for j=0 to 3 do in parallel
       b_ij=h[4i+j];
k=1;

while (interrupt) do
```

```
begin
p=buffer[transmitted_data];
q=buffer[received_data];

 for i=0 to 3 do in parallel
   for j=0 to 3 do in parallel
      a_ij=X[((4i+j)+k) mod 16];

 for i=0 to 3 do in parallel
   for j=0 to 3 do in parallel
      c_ij=b_ij*a_ij;

 for i=0 to 3 do in parallel
    begin
    c_1i=c_1i+c_0i;
    c_2i=c_2i+c_3i;
    end;

 for i=1 to 2 do in parallel
    begin
    c_i1=c_i0+c_i1;
    c_i2=c_i2+c_i3;
    end;

 for i=1 to 2 do in parallel
     c_1i=c_1i+c_2i;
 c_11=c_11+c_12;

 d_11 = q ;
 c_11 = d_11- c_11;
 buffer[out]=c_11;

if update then
 begin
 b_11=beta;
 c_11=c_11 * b_11;
 c_12=c_11;


for i=1 to 2 do in parallel
     c_2i = c_1i;

  for i=1 to 2 do in parallel
     begin
      ci0=ci1;
      ci3=ci2;
     end;
```

```
for i=0 to 3 do in parallel
      begin
      c0i=c1i;
      c3i=c2i;
      end;

  for i=0 to 3 do in parallel
    for j=0 to 3 do in parallel
      begin
      bij=bij + cij;
      h[((4i+j)+k) mod 16)]=bij;
      end;
  end;

   k=(k+1) mod 16;
 end;
end;
```

When the procedure echo_canceler is called the tap coefficients are loaded into the register b of the PE and when the interrupt occurs the transmit data and the receive data are placed in the variables p and q respectively. The data from the circular buffer X is read into the registers a of the processing elements. The convolution is then performed, the register c of the PE, P(1,1) holds the difference between the received signal and the output of the FIR filter, the result is then placed in the output buffer which then converted into the analog signal using the D/A converter as shown in the figure 8.6. When the update bit is enabled the adaptive algorithm is used to vary the coefficients of the taps of the FIR filter accordingly to adapt to changing characteristics of the channel. The signal r'(n) is obtained after the echo in the received signal r(n) is reduced or removed as the case may be.

8.10 Performance Issue

The adaptive echo canceler using the MMCA with VLSI implementation will be able to perform much better than the existing DSP's. Assuming that the multiply/accumulate operation takes about two cycles for a complex operation and transfer/accumulate operation for the transfer of data takes about one cycle and about four to six cycles as an additional overhead for data I/O operations it can be shown that computing the output y(n), reducing the echo and updating the tap coefficients can be done much faster thus making it an ideal architecture for video and other high speed data communication on the subscriber loops.

References

[1] A. Reddy, "A Modified Mesh Architecture for Summation", ISCA CAINE 1993, 126-129.

[2] A.Reddy & S.V.Ahamed, "A Parallel Adaptive Echo Canceller", ICCAI 94, Dec. 94, pp. 13-16.

[3] F. Kamilo & D. Messerschmitt, "Advanced Digital Communication", Prentice Hall, New York.

[4] M. J. Miller & S.V. Ahamed, "Digital Transmission Systems and Networks: Principles", Vol. 1, Computer Science Press.

[5] M. J. Miller & S.V. Ahamed, "Digital Transmission Systems and Networks: Applications, Vol. 2, Computer Science Press.

[6] S. V. Ahamed, P. P. Bohn & N. L. Gottfried, "A Tutorial on Two Wire Digital Transmission in Loop Plants", IEEE Trans. Commun., Vol. COM 29, no. 11, pp. 1554-1564, Nov. 1981.

[7] S. V. Ahamed, "Simulation and Design Studies of the Digital Subscriber Lines", Bell System Technical Journal 61, no. 6:1003-77, July-Aug. 1982a.

[8] N. Holte & S. Stueflotten, "A New Digital Echo Canceler for Two Wire Subscriber Lines", IEEE Trans. on Commun. Vol. Com 29, no. 11, Nov. 1981.

[9] W. Y. Chen, J. L. Dixon & D. L. Waring, "High Bit Rate Digital Subscriber Line Echo Cancellation", IEEE JSAC Vol. 9, no. 6, Aug. 1991, pp. 848-860.

Appendix A

Modeling of Digital Transmission Line

From the two port network theory or the four terminal wire theory the steady state behavior can be characterized by a set of linear equations.

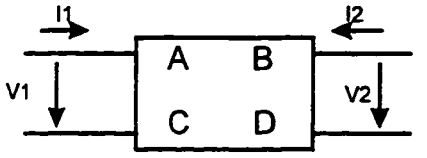

Figure A.1: Two port Network

$$\begin{bmatrix} V_1 \\ I_1 \end{bmatrix} = \begin{bmatrix} A & B \\ C & D \end{bmatrix} \begin{bmatrix} V_2 \\ I_2 \end{bmatrix}$$

where V_1 and I_1 is the voltage and current of the input port and V_2 and I_2 are the corresponding voltage and current of the output port. A, B, C and D are the complex functions which are dependent on the frequency, length, temperature and R, L G and C parameters which are also referred to as the primary constants of the wire gauge used. R is the resistance in ohms/unit length, L is the inductance in Henries/unit length, G is the conductance/unit length and C is the capacitance in Farads/unit length.

Consider an element of the homogenous line of length dx with its origin at the point x as shown in the figure 2. Considering the element of the line to be between x and x + dx, let the input current be I and the output current be I + dI and also let V be the input voltage and V + dV be the output voltage.

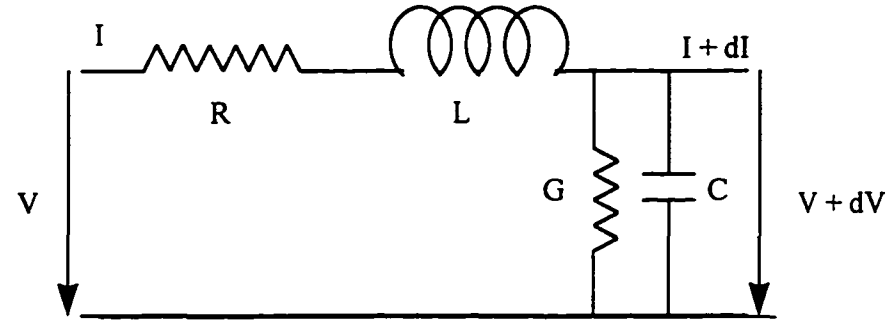

Figure A.2: Element of Transmission Line

Let V(x,f) and I(x,f) be the complex voltage and current at the point x and frequency f. The frequency variation in general could take any form, assuming a sinusoidal frequency varied input we can represent $I(x,f) = I(x) \exp(j\omega t)$ and $V(x,f) = V(x) \exp(j\omega t)$ where V(x) and I(x) are complex quantities at the point x. When we move a distance dx on the line from the left to the right there is a drop in the voltage and the current for the positive increment of x. The drop in the voltage is due the resistance and the inductance of the line for a fixed current I and the drop in the current is due to the conductance and the capacitance of the line for a fixed voltage V. From the figure

2 and from Kirchoffs current law which states that *the sum of all the currents in the network at a node or a point is equal to zero* we get

$$I = (G + j\omega C)Vdx + I + dI$$

$$dI/dx = -(G + j\omega C)V = -YV \quad -(1)$$

$$Y = G + j\omega C \quad -(2)$$

From the Kirchoff's voltage law which states that *the algebraic sum of all the voltages in a closed electrical circuit is equal to zero*, we get

$$V = (R + j\omega L)Idx + V + dV$$

$$dV/dx = -(R + j\omega L)I = -ZI \quad -(3)$$

$$Z = (R + j\omega L) \quad -(4)$$

When the inputs considered are sinusoidal equations (1) to (4) get modified to

$$\partial^2 I/\partial x^2 = [R + j\omega L]\,[G + j\omega C]\,I \quad -(5)$$

$$= ZYI \quad -(6)$$

$$\partial^2 V/\partial x^2 = [R + j\omega L]\,[G + j\omega C]\,V \quad -(7)$$

$$= ZYV \quad -(8)$$

In the above equations $\omega = 2\pi f$ where f is the frequency in Hertz and ω is the angular velocity measured in radians/sec.

Let $\gamma = \sqrt{(R + j\omega L)(G + j\omega C)} = \sqrt{ZY}$ which is a complex quantity called as the ***propagation constant***, now equations (5) and (7) can be written as

$$\partial^2 I/\partial x^2 = \gamma^2 V \qquad -(9)$$

$$\partial^2 V/\partial x^2 = \gamma^2 I \qquad -(10)$$

Assuming x = L at the load and x = 0 at the source or the transmitter, the voltage and current which is function of both distance x and the frequency f of the line consists of two superimposed waves, one of which V_i is called the source or the incident wave starts from the transmitter side and moves towards the load or the termination side whose amplitude has an exponential decay of $e^{-\gamma x}$ with the increase in the distance x and the other V_r called the reflected wave starts from the load side and moves towards the transmitter side whose amplitude increases with the increase in the distance x at an exponential rate of $e^{\gamma x}$. The voltage and the current at any point x is the sum of the two waves given by

$$V(x) = V_i e^{-\gamma x} + V_r e^{\gamma x} = Z_c [I_i e^{-\gamma x} - I_r e^{\gamma x}] \qquad -(11)$$

$$I(x) = I_i e^{-\gamma x} + I_r e^{\gamma x} = 1/Z_c [V_i e^{-\gamma x} - V_r e^{\gamma x}] \qquad -(12)$$

In the above equation $I_i = V_i / Z_c$ and $I_r = -V_r / Z_c$ and Z_c is the ***characteristic impedance.***

The source wave differs from the reflected wave in the following things

1. The amplitude and phase of V_i and V_r are different.

2. I_i and I_r oppose each other.

3. Sign of exponent is different negative being for the source wave and positive being for the reflected wave.

The reason for a change of sign in the exponent is because of the following. Consider a voltage source with a sinusoidal variation. The wave at point x on the line of length is given by $V(x,f) = V e^{-\gamma x} = V e^{-\alpha x} e^{-\beta x}$. The propagation constant $\gamma = \alpha + j\beta$, α the real part is referred to as the ***attenuation constant*** measured in nepers/meter or decibels/meter and the imaginary part β is called as the ***phase constant*** expressed in radians/meter. Let x be the origin or the transmitting point the wave is a sinusoidal wave of amplitude A and of wavelength $\lambda = 2\pi/\beta$. The amplitude of the wave decreases as we move along the line for increasing x away from the transmitter towards the load. This wave continues to have the same wavelength λ and is called as the incident or the source wave having a voltage V_i and current I_i. The second wave starts from the load side and moves backwards towards the transmitter. This wave which originates from the load side as result of reflection is called the reflected wave whose voltage and current is denoted by V_r and I_r respectively has also decreasing amplitude as discussed before with decreasing x. The propagation velocity of the

wave along the transmission line of length L is given by $V_p = \omega/\beta$ where $\omega = 2\pi f$ and β is the phase constant in radians/meter.

The ***characteristic impedance*** Z_c of the line is defined as the ratio of the voltage to current at any point in the line independent of x for either the source or the reflected wave

$$Z_c = V_i/I_i = -V_r/I_r$$

Differentiating the equation (11) we get

$$\partial V/\partial x = \gamma\,[-V_i\, e^{-\gamma x} + V_r\, e^{\gamma x}] = -[R + j\omega L]I \qquad -(13)$$

From equation (11), (12) and (13) it follows

$$\gamma\,[V_i\, e^{-\gamma x} - V_r\, e^{\gamma x}] = 1/Z_c\{[R + j\omega L][\, V_i\, e^{-\gamma x} - V_r\, e^{\gamma x}]\}$$

$$Z_c = [R + j\omega L]\,/\sqrt{(R + j\omega L)\,(G + j\omega\, C)}$$

$$Z_c = \sqrt{\frac{R + j\omega L}{G + j\omega L}} \qquad -(14)$$

Let V_s and I_s be the source voltage and current respectively. Let Z_s be the source impedance, γ be the propagation constant of the line of length l and Z_c the characteristic impedance of the line. At the transmitter of the source x = 0, and we wish to compute V(x) and I(x) as a function of these quantities

$$V_s = V_i + V_r = Z_c(I_i - I_r) \qquad - (15)$$

$$I_s = I_i + I_r = (V_i - V_r)/Z_c \qquad - (16)$$

From equations (15) and (16) we get

$$V_i = (V_s + I_s Z_c) / 2 \qquad - (17)$$

$$V_r = (V_s - I_s Z_c) / 2 \qquad - (18)$$

$$I_i = (I_s + V_s/Z_c) / 2 \qquad - (19)$$

$$I_r = (I_s - V_s/Z_c) / 2 \qquad - (20)$$

We know that from (11) $V(x) = V_i e^{-\gamma x} + V_r e^{\gamma x} = Z_c [I_i e^{-\gamma x} - I_r e^{\gamma x}]$ and from equations (17) and (18) we get

$$= [(V_s + I_s Z_c) / 2] e^{-\gamma x} + [(V_s - I_s Z_c) / 2] e^{\gamma x}$$

$$= V_s [(e^{\gamma x} + e^{-\gamma x}) / 2] - I_s Z_c [(e^{\gamma x} - e^{-\gamma x}) / 2)]$$

$$= V_s \cosh(\gamma x) - I_s Z_c \sinh(\gamma x) \qquad - (21)$$

and we know that from (12) $I(x) = I_i e^{-\gamma x} + I_r e^{\gamma x} = 1/Z_c [V_i e^{-\gamma x} - V_r e^{\gamma x}]$ and from equations (19) and (20) we get

$$= [(I_s + V_s/ Z_c) / 2] e^{-\gamma x} + [(I_s - V_s/ Z_c) / 2] e^{\gamma x}$$

$$= I_s [(e^{\gamma x} + e^{-\gamma x}) / 2] - V_s/ Z_c [(e^{\gamma x} - e^{-\gamma x}) / 2)]$$

$$= I_s \cosh(\gamma x) - V_s / Z_c \sinh(\gamma x) \qquad \text{- (22)}$$

From (21) and (22) the impedance at point x is

$$Z(x) = Z_c \left[(Z_s - Z_c \tanh(\gamma x)) / (Z_c - Z_s \tanh(\gamma x)) \right] \qquad \text{- (23)}$$

The line input impedance in terms of load impedance Z_l is

$$Z_s = Z_c \left[(Z_l + Z_c \tanh(\gamma l)) / (Z_c + Z_l \tanh(\gamma l)) \right] \qquad \text{- (24)}$$

Now we consider three special cases

Case (1) when $Z_l = Z_c$

This means that at $x = l$, $Z(l) = Z_c$ and from equation (23) we get

$$Z_c = Z_c \left[(Z_s - Z_c \tanh(\gamma l)) / (Z_c - Z_s \tanh(\gamma l)) \right]$$

$$Z_s = Z_c$$

This means that when the load impedance is equal to the characteristic impedance of the line then the line impedance at any point x on the line is also equal to the characteristic impedance Z_c.

$$V_i = I_s / 2 (Z_s + Z_c) = I_s Z_s = V_s$$

$$I_i = I_s / 2 (1 + Z_s/Z_c) = I_s / 2 (1 + Z_s/Z_s) = I_s$$

$$V_r = I_s / 2 (Z_s - Z_c) = I_s / 2 (Z_s - Z_s) = 0$$

$$I_r = I_s / 2 (1 - Z_s / Z_c) = I_s / 2 (1 - Z_s/Z_s) = 0$$

$$V(x) = V_s e^{-\gamma x} \text{ and } I(x) = I_s e^{-\gamma x}$$

Case (2) short circuited line $Z_l = 0$, $V(l) = 0$

From equation (23) we get

$$0 = Z_c [(Z_s - Z_c \tanh(\gamma l)) / (Z_c - Z_s \tanh(\gamma l))]$$

$$Z_s = Z_c \tanh(\gamma l)$$

Case (3) open circuited line, $Z_l = \infty$, $I(l) = 0$

From equation (23) we get

$$\infty = Z_c [(Z_s - Z_c \tanh(\gamma l)) / (Z_c - Z_s \tanh(\gamma l))]$$

$$Z_s = Z_c / \tanh(\gamma l)$$

Now let us consider $x = 0$ at the receiving or the load end and $x = l$ at the transmitter or the source end. The general solutions for the voltage and current would now take the form

$$\partial I/\partial x = [G + j\omega C]V \qquad - (25)$$

$$\partial V/\partial x = [R + j\omega L]I \qquad - (26)$$

and

$$V(x) = V_i e^{\gamma x} + V_r e^{-\gamma x} = Z_c [-I_r e^{-\gamma x} + I_i e^{\gamma x}] \quad - (27)$$

$$I(x) = I_i e^{\gamma x} + I_r e^{-\gamma x} = 1/Z_c [-V_r e^{-\gamma x} + V_i e^{\gamma x}] \quad - (28)$$

which means

$$Z_c = V_i / I_i = -V_r / I_r$$

$$V_i = (V_l + I_l Z_c) / 2 \quad - (29)$$

$$V_r = (V_l - I_l Z_c) / 2 \quad - (30)$$

$$I_i = (I_l + V_l / Z_c) / 2 \quad - (31)$$

$$I_r = (I_l - V_l / Z_c) / 2 \quad - (32)$$

$$V(x) = V_l \cosh(\gamma x) + I_l Z_c \sinh(\gamma x) \quad - (33)$$

$$I(x) = I_l \cosh(\gamma x) + V_l / Z_c \sinh(\gamma x) \quad - (34)$$

$$Z(x) = Z_c [(Z_l + Z_c \tanh(\gamma x)) / (Z_c + Z_l \tanh(\gamma x))] \quad - (35)$$

By the two port network theory these set of linear equations can be represented as

$$\begin{bmatrix} V_s \\ I_s \end{bmatrix} = \begin{bmatrix} A & B \\ C & D \end{bmatrix} \begin{bmatrix} V_l \\ I_l \end{bmatrix}$$

when $x = l$, $V(l) = V_s$ and $I(x) = I_s$

$$\begin{bmatrix} V_s \\ I_s \end{bmatrix} = \begin{bmatrix} cosh\gamma l & Z_c \sinh\gamma l \\ 1/Z_c \sinh\gamma l & \cosh\gamma l \end{bmatrix} \begin{bmatrix} V_l \\ I_l \end{bmatrix}$$

$A = \cosh(\gamma l)$, $B = Z_c \sinh(\gamma l)$, $C = 1/Z_c \sinh(\gamma l)$ and $D = \cosh(\gamma l)$.

$$Z_s = Z_c \left[(Z_r + Z_c \tanh(\gamma x)) / (Z_c + Z_r \tanh(\gamma x)) \right]$$

A.1 Reflection Coefficient ρ

Reflection coefficient is defined as the ratio of the amplitude of the reflected wave to the incident or the source wave at any point x on the line where $0 \leq x \leq l$.

$$\rho(x) = (V_r e^{-\gamma x}) / (V_i e^{\gamma x}) = (V_r / V_i) e^{-2\gamma x}$$

$$V_r / V_i = [(V_l + I_l Z_c) / 2] / [(V_l - I_l / Z_c) / 2] = (Z_l + Z_c) / (Z_l - Z_c)$$

$$\rho(x) = [(Z_l + Z_c) / (Z_l - Z_c)] e^{-2\gamma x} \qquad - (36)$$

At $x = 0$

$$\rho(x) = [(Z_l + Z_c) / (Z_l - Z_c)]$$

A.2 Computation of α and β from the propagation constant γ in terms of the primary constants

$$\gamma = \alpha + j\beta = \sqrt{(R + j\omega L)\,(G + j\omega C)}$$

$$\gamma^2 = \alpha^2 + j2\alpha\beta - \beta^2 = (RG - \omega^2 LC) + j\omega(LG + RC)$$

$$\alpha^2 - \beta^2 = (RG - \omega^2 LC)$$

$$2\alpha\beta = \omega(LG + RC)$$

$$\alpha^2 + \beta^2 = \sqrt{((R^2 + \omega^2 L^2)(G^2 + \omega^2 C^2))}$$

$$\alpha = \sqrt{\left[1/2\left\{\sqrt{((R^2 + \omega^2 L^2)(G^2 + \omega^2 C^2))} + (RG - \omega^2 LC)\right\}\right]} \quad -(37)$$

$$\beta = \sqrt{\left[1/2\left\{\sqrt{((R^2 + \omega^2 L^2)(G^2 + \omega^2 C^2))} - (RG - \omega^2 LC)\right\}\right]} \quad -(38)$$

Alternatively the ABCD parameters for the transmission can also be derived by modelling it as a two port 'T' network.

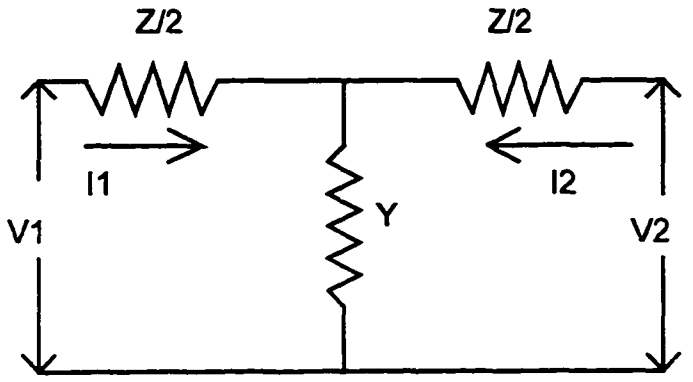

Figure A.3: Two Port Network

By using the impedance matrix the equations of the network are of the form

$$\begin{bmatrix} Z_{11} & Z_{12} \\ Z_{21} & Z_{22} \end{bmatrix} \begin{bmatrix} I_1 \\ I_2 \end{bmatrix} = \begin{bmatrix} V_1 \\ V_2 \end{bmatrix}$$

$$\mathbf{Z\,I = V}$$

where the column matrices **I** and **V** are the input and the output ports respectively. **Z** is called as the impedance matrix.

A.3 Coefficients of the Z matrix

In order to determine the coefficients of the **Z** matrix we consider the following cases. The coefficients for the impedance matrix is computed by imposing the open circuit condition.

Case 1: $I_2 = 0$

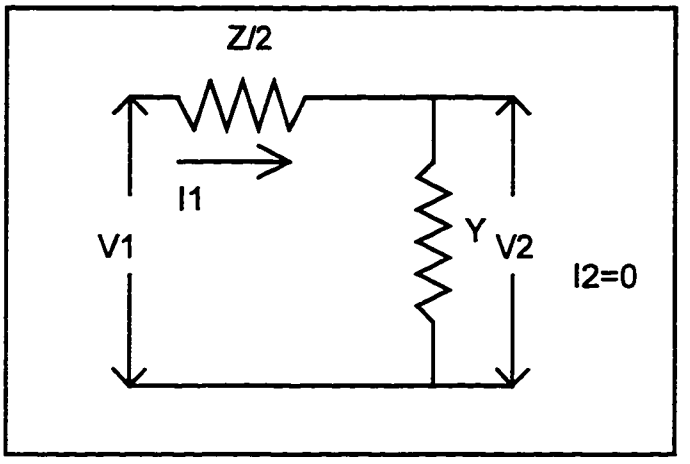

Figure A.4: Network with Port 2 Open

$$Z_{11} = V_1 / I_1$$

$$Z_{11} = (Z / 2 + 1 / Y)$$

$$V_2 / I_1 = 1 / Y$$

Case 2 : $I_1 = 0$

$$Z_{22} = V_2 = (Z / 2 + 1 / Y)$$

$$V_1 / I_2 = 1 / Y$$

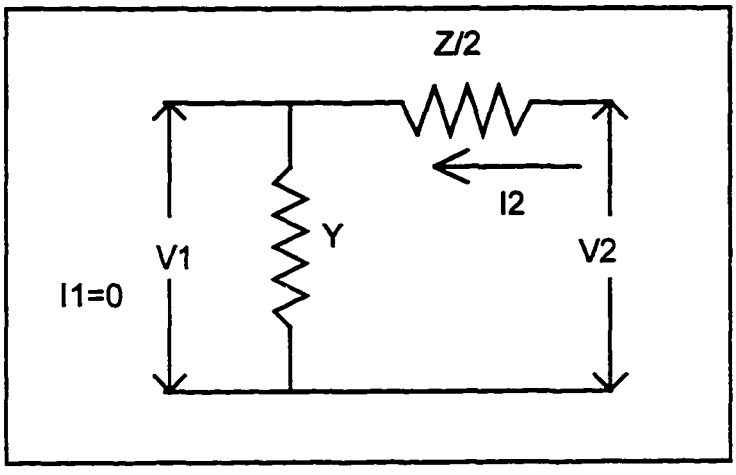

Figure A.5: Network with Port 1 Open

A.4 ABCD Parameters

A is the reciprocal of the open circuited voltage ratio

$$A = V_1 / V_2 \text{ at } I_2 = 0$$

$$= Z_{11} / Z_{21.}$$

D is the reciprocal of the short circuited current ratio

$$D = I_1 / I_2 \text{ at } V_2 = 0$$

$$= Z_{22} / Z_{21.}$$

C and B is the reciprocal open circuit admittance and impedance respectively.

$$B = V_1/I_2 \text{ at } V_2 = 0$$

$$Z/Z_{21} = 1/Z_{21}(Z_{11}Z_{22} - Z_{12}Z_{21})$$

$$C = I_1/V_2 \text{ at } I_2 = 0$$

$$B = Z_{11}Z_{22}/Z_{21} - Z_{12}$$

$$A = Z_{11}/Z_{21} = Y(Z/2 + 1/Y) = (ZY/2 + 1)$$

$$B = Y(Z/2 + 1/Y)\,(Z/2 + 1/Y) - 1/Y$$

$$C = 1/Y$$

$$D = Y(Z/2 + 1/Y) = (ZY/2 + 1)$$

A.5 Matrices for the following circuits

Case 1:

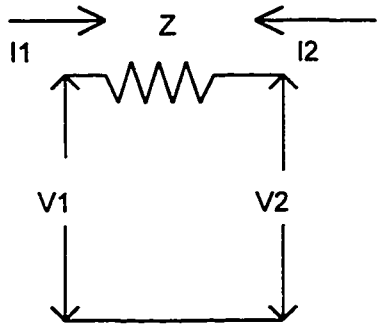

Figure A.6: Impedance Network

$$\begin{bmatrix} V_1 \\ I_1 \end{bmatrix} = \begin{bmatrix} 1 & Z \\ 0 & 1 \end{bmatrix} \begin{bmatrix} V_2 \\ I_2 \end{bmatrix}$$

Case 2:

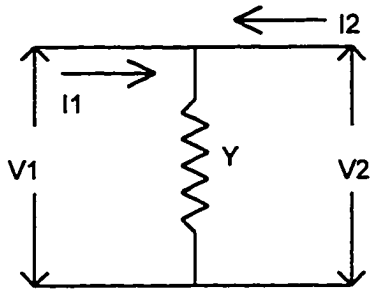

Figure A.7: Admittance Network

$$\begin{bmatrix} V_1 \\ I_1 \end{bmatrix} = \begin{bmatrix} 1 & 0 \\ 1/Z & 1 \end{bmatrix} \begin{bmatrix} V_2 \\ I_2 \end{bmatrix}$$

Case 3:

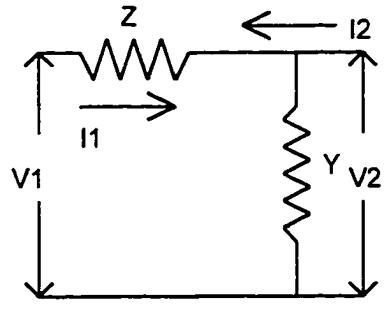

Figure A.8: Impedance Network with Load Admittance

$$\begin{bmatrix} V_1 \\ I_1 \end{bmatrix} = \begin{bmatrix} ZY + 1 & Z \\ Y & 1 \end{bmatrix} \begin{bmatrix} V_2 \\ I_2 \end{bmatrix}$$

Case 4:

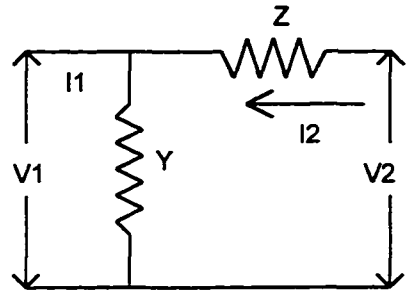

Figure A.9: Impedance Network with Source Admittance

$$\begin{bmatrix} V_1 \\ I_1 \end{bmatrix} = \begin{bmatrix} 1 & Z \\ Y & ZY + 1 \end{bmatrix} \begin{bmatrix} V_2 \\ I_2 \end{bmatrix}$$

Case 5:

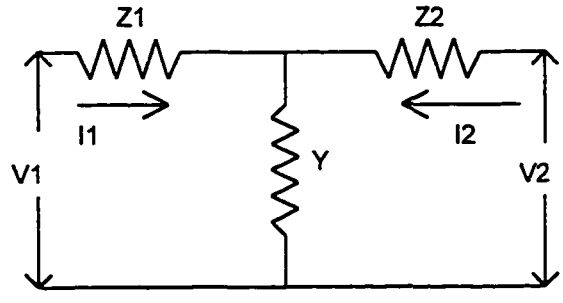

Figure A.10: Impedance Network with Center Tap Admittance

$$\begin{bmatrix} V_1 \\ I_1 \end{bmatrix} = \begin{bmatrix} Z_1Y + 1 & Z_1 + Z_2 + YZ_1Z_2 \\ Y & Z_2Y + 1 \end{bmatrix} \begin{bmatrix} V_2 \\ I_2 \end{bmatrix}$$

Now consider a two port network with a load impedance Z_L

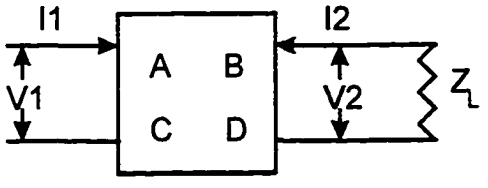

Figure A.11: Two Port Network with Load

$$V_1 = AV_2 + BI_2$$

$$I_1 = BV_2 + DI_2$$

Since $V_2 = I_2Z_L$

$$Z_1 = \frac{AZ_L + B}{CZ_L + D}$$

Using the matrix format Z_1 can be represented as

$$Z_1 = \begin{bmatrix} A & B \\ C & D \end{bmatrix} \begin{bmatrix} 1 \\ 1/Z_L \end{bmatrix} = \frac{A + B/Z_L}{C + D/Z_L}$$

When source impedance is added to the above two port network the input line impedance gets modified as follows

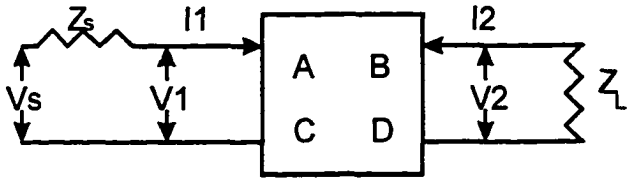

Figure A.12: Two Port Network with Source and Load

$$\begin{bmatrix} V_s \\ I_s \end{bmatrix} = \begin{bmatrix} 1 & Z_s \\ 0 & 1 \end{bmatrix} \begin{bmatrix} A & B \\ C & D \end{bmatrix} \begin{bmatrix} V_2 \\ I_2 \end{bmatrix}$$

$$V_S = V_1 + I_1 Z_S = AV_2 + BI_2 + (CV_2 + DI_2)Z_S$$

$$= (AZ_L + B)I_2 + (CZ_L + D)I_2 Z_S$$

$$= I_2[(AZ_L + B) + (CZ_L + D)Z_S]$$

$$Z_{in} = \frac{Z_L(A + CZ_s) + (B + DZ_s)}{Z_L C + D}$$

Using a quadripole model with the terminating load impedance Z_L and terminating source impedance Z_S we know that from the above derivations that

$$Z_{in} = \frac{AZ_L + B + Z_s(CZ_L + D)}{Z_L C + D}$$

Bibliography

Chapter 1

[1] J.G. Proakis, Digital Communications, MacGraw Hill, New York.

[2] B.E.Keiser, Broadband Coding, Modulation and Transmission Engineering", Prentice Hall.

[3] W.Y.Chen, J.L.Dixon and J.L.Waring, "High-Bit Rate Digital Subscriber Line Echo Cancellation", IEEE JSAC, Vol. 9, No. 6, August 1991, pp. 848-860.

[4] S.V.Ahamed, P.P.Bohn and N.L.Gottfried, "A Tutorial on Two Wire Digital Transmission in the Loop Plant", IEEE Transactions on Communications, Vol. COM 11, Nov. 1981, pp.1554-1564.

[5] J.J.Werner, "The HDSL Environment", IEEE JSAC, Vol. 9, No. 6, August 1991.

[6] W.Stallings, "Data and Computer Communications Systems", MacMillan, New York.

[7] J.Sutherland and L.Litteral, "Residential Video Services", IEEE Comm. Mag. July 1992.

Chapter 2

[1] K.W. Cattermole, "Principals of Digital Line Coding," Int. J. Electron., Vol. 55, no. 1, pp. 3-33, 1983.

[2] S.V. Ahamed , P.P. Bohn, and N.L. Gottfried, "A Tutorial on Two Wire Data Transmission in the Loop Plant," IEEE Trans. on Commun., Vol. COM-29, no. 11, pp. 1,554-1,564, Nov. 1981.

[3] J.W. Lechleider, "DSLs for use with Correlated Line Codes," IEEE Trans. on Commun., Vol. COM-35, no. 10, pp. 1,029-1,036, Oct. 1987.

[4] British Telecommunications Research Laboratories, "Further Comparisons of Line Codes for the Network Side of NT1, "ECSA contribution T1D1.3

Chapter 3

[1] Bellcore, "Generic Requirements for High-Bit-Rate Digital Subscriber Lines", Technical Advisory TA-NWT-001210, issue 1, Oct. 1991.

[2] A.Reddy & S.V.Ahamed, "Parallel Digital Cap Transmitter", ISCA, Vol.3, No. 2, Aug. 1996, pp. 86-91.

[3] W.Y.Chen, G.H.Im & J.J.Werner, "Design of Digital Carrierless AM/PM Transceivers", T1E1.4/92-149.

[4] I.Kalet, "The Multitone Channel", IEEE Trans. Commun., Vol. 37, no. 2, pp. 119-124, Feb. 1989.

[5] J.S.Chow, J.C.Tu & J.M.Cioffi, " A Computationally Efficient Adaptive Transceiver for High-Speed Digital Subscriber Lines", ICC '90, Vol. 4, pp. 1750-1753.

[6] T.Russel Hsing & J.W.Lechleider, "Digital Signal Processing for High-Speed Digital Transport Technology in the Copper Loop Plant", Globecom '91, pp. 1987- 1991.

[7] R.D.Gitlin & S.B.Weinstein, "Fractionally-Spaced Equalization: An improved Digital Tranversal Equalizer ", Bell System Technical Journal, Vol. 60. 1981, pp. 275-296.

Chapter 4

[1] G.S. Moschytz and S.V. Ahamed, "Transhybrid loss with RC Balance Circuits for Primary Rate ISDN Transmission Systems", IEEE JSAC, August 1991, Vol. 9, no. 6, pp. 951-959.

[2] S.V.Ahamed, P.P.Bohn and N.L.Gottfried, "A Tutorial on Two Wire Digital Transmission in the Loop Plant", IEEE Transactions on Communications, Vol. COM 11, Nov. 1981, pp. 1554-1564.

[3] Bellcore, "Generic Requirements for High-Bit-Rate Digital Subscriber Lines", Technical Advisory TA-NWT-001210, issue 1, Oct. 1991.

Chapter 5

[1] G.S. Moschytz and S.V. Ahamed, "Transhybrid loss with RC Balance Circuits for Primary Rate ISDN Transmission Systems", IEEE JSAC, August 1991, Vol. 9, no. 6, pp. 951-959.

[2] S.V.Ahamed and G.S.Moschytz, "Optimization of the RC Matching Network in Adaptive Active Hybrids for High-Speed Data Communications", IEEE ISAS, June 1991.

[3] S.V.Ahamed, "Simulation Environments for the High-Speed Digital Subscriber Lines (HDSL)", IEEE ICC May 1993, pp. 811-815.

[4] G.S.Moschytz and Ahamed, "Transhybrid Loss with RC Balance Circuits for High Speed Full Duplex Modems", AT&T Bell Laboratories XGN360000-891214-01-TM, Dec. 1989.

[5] A.Reddy and S.V.Ahamed, "Simulation Study of CAP in High Bit Rate Asymmetrical Digital Subscriber Line (ADSL) Environment", ICCC '95, Aug. 1995, pp. 177-181.

[6] B.Widrow and S.D.Stearns, "Adaptive Signal Processing", Prentice Hall , New York.

Chapter 6

[1] G.S.Moschytz and S.V.Ahamed, "Transhybrid loss with RC Balance Circuits for Primary Rate ISDN Transmission Systems", IEEE JSAC, August 1991, Vol. 9, No. 6, pp. 951-959.

[2] S.V.Ahamed and G.S.Moschytz, "Optimization of the RC Matching Network in Adaptive Active Hybrids for High-Speed Data Communications", IEEE ISCAS, June 1991.

[3] S.V.Ahamed, "Simulation Environments for the High-Speed Digital Subscriber Lines (HDSL)", IEEE, ICC May 1993, pp. 811-815.

[4] G.S.Moschytz and S.V.Ahamed, "Transhybrid Loss with RC Balance Circuits for High Speed Full Duplex Modems", AT & T Bell Laboratories XGN360000-891214-01-TM, Dec. 1989

[5] A.Reddy and S.V.Ahamed, "Matching Functions by Component Relaxation Method for Asymmetrical Digital Subscriber Line (ADSL)", AEIC' 95, Dec. 1995, pp. 306 - 310.

Chapter 7

[1] O.Agazzi, D.A.Hodges & D.G.Messerschmitt, "Large Scale Integration of Hybrid Method Digital Subscriber Loops", IEEE Trans. on Comm., Vol. COM-30, No.9, Sept. '82.

[2] W.Y.Chen, J.L.Dixon & D.L.Waring, "High Bit Rate Digital Subscriber Line Echo Cancellation", IEEE JSAC, Vol. 9, No. 6, August 1991, pp. 848-860.

[3] K.Feher, "Advanced Digital Communications: Systems and Signal Processing Techniques", Prentice Hall, New York.

[4] R.L.Geiger, P.E.Allen & N.R.Strader, "VLSI Design Techniques for Analog and Digital Circuits", McGraw Hill, New York.

[5] S. V. Ahamed, "Simulation and Design Studies of the Digital Subscriber Lines", Bell System Technical Journal Vol. 61, No. 6.1003-77, July-Aug. 1982a.

[6] S.V.Ahamed, "Simulation Environments for the High-speed Digital Subscriber Line (HDSL)", IEEE International Conference on Communications ICC '93, May 1993.

[7] G.S.Moschytz & S.V.Ahamed, "Transhybrid Loss with RC Balance Circuits for Primary-Rate ISDN Transmission Systems", IEEE JSAC Vol. 9, No. 6, August 1991.

[8] S.V.Ahamed & V.B.Lawrence, "Simulation Studies of Higher Rates in Subscriber Loop Plant", ISSSE '89.

[9] B.Widrow and S.D.Stearns, "Adaptive Signal Processing", Prentice Hall , New York.

Chapter 8

[1] A. Reddy, "A Modified Mesh Architecture for Summation", ISCA CAINE 1993, pp. 126-129.

[2] A.Reddy & S.V.Ahamed, "A Parallel Adaptive Echo Canceller", ICCAI 94, Dec. 94, pp. 13-16.

[3] F. Kamilo & D. Messerschmitt, "Advanced Digital Communication", Prentice Hall 1987.

[4] M. J. Miller & S.V. Ahamed, "Digital Transmission Systems and Networks: Principles", Vol. 1, Computer Science Press, 1987.

[5] M. J. Miller & S.V. Ahamed, "Digital Transmission Systems and Networks: Applications, Vol. 2, Computer Science Press, 1987.

[6] S. V. Ahamed, P. P. Bohn & N. L. Gottfried, "A Tutorial on Two Wire Digital Transmission in Loop Plants", IEEE Trans. Commun., Vol. COM 29, no. 11, pp. 1554-1564, Nov. 1981.

[7] S. V. Ahamed, "Simulation and Design Studies of the Digital Subscriber Lines", Bell System Technical Journal 61, no. 6.1003-77, July-Aug. 1982a.

[8] N. Holte & S. Stueflotten, "A New Digital Echo Canceler for Two Wire Subscriber Lines", IEEE Trans. on Commun. Vol. Com 29, no. 11, Nov. 1981.

[9] W. Y. Chen, J. L. Dixon & D. L. Waring, "High Bit Rate Digital Subscriber Line Echo Cancellation", IEEE JSAC Vol. 9, no. 6, Aug. 1991, pp. 848-860.